



The University of
Nottingham

UNITED KINGDOM · CHINA · MALAYSIA

**IDENTIFYING MATRIX METALLOPROTEINASE-12
SUBSTRATES AS THERAPEUTIC TARGETS IN
CHRONIC OBSTRUCTIVE PULMONARY DISEASE**

By

Brendan Mallia-Milanes MD, MRCP (UK)

**MEDICAL LIBRARY
QUEENS MEDICAL CENTRE**

**Thesis submitted to the University of Nottingham for the degree of
Doctor of Philosophy**

December 2015

Abstract

Chronic Obstructive Pulmonary Disease (COPD) is the third most common cause of death worldwide. Its natural course is a decline in lung function, punctuated by acute exacerbations, leading to hospitalizations and, ultimately, death. The disease is widely accepted to result from an ongoing process of

This thesis is dedicated to my parents for their unconditional love and limitless support

Matrix metalloproteinase (MMP)-12 was originally implicated in COPD by its degradation of elastin in the lung ECM. However, newer in vivo evidence reveals MMP-12 to target substrates outside the ECM. Given these newer findings it was hypothesized that MMP-12 cleaves non-ECM proteins in COPD which may contribute to the disease process. This hypothesis was addressed initially using a candidate-based approach by testing osteopontin and desmin for pathway activation as potential MMP-12 substrates. However, these proved to be non-specific cleavage sites. Next, a novel proteomic technique called TAP (Tandem Affinity Purification of Substrates) was employed to identify potential MMP-12 substrates using a affinity-coupled mouse model. This led to the discovery of several ECM MMP-12 substrates in the mouse model. Next, these findings were translated to human COPD sputum to identify potential MMP-12 targets in COPD, both in exacerbation and during stable disease. Studies with human COPD sputum for MMP-12 substrates were discovered, of particular interest, Complement factor D and the anticoagulant anti-thrombin III, revealing ever new substrates for MMP-12 in COPD.

Abstract

Chronic Obstructive Pulmonary Disease (COPD) is the third commonest cause of death worldwide. Its natural course is a decline in lung function, punctuated by exacerbations, leading to premature death. COPD pathogenesis remains incompletely understood. The disease is widely accepted to result from an excess protease over protective anti-protease activity, leading to extracellular matrix (ECM) damage in the lungs. However, this belief is oversimplified since both harmful pro-inflammatory and protective anti-inflammatory roles are now described for proteases in animal and cell culture models.

Matrix Metalloproteinase (MMP)-12 was originally implicated in COPD by its degradation of elastin in the lung ECM. However, newer *in vitro* evidence reveals MMP-12 to target substrates outside the ECM. Given these newer findings it was hypothesized that MMP-12 cleaves non-ECM proteins in COPD which may contribute to the disease process. This hypothesis was addressed initially using a candidate-based approach, by testing osteopontin and tissue factor pathway inhibitor as potential MMP-12 substrates. However, these proved to be neutrophil elastase targets. Next, a novel proteomic technique called TAILS (Terminal Amine Isotopic Labelling of Substrates) was employed to identify potential MMP-12 substrates using a *Mmp12*^{-/-} smoking mouse model. This led to the discovery of new non-ECM MMP-12 substrates in the mouse model. Next, these findings were translated to human COPD sputum to identify potential MMP-12 targets in COPD, both at exacerbation and during stable disease. Similarly, within human COPD sputum non-ECM MMP-12 substrates were discovered, of particular interest, complement factor C3 and the anticoagulant anti-thrombin III, revealing ever new potential roles for MMP-12 in COPD.

Publications

Cane J, **Mallia-Milanes B**, Forrester D, et al. *Matrix metalloproteinases -8 and -9 in the airways, blood and urine during exacerbations of COPD*. Journal of Chronic Obstructive Pulmonary Disease. In press.

Abstracts

Mallia-Milanes B, Bolton CE, Johnson SR. *Tissue factor pathway inhibitor (TFPI) is cleaved by multiple proteases in COPD lungs to affect circulating TFPI levels*: Poster presentation at the British Thoracic Society Winter Meeting, London, UK December 2015

Mallia-Milanes B, Meakin G, Bailey H, et al. *Identifying MMP-12 substrates in COPD*: Poster presentation at the British Association for Lung Research, Nottingham, UK, July 2013.

Mallia-Milanes B, Meakin G, Bailey H, et al. *Identifying MMP-12 substrates in COPD*: Poster presentation at the American Thoracic Society, Philadelphia, USA, May 2013.

Mallia-Milanes B, Meakin G, Bailey H, et al. *Identifying MMP-12 substrates as therapeutic substrates in COPD*: Poster presentation at the British Thoracic Society Winter Meeting, London, UK December 2012.

Oral Presentations

Mallia-Milanes B, Dufour A, Leme A, et al. *A two species proteomics approach to determine MMP-12 substrates in COPD*, British Thoracic Society Winter Meeting, London, UK December 2015.

Mallia-Milanes B. *MMP-12 and TFPI cleavage in COPD airways*. Presentation to the Overall Laboratory Team, University of British Columbia, Vancouver, Canada, July 2014

Acknowledgements

This thesis would not be possible without the help and support of several people. Firstly, I must express my utmost gratitude to my supervisors Professor Simon R Johnson and Dr Charlotte E Bolton. I am grateful to Professor Johnson for his ideas, intellectually stimulating meetings, pushing me out of my comfort zone and allowing me the freedom to explore my own ideas. I am grateful to Dr Bolton for her constant support, encouragement and positivity. Her passion for research and COPD is truly inspirational.

I must thank Adeleine Sheehan for her hard work in recruiting and enrolling patients with COPD into the cohort used for this thesis and Helen Bailey, Gary Meakin and Rebecca Simms for processing what must have seemed endless sputum and blood samples! I am extremely grateful to Dr Michelle John for providing the arterial stiffness data for this thesis. I would also like to thank all the participants in the study who selflessly enrolled onto the studies despite struggles with their daily symptoms.

A special thank you is due to the team at Respiratory Medicine QMC for providing such a friendly working environment, with a special mention to our team's post-doctoral researchers, Drs Debbie Clements and Ivonne Siebeke. I am grateful to Dr Clements for teaching me laboratory techniques and for help with troubleshooting. I am especially thankful to Ivonne for her friendship, encouragement, critical advice and for being so thorough and meticulous. A special thank you goes to the other PhD students Arundhati Dongre-Patel, Chris Philp and Shams-un-nisa Naveed who made work such a pleasurable experience. They have become treasured friends.

I would like to acknowledge the indispensable role of the Overall laboratory at the University of British Columbia, Vancouver in the preparation of this thesis. I am most grateful to Professor Overall and Dr Reini Kappelhoff ("Die Reini"!) for such a warm welcome to the lab and Drs Antoine Dufour and Nestor Solis for their patience, expertise

and enthusiasm in teaching me proteomic techniques. My experience in Vancouver is unforgettable.

Lastly, but definitely not least, a most sincere thank you is due to my parents to whom I dedicate this thesis, and to my sister Andrea, brother Luca, brother-in-law Wilfred and nephew Matteo. I cannot imagine my life without you. You truly all make me complete.

	Page Number
Acknowledgements	v
Abbreviations	viii
List of Figures	xv
List of Table	xviii
Chapter 1 Literature Review	1
1.0 COPD- Background, Disease Prevalence and Importance	1
1.1 Risk Factors for COPD	2
1.2 COPD- just an airway disease?	3
1.3 Mechanics of Airflow Limitation in COPD	4
1.4 Cellular Basis of COPD Pathogenesis	5
1.5 Correlation of Cellular Pathogenesis to Airflow Limitation	7
1.6 COPD Pathobiology	7
1.7 The Protease-Anti-protease Theory	9
1.8 Reactive Oxygen Species	10
1.9 Inflammatory Cells in COPD- Macrophages	12
1.10 Inflammatory Cells in COPD- Macrophages	18
1.11 Matrix Metalloproteinases- an Overview	16
1.12 Matrix Metalloproteinases- General Structure and Function	19
1.13 Macrophage Metalloproteinase/ Matrix Metalloproteinase-12	20
1.14 Relationship of Matrix Metalloproteinase-12 in COPD	21
1.15 Methods of Identifying MMP-12 substrates	24

Contents

Section	Page Number
Abstract	iii
Publications	v
Abstracts	v
Oral Communications	v
Acknowledgements	vi
Abbreviations	xix
List of Figures	xv
List of Table	xviii
Chapter 1 Literature Review	1
1.0 COPD- Background, Disease Prevalence and Importance	1
1.1 Risk Factors for COPD	3
1.2 COPD- just an airway disease?	3
1.3 Mechanics of Airflow Limitation in COPD	4
1.4 Cellular Basis of COPD Pathogenesis	5
1.5 Correlation of Cellular Pathogenesis to Airflow Limitation	7
1.6 COPD Exacerbations	7
1.7 The Protease-Anti-protease Theory	9
1.8 Reactive Oxygen Species	10
1.9 Inflammatory Cells in COPD-Neutrophils	12
1.10 Inflammatory Cells in COPD-Macrophages	13
1.11 Matrix Metalloproteinases-an Overview	16
1.12 Matrix Metalloproteinase-General Structure and Function	19
1.13 Macrophage Metalloelastase/ Matrix Metalloproteinase-12	20
1.14 Importance of Matrix Metalloproteinase-12 in COPD	21
1.15 Methods of Identifying MMP-12 substrates	24

1.16 Osteopontin, a MMP-12 substrate <i>in vitro</i>	29
1.17 Tissue Factor Pathway Inhibitor (TFPI), an MMP-12 substrate <i>in vitro</i>	34
1.18 Pharmacological Inhibition of MMP-12	35
1.19 Conclusion	36
1.20 Aims	37
Chapter 2 Methods	38
2.0 <i>In vitro</i> cleavage assays	38
2.1 Patients	38
2.2 Spirometry	38
2.3 Cardiovascular measurements	39
2.4 Thoracic CT scans	40
2.5 Sputum induction	40
2.6 Sputum processing	40
2.7 Protein determination assay	41
2.8 Sputum spiking <i>ex vivo</i> experiments	41
2.9 Immunoprecipitation	43
2.10 Sodium Dodecyl Sulphate-Polyacrylamide Gel Electrophoresis (SDS-PAGE)	44
2.10.1 Sample preparation	44
2.10.2 Preparation of acrylamide gels	44
2.10.3 Running SDS-PAGE gels	45
2.11 Western blotting	45
2.12 ECL Method of Protein Detection	46
2.13 Stripping Western Blots	47
2.14 Silver Staining Method of Protein Detection	47
2.14.1 Fixative step	47

2.14.2 Wash step	47
2.14.3 Staining step	48
2.14.4 Stop step	48
2.15 Enzyme-Linked Immunosorbent Assay (ELISA)	48
2.16 Proteome Profiler Antibody Arrays	49
2.17 Western blotting and Proteome profiler human protease array Data Analysis	50
2.18 Human Monocyte Preparation	50
2.19 Reactive Oxidative Species (ROS)	51
2.20 Macrophage Differentiation Protocol	52
2.21 Real-time Polymerase Chain Reaction (qPCR)	53
Chapter 3 The Presence and Cleavage of OPN in COPD Airways	54
3.0 Background	54
3.1 Methods	56
3.1.1 <i>In vitro</i> cleavage assays	56
3.1.2 Patient cohort and study design	57
3.1.3 Spirometry and CT scans	57
3.1.4 Sputum induction	57
3.1.5 Sputum processing	58
3.1.6 Sputum spiking <i>ex vivo</i> experiments	58
3.1.7 Western blotting	59
3.1.8 Silver stain	59
3.1.9 Proteome profiler human protease array	60
3.1.10 Sputum Protein Level Determination	60
3.1.11 Human Monocyte Preparation	61

3.1.12 ROS Measurement	61
3.1.13 Macrophage Differentiation Protocol	61
3.1.14 qPCR	61
3.1.15 Analysis and Statistics	62
3.2 Results	62
3.2.1 MMP-12 cleaves osteopontin <i>in vitro</i>	62
3.2.2 OPN is present in human COPD sputum in cleaved and uncleaved forms	66
3.2.3 MMP-12 is present in human COPD sputum	66
3.2.4 OPN is cleaved <i>in situ</i> in human COPD sputum	67
3.2.5 Comparison of OPN cleavage in COPD sputum at exacerbation and recovery	69
3.2.6 Proteome profiler assay	70
3.2.7: Inhibition Assays: <i>ex vivo</i> sputum cleavage of OPN in presence of protease inhibitors	72
3.2.8 OPN is cleaved by NE and uPA	80
3.2.9 Clinical characteristics of fast OPN cleavers and slow OPN cleavers	82
3.2.10 Functional assays of MMP-12-cleaved OPN: ROS assay	84
3.2.11 Functional assays of MMP-12-cleaved OPN: qPCR	87
3.3 Discussion	88
Chapter 4 The Presence and Cleavage of TFPI in COPD Airways	92
4.0 Background	92
4.1 Methods	94
4.1.1 <i>In vitro</i> cleavage	94

4.1.2 Patient cohort and study design	95
4.1.3 Spirometry and CT scans	95
4.1.4 Cardiovascular measurements	95
4.1.5 Lithium heparin plasma preparation	96
4.1.6 EDTA plasma preparation	96
4.1.7 Sputum induction	96
4.1.8 Sputum processing	96
4.1.9 Sputum spiking <i>ex vivo</i> experiments	96
4.1.10 Western blotting	97
4.1.11 Proteome profiler human protease array	98
4.1.12 ELISA	98
4.1.13 Analysis and statistics	99
4.2 Results	99
4.2.1 MMP-12 cleaves TFPI <i>in vitro</i>	99
4.2.2 TFPI is present in human COPD sputum in cleaved and uncleaved forms	100
4.2.3 TFPI is cleaved <i>in situ</i> in human COPD sputum	101
4.2.4 Comparison of cleavage of TFPI in COPD sputum at exacerbation and recovery	104
4.2.5 Proteome profiler assay	106
4.2.6 Inhibition Assays: <i>ex vivo</i> sputum cleavage of TFPI in presence of protease inhibitors	107
4.2.7 TFPI is cleaved by NE and uPA	113
4.2.8 Clinical characteristics of fast TFPI cleavers and slow TFPI cleavers	114
4.2.9 Heparin plasma TFPI levels at exacerbation and recovery	117

4.2.10 Correlation of plasma TFPI levels to aortic stiffness	120
4.3 Discussion	121
Chapter 5 Identifying MMP-12 substrates in COPD	127
5.0 Background	125
5.1 Methods	128
5.1.1 BALF samples from <i>Mmp-12^{-/-}</i> and <i>Mmp-12^{+/+}</i> mice	128
5.1.2 Sputum samples	128
5.1.3 Whole Protein TMT Labelling	129
5.1.4 Whole Protein Dimethylation	130
5.1.5 N-terminal Enrichment	131
5.1.6 High Performance Liquid Chromatography (HPLC) and Mass Spectrometry (MS)	131
5.1.7 Spectrum-to-sequence Matching and Statistics	132
5.2 Results	133
5.2.1 Mice samples	133
5.2.2 Human COPD exacerbation and recovery samples	136
5.2.3 The human sputum degradome in COPD	145
5.3 Discussion	153
Chapter 6 Discussion and Further Work	157
6.0 Introduction	157
6.1 MMP-12 is present and active in COPD sputum	157
6.2 OPN and TFPI were identified as new substrates for NE	158
6.3 Protease activity in COPD airways is complex	159
6.4 MMP-12 targets a large variety of substrates outside the ECM	160
6.5 TAILS on human COPD sputum identified the presence of MMP-12 substrates	160

6.6 TAILS was used successfully to identify the human COPD	
sputum degradome	161
6.7 Neutrophils are chiefly involved in proteolytic events in	
COPD airways	162
6.8 The lungs are involved in coagulation in COPD	162
6.9 Conclusion	163
7.0 References	164

Fig. 3.1 MMP-12 cleaves OPN in a -20kDa fragment in vitro	64
Fig. 3.2 MMP-12 cleaves OPN in a multiple fragment in vitro	64
Fig. 3.3 OPN is present in COPD sputum in polymeric, monomeric and dimeric forms	65
Fig. 3.4 Sputum protein levels are similar at exacerbation and recovery	66
Fig. 3.5 All three forms of MMP-12 are present in COPD sputum	67
Fig. 3.6 Redensitating anti-OPN western blots from 4 patients	68
Fig. 3.7 Cleavage of MX HS tagged OPN occurs at different rates in sputum from differing COPD patients	69
Fig. 3.8 No differences in sputum protease levels between fast OPN cleavers and slow OPN cleavers	71
Fig. 3.9 Differences in sputum protein levels between fast and slow OPN cleavers	72
Fig. 3.10 Benzamide does not inhibit recombinant OPN cleavage in COPD sputum	74
Fig. 3.11a and b: MX SPIC inhibits recombinant OPN cleavage in sputum	75
Fig. 3.11c: GDI SPIC failed to inhibit recombinant OPN cleavage in sputum	76
Fig. 3.12a and b: Benzamide does not inhibit OPN cleavage in COPD sputum	78
Fig. 3.12a and b: Recombinant OPN cleavage decreased the presence of benzamide	79
Fig. 3.13: Benzamide does not inhibit recombinant OPN cleavage in sputum	80

List of Figures

Fig. 1.1 Schematic overview of inflammatory cell involvement in COPD	6
Fig. 1.2 Macrophage differentiation	16
Fig. 1.3 Schematic representation of the general structure of MMPs	20
Fig. 1.4 TAILS procedure	28
Fig. 2.1 Recombinant 6XHIS tagged-OPN is increasingly cleaved in increasing concentrations of sputum	43
Fig. 3.1 MMP-12 cleaves OPN to a ≈20kDa fragment <i>in vitro</i>	63
Fig. 3.2 MMP-12 cleaves OPN to a ≈20kDa fragment <i>in vitro</i>	64
Fig. 3.3 OPN is present in COPD sputum in polymeric, monomeric and cleaved forms	65
Fig. 3.4 Sputum protein levels are similar at exacerbation and recovery	66
Fig. 3.5 All three forms of MMP-12 are present in COPD sputum	67
Fig. 3.6 Representative anti-OPN western blots from 4 patients	68
Fig. 3.7 Cleavage of 6X HIS tagged-OPN occurs at different rates in sputum from different COPD patients	69
Fig. 3.8a-d Differences in sputum protease levels between fast OPN cleavers and slow OPN cleavers	71
Fig. 3.9 Differences in sputum protein levels between fast and slow OPN cleavers	72
Fig. 3.10 Ilomastat does not inhibit recombinant OPN cleavage in COPD sputum	74
Fig. 3.11a and b 50X SPIC inhibits recombinant OPN cleavage in sputum	75
Fig 3.11c 50X SPIC failed to inhibit recombinant OPN cleavage in sputum	76
Fig. 3.12a and b Amiloride does not inhibit OPN cleavage in COPD sputum	78
Fig. 3.13a and b Recombinant OPN cleavage decreased the presence of sivelestat	79
Fig 3.14 Hirudin does not inhibit recombinant OPN cleavage in sputum	80

Fig. 3.15 NE cleaves OPN <i>in vitro</i> to a <20kDa fragment	81
Fig. 3.16 uPA cleaves OPN <i>in vitro</i> to a ≈20kDa fragment	81
Fig. 3.17 Fast OPN cleavers have higher sputum neutrophil percentages	84
Fig. 3.18 ROS production by PBMC undergoing zymosan phagocytosis is not altered by OPN	85
Fig. 3.19 No difference in PBMC ROS production was noted between uncleaved and MMP-12-cleaved OPN	86
Fig. 3.20 qPCR showing RNA levels of Mannose Receptor in macrophages incubated under different conditions	87
Fig. 3.21 qPCR showing RNA levels of IL-12 in macrophages incubated under different conditions	88
Fig. 4.1 MMP-12 cleaves TFPI <i>in vitro</i> to a ≈20kDa fragment	100
Fig. 4.2 TFPI monomer and fragments are present in human COPD sputum	101
Fig. 4.3 TFPI cleavage in COPD sputum is time-dependent	102
Fig. 4.4 Cleavage of 10X HIS tagged-TFPI occurs at different rates in sputum from different COPD patients	103
Fig. 4.5 Cleavage of 10X HIS tagged-TFPI occurs at different rates in sputum from different COPD patients	104
Fig. 4.6 Level of cleavage of human recombinant 10X HIS tagged-TFPI in sputum supernatant was similar at Visit 1 (exacerbation) and Visit 3 (recovery)	105
Fig. 4.7 Representative anti-6X HIS antibody probed western blot comparing degradation of 10X HIS tagged-TFPI in COPD PBS supernatant sputum in paired samples taken at exacerbation and recovery	106
Fig. 4.8a-d Differences in sputum protease levels between fast TFPI cleavers and slow TFPI cleavers	107
Fig. 4.9 Ilomastat does not inhibit TFPI cleavage in COPD sputum	108
Fig. 4.10 TFPI cleavage in sputum is serine protease dependent	109

Fig. 4.11 TFPI cleavage in sputum is partially inhibited by a serine/cysteine/amidopeptidases/aspartic protease inhibitor cocktail	110
Fig. 4.12 Cysteine protease inhibition does not inhibit TFPI cleavage in COPD sputum; immunoblot probed with anti-6X HIS tag antibody	110
Fig. 4.13 No clear differences were noted between samples treated with 10X SPIC/ Ilomastat and 10X SPIC only	111
Fig. 4.14 The uPA inhibitor, amiloride does not inhibit TFPI cleavage in COPD sputum; immunoblot probed with anti-6X HIS tag antibody	112
Fig. 4.15 The NE inhibitor, sivelestat inhibits TFPI cleavage in COPD sputum	112
Fig. 4.16 NE cleaves TFPI <i>in vitro</i> to a <20kDa fragment	113
Fig. 4.17 uPA cleaves TFPI <i>in vitro</i> to a ≈35kDa fragment	114
Fig. 4.18 Sputum indices were compared between fast and slow TFPI cleavers	116
Fig. 4.19 Fast TFPI cleavers had lower heparin plasma TFPI levels compared to slow TFPI cleavers	117
Fig. 4.20 Plasma TFPI levels are elevated at exacerbation (Visit 1) compared to recovery (Visit 3)	118
Fig. 4.21 Sputum neutrophil counts indirectly correlate with plasma TFPI levels at recovery (Visit 3)	120

List of Tables

Table 1.1 Diagnosis and classification of severity of airflow limitation in COPD using spirometry, as per GOLD guidelines	5
Table 1.2 Classification of human MMPs	8
Table 1.3 Summary of identified MMP-12 substrates	25
Table 1.4 Summary of studies on OPN cleavage	31
Table 3.1 Clinical characteristics of fast OPN cleavers and slow OPN cleavers	83
Table 4.1 Comparison of fast TFPI cleavers and slow TFPI cleavers	115
Table 4.2 Correlation of heparin plasma TFPI values at Visit 1 and Visit 3 to sputum cell indices	119
Table 4.3 Demographic data at baseline visit (clinical trial NCT01151306)	120
Table 5.1 Cleavage sites and <i>Mmp-12^{-/-}/Mmp-12^{+/+}</i> ratios for the differentially cleaved peptides	135
Table 5.2 Murine MMP-12 targets are present in human COPD sputum	136
Table 5.3 Proteins with peptides increased both at exacerbation and recovery	137
Table 5.4 Proteins with peptides increased at exacerbation only	140
Table 5.5 Proteins with peptides increased at recovery only	143
Table 5.6 Clinical and sputum characteristics of COPD patients	146
Table 5.7 Proteins identified in human COPD sputum by TAILS grouped according to their function/s	147

Abbreviations

-/- Knockout

+/+ Wild type

2-D Two-Dimensional

aa Amino acid

A1AT Alpha-1-antitrypsin

ACN Acetonitrile

ADAM A disintegrin and metalloprotease

ADAM-TS ADAM subfamily with thrombospondin (TS)-like motifs

AM Alveolar macrophages

APMA 4-aminophenylmercuric acetate

Arg Arginine

Arg-C Arginase-C

BAL Bronchoalveolar lavage

CCL Chemokine ligand

CD Cluster of differentiation

CD₂O Deuterated formaldehyde

¹³CD₂O ¹³Carbon labelled, deuterated formaldehyde

CH₂O Formaldehyde

cm Centimetre

COPD Chronic obstructive pulmonary disease

CRP C-reactive protein

CT-PCPE C-terminal proteinase enhancer

CVD Cardiovascular disease

D Aspartic acid

DDP_{IV}/CD26 Dipeptidyl-peptidase 4

DLCO Transfer factor

DNA Deoxyribonucleic acid

DTT Dithiothreitol

E Exacerbation

ECM Extracellular matrix

e.g. *exempli gratia*, for example

ELISA Enzyme-linked immunosorbent assay

ERK Extracellular signal kinase

Eta-1 Early T-cell activation-1

F Factor

FDR False discovery rate

FEV₁ Forced expiratory volume in 1 second

Fig Figure

FVC Forced vital capacity

G Glycine

GIMP GNU image manipulation programme

GLN Glutamine

GM-CSF Granulocyte-macrophage colony-stimulating factor

GOLD Global initiative for chronic obstructive lung disease

GPI Glycophosphatidylinositol

GRO- α Growth related oncogene-alpha

GSH Glutathione

GWAS Genome-wide association studies

h helper

HCL Hydrochloride

HIS Histidine

H₂O₂ Hydrogen peroxide

HPLC High performance liquid chromatography

HRP Horseradish peroxidase

i.e. id est, that is

IFN- γ Interferon-gamma

Ig Immunoglobulin

IL Interleukin

ILR1 Interleukin-1receptor type 1

i.v. Intravenous

JNK c-Jun kinase

K Lysine

kDa kiloDalton

Ki Inhibitory constant

KO Knockout

KOS Knockout mice exposed to cigarette smoke

L Litre

Leu Leucine

LPS Lipopolysaccharide

M Molar

mM Millimolar

MCP Monocyte chemoattractant protein

M-CSF Macrophage colony-stimulating factor

MAP Mean arterial pressure

Met Methionine

MHC Major histocompatibility complex

MIP Macrophage Inflammatory Protein

min minutes

MME Matrix metalloelastase

MMP Matrix metalloproteinase

MPO Myeloperoxidase
mRNA Messenger RNA
MSP Macrophage-stimulating protein
MT-MMP Membrane-type matrix metalloproteinase
MyD88 Myeloid differentiation primary response 88
N amino group
NaBH₃CN Sodium cyanoborohydride
NaBD₃CN Sodium cyanoborodeuteride
NaCl Sodium chloride
NaOH Sodium hydroxide
NE Neutrophil elastase
NF Nuclear factor
ng nanograms
NH₂ amino group
NHS National Health Service
OPN Osteopontin
O₂ Oxygen
O₂⁻ Superoxide radical
PAGE Polyacrylamide gel electrophoresis
PBMC Peripheral blood mononuclear cells
PBS Phosphate buffered saline
qPCR Real-time polymerase chain reaction
PI3K Phosphatidylinositol-3 kinase
p.p.m parts per million
PR3 Proteinase 3
PVDF Polyvinylidene fluoride
PWV Pulse wave velocity

r recombinant

R Arginine, Recovery

RNA Ribonucleic acid

ROS Reactive oxygen species

rpm Revolutions per minute

RTK Receptor-type protein tyrosine kinase

S Substrate

S'1 Specificity

SDS Sodium dodecyl sulphate

SLPI Secretory leukocyte protease inhibitor

SNP Single nucleotide polymorphism

SOD Superoxide dismutase

SPIC Serine protease inhibitor cocktail

spp-1 secreted phosphoprotein-1

TAILS Terminal amine isotopic labelling of substrates

TCA Trichloroacetic acid

TCC total cell count

TCEP Tris (2-carboxyethyl)phosphine

TF Tissue factor

TFPI Tissue factor pathway inhibitor

TIMP Tissue inhibitor of metalloproteases

TNF- α Tumour necrosis factor-alpha

TLR Toll-like receptor

uPA Urokinase-type plasminogen activator

v versus

V Visit

V_A alveolar volume

VLDL Very low density lipoprotein

WCC White cell count

WT Wild type

WTS Wild type mice exposed to cigarette smoke

Chapter 1 Literature review

1.0 COPD- Background, Disease Prevalence and Importance

Chronic Obstructive Pulmonary disease (COPD) currently affects around 210 million people globally [1]. It is the third commonest cause of death worldwide [2] and the only leading cause of mortality whose prevalence continues to rise [3]. While between 1966 and 1995 the age-adjusted death rates for coronary heart disease and stroke declined by 45% and 58% respectively, COPD death rate increased by 71% [3]. The WHO predicts the disease to become the fifth leading cause of disability worldwide by 2020 [3, 4]. The commonest aetiological factor is cigarette smoking and the natural history of the disease is one of a gradual decline in lung function, frequently punctuated by exacerbations, deterioration in quality of life and reduced life expectancy [5].

The true prevalence of COPD is difficult to ascertain. Reported prevalence figures for the disease are often underestimated [6-8] due to varying methods of diagnosis [7], inaccuracy in death certificate reporting [6], gender bias in population studies [8] and difficulty in diagnosing COPD due to overlapping symptoms with commonly associated conditions, such as ischemic heart disease [9]. Data from an international telephone survey carried out in the USA, Canada and six European countries estimated the prevalence of COPD at around 4% [10] while a systematic review of COPD prevalence studies estimated a range of 4-10% in countries where spirometry was used for diagnosis [7]. Perhaps the most accurate estimation is that from an international worldwide study (BOLD) in which spirometry was used for diagnosis as per the internationally recognised Global Initiative for Chronic Obstructive Lung Disease (GOLD) guidelines. This study placed the prevalence figure at 10.1% for GOLD stage II or higher [8].

COPD is a huge economic burden. In Britain, it is the second commonest cause of emergency admissions, causing more than 25,000 deaths each year and costing the National Health Service (NHS) more than £800 million annually [1]. In the United States of America COPD accounts for around 750,000 admissions to hospital each year, with 10-12% of stays occurring in critical care units [4]. The estimated annual cost is in the region of US\$24 billion, 61% of which is due to direct medical spending, such as hospital based care [11]. With a continued rise in the COPD mortality rate [12] and disappointing smoking cessation rates [13] COPD management poses a unique challenge for us and future generations.

One urgent requirement in the battle against COPD is the development of new strategies to develop drugs to combat the disease. The mainstay of current treatment is inhaled corticosteroids [5] which exert a non-discriminatory anti-inflammatory effect on the airways [14]. Unfortunately, COPD responds poorly to corticosteroid treatment, so mortality and disease progression remain unaffected [15]. In addition, such therapy leads to side effects which contribute to disease morbidity, such as osteoporosis and adrenal insufficiency [16]. Hence new drugs are needed.

The recognized importance of proteases in COPD pathology [17-20] has led to clinical trials of anti-proteases targeting some of the main suspects in pathogenesis, notably matrix metalloprotease (MMP)-12 [21, 22] and neutrophil elastase (NE) [23], in an effort to halt disease progression. Despite this, anti-protease trial outcomes in COPD have been disappointing in their lack of drug efficacy [21-23]. Furthermore, anti-MMP drugs investigated in other illnesses have been associated with significant side effects [24, 25]. In hindsight, this is unsurprising given the intricacies of the protease web, with crosstalk and similar substrate profiles existing between different proteases [26]. New strategies should therefore focus on protease targets, *i.e.* downstream of the protease. This should lead to newer more specific drugs with a narrower side effect profile than

those targeting the protease. To achieve this, the substrate profile of proteases, or 'degradome' involved in COPD needs to be identified.

The following literature review will focus on the mechanisms involved in COPD, highlight what is unknown in disease pathogenesis, and determine how identifying suspected MMP-12 substrates may develop better treatment. This thesis therefore aims to identify new targets within the degradome of MMP-12 in the airways in COPD.

1.1 Risk Factors for COPD

Smoking is the strongest known risk factor for COPD [5, 27, 28]. However, not all smokers develop COPD [8] and fixed airflow obstruction occurs in non-smokers [29], meaning other factors are involved. Among genetic factors, alpha-1-antitrypsin (A1AT) deficiency is known to cause premature emphysema [18], although this condition is rare. Single nucleotide polymorphisms in certain genes, such as the MMP-12 gene have been associated with COPD [30-32]; however further studies are needed to understand these associations further. More recently, exposure to indoor fumes derived from biomass fuels in dwellings with poor ventilation has been recognized as an important cause for COPD worldwide[33]. The role of air pollution, while known to exacerbate existing lung disease [34, 35], is thought to play a minimal role in COPD prevalence in comparison to the effect of cigarette smoking [36].

1.2 COPD- just an airway disease?

COPD is defined as progressive, poorly reversible airflow limitation caused by an abnormal inflammatory response in the lungs to noxious stimuli [5], usually cigarette smoke [37]. Pathogenesis involves small airways inflammation and alveolar destruction, termed emphysema [38, 39]. "COPD" is hence an umbrella term encompassing a range of respiratory conditions, including chronic bronchitis and emphysema, all with the

common feature of non-fully reversible airflow obstruction. Mounting evidence suggests that there is an extra-pulmonary component to the disease which is responsible for associated co-morbidities, most especially cardiovascular disease (CVD) [4, 9, 40-42]. Indeed, the risk of CVD in COPD is two to three times greater than that attributed to smoking alone [4] and CVD accounts for a quarter of deaths in COPD [43]. Despite a recognized link between CVD and airway and systemic inflammation in COPD [44], the underlying mechanisms still require exploration.

1.3 Mechanics of Airflow Limitation in COPD

In COPD airflow limitation measured during forced expiration results from increased resistance in the small conducting airways, *i.e.* those with an internal diameter of <2mm present in the 4th to the 14th generation of branching [45-48], and/or increased lung compliance as a result of alveolar destruction [49]. The units for airway resistance are cm H₂O/L per second, and for lung compliance L/cmH₂O, and their product (time) provides the time constant for lung emptying [50]. This is reflected in spirometry measurements, *i.e.* FEV₁ (forced expiratory volume in 1 second or the amount of air exhaled forcibly from the lungs in 1 second) and its ratio to FVC (forced vital capacity or the maximum volume of air forcibly exhaled), which remain the gold standard for diagnosing, monitoring and staging severity of COPD in clinical practice (Table 1.1) [5].

Table 1.1 Diagnosis and classification of severity of airflow limitation in COPD using spirometry, as per GOLD guidelines [5]

In patients with FEV₁/FVC <0.7:		
Stage of Disease	Severity of Airflow Limitation	FEV₁ Percent Predicted
GOLD I	Mild	≥80%
GOLD II	Moderate	≥50% <80%
GOLD III	Severe	≥30% < 50%
GOLD IV	Very Severe	<30%

1.4 Cellular Basis of COPD Pathogenesis

In COPD, chronic inhalation of toxic gases, most commonly cigarette smoke, triggers activation of both the host's innate and adaptive immune response [51]. This activation persists even after cessation of exposure to noxious stimuli [52, 53]. Within the innate system, the mucociliary clearance works with the monocyte/macrophage system to clear the airways of deposited particles [51]. Cigarette smoke, both directly [54] and through loss of epithelial cell tight junctions, triggers the release of cytokines [51]. These include interleukin (IL)-6, 8 and macrophage chemoattractant protein (MCP)-1, resulting in mobilization of neutrophils and macrophages from the circulation into the epithelium [51, 54-58]. These newly recruited inflammatory cells release proteolytic enzymes, most notoriously the MMPs and NE that degrade components of the extracellular matrix (ECM), notably elastin, causing emphysema [59, 60]. Damaged epithelium and endothelium as well as the release of elastin fragments activate the adaptive immune system via antigen-presenting cells using Major histocompatibility complex (MHC) class II molecules leading to a T-cell immune response which, in turn, activates B-cell mediated immunity within the lungs [61-65]. This process of "autoimmunity" has been proposed as a mechanism for the propagated inflammation

seen in COPD even after smoking cessation. A schematic representation of the inflammatory pathways in COPD is shown in the figure below (Figure 1.1)

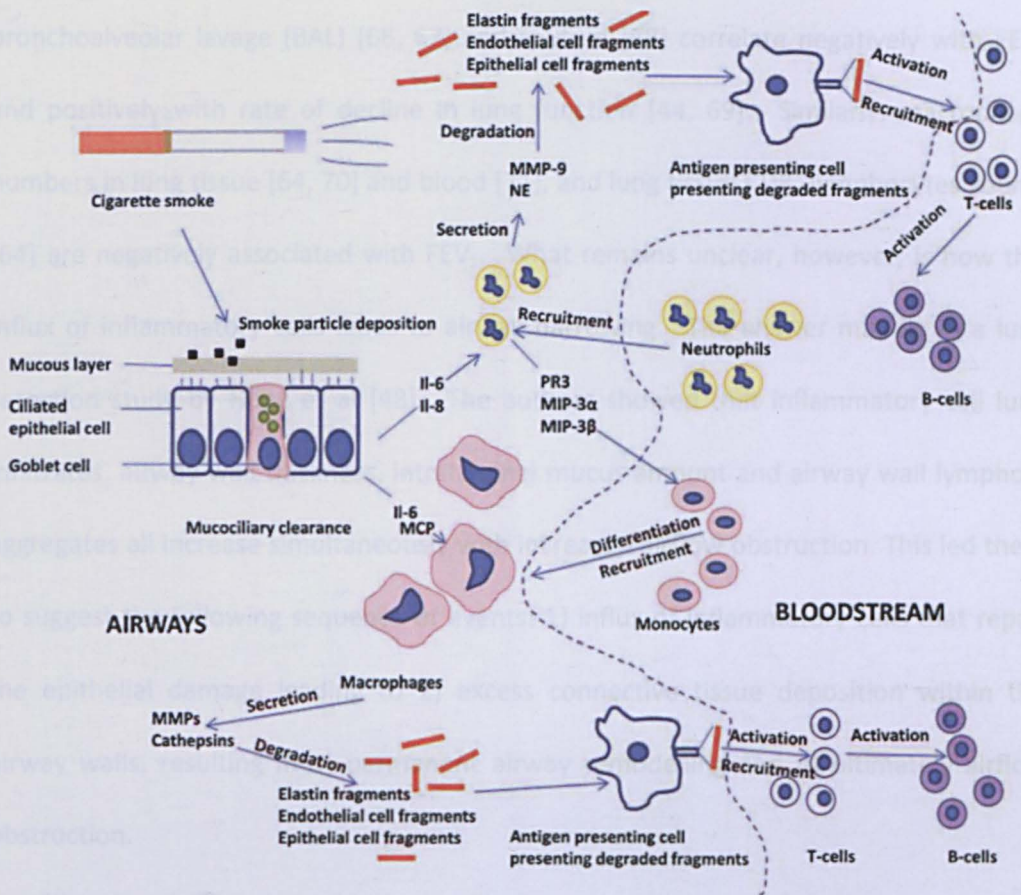


Fig. 1.1 Schematic overview of inflammatory cell involvement in COPD. Cigarette smoke damages epithelial cells, leading to release of cytokines, such as IL-6, 8 and MCP. This triggers the recruitment of neutrophils and monocytes into the airways, the latter differentiating into macrophages. Both neutrophils and macrophages release proteolytic enzymes that degrade cellular and extracellular matrix components in the lung, releasing digested fragments, such as elastin fragments. These are picked up and presented to the T-cell system by antigen presenting cells which in turn activate a B-cell response. Abbreviations: IL, interleukin; MCP, macrophage chemoattractant protein; MIP, macrophage inflammatory protein; MMP matrix metalloproteinase; NE, neutrophil elastase; PR3, proteinase 3.

1.5 Correlation of Cellular Pathogenesis to Airflow Limitation

Cell numbers in both the innate and adaptive immune system are associated with airflow obstruction in COPD. Intraluminal neutrophil counts sampled from bronchoalveolar lavage (BAL) [66, 67] and sputum [68] correlate negatively with FEV₁ and positively with rate of decline in lung function [44, 69]. Similarly, macrophage numbers in lung tissue [64, 70] and blood [71], and lung tissue CD8⁺ lymphocytes counts [64] are negatively associated with FEV₁. What remains unclear, however, is how this influx of inflammatory cells leads to airway narrowing. The answer may lie in a lung resection study by Hogg et al [48]. The authors showed that inflammatory cell lung infiltrates, airway wall thickness, intraluminal mucus amount and airway wall lymphoid aggregates all increase simultaneously with increased airflow obstruction. This led them to suggest the following sequence of events: 1) influx of inflammatory cells that repair the epithelial damage leading to 2) excess connective tissue deposition within the airway walls, resulting in 3) permanent airway remodelling and 4) ultimately airflow obstruction.

1.6 COPD Exacerbations

COPD exacerbations are an acute worsening in patients' daily respiratory symptoms which may or may not lead to medical help being sought [72, 73]. At the more severe end hospitalisation is required. Exacerbations punctuate the natural course of COPD, accelerating lung function decline [74, 75], worsening health status [76] and increasing the risk of mortality [77, 78]. During the time of an exacerbation there is a heightened risk of myocardial injury [42], and further exacerbations suffered cumulatively increase the risk of myocardial infarction [41]. Although patients with more severe COPD are more likely to develop an exacerbation [73], the strongest independent risk factor for an exacerbation is a history of previous exacerbations,

irrespective of COPD stage [79]. This has led to the recognition of a distinct COPD phenotype, the “frequent exacerbator”, a patient experiencing 2 or more exacerbations per year [79]. Given the aforementioned risks associated with exacerbation, the frequent exacerbator is an important subject to focus on both clinically and in clinical trials.

Exacerbations are associated with an increase in airway inflammation [80-83]: levels of neutrophils [80, 82, 84], lymphocytes [80, 83] and eosinophils [81-83] increase to varying levels in patients, as do proteases, such as NE [80, 82] and MMPs [85, 86]. The underlying cause for this heightened inflammatory status is not always evident [87]. Both bacterial [82, 88-91] and viral infections [82, 90, 92] occur with increased frequency at exacerbation, with acquisition of a new bacterial strain recognized as a cause for exacerbation [88]. A drop in environmental temperature has also been reported to increase exacerbation frequency [93]. However, whether this is due to the effect of low temperature alone or the increased incidence of viral infections in the winter is unknown. Other causative factors include atmospheric pollutants, as suggested by epidemiological data [94-97].

Similar to COPD, the nature and origin of exacerbations are heterogeneous. This explains why the current “one size fits all” management with corticosteroid treatment, often with the supplementation of antibiotics, is far from ideal. There is an imperative need to work towards individualized treatment. This requires a better understanding of exacerbation pathophysiology and aetiology for the development of more specific methods of diagnosis and treatment. Given the heightened release of proteases at exacerbation, one strategy should involve a better understanding of the substrate targets of these proteases.

1.7 The Protease-Anti-protease Theory

It is widely accepted, although by no means definite, that in COPD the destruction of ECM components and resulting alveolar damage is due to an excess of protease activity over inhibition by anti-proteases. In support of this theory, intratracheal instillation of human neutrophil proteases induces emphysema in rodents [17, 19, 98]; conversely, NE knockout (KO) mice are significantly protected against cigarette smoke-induced emphysema [99]. Similarly, MMP-12 KO mice are completely emphysema-resistant [100], unlike their wild type counterparts. Furthermore, in humans, the genetic condition A1AT deficiency leads to premature emphysema due to insufficient inhibition of NE [18] by its main anti-protease A1AT [101]. Similarly, in COPD, levels and destructive ability of proteases in the lung are increased [20, 60, 102].

The release of proteases by neutrophils is stimulated by their activation following interaction with endothelial cell surface selectins [103], cytokines, such as tumor necrosis factor (TNF)- α and chemoattractants, such as IL-8 or bacterial lipopolysaccharide (LPS) [104, 105]. These act via Toll-like receptors (TLR), myeloid differentiation primary response 88 (MyD88) adaptor protein and Interleukin-1 Receptor type 1 (IL-1R1) [54]. On activation, the protease-containing granules within the neutrophil cytoplasm fuse to the plasma cell membrane, thereby releasing the contents into the surrounding tissue [104, 105]. Neutrophil secretion of chemoattractants, such as macrophage inflammatory protein (MIP)-3 α (CCL-19), MIP-3 β (CCL-20) [106] and proteinase 3 (PR3) [104] leads to recruitment of monocytes into the lung interstitium. These differentiate into macrophages with the potential to secrete a whole host of proteases, including MMP-1, 2, 9, 12, cathepsins K,L, S [107, 108] and phagocytosed NE of neutrophil origin [109-111]. The precise mechanisms responsible for stimulating macrophages to secrete proteases in COPD are still unclear. However, *in*

vitro data demonstrate significantly increased protease release by macrophages in the presence of interferon (IFN)- γ and LPS and a slight increase induced by IL-4 [112].

The physiological role of proteases is to maintain healthy tissue homeostasis; therefore they demonstrate both pro-inflammatory roles *e.g.* when clearing bacterial infection as well as anti-inflammatory properties necessary to limit proteolytic damage of their surrounding tissues. Expectedly, their roles are extensive and include 1) activating microbicidal proteins [103], 2) processing cytokines [113, 114], chemokines [115-117], growth factors [118], other proteases and anti-proteases [99], 3) activating receptors [119] and 4) inducing apoptosis [105]. In COPD, it appears that the initial protease release in response to tissue damage fails to self-regulate and abate, and while this is often attributed to the imbalance between protease and anti-protease activity, serious evidence for this occurring in human non-A1AT induced COPD is strikingly lacking. It is true that several protease levels are increased in human COPD airways; however, with the exception of a few studies [85, 86, 120-123], often small in number of patients, and with conflicting findings of a protease-anti-protease imbalance, protease levels are often not measured in relation to their physiological inhibitors. Perhaps this imbalance only partially explains the pathogenesis in COPD and other hypotheses, such as different protease substrate profiles between COPD and healthy individuals need to be tested.

1.8 Reactive Oxygen Species

The term “reactive oxygen species” (ROS) refers to any oxygen-containing molecule (radical or non-radical) capable of initiating a harmful reaction to the host [124, 125]. ROS are generated in redox reactions in phagocytic cells during mitochondrial metabolism and processes involving NADPH oxidase (NOX) [125]. Examples of ROS include the superoxide anion O_2^- and hydrogen peroxide H_2O_2 [124, 125]. While ROS may be harmful due to their oxidation of intracellular lipids, proteins and DNA, they are

also involved in bacterial killing within macrophages and neutrophils and therefore beneficial to the host [124, 126]. In the normal functioning cell, there is interplay between the generation and “mopping up” of ROS, i.e. the oxidant-anti-oxidant system, of which superoxide dismutase (SOD), catalase and glutathione (GSH) are the major pulmonary enzymatic anti-oxidant systems [125]. Loss of this oxidant-anti-oxidant balance, termed “oxidative stress,” has been proposed as a mechanism involved in COPD pathogenesis [125].

The role of ROS in COPD is recognized in various studies. Firstly, cigarette smoking has been linked to ROS generation: 1) both the tar and gas components of cigarette smoke are rich sources of ROS-generating oxidants [125]; 2) smoking causes a rise in BAL and alveolar macrophage iron levels which are involved in ROS production [127, 128]; 3) smoking is linked to an increase in exhaled breath oxidant derived products, such as F2-isoprostanes [129]; and 4) monocytes and alveolar macrophages derived from smokers generate more H_2O_2 [125] and O_2^- [130], respectively than those isolated from non-smokers. Secondly, there is evidence for increased ROS production in COPD: 1) exhaled breath ROS levels increase in stable COPD and further still in unstable COPD in comparison to healthy individuals [131]; and 2) BAL xanthine oxidase activity, an enzyme that generates O_2^- and H_2O_2 , is elevated in COPD compared to controls [132].

Linking the oxidant-anti-oxidant imbalance seen in COPD with the protease-anti-protease theory is particularly intriguing and may help discover mechanisms in COPD pathogenesis. One theory is that ROS inactivate anti-proteases in COPD. This has been shown in animal studies where acute exposure to cigarette smoke reduced the inhibitory effect of the anti-protease secretory leukocyte protease inhibitor (SLPI) on trypsin, an effect not seen in the presence of the anti-oxidant N-acetylcysteine [133]. *Ex vivo*, A1AT exposed to smokers' BAL macrophages less readily inhibited elastase than when exposed to non-smokers' macrophages. However, the latter improved in the

presence of antioxidants [134]. Another theory that may explain a potential link between oxidative stress and the protease/ anti-protease imbalance in COPD is the direct activation of proteases from their latent form by ROS. This has been shown by activation of neutrophil collagenase (MMP-8) *in vitro* [135] and gelatinase B (MMP-9), both *in vitro* and *in vivo* [136], in the presence of ROS, such as nitric oxide [135]. Similarly, the oxidant hypochlorous acid activates MMPs [137].

While the above studies provide links between oxidants and excess protease activity in COPD, more work is still needed. Indeed, the link between ROS and MMP-12 has not been explored.

1.9 Inflammatory Cells in COPD-Neutrophils

Neutrophils originate in the bone marrow as pluripotent haematopoietic stem cells that first differentiate into myeloblasts [104]. These develop into promyelocytes, the stage at which granule protein synthesis commences [103]. On full differentiation neutrophils acquire their characteristic polymorphous nucleus and ability to retain neutral dyes [104]. Neutrophils are the host's initial defence against infection whereby they are recruited by chemotactic factors to sites of tissue inflammation to exert their anti-microbial activity by protease release [105, 138] and ROS production [138]. Once released from the bone marrow, neutrophils circulate in the bloodstream for only 6-8 hours, thus placing them among the shortest lived cells [104].

In COPD, neutrophils accumulate in the lumen of large airways [52, 139, 140] and bronchial wall [70, 141, 142], with further airway accumulation at exacerbation [80, 82, 84]. Airway neutrophil levels correlate negatively with airflow obstruction [68] and positively with a faster decline in lung function [69, 140] and greater degree of peripheral airway dysfunction [68, 143]. The number of neutrophils, however, is unlikely to fully explain lung function decline in COPD as other neutrophilic lung diseases, such as cystic fibrosis and bronchiectasis show no such link [109]. Neutrophils in COPD

may perhaps be intrinsically different and more destructive than in other conditions. Indeed, data show that neutrophils have enhanced proteolytic activity [20] and their chemotactic responses are both increased [20] and more erratic [144], leading to more damage in COPD.

One of the most extensively studied neutrophil proteases is NE. While it has long been established that NE digests elastin [17-20], leading to alveolar destruction, newer evidence has shown that its repertoire includes substrates outside the ECM, such as growth factors [118], naturally occurring anti-coagulants [145] and other proteases, such as MMPs [146], some of which, following NE proteolysis, have the potential to be involved in COPD pathogenesis. Hypothetically, given this large range of NE substrates, some of which are involved in normal tissue homeostasis, it may be more beneficial to therapeutically target NE substrates linked with COPD pathology, rather than NE itself. As with MMP-12, this requires more research into NE substrates and their role in COPD.

1.10 Inflammatory Cells in COPD-Macrophages

Alveolar macrophages (AM) are derived from peripheral blood monocytes that mature into resident airway phagocytes [147], via an intermediate stage within the lung interstitium [148] in response to metabolic, immune-mediated and/ or pro-inflammatory stimuli, [147] *e.g.* cigarette smoke. AM express pattern recognition receptors, thereby promoting tissue remodelling and homeostasis [147, 149, 150].

AM are a heterogeneous population that demonstrate plasticity in response to various cytokines and microbial products. In a simplified overview this plasticity or polarization manifests itself as a M1 or M2 phenotype [151-155] (Figure 1.2). M1 macrophages are known as classically activated cells and develop in response to IFN- γ , microbial products, *e.g.* LPS and/ or cytokines, such as granulocyte macrophage-colony stimulating factor (GM-CSF) and TNF- α [152, 153]. Such AM are distinguished by their

release of pro-inflammatory cytokines, including IL-1 β , TNF- α , IL-6, IL-12 and an increased production of ROS [152]. In contrast, exposure to IL-4 and IL-13 leads to alternatively activated M2 macrophages, characterized by expression of the mannose receptor and cluster of differentiation (CD) 163 [151], as well as an anti-inflammatory phenotype with a lower production of IL-12 and increased production of IL-10 compared to M1 [153]. The M2 phenotype is arbitrarily further subdivided into 3 subphenotypes: M2a, b and c [152, 154]. Release of IL-4 and/or IL-13 by T helper (h) 2 cells differentiates AM into a M2a phenotype involved in wound healing, suppression of immune-mediated inflammation and promotion of Th2 cell differentiation [152]. M2b and 2c produce IL-10 and/or TGF- β in response to IL-1R signalling and TGF- β respectively, thus promoting the differentiation of T regulatory cells [152]. In addition to cytokines, corticosteroids may also influence macrophage polarization by promoting differentiation into the M2c subphenotype [152, 155].

Within the setting of COPD pathogenesis AM are particularly important. They accumulate in the respiratory bronchioles in healthy cigarette smokers where emphysema first manifests [107] and their numbers increase further in COPD [108]. Among COPD patients, levels are increased in more severe stages of COPD compared with lower stage disease [156]. Their presence in the submucosa is linked to the degree of airflow obstruction [70] and their presence in the alveolar walls correlates with mild and moderate degrees of emphysema [157]. As previously mentioned, recruitment of macrophages to the airways is thought to occur via the monocyte-selective MCP-1 and the CXC chemokines, such as GRO- α via CXCR2 [58]. Both MCP-1 and GRO- α levels are increased in sputum and BAL in COPD [158]. Within the recruited macrophages the pattern recognition TLR, IL-1R and MyD88 signalling pathways are activated, leading to an up-regulation in the transcription of pro-inflammatory cytokines, such as TNF- α and IL-6 [54], via the transcription factor NF- κ B [159]. In addition, receptor-type protein

tyrosine kinases (RTKs) and their ligands, such as Macrophage-Stimulating Protein (MSP) are also involved in the synthesis of cytokine production and also enable other macrophage functions, such as migration and phagocytosis [160].

Despite the pro-inflammatory nature of COPD, the distinction between M1 and M2 populations in this condition is not clear cut. Studies have unexpectedly shown a down-regulation of M1 associated genes [161, 162] and cytokines [162] in AM from smokers compared to non-smokers [161, 162], and COPD smokers compared to healthy smokers [161], as well as an upregulation of M2 related genes in AM isolated from COPD smokers compared to healthy smokers and in AM isolated from healthy smokers compared to healthy non-smokers [161]. This is in contrast to the findings by Yang *et al.* who showed an increase in pro-inflammatory mediator release by monocytes on exposure to cigarette smoke [163]. Among a COPD GOLD stage II-III cohort of ex-smokers and smokers, the former had a higher percentage of CD163⁺ (a marker for M2 phenotype) BAL AM while no difference in anti-inflammatory or pro-inflammatory mediator levels was noted between the two groups [164]. More recently, Chana *et al.* showed that macrophage phenotypes in COPD are more complex than the currently accepted M1 and M2 populations [165]. The authors were unable to clearly define two disparate sets of AM isolated from COPD lung tissue based on M1 and M2-defining cell surface receptors: >80% of CD14⁺CD16⁻ cells were CD40⁻ (a M1 marker), yet all were also CD163⁺; of the CD14⁺CD16⁺ cells there was an equal distribution of CD163⁺ and CD163⁻ [165]. Instead, a new subpopulation or phenotype of macrophages isolated from the 30-40% Percoll interface was described that was less glucocorticoid sensitive compared to healthy smokers' and non-smokers' macrophages isolated from the same interface [165].

The differences seen in outcomes in the above studies may reflect the use of monocytes compared to differentiated AM, and/or reflect the heterogeneity as well as

the alternating plasticity of monocyte/ macrophage populations and the complex nature of macrophage biology in COPD. These discrepancies highlight the need for further studies on macrophage phenotype and biology in COPD.

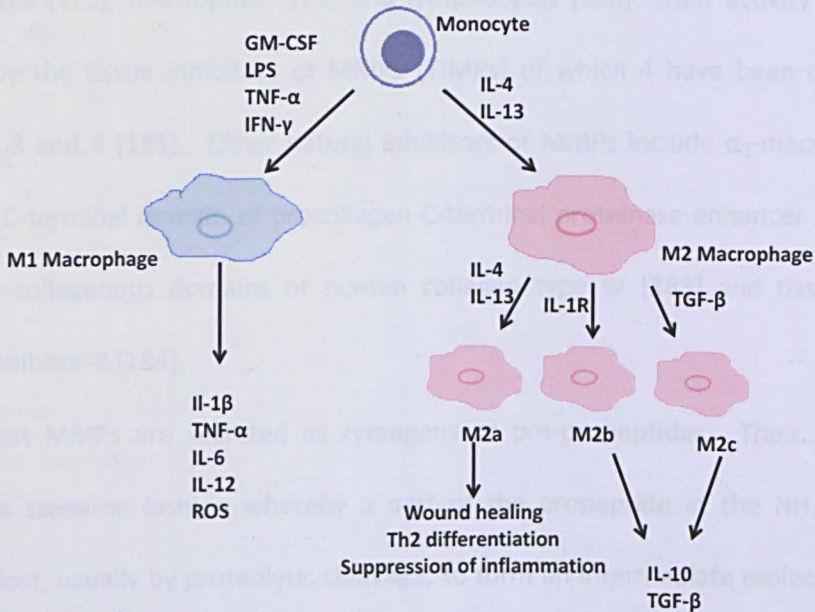


Fig. 1.2 Macrophage differentiation. Monocytes may be classically activated to a pro-inflammatory M1 phenotype whereby they produce cytokines, such as IL-6 and TNF- α and release ROS. In contrast, monocytes stimulated by IL-4 or IL-13 have an anti-inflammatory phenotype, characterised by lower IL-12 and higher IL-10 levels than M1 macrophages. These are known as alternatively activated or M2 macrophages. Abbreviations: GM-CSF, granulocyte macrophage-colony stimulating factor; IL, interleukin; IL-1R, interleukin-1 receptor; LPS, lipopolysaccharide; ROS, reactive oxygen species; TGF, transforming growth factor; TNF, tumour necrosis factor.

1.11 Matrix Metalloproteinases-an Overview

MMPs were first discovered in tadpole tails as enzymes possessing collagenolytic activity [166]. There are now 26 MMPs described [167] of which 23 have been found in humans [168]. MMPs belong to a large family of calcium-containing, zinc-dependent endopeptidases capable of degrading ECM components, including elastin,

glycoproteins, proteoglycans and collagen [167]. They play important roles in tissue repair and remodelling, *e.g.* after myocardial infarction [169], and in the progression of diseases, such as atherosclerosis [170, 171], arthritis, cancer, chronic tissue ulcers and COPD [172, 173]. They are regulated by hormones [174], growth factors [175] and cytokines [174] and are secreted by a variety of connective tissue, pro-inflammatory and structural cells, including fibroblasts [176], osteoclasts [177], endothelial cells [178], macrophages [173], neutrophils [179] and lymphocytes [180]. Their activity is mainly inhibited by the tissue inhibitors of MMPs (TIMPs) of which 4 have been described: TIMP-1, 2, 3 and 4 [181]. Other natural inhibitors of MMPs include α_2 -macroglobulin [181], the C-terminal domain of procollagen C-terminal proteinase enhancer (CT-PCPE) [182], non-collagenous domains of human collagen type IV [183] and tissue factor pathway inhibitor-2 [184].

Most MMPs are secreted as zymogens or pre-propeptides. Their activation occurs in a stepwise fashion whereby a part of the propeptide at the NH₂-terminal domain is lost, usually by proteolytic cleavage, to form an intermediate molecule which is then catalysed, occasionally by autocatalysis, to release the active form [167, 168, 185]. Activation of MMPs can be replicated *in vitro* by the use of mercury containing compounds, such as 4-aminophenylmercuric acetate (APMA) [168, 186]. Extracellular release usually occurs immediately after synthesis, with the exception of MMP-8 and MMP-9 which are stored intracellularly within neutrophil granules and released during inflammatory conditions [187]. MMPs are classified according to their domain arrangements and substrate specificities. A list of the MMPs in humans is provided in the table below (Table 1.2).

Table 1.2 Classification of human MMPs. Abbreviations: GPI, glycosylphosphatidylinositol. Adapted from Nagase *et al.* [168] and Verma *et al.* [167].

Enzyme Type	MMP
Collagenases	
Interstitial collagenase; Collagenase 1	MMP-1
Neutrophil collagenase; Collagenase 2	MMP-2
Collagenase 3	MMP-13
Gelatinases	
Gelatinase A	MMP-2
Gelatinase B	MMP-9
Stromelysins	
Stromelysin 1	MMP-3
Stromelysin 2	MMP-10
Matrilysins	
Matrilysin 1	MMP-7
Matrilysin 2	MMP-26
Stromelysin 3	MMP-11
Membrane-type (MT) MMPs	
a) <i>Transmembrane type</i>	
MT-1 MMP	MMP-14
MT-2 MMP	MMP-15
MT-3 MMP	MMP-16
MT-5 MMP	MMP-24
b) <i>GPI-anchored</i>	
MT4-MMP	MMP-17
MT6-MMP	MMP-25

Table 1.2 Classification of *human* MMPs; Abbreviations: GPI, glycosylphosphatidylinositol. Adapted from Nagase *et al.* [168] and Verma *et al.* [167].

Others	
Macrophage elastase	MMP-12
Rheumatoid Arthritis Synovial Inflammation (RASI)-1	MMP-19
Enamelysin	MMP-20
MMP identified on chromosome 1	MMP-21
MMP identified on chromosome 1	MMP-12
From Human Ovary cDNA	MMP-23
Epilysin	MMP-28

1.12 Matrix Metalloproteinase-General Structure and Function

In general, MMPs consist of a propeptide or pro-domain made up of about 80 amino acids (aa), a catalytic domain (≈ 170 aa) and a haemopexin domain (≈ 200 aa). The haemopexin domain is joined to the catalytic domain by a linker peptide of variable length also known as the hinge region (Figure 1.3) [167, 168, 185]. Variations in structure complexity and consistency exist between the MMP classes, often relating to their substrate specificity and differing functions [167, 168, 188-190]. The following section describes the commonest features in the MMP structure and how these relate to enzyme function.

The propeptide domain maintains latency of the MMP molecule by binding of its cysteine “switch” motif to the zinc ion in the catalytic domain [168]. The catalytic domain contains two zinc ions, one catalytic, the other structural, and up to 3 calcium ions that stabilize the structure [188]. The zinc binding motif in the catalytic domain consists of an amino acid sequence [191] which is necessary for substrate cleavage [168]. Once the MMP is activated substrate binding starts at the side closer to the N-terminus of the enzyme, with the substrate anchoring in its hydrophobic S'1 (specificity) pocket [190]. The depth of S'1 determines MMP substrate specificity, a property which has

been explored in the development of specific MMP inhibitors [167, 188, 189, 192]. On substrate binding, a water molecule is displaced from the zinc ion, and one of its protons is taken up by the glutamate carboxyl group of the catalytic domain, permitting peptide bond hydrolysis by a nucleophilic attack on the carbonyl carbon of the peptide bond by the polarized water [167]. The haemopexin domain is present at the C-terminal end of

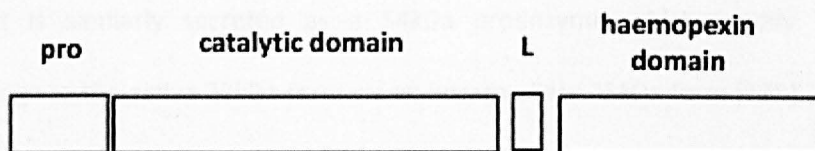


Fig. 1.3 Schematic representation of the general structure of MMPs. Certain domains vary between classes of MMPs. However, with the exception of matrilysins, which lack a haemopexin domain and linker region, all MMPs consist of a pro-, catalytic and haemopexin domain. Abbreviations: L, linker or hinge region; pro, pro-domain.

MMPs [193]. Unlike the propeptide and catalytic domain, the haemopexin domain may be absent in certain MMPs, such as the matrilysins (MMP-7 and 26) [192]. While the structure is conserved in the domains around the catalytic site variation occurs between the haemopexin domains of different MMPs [193], a feature which may be important to target in the development of specific MMP inhibiting drugs. The haemopexin domain serves a number of functions depending on the MMP. These include inhibitor and substrate binding, MMP activation, cell surface attachment, endocytosis and MMP degradation, and the formation of MMP multimers which may be essential for substrate cleavage by certain MMPs, *e.g.* MT-1 MMP cleavage of collagen type I fibres [185]. In contrast, the activity of MMP-12, such as elastin degradation appears to be unaffected by loss of the haemopexin domain [194].

1.13 Macrophage Metalloelastase/ Matrix Metalloproteinase-12

Macrophage metalloelastase, or simply macrophage elastase (MME) was first isolated in 1975 from thioglycollate-stimulated murine peritoneal macrophages [195].

Similar to other mammalian elastases it was found to degrade elastin, yet possessed a narrower substrate range and a wider resistance to elastase inhibitors [195]. Subsequent analysis identified it as a 22kDa metalloproteinase [196], derived from a 53kDa proform [197]. The human counterpart (MMP-12), first isolated from alveolar macrophages, is a distinct MMP that shares 74% of its amino acid sequence with MME [198]. It is similarly secreted as a 54kDa proenzyme which readily undergoes autocleavage to the active 22kDa form via an intermediate 45kDa form [198].

Structurally, MMP-12 shares its common domains with other MMPs, most closely resembling MMP-1 and 3 [199]. In common with MMP-8 and 13 [168], MMP-12 possesses a particularly deep S1' loop [199]. Its expression and secretion is upregulated by pro-inflammatory mediators, such as IL-1 β and TNF- α via extracellular signal-regulated kinase (ERK), c-Jun kinase (JNK), phosphatidylinositol-3 kinase (PI3K) and activator protein-1 activity pathways [200]. Similar to other MMPs, the activity of MMP-12 is thought to be inhibited by TIMPs [201], although as it is part of the intricate protease web, regulation of its activity is likely to be a lot more complex with involvement of other proteases, substrates, co-factors and receptors [202].

1.14 Importance of Matrix Metalloproteinase-12 in COPD

Since the development of the MME knockout (MME^{-/-}) mouse, MMP-12 has gained increasing recognition as a protease central to COPD pathogenesis. MME^{-/-} mice are bred from embryonic stem cells lacking most of exon 2 in the MME genome [100, 146, 203]. Their macrophages show < 5% of the elastinolytic capacity of wild type (MME^{+/+}) macrophages, thus reducing their ability to digest elastin in the pulmonary ECM [203]. This protects MME^{-/-} mice from cigarette smoke-induced emphysema [100]. In addition to the decrease in elastin degrading capacity of lung macrophages, MME^{-/-}

mice have lower levels of macrophages in their lungs; the lack of MME leads to a reduction in BAL elastin fibres which are chemoattractant to monocytes [146, 204-206]. Since MME also contributes to emphysema development indirectly by cleaving and inactivating the NE inhibitor A1AT, MME^{-/-} mice may also be protected from emphysema by increased NE inhibition through A1AT activity [99].

The involvement of MME in emphysema in mice provides a limited view of the role of MMP-12 in human COPD. In the first instance, murine lungs differ from humans' in their absence of respiratory bronchioles and mucous glands in the larger airways [207], so while mice develop emphysema without a chronic bronchitis component, the opposite is true in human COPD. Furthermore, MME and MMP-12 target different aa sequences within similar substrates which may lead to opposite effects on downstream signalling pathways. For instance, cleavage of CXCL-5 by MME and MMP-12 results in opposite effects on neutrophil recruitment [115]. In terms of COPD development, mice only develop emphysema in response to continued cigarette smoke exposure; once exposure ceases emphysema resolves [208]. Additionally, exacerbations and small airways inflammation, key features of human COPD which require further research, do not occur in mice [208]. Therefore, understanding the role of MMP-12 in human COPD through mouse studies requires validation in human studies and interpretation with caution.

Studies on the role of MMP-12 in human COPD are disappointingly few, conflicting in their outcomes and occasionally small in number of participants. Among the genome-wide association studies (GWAS) Haq *et al.* described an increased frequency of two *MMP-12* SNPs, 14 and 18, rs652438 and rs2276109 respectively in Caucasian patients with GOLD stages III and IV COPD [209]. In a separate study, SNP 14 was linked to a decline in lung function when considered as a haplotype with the *MMP-1* promoter SNP 13 rs1799750 in a largely (95%) Caucasian group [210]. In contrast, no

association between SNP 18 and COPD was reported in this study [210] possibly reflecting a different population phenotype. In a GWAS on 1643 Caucasian COPD and healthy smoking control subjects no link was described between *MMP-12* SNPs 14 and 18 and COPD [30]. Similarly, a study on 111 COPD patients in Brazil found no association between SNP 18 and COPD [31], although numbers were small and the range of severity of COPD in the population was not clearly defined. More recently, in the COPDGene study carried out on 10,192 smokers with varying lung function, another SNP on the *MMP-12* gene, rs17368582, was associated with an increased risk of a moderate centrilobular emphysema as measured on CT scan [32].

SNP14 is present in the haemopexin encoding region of the gene and results from an arginine to serine mutation. It has been linked to increased *MMP-12* proteolytic activity, increased sputum macrophage numbers and greater emphysema severity in COPD [211]. SNP 18 increases activator protein-1 binding and *MMP-12* expression [212]. Despite conflicting outcomes there still is evidence in some of the above studies that suggests a link between *MMP-12* SNP expression and airflow obstruction and emphysema. These *MMP-12* SNPs have been associated with increased protease activity, making them likely candidates in COPD pathogenesis. Further research into the role of *MMP-12* in COPD is therefore warranted.

Similar to genetic studies, the literature is quite sparse on *MMP-12* protein levels and function within COPD airways. Patients with COPD have higher levels of *MMP-12* positive BAL macrophages [213, 214], *MMP-12* positive sputum macrophages [213] and higher levels of *MMP-12* within BAL supernatant [214] than healthy controls [213, 214], former smokers [213] and smokers without lung disease [213]. Similarly, *MMP-12* levels in COPD sputum supernatant were increased compared to sputum from healthy smokers, non-smokers and never smokers in one study [215] and increased in COPD patients compared to healthy non-smokers in another cohort [122]. In a separate

study no difference in sputum MMP-12 levels or activity was noted between COPD patients, asthmatics or healthy volunteers [216]. Smoking also has an effect on MMP-12 levels, increasing the number of MMP-12 positive macrophages in sputum and BAL [213], although in one study sputum supernatant MMP-12 levels were reported to be similar between smoking and non-smoking COPD subjects [122]. In this study sputum MMP-12 activity was higher in COPD ex-smokers than COPD current smokers as was the MMP-12 concentration/TIMP-1 level ratio and the MMP-12 activity/TIMP-1 and MMP-12 activity/TIMP-2 ratios [122], suggesting that smoking may also affect MMP-12 activity.

While some studies report higher airway MMP-12 levels in COPD compared to subjects without airflow obstruction [122, 213-215], no significant direct correlation between MMP-12 airway levels and degree of airflow obstruction has been described. A direct relationship, however, has been described between MMP-12 and emphysema measurements. Both sputum MMP-12 concentration and MMP-12 activity have been directly associated with extent of emphysema (measured in percentage of low-attenuation areas on CT at < -950 Hounsfield units) in asthma and COPD subjects ($r = 0.377$; 95% CI, 0.126 to 0.591 and $r = 0.442$; 95% CI, 0.198 to 0.639, respectively) [122]. Similarly, alveolar macrophage MMP-12 mRNA levels have been linked to emphysema extent, measured by the percent predicted transfer factor corrected for alveolar volume ($DLCO/V_A$) in COPD patients GOLD staged 0-4 ($r^2=0.2112$, $p=0.0004$) [217]. These studies therefore suggest involvement of MMP-12 in emphysema, but also reveal the need for further studies to better understand how it is involved.

1.15 Methods of Identifying MMP-12 substrates

While originally identified as an elastolytic protease, studies [218, 219] have shown MMP-12 to degrade a host of other substrates both within and outside the ECM

(summarised in Table 1.3). Most of these MMP-12-substrate cleavage reactions have

Table 1.3 Summary of identified MMP-12 substrates

Author/Year	Experiment	MMP-12 substrate
Da Silva <i>et al.</i> [220], 2010	Mouse models (<i>in vivo</i>); <i>in vitro</i>	Osteopontin
Dean <i>et al.</i> [115], 2008	<i>In vitro</i> cleavage analysis; <i>In vitro</i> chemotaxis; Transalveolar <i>in vivo</i> chemotaxis	Human MMP-12 CXCL1, 2, 3, 5, 8; CCL2,7,8,13 Murine MME CXCL1, 2, 3
Churg <i>et al.</i> [113] 2003	<i>In vivo</i> smoke exposed WT/KO mice Murine AM (<i>in vitro</i>)	Pro-TNF α
Koolwijk <i>et al.</i> [119], 2001	Cell culture	u-PAR
Belaouaj <i>et al.</i> [221], 2000	<i>In vitro</i> , <i>in vivo</i>	Tissue factor pathway inhibitor
Gronski <i>et al.</i> [219], 1997	<i>In vitro</i>	Fibronectin, laminin, entactin, chondroitin sulphate, heparin sulphate, α_1 antitrypsin, type 4 collagen
Dong <i>et al.</i> [222], 1997	<i>In vivo</i> , Cell culture	Plasminogen
Chandler <i>et al.</i> [218], 1996	<i>In vitro</i>	GST-TNF Myelin basic protein Fibronectin Laminin Vitronectin Elastin Type 4 collagen
Banda <i>et al.</i> [223], 1988	Cell culture	Alpha-1 anti-trypsin

only been characterised *in vitro* and there may be other potentially important ones which remain undiscovered. Identifying new MMP-12 substrates will increase knowledge of MMP-12 biology, help identify signalling pathways in disease pathogenesis, and enable the development of new drugs targeting mediators downstream from the enzyme. This latter point is particularly important in light of the disappointing MMP inhibitor clinical trial outcomes which showed no improvement or indeed poorer

survival, albeit in cancer patients on MMP inhibitors, such as marimastat, prinomastat and tanomastat compared to standard treatment or placebo [224]. Targeting a specific protease substrate rather than the protease itself is likely to yield a drug with a more favourable side effect profile.

One of the simplest ways of identifying new protease substrates is to incubate the recombinant protease with a suspected recombinant substrate *in vitro* and then determine the presence of cleaved products using a protein separation technique, such as protein electrophoresis (PAGE) followed by Western blot. The characteristic pattern obtained on Western blot can then be used to identify similarly cleaved products in biological samples. A limitation of this method is the presence of bias as it is hypothesis driven and dependent on selecting suspected substrates beforehand based on the scientific literature. In addition, it is limited when applied to biological samples due to the simultaneous targeting of a particular substrate by different proteases *in vivo* which may all produce fragments too similar in weight to be distinguished by electrophoresis. The additional use of other techniques such as amino acid sequencing and mass spectrometry (MS) allows more accurate determination of the cleaved fragments, and hence the responsible protease/s *in vivo* [225].

More recent advances in the field of proteomics address the problem of using a biased approach as they allow the large scale identification of a particular protease substrate profile using specific knockout (KO) mouse samples [226, 227]. TAILS (Terminal Amine Isotopic Labelling of Substrates) has been developed to identify protease-generated neo-N-termini on an organism-wide scale [228-230]. It can therefore be utilized to distinguish peptide differences between wild type (WT) and KO mice samples, *e.g.* MMP-12. The process involves differential labelling of whole proteins in KO and WT samples with an isobaric tag known as iTRAQ (isobaric tag for relative and absolute quantitation). This allows labelling and blocking of all primary amines including

the NH₂- termini and lysine side chains. After labelling, the samples are pooled and trypsinized. Since the lysine residues have been labelled with an isobaric tag, trypsin digestion is limited to arginine, resulting in longer cleaved peptides for improved identification by mass spectrometry. Next, samples are added to a polyaldehyde dendritic polymer which negatively selects the trypsin generated free NH₂-termini. NH₂-amines present in the original samples have been labelled and therefore do not bind to the polymer. Similarly, naturally acetylated or cyclized NH₂-amines remain unselected. Following ultrafiltration the labelled substrates are separated from the polymer and its bound peptides and identified by tandem mass spectrometry (MS²). WT: KO peptide ratios equal to 1.0 represent substrates present in equal amounts in both WT and KO samples, and therefore unlikely to be targeted by the protease absent in the KO mouse. Ratios greater or less than 1.0 represent the gain or loss, respectively, of a peptide due to the protease absent in the KO sample. A schematic representation of TAILS is shown in figure 1.4

1.16 Osteopontin, a MMP-12 substrate *in vitro*

Osteopontin (OPN), also known as Ets-1 (early T-cell activation 1) and *osp-1*

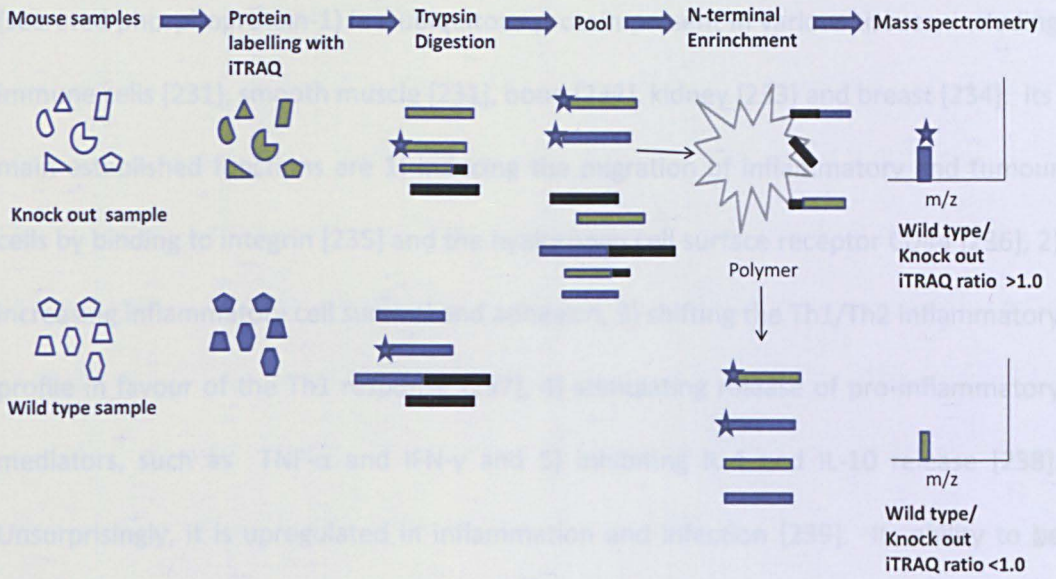


Fig. 1.4 TAILS procedure: KO and WT whole proteins are differentially labelled with isobaric tags, trypsin digested and pooled. Samples are added to a polyaldehyde polymer which binds the neo-NH₂ termini generated by trypsin cleavage. Peptides present in the original samples remain unbound and are separated from the polymer by ultrafiltration. Peptides are then identified by MS2. WT: KO peptide ratios equal to 1 represent substrates present in equal amounts in both WT and KO samples. Ratios greater or less than 1.0 represent the gain or loss of a peptide due to the protease absent in the KO sample. Abbreviations: KO, knock out; MS2, tandem mass spectrometry; WT, wild type; black rectangles represent neo-NH₂ termini; stars represent acetylation of NH₂-terminal peptides in the original proteins. Adapted from Prudova *A et al.* [230]

1.16 Osteopontin, a MMP-12 substrate *in vitro*

Osteopontin (OPN), also known as Eta-1 (early T-cell activation-1) and spp-1 (secreted phosphoprotein-1) is a ubiquitous protein present in various tissues, including immune cells [231], smooth muscle [231], bone [232], kidney [233] and breast [234]. Its main established functions are 1) inducing the migration of inflammatory and tumour cells by binding to integrin [235] and the hyaluronan cell surface receptor CD44 [236], 2) increasing inflammatory cell survival and adhesion, 3) shifting the Th1/Th2 inflammatory profile in favour of the Th1 response [237], 4) stimulating release of pro-inflammatory mediators, such as TNF- α and IFN- γ and 5) inhibiting IL-4 and IL-10 release [238]. Unsurprisingly, it is upregulated in inflammation and infection [239]. Its ability to be cleaved by MMP-12 [177, 220], its presence in obstructive airways disease [231] and its association with emphysema in mouse models [240] makes it a relevant MMP-12 substrate to study in the context of COPD. However, while known to be degraded by MMP-12 *in vitro*, such cleavage has not yet been described *in vivo* in human COPD.

Structurally, OPN consists of a central integrin binding sequence, arginine-glycine-aspartic acid (RGD), the neighbouring thrombin cleavage site SVVYGLR and several phosphorylated and glycosylated sites which are well-conserved between species [238]. Also conserved are the 2 glutamine residues GLN-34 and GLN-36 via which transglutamination occurs [238], allowing the molecule to form crosslinks with itself, known as polymer formation, and other molecules [241], such as fibronectin, necessary for ECM formation in tissues, such as bone [232, 242]. Of note, OPN polymers have been linked to diseases, such as atherosclerosis [243] and osteoarthritis [244], and with inflammatory processes, such as increased neutrophil recruitment in mice models [245] and increased sputum alveolar macrophage numbers in healthy and asthmatic subjects [246].

The cleavage of OPN is of particular biological importance. OPN is cleaved by a various proteases, such as MMPs and the serine protease, thrombin, whose cleavage of the molecule is most documented. Thrombin potentiates the function of OPN by revealing the main $\alpha\beta$ integrin binding site RGD, resulting in increased cell migration [235] and adhesion [247]. Thrombin cleavage of human OPN occurs just C-terminal to the RGD integrin binding site Arg¹⁶⁹–Ser¹⁷⁰ [248]. Cleavage by MMP- 3 and 7 occurs at different sites to thrombin and includes the GL site immediately preceding the thrombin cleavage site [249]. *In vitro* data [177] have revealed MMP-12 isolated from rabbit osteoclasts to cleave bovine OPN between Gly¹⁵⁹ and Leu¹⁶⁰ motifs. While this had no effect of mobilization of osteoclasts, a separate study [220] investigating the stimulation of human T-cells by MMP-12-cleaved OPN fragments demonstrated an association between OPN cleavage and increased release of the pro-inflammatory cytokine IL-17. Table 1.4 below summarises some of the studies on OPN cleavage and the associated functional consequences on immune, tumour and other cells.

The above studies show that, in general, cleavage of OPN renders the protein more active in terms of inducing cell adhesion and migration. However, most of this work has been done using thrombin as a protease. Further studies on the functional effect of OPN cleavage by MMP-12 in COPD are needed. Given the pro-inflammatory role of OPN, its link to emphysema in mice models, and its susceptibility to cleavage by MMP-12 *in vitro*, OPN is an important MMP-12 substrate to study in COPD.

Table 1.4 Summary of studies on OPN cleavage

Author, Journal, Year	Protease for OPN cleavage	Main Tissue/ Cell type studied	Main findings
Senger, D. <i>et al.</i> , Molecular Biology of the Cell, 1994 [250]	Human Thrombin	Human fibrosarcoma, human bladder carcinoma, human intestinal smooth muscle and human foetal lung fibroblast cell lines	Thrombin cleaved OPN increases attachment and spreading of human foetal lung fibroblasts, human bladder carcinoma cells and human fibrosarcoma cells compared to full length OPN; attachment of human foetal lung fibroblasts is blocked by antibodies to GRGDS and $\alpha_v\beta_3$.
Senger, D. <i>et al.</i> , Annals of the New York Academy of Sciences, 1995 [247]	Human Thrombin	Human fibrosarcoma, human bladder carcinoma, human intestinal smooth muscle and human foetal lung fibroblast cell lines	Human foetal lung fibroblasts, human bladder carcinoma cells and human fibrosarcoma cells bind and spread more readily to thrombin cleaved OPN than full length OPN
Smith, L. <i>et al.</i> , Journal of Biological Chemistry, 1996 [248]	Human Thrombin	M21 melanoma cell lines Bovine aortic endothelial cells	Bovine aortic cells attach to the full length/ cleaved OPN in the following descending order: 30N-terminal fragment>10N-terminal fragment>uncleaved OPN>C-terminal fragment. Binding of M21 cells to OPN is dependent on sequence within the 30N-terminal and 10N-terminal fragments which binds to $\alpha_9\beta_1$.
Barry, S. <i>et al.</i> , Experimental Cell Research 2000 [251]	Human Thrombin	Jurkat (J6) cells	N-terminal thrombin cleaved OPN fragment is involved in binding of J6 cells to $\alpha_4\beta_1$

Table 1.4 Summary of studies on OPN cleavage

<p>Agnihotri, R. <i>et al.</i>, Journal of Biological Chemistry, 2001 [249]</p>	<p>Human MMP-3, MMP-7, thrombin</p>	<p>AsPC-1 (Pancreatic adenoma cell line), HeLa (Cervical cancer cell line), primary mouse macrophages</p>	<p>MMP-3/MMP-7 cleaved OPN acts via RGD sequence to increase AsPC-1 adhesion compared to uncleaved OPN. Cleaved OPN increases adhesion of HeLa cells in the following descending order: thrombin cleaved OPN>MMP-7 cleaved OPN>MMP-3 cleaved OPN>uncleaved OPN. Migration of primary mouse macrophages decreases in the following descending order: MMP-3 cleaved OPN>uncleaved OPN.</p>
<p>Weber, G. <i>et al.</i>, Journal of Leukocyte Biology, 2002 [236]</p>	<p>Human Thrombin</p>	<p>MH-S murine macrophage cell line; MT-thymus derived macrophages from BALB/c mouse</p>	<p>Uncleaved murine OPN induces IL-12 and TNF-α secretion in macrophages. N- terminal thrombin cleaved murine OPN fragment increases macrophage secretion of pro-MMP-9 and causes macrophage haptotaxis, though latter effect was no greater than that seen with uncleaved OPN.</p>
<p>Hou, P. <i>et al.</i>, Bone, 2003 [177]</p>	<p>Rabbit MMP-12</p>	<p>Rabbit Osteoclasts</p>	<p>Rabbit MMP-12 cleaved human OPN at G166- L168 to 30kDa and 20kDa fragments identified as LPVKPTSSGSS and LKSRSKFRRS by N- terminal sequencing. MMP-12 did not affect osteoclast recruitment.</p>
<p>Mi, Z. <i>et al.</i>, Cancer Research, 2007 [235]</p>	<p>Thrombin</p>	<p>Murine breast cancer cell lines</p>	<p>C-terminal fragment of thrombin cleaved murine OPN increases the migration and invasion of murine breast cancer cells compared to uncleaved murine OPN</p>

Table 1.4 Summary of studies on OPN cleavage

Grassinger, J. <i>et al.</i> , Blood, 2009 [252]	Human MMP-3, MMP-7, thrombin	Human haemopoietic progenitor and stem cells	N-terminal fragment of thrombin cleaved OPN binds to human blood stem cells via $\alpha_9\beta_1$ and $\alpha_4\beta_1$; MMP-3 and MMP-7 cleaved OPN does not bind to human blood stem cells. Thrombin cleaved OPN increases human haemopoietic progenitor and stem cell chemotaxis compared to uncleaved OPN.
Nishimichi, N. <i>et al.</i> , Journal of Biological Chemistry, 2009 [245]	Human Thrombin	SW480 primary adenocarcinoma colon cells	SW480 cells bind similarly to polymeric and thrombin cleaved OPN and less to uncleaved OPN. Cells bind to cleaved OPN via SVVYGLR sequence.
Da Silva A <i>et al.</i> , The American Journal of Pathology, 2010 [220]	Human MMP-12	Human T-cells	MMP-12 cleavage of OPN <i>in vitro</i> produces 40kDa and 37kDa bands on Western blot probed with anti-OPN; two of the MMP-12 cleaved OPN fragments identified by mass spectrometry, SVVYG and IPVKQ increased IL-17 production by T cells in culture but had no effect on IFN- γ secretion.
Arjormandi, M. <i>et al.</i> , PLOS one 2011 [246]	Human thrombin	Sputum and BAL from healthy and asthmatic volunteers	While polymeric OPN BAL levels are associated with higher concentrations of BAL macrophages, no link between cleaved OPN and macrophage levels was noted in human airways.
Yamaguchi, Y. <i>et al.</i> , Journal of Biological Chemistry, 2013 [253]	Thrombin Plasma Carboxypeptidase2 (CPB2)	Human glioma cells	Glioma cells more adherent to thrombin cleaved OPN and CPB2/thrombin double cleaved OPN than uncleaved OPN

1.17 Tissue Factor Pathway Inhibitor (TFPI), an MMP-12 substrate *in vitro*

TFPI is a glycoprotein present in 2 forms, TFPI-1 and 2. The 40kDa TFPI-1 is the main secreted form and circulates in plasma [254] at concentrations of 2.5-5nM [255]. It is chiefly secreted by endothelial cells [256, 257], platelets [258] and monocytes [259], and is recruited to sites of thrombus formation [145]. TFPI-2 occurs in 3 differentially glycosylated isoforms, 27kDa, 31kDa and 33kDa, and is largely restricted to the extracellular matrix [260]. While both molecules function as a serine proteinase inhibitor, TFPI-1 is the main influence on the tissue factor pathway [261]. TFPI binds to the VIIa/TF complex as well as Xa [262], enabling it to function as the main inhibitor of the tissue factor (extrinsic) coagulation pathway [263].

The anti-thrombotic function of TFPI is limited by its susceptibility to proteolysis. *In vitro* studies reveal the molecule to be cleaved by the serine protease plasmin with a reduction in its ability to inhibit clotting [264]. Similarly, cleavage of TFPI *in vitro* by the serine protease NE leads to a reduction in its anticoagulant activity [145] as does cleavage by MMP-1, 3, 7, 8, 9 and 12 [221], albeit at different sites to those targeted by the serine proteases. Among the MMPs, cleavage of TFPI by MMP-1 and 12 causes the greatest reduction in anticoagulation [221]. Similar to *in vitro* studies, mouse models and *ex vivo* data have shown susceptibility of TFPI to proteolysis with loss of its anticoagulant properties. In mouse models bleeding times were prolonged and fibrin clot formation reduced in Cathepsin G and NE KO mice (Elane^{-/-}; Ctsg^{-/-}) compared to WT controls, an effect reversed by anti-TFPI antibody [145]. *Ex vivo*, urokinase supplemented plasma (which leads to higher levels of plasmin) degraded the molecule with loss of function [264], and human platelets demonstrated a decrease in Xa production (inhibited by TFPI) in the presence of specific NE and Cathepsin G inhibitors, and a similar reduction in Xa production on exposure to mutant strains of TFPI resistant to NE and Cathepsin G cleavage [145]. *In vivo* data reveal co-localization of TFPI and its

upregulation with MMP-12 in human carotid atherosclerotic plaques [221], suggesting cleavage of TFPI by MMP-12 promotes CVD.

The above studies highlight the need for further studies to investigate the role of MMP-12 cleavage of TFPI in promoting thrombotic events in COPD, as these may lead to the known increased risk of CVD. Indeed, the involvement of TFPI in preventing intravascular thrombosis, its loss of inhibitory action after proteolysis [145, 221], its localization to sites of thrombus formation [145], and its co-localization and upregulation with MMP-12 in atherosclerotic plaques [221] make it an important substrate to study in improving our understanding of the increased risk of CVD events in COPD [4].

1.18 Pharmacological Inhibition of MMP-12

Since the disappointing MMP-inhibitor clinical trial outcomes, partly due to their unfavourable side effect profile [224], there has been interest in creating more selective MMP inhibitors with a narrower therapeutic selectivity. This has been met with considerable difficulty due to the sequence similarity in the MMP catalytic domains [265, 266]. In addition, MMPs have roles in several disease processes, *e.g.* MMP-12 is implicated in emphysema development [146, 209, 211] as well as suppression of lung cancer metastasis [267]. Interfering with one pathway in a certain illness may lead to unwanted outcomes in another. Indeed, earlier strategies involving the development of chelating compounds, such as hydroxamate that bind to the MMP zinc atoms, led to indiscriminate targeting of MMPs, resulting in undesirable side effects [268].

Newer compounds that replaced the hydroxamate group for weaker zinc binding groups, such as carboxylate and phosphatidyl groups demonstrated increased selectivity to MMPs, such as MMP-12 [269, 270]. Wu et al developed a series of dibenzofuran sulphonamides, leading to the selection of a compound which showed

good selectivity against MMP-12 over other MMPs with good anti-inflammatory properties in a lung inflammation mouse model [271]. Devel et al developed non-zinc binding, non-phosphinic inhibitors with a longer and bent P1' side chain designed to fit into the lower half of the S1' cavity [272]. The lack of positional constraints from zinc binding and alteration in the P1' side chain allowed the development of an inhibitor with improved selectivity and potency. More work however is needed before translating these findings to human studies. Recently, a multinational 6 week, double blind, placebo controlled, randomized Phase II clinical trial was conducted to study the therapeutic and adverse effects of the MMP-9,-12 inhibitor, AZD1236, on patients with moderate/ severe COPD [22]. AZD1236 promised to be more selective than older inhibitors and indeed the adverse effect profile was similar between the study drug and placebo. However, no differences in inflammatory biomarkers or clinical effects were noted between the placebo and treatment arm. Clearly more work is needed to develop a MMP-12 inhibitor that is both efficient and limited in its side effects. The answer may therefore be to target molecules downstream from MMP-12 itself and focus on some of its substrates for a more favourable side effect profile.

1.19 Conclusion

The literature provides an exciting and potentially important role for MMP-12 and its substrates in COPD. *Mmp-12*^{-/-} mouse models are consistent in showing their inability to develop smoking related emphysema and human studies have shown both the presence and activity of MMP-12 in COPD airways. There is increasing evidence that the substrate profile of MMP-12 extends beyond ECM proteins to include both anti- and pro-inflammatory mediators with potential involvement in COPD pathogenesis. Further work is therefore needed to identify the substrate repertoire of MMP-12 that is involved in COPD. This will lead to the development of more focused therapies aimed

downstream of MMP-12 for better disease outcomes and a more favourable side effect profile.

1.20 Aims

Given the need to further determine the substrate repertoire of MMP-12 in COPD the aims of this thesis were:

1a) to use a candidate approach to determine if OPN is a substrate of MMP-12 in COPD airways;

1b) to determine the association between OPN cleavage and inflammation in COPD airways;

1c) to determine the pro-inflammatory effect of MMP-12-cleaved OPN on monocytes and macrophages;

2a) to use a candidate based approach to determine if TFPI is a substrate of MMP-12 in COPD airways;

2b) to determine the association between TFPI cleavage and inflammation in COPD airways;

2c) to determine the link between cleavage of TFPI in the airways, circulating TFPI levels and CVD risk in COPD;

3a) to use a novel proteomic approach, TAILS, to identify MMP-12 substrates in COPD using a smoking *Mmp-12*^{-/-} mouse model

3b) to determine which MMP-12 substrates identified in the smoking *Mmp-12*^{-/-} mouse model were present in COPD sputum at exacerbation and stable disease.

Chapter 2 Methods

2.0 *In vitro* cleavage assays

All cleavage experiments were carried out at 37°C. Details of individual cleavage assays are described in the relevant methods sections of the results chapters.

2.1 Patients

For the “Investigating Biomarkers in Acute Exacerbations of Chronic Obstructive Disease” study patients with a physician diagnosis of an exacerbation of COPD were recruited at presentation to hospital with an exacerbation (Visit 1). They were followed up 5-7 days later (Visit 2) and 4 weeks later (visit 3/ recovery visit). The study was approved by the National Ethics Research Service (NRES), REC reference 10/H0403/85.

For monocyte and macrophage experiments blood was taken from healthy never smoked volunteers. The study was approved by NRES, REC reference BT17012011.

For the “The Effect of Statins in Patients with COPD” clinical trial (clinical trials identifier NCT01151306) patients with COPD with FEV₁ 30-80% predicted were recruited. None of the patients had a self-reported history of diabetes mellitus or ischaemic heart disease. None had been prescribed statins prior to the start of the trial. Baseline, pre-intervention data were used for this thesis. Ethical (REC 10/H0408/10) and governance (including Medicines and Healthcare Products Regulatory agency) approvals were granted.

In all the above studies patients gave written informed consent before any investigations were carried out. All procedures were carried out in accordance with the Declaration of Helsinki [273].

2.2 Spirometry

Post-bronchodilator spirometry was carried out in the “Investigating Biomarkers in Acute Exacerbations of Chronic Obstructive Disease” study at visit 3 when patients

were stable and the “The Effect of Statins in Patients with COPD” clinical trial. Forced expiratory manoeuvres FEV₁ and forced vital capacity (FVC) were measured in accordance with the ATS/ERS task force recommendations for lung function [274] testing using a desktop spirometer Microlab MK6 spirometer (*Micro Medical Ltd, Rochester, UK*).

2.3 Cardiovascular measurements

These were taken in the “The Effect of Statins in Patients with COPD” trial only. Patients were asked to refrain from inhaling short- and long-acting bronchodilators 4h and 12h, respectively, prior to measuring peripheral blood pressure (*705-IT, Omron, Milton Keynes, UK*). Mean arterial pressure (MAP) was calculated. Aortic Pulse Wave Velocity (PWV) (carotid-femoral) was performed after resting supine for 10 min by the same experienced operator using a Sphygmocor device (*Atcor Medical, West Ryde, Australia*). Arterial PWV is the most accepted method of measuring arterial stiffness whereby the arterial tree is seen as a viscoelastic tube whose elastic properties generate a forward pressure wave along the tree, with arterial branch points and high resistance at the tube end generating retrograde waves. Increased arterial stiffness generates faster forward and retrograde waves. This is known as the propagative model [275-277]. Carotid-femoral PWV measurement is based on the propagative model. It is accepted as the standard method of measuring aortic stiffness which increases with age hypertension and diabetes and has been shown to predict CV risk in epidemiological studies. It is measured by obtaining a variety of waveforms (including distension, pressure or Doppler) transcutaneously at the right common carotid and right femoral arteries. The time delay (t) is the time between the feet of the two waveforms and D is the surface distance between the two recording sites; PWV is thus calculated as $PWV = D / t$ (metres) / t (seconds) [277].

2.4 Thoracic CT scans

CT scans of the thorax were carried out in the “Investigating Biomarkers in Acute Exacerbations of Chronic Obstructive Disease” study, where patients consented four weeks after the end of an exacerbation. Scans were taken with the following parameters: rotation time, 0.5s; slice thickness, 0.625mm; interval, 0.5mm; peak, 120kV. Both lungs were scanned from top to bottom. Subjects were asked to hold their breath at deep inspiration in the supine position during scanning. Scans were interpreted by a NHS consultant radiologist.

2.5 Sputum induction

Sputum was only collected in the “Investigating Biomarkers in Acute Exacerbations of Chronic Obstructive Disease” study. Sputum was expectorated spontaneously at visits 1 and 2 and where possible induced at visit 3 when spontaneous expectoration was not possible, when consent given and patients met the criteria for safe induction. Twenty minutes prior to sputum induction 400µg salbutamol was administered via spacer. Patients were then asked to sequentially inhale 3%, 4% and 5% saline for 5 min via an ultrasonic nebulizer. Spirometry was checked after each inhalation and prior to patient discharge from the unit to ensure that airflow obstruction had not dropped by more than 10% from baseline.

2.6 Sputum processing

Sputum was processed within 2 h of expectoration. Sputum plugs were selected from saliva, added to a volume of PBS 8 ml X the sputum weight in grams and mixed by vortex and a rolling mixer. Next, the mixture was centrifuged at 790xg, at 4°C for 10 min and 4 volumes of the supernatant stored at -80°C for future analysis. Next, freshly made 0.2% DTT was added to the remaining PBS/sputum mixture in a 4:1 ratio to the original sputum weight, the mixture placed on the vortex, then a rolling mixer for 15 min and then filtered through a PBS-pre wet 48µm nylon mesh filter (*Sefar, Bury, UK*). The total

cell count and viability of the sputum filtrate sample was determined by the trypan blue exclusion method using a modified Neubauer haemocytometer. Only samples with a cell viability of >50% and squamous cell contamination <30% were processed further. Next, the sample was centrifuged at 790xg at 4°C for 10 minutes and the resulting supernatant stored at -80°C for future analysis. The remaining cell pellet was resuspended in a volume of PBS adjusted to give a suspension of 0.5×10^6 cells/mL for cytopsin preparation. Cytospins were air dried, fixed with methanol for 15 minutes and stained with Rapi-diff (*Triangle, Skelmersdale, UK*). For cell counts 400 leukocytes were counted; results were expressed as absolute counts/g of sputum as well as a percentage of the total leukocyte count.

2.7 Protein determination assay

The Bio-Rad protein determination assay (*Bio-Rad Laboratories, Hertfordshire, UK*) was used to measure the protein concentration in human sputum supernatant and mouse BALF samples. Bovine serum albumin (BSA) (*Millipore Limited, Co Durham, UK*) was used as the standard. It was serially diluted twofold in PBS, starting from $2,000\mu\text{gml}^{-1}$ to $62.5\mu\text{gml}^{-1}$. Next, 500 μL Bio-Rad protein assay reagent, diluted 1:5 in deionized water, was added to 10 μL of each standard or sample. Next, 200 μL of the reagent/standard or reagent/sample mixture was plated onto a 96-well plate and allowed to incubate at room temperature for 5 min. The optical density of samples was measured against the standards at a 595nm wavelength using a microplate reader (*Flexstation 3, Sunnyvale, CA, USA*). All samples were analysed twice.

2.8 Sputum spiking *ex vivo* experiments

Experiments were designed to determine whether MMP-12 cleaved particular substrates, *i.e.* osteopontin (OPN) and tissue factor pathway inhibitor (TFPI) in sputum. An *ex vivo* model was set up in which COPD PBS sputum supernatant was spiked with

recombinant histidine (HIS)tagged-OPN or TFPI and their cleavage pattern detected by probing with anti-6XHIS antibody by Western blotting.

Undiluted sputum supernatant as well 1:5 and 1:25 diluted sputum deionized water was used for optimization of the experiment. Sputum samples were incubated with 200ng recombinant 6XHIS-tagged OPN or 100ng recombinant 10XHIS-tagged TFPI (both *R+D, Abingdon, UK*) at 37°C for 30min, 1 h, 2 h, 3 h, 4 h, 20 and 52 h. Sputum alone placed in the incubator at 37°C at similar time points was used as a negative control; 44ng active MMP-12 (*Enzo Life Sciences, Exeter, UK*) incubated with 200ng recombinant 6XHIS-tagged OPN or 100ng recombinant 10XHIS-tagged TFPI at 37°C for 30min and 180min, respectively was the positive control. All reaction samples had equal volumes. Following incubation, reaction samples were analysed by SDS-PAGE method and Western blotting using an anti-6X HIS antibody (*Abcam, Cambridge, UK*). Since best results with a minimal noise to signal ratio were achieved with 1:5 diluted sputum, this dilution was used in further spiking experiments. A representative blot is shown in fig. 2.1. To determine the proteinase/s involved in OPN and TFPI cleavage in sputum, the experiments were also carried out in the presence of protease inhibitor. These inhibition assays are detailed in the methods section of the results chapter.

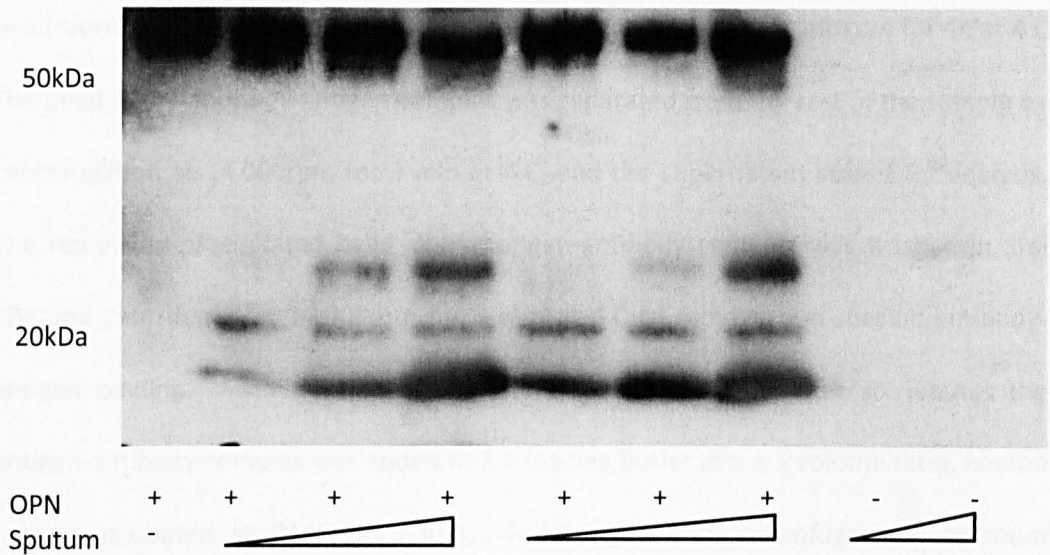



Fig. 2.1 Recombinant 6XHIS tagged-OPN is increasingly cleaved in increasing concentrations of sputum. Representative anti-6XHIS tag Western blot: 200ng recombinant 6XHIS tagged-OPN was spiked in undiluted sputum, 1:5 and 1:25 diluted sputum for 2h and the cleaved fragments identified by Western blot. Unspiked sputum was used as negative control. Abbreviations: OPN, osteopontin;  represents increasing concentration of sputum.

2.9 Immunoprecipitation

Immunoprecipitation was employed to test whether sputum MMP-12 was responsible for cleaving spiked recombinant proteins in *ex vivo* experiments. First, PBS sputum supernatants were pre-cleared to reduce non-specific binding to beads by incubating 30 μ L of sputum supernatant with 12 μ L of non-specific IgG (2 μ gml⁻¹) for 1h on ice. Next, 20 μ L of bead slurry (*Sigma-Aldrich, Dorset, UK*) were added to the mixture and incubated for 30min at 4°C with gentle agitation. The mixture was then spun at 14,000xg at 4°C for 10 min, keeping the supernatant while discarding the bead slurry. Mouse monoclonal anti-human MMP-12 antibody (*R+D, Abingdon, UK*) and rabbit polyclonal anti-human MMP-12 antibody (*AbCam, Cambridge, UK*), both diluted to 2 μ gml⁻¹ in deionized water, were assayed as immunoprecipitating antibodies. In-house animal matched isotype antibodies were used as negative controls. Each 30 μ L sputum supernatant aliquot was incubated overnight with gentle agitation at 4°C with 10 μ L of either of the immunoprecipitating antibody or the matched isotype. The next day, 20 μ L

bead slurry was incubated with each antibody-sputum supernatant mixture for 4h at 4°C. The bead slurry-antibody-antigen complex was separated from the rest of the sample by centrifugation at 14,000rpm for 3 min at 4°C, and the supernatant stored for analysis. The remaining precipitated bead slurry-antigen-antibody complex was washed in 1ml PBS and centrifuged at 14,000rpm for 3 min at 4°C to remove non-specific antibody-antigen binding. Each time the supernatant was discarded. After six washes the antigen-antibody complex was added to 2 X loading buffer in a 1:1 volume ratio, heated to and incubated at 94°C for 5 min. Following a brief microfuge spin at room temperature the supernatant was ready for analysis by SDS-PAGE and Western blotting. Unfortunately, this technique proved unsuccessful at isolating MMP-12 from sputum supernatant. It was therefore abandoned in favour of inhibition assays.

2.10 Sodium Dodecyl Sulphate-Polyacrylamide Gel Electrophoresis (SDS-PAGE)

2.10.1 Sample preparation

First, a stock of 2 X reducing buffer was made by the addition of 3.2ml 1M Tris-HCl (pH 6.8) to 8ml 10% SDS (*Sigma-Aldrich, Dorset, UK*), 4ml 100% glycerol (*Fisher Scientific, Loughborough, UK*), 2ml b-mercaptoethanol blue solution (*Sigma-Aldrich, Dorset, UK*) and 2.8ml deionized water. Next, 15µL of each sample were added to 15µL 2 X reducing gel loading buffer. Each mixture was briefly centrifuged at 13,000rpm at room temperature, then heated to 94°C for 5 min and similarly centrifuged again. The sample/ reducing buffer mixture was then ready for electrophoresis.

2.10.2 Preparation of acrylamide gels

Gels were made using the Bio-Rad Mini-protean III gel electrophoresis apparatus (*Bio-Rad Laboratories, Hertfordshire, UK*). A 10-well comb and 1.5mm spacer plate gel were selected to allow the running of up to 10 x 15µL samples per gel. A 10% percent acrylamide gel was chosen to allow separation of proteins.

Each resolving gel was prepared by the sequential addition of the following to a universal container: 4ml deionised water, 3.3ml 30% acrylamide (*Sigma-Aldrich, Dorset, UK*), 100µL 10% SDS (*Sigma-Aldrich, Dorset, UK*), 2.5ml 1.5M Tris-HCl (pH8.8), 10% ammonium persulphate (*Promega, Southampton, UK*) and 4µL tetramethylethylenediamine (*Sigma-Aldrich, Dorset, UK*). The gel was added to the gap between the glass plates, allowing a depth of 1 cm for the later addition of the stacking gel. A few drops of water-saturated isobutanol (*Fisher Scientific, Loughborough, UK*) were then added to the gel which was allowed to set at room temperature. Next, the isobutanol was washed off and the stacking gel prepared by the sequential addition of the following components to a universal container: 3.4ml deionized water, 830µL 30% acrylamide, 50µL 10% SDS, 630µL 1.0M Tris-HCl (pH 6.8), 50µL 10% ammonium persulphate and 5µL tetramethylethylenediamine. This was added to the resolving gel until the space between the glass plates was filled. The comb was then inserted into the stacking gel and removed once set. For some experiments ready-made 10% polyacrylamide gels were used (*Bio-Rad Laboratories*).

2.10.3 Running SDS-PAGE gels

First, the gel tank was filled with 1x Tris-glycine/SDS running buffer (25mM Tris base, 192mM glycine, 0.1% SDS). Next, the gels were transferred to the gel tank filled with running buffer. The samples were run through the stacking gel at 100V and then through the resolving gel at 200V. The power supply was disconnected just before the samples reached the bottom of the glass plates. Sample weight was checked against a pre-stained molecular weight standard (*Bio-Rad Laboratories*).

2.11 Western blotting

The Bio-Rad protein transfer apparatus (*Bio-Rad Laboratories*) was used for Western blotting. First, stacking gels was cut away from resolving gels and discarded. The resolving gels, filter paper sheets and fibre pads (all *Bio-Rad Laboratories*) were

allowed to equilibrate for a minimum of 15 min in 1 X transfer buffer (25mM Tris base, 192mM glycine). The PVDF membrane (*Millipore Limited, Co Durham, UK*) was cut to size and soaked in 100% methanol (*Fisher Scientific, Loughborough, UK*) for 15 min to activate, followed by 1 X transfer buffer for a further 15 min to equilibrate. The transfer tank was filled with 250ml of refrigerated 1 X transfer buffer and placed on ice. The gel sandwich was assembled and placed into a cassette. The blot was run at 100V, 350mA for 60 min. On completion the PVDF membrane was separated from the rest of the gel sandwich and blocked for 60 min in 5% BSA (*Millipore Limited, Co Durham, UK*) dissolved in 0.1% phosphate-buffered saline (*Oxoid Limited, Hampshire, UK*) –Tween20 (*Sigma-Aldrich, Dorset, UK*) (PBS-T). The blot was then placed in primary antibody diluted in 5% BSA-0.1% PBS-T overnight at 4°C. The next day the blot was washed for 10 min in 0.1% PBS-T, three times, then placed in horseradish peroxidase (HRP)-conjugated secondary antibody for 60 min. After three 10 min washes in 0.1% PBS-T, the blot was ready for enhanced chemiluminescence (ECL) detection. When a HRP-conjugated primary antibody was used, *e.g.* anti-6 X histidine (HIS) antibody, the protocol varied by placing the blot in primary antibody for 60 min and washing three times in 0.1% PBS-T before detection by ECL.

2.12 ECL Method of Protein Detection

After blotting away excess PBS-T, the PVDF membrane was placed in pre-mixed ECL reagents 1 and 2 (*GE Healthcare, Amersham, UK*) for 1 min at room temperature, away from direct light. Next, the membrane was placed in a plastic bag in a developing cassette. Photographic film (*GE Healthcare, Amersham, UK*) was loaded onto the plastic bag in a dark room and the film exposed. The film was then immersed in developing fluid (*Kodak, Sigma-Aldrich, Dorset, UK*), diluted 1:5 in deionized water, until bands became visible. The film was then washed in water and fixed in fixing solution (*Kodak, Sigma-Aldrich, Dorset, UK*), diluted 1:5 for analysis later.

2.13 Stripping Western Blots

Occasionally blots were stripped to allow blot probing with a different antibody. First, Restore Stripping Buffer (*Thermo Scientific, Langensfeld, Germany*) was warmed to 37°C for 30 min. Next, the blot was immersed into the buffer and allowed to incubate for 30 min at 37°C. The blot was then washed in 0.1% PBS-T for 10 minutes, three times, and then blocked for one hour in 5% BSA-0.1%PBS-T at room temperature. The blot was then ready for probing with a different primary antibody.

2.14 Silver Staining Method of Protein Detection

Silver staining allows the detection of proteins in as low an amount as nanogram quantities [278]. Peptide fragments not recognized by primary antibodies specific for the C-or N-terminal end may be detectable by silver stain.

Unless otherwise stated, all reagents used were obtained from Bio-Rad Laboratories. Following electrophoresis, gels were fixed, washed and stained as described below.

2.14.1 Fixative step

Fixative enhancer solution was prepared by the addition of 200ml reagent grade methanol, 40ml reagent grade acetic acid (both *Fisher Scientific, Loughborough, UK*) and 40ml fixative enhancer concentrate to 120ml deionized water. Gels were placed in the fixative enhancer solution for 18 h at 4°C. Different durations were tested for this step starting from 30min. An 18h incubation period was consistently found to yield the clearest protein bands.

2.14.2 Wash step

After decanting the fixative enhancer solution, the gel was gently agitated in 400ml deionized water for 10 min at room temperature. The process was repeated three times. Washes lasting less than 40min in total were noted to lead to an increase in background staining.

2.14.3 Staining step

This required the sequential addition of 35ml deionized water, 5ml silver complex solution, 5ml reduction moderator solution and 5 ml of image development solution to a beaker within 5 min of use. Immediately before staining 50ml development accelerator solution, brought to room temperature, was added to the mixture. The gel was then immersed in the staining solution and agitated on a rocker for 20 min. Once the desired level of staining was reached the staining step was halted.

2.14.4 Stop step

Staining was stopped by placing the gel in 5% acetic acid solution on a rocker for 15 min. Next, the gel was rinsed in deionized water and imaged using the GeneGenius bioimaging system (*Syngene, Cambridge, UK*).

2.15 Enzyme-Linked Immunosorbent Assay (ELISA)

MMP-12 was measured in sputum supernatant by ELISA (*Dendritics, Lyon, France*). This kit identifies both the pro- and catalytic domains of the enzyme. Plates were coated with 120 μ L of capture antibody diluted to 2.5 μ g/ml in 0.1M carbonate/bicarbonate buffer pH 9.55-9.65 and left overnight on a rocker at room temperature. The following day, plates were washed with 0.05% Tween in PBS (PBS-T). Next, 100 μ L of samples or standards, diluted in 1% BSA in PBS-T were added to the plates and incubated at 37°C for 2 h. Next, plates were washed in PBS-T, followed by the addition of 100 μ L HRP-conjugated detection antibody diluted to 3 μ g/ml in 1% BSA in PBS-T. Plates were incubated at 37°C for 1 h. Next, plates were washed 3 times in PBS-T, followed by the addition of 100 μ L of 3, 3', 5, 5'-tetramethylbenzidine HRP supersensitive microwell substrate (*Tebu Bio Laboratories, Peterborough, UK*). The optical density of each well was then read using a microplate reader (*Flexstation 3, Sunnyvale, CA, USA*) set at 620nm. The standard curve was set to a 4 parameter fit; the lower limit of the

assay was <50pg/ml. This investigation was abandoned as MMP-12 levels in sputum were below the lower limit of detection of this assay.

TFPI-1 levels in heparin and EDTA plasma samples were measured using a DuoSet ELISA kit (*R+D, Abingdon, UK*). Further details are provided in the methods section of the relevant results chapter.

2.16 Proteome Profiler Antibody Arrays

The Proteome Profiler Human Protease Array kit was used to determine relative differences in protease expression between sputum supernatant samples. All materials used were obtained from the Proteome profiler human protease array kit, catalogue number ARY021 (*R+D, Abingdon, UK*). Equal volumes of samples to be analysed were thawed. Next, nitrocellulose membranes containing capture antibody spots were blocked in 2ml Array Buffer 6 on a rocker at room temperature for 1 h. Meanwhile, samples were added to 0.5ml of Array Buffer 4 and the final volume adjusted to 1.5ml with Array Buffer 6. Next, 15 μ L of detection antibody cocktail was added to each sample aliquot and allowed to incubate at room temperature for 1 h. Next, Array Buffer 6 was replaced with the sample/ detection antibody mixture; membranes were left to incubate in the mixture overnight at 4°C. The following day, membranes were washed for 10min in 1 X wash buffer at room temperature three times. Next, membranes were incubated in Streptavidin-HRP diluted in Array Buffer 6 for 30min at room temperature. Next, the membranes were washed three times, followed by incubation in a chemiluminescent mixture, Chemi Reagent Mix, for 1 min at room temperature. Next, the membranes were covered in a plastic membrane and exposed to X-ray film within an autoradiography film cassette till signals were visualised as spots. Further details are provided in the methods section of the relevant results chapter.

2.17 Western blotting and Proteome profiler human protease array Data Analysis

Western blot bands and Proteome Profiler Human Protease Array Kit spots were developed on X-ray films and analysed using a transmission-mode scanner and image analysis software (GIMP2.6 1.0). Signal intensities (pixel densities) for each spot/band were measured as grayscale images using the histogram dialog in GIMP where values 0-255 represented a scale of signal intensities ranging from black to white. The pixel density of each signal was measured using the “fuzzy select” tool. This value was then subtracted from the background value measured from a clear area of the array so that a positive value for each signal was obtained. This value was then normalised to the value obtained from the signal obtained from a reference standard. Further details are provided in the methods section of the relevant results chapter.

2.18 Human Monocyte Preparation

Human peripheral blood monocytes (PBMC) were obtained by standard venepuncture of 50ml blood into EDTA tubes from each healthy volunteer. Blood was diluted with an equal volume of Hank's balanced salt solution (*Sigma-Aldrich, Dorset, UK*) and overlain onto an equal volume of Histopaque-1077 (*Sigma-Aldrich*). Next, the blood mixture was centrifuged at 800xg for 30 min and the PBMC ring collected. Next, a positive selection of CD14⁺ cells was performed by incubating the PBMC, resuspended in MACS buffer [2mM EDTA (*Sigma-Aldrich*) and 0.5% foetal bovine serum (*Sigma-Aldrich*) in PBS], with MACS colloidal supermagnetic microbeads conjugated with monoclonal anti-human CD14⁺ antibodies (*Miltenyi Biotec, Bergisch Gladbach, Germany*). Next, the cells were washed in MACS buffer, centrifuged at 350xg for 10 min at 4°C, resuspended in 500µL MACS buffer, and loaded onto a separation column (*MS column, Miltenyi Biotec*) placed in the magnetic field of a MiniMACS separator (*Miltenyi Biotec*). The trapped CD14⁺ cells were then eluted from the column in MACS buffer. They were then

centrifuged at 350xg for 5 min at 4°C and resuspended in the appropriate buffer. Cells were resuspended in buffer A (Section 2.20) for a final cell concentration of 1.1×10^6 cells/ml for reactive oxidative species measurements or in complete RPMI for a final concentration of 0.5×10^6 cells/ml for macrophage differentiation experiments (Section 2.21).

2.19 Reactive Oxidative Species (ROS)

PBMC were isolated as previously described (section 2.19), resuspended in Buffer A [Hank's balanced salt solution with $\text{Ca}^{2+}/\text{Mg}^{2+}$ without phenol red containing 20mM HEPES (all *Gibco, Life Technologies, Paisley, UK*) and 0.1% BSA] at a final concentration of 1.1×10^6 cells/ml, 45 μL of which were plated per well in a 96 well plate. To test the effect of OPN concentration on PBMC ROS production OPN was added in a final concentration of 10 $\mu\text{g}/\text{ml}$, 1 $\mu\text{g}/\text{ml}$ or 0.1 $\mu\text{g}/\text{ml}$ to each well at 37°C and 5% CO_2 for 20 min. PBS was used as negative control to OPN. Next, 100 μL luminol (67 $\mu\text{g}/\text{ml}$) (*Sigma-Aldrich, Dorset, UK*) followed by 50 particles/ cell zymosan (*Life Technologies, Paisley, UK*) was added to half of the OPN and PBS-containing wells (experimental wells) while Buffer A was added to the other half of the OPN and PBS-containing wells as a negative control to zymosan. Next, plates were immediately placed in a luminometer (*FLUOstar OPTIMA, BMG Labtech, Offenburg, Germany*) programmed to take readings every 2 min for 2 h at 37°C. Each condition was carried out at least in duplicate. Similarly, to compare the effect of OPN to MMP-12-cleaved OPN on PBMC ROS production 4 separate conditions were tested: 1) OPN (*R+D*) alone at a final concentration of 10 $\mu\text{g}/\text{ml}$ 2) OPN 10 $\mu\text{g}/\text{ml}$ and 11ng MMP-12 (*Enzo Life Sciences*) in a ratio of 4.5:1 by weight respectively added to the well 3) 11ng MMP-12 alone and 4) PBS as the negative control to OPN and MMP-12. All conditions were allowed to incubate alongside the monocytes at 37°C for 20 minutes before adding to the corresponding wells. As before, luminol followed by zymosan was added to the experimental wells

while luminol followed by Buffer A provided the negative control to zymosan. Plates were read in a luminometer (*FLUOstar OPTIMA*) as before with each condition carried out in duplicate.

2.20 Macrophage Differentiation Protocol

The following experiment was set up to determine the effect of OPN and MMP-12-cleaved OPN on the differentiation of M1 Macrophages. PBMC were isolated from healthy human volunteers as above (Section 2.19), resuspended in complete RPMI [RPMI-1640 (Sigma-Aldrich) containing 10% human AB serum (Sigma-Aldrich), 2mM L-glutamine (Sigma-Aldrich), 100U/ml penicillin (Sigma-Aldrich), 100µg/ml streptomycin (Sigma-Aldrich), and 10mM HEPES] containing 10ng/ml GM-CSF (*Miltenyi Biotec*) and seeded at 0.5×10^6 cells/ml onto each well of a 24 well tissue culture plate (*Costar, Sigma-Aldrich, Dorset, UK*). On day 3 a further 500µL complete RPMI containing 2X GM-CSF 10ng/ml were added per well. On day 7 the medium in each well was replaced with 1.5ml of complete RPMI containing 10ng/ml GM-CSF and 10ng/ml IFN- γ (*R+D*). To determine the effect of OPN or MMP-12-cleaved OPN on macrophage differentiation OPN (*R+D*) was added at a final concentration of 0.5µg/ml per well on its own or together with 0.1µg/ml MMP-12 (*Enzo Life Sciences*). The effect of MMP-12 was determined by the addition of MMP-12 (0.1µg/ml) on its own. Neither OPN nor MMP-12 was added to wells designated negative controls. On day 8 the medium was spiked with 10ng/ml LPS. The next day the supernatant was harvested and stored at -80°C until further analysis while RLT lysis buffer (*RNeasy Mini Kit, Qiagen, Hilden, Germany*) was added to the cells for RNA extraction. All experimental conditions were carried out in triplicate.

2.21 Real-time Polymerase Chain Reaction (qPCR)

Monocyte derived macrophages were lysed in RLT buffer (*RNeasy Mini kit, Qiagen*) and homogenized using a shredder column (*Qiagen*). Homogenates were stored at -80°C until further use. Total RNA was extracted according to the manufacturer's instructions using an *RNeasy Mini kit* and RNA was eluted in $30\mu\text{l}$ RNase free distilled water. The amount of RNA eluted was determined using a *Nanodrop-100* spectrophotometer. Extracted RNA was reverse transcribed using *SuperScript Reverse Transcriptase (Life technologies, Paisley, UK)* and cDNA was amplified using a *Brilliant III Ultra-Fast SYBR Green qPCR Master Mix kit (Agilent Technologies, CA, USA)* according to manufacturer's instructions. Target genes, Mannose Receptor (MR), a marker of macrophage M2 differentiation, and IL-12, a marker of macrophage M1 differentiation, as well as housekeeping gene β -actin transcripts were real-time quantified from cDNA using a *QuantiFast SYBR Green PCR kit and gene specific primer assays (Sigma Aldrich, Dorset, UK)*. Since β -actin was used for normalisation, β -actin PCR was included in each reaction plate. PCRs were all set up in triplicate reactions. Primer sequences were as follows: IL-12 forward: AGAAAGATAGAGTCTTCACGG; IL-12 reverse: AAGATGAGCTATAGTAGCGG; MR forward: AAATTTGAGGGCAGTGAAAG; MR reverse: GGATTTGGAGAAAATCTG; β -actin forward: GACGACATGGAGAAAATCTG; β -actin reverse: ATGATCTGGGTCATCTTCTC.

Chapter 3 The Presence and Cleavage of OPN in COPD Airways

3.0 Background

MMP-12 cleaves OPN *in vitro* four amino acids N-terminal to the well-documented thrombin cleavage site, similarly exposing its RGD sequence [177]. Following thrombin proteolysis, this exposed motif facilitates OPN binding to $\alpha\beta$ integrins on a number of cell types [236, 245, 248, 250, 253], thereby increasing their adhesive [245, 248, 250, 253] and migratory properties [236, 250]. For instance, murine macrophages [236] and human foetal lung fibroblasts [250] bind and spread more readily along thrombin-cleaved OPN than the full length protein. Similar to thrombin, MMP-3 and 7 increase adhesion of OPN to pancreatic adenoma cells via the exposed RGD motif, and murine macrophage chemotaxis to OPN is increased following its cleavage by MMP-3 [249]. Since cellular adhesion and migration are linked to cellular inflammatory roles, the above studies have led to the speculation that the pro-inflammatory effect of OPN is increased following its proteolysis.

Despite both thrombin and MMP-12 having close cleavage sites on the OPN molecule, the functional consequences of MMP-12 proteolysis of OPN are not clear. There are fewer studies on MMP-12 cleavage of OPN, and results from available studies are conflicting in terms of whether MMP-12 potentiates the inflammatory role of OPN. For example, Hou et al documented no difference in rate of rabbit osteoclast migration to full length OPN or MMP-12-cleaved OPN [177]. Goncalves Da Silva *et al.* showed no difference in T cell release of the classical macrophage activator IFN- γ in the presence of MMP-12-cleaved or full length OPN, but noted that MMP-12-cleaved OPN increased T-cell release of the pro-inflammatory mediator IL-17 compared to uncleaved OPN [220]. These studies indicate that MMP-12 cleaved OPN has different inflammatory

consequences on different cell types. Therefore the findings from one cell type cannot be easily applied to another.

Both OPN [240] and MMP-12 [146, 203] have been linked to emphysema in mouse model studies and both are secreted by macrophages [198, 279] which are central to COPD pathogenesis [107, 108, 156, 157]. However, the effect of MMP-12-cleaved OPN on human macrophages in COPD has not yet been explored. In the adenosine deaminase KO mouse (*Ada*^{-/-}), developed as a model of lung injury and emphysema, OPN RNA was upregulated in lung tissue extracts and BALF cell pellets compared with wildtype strains, with OPN being localized to BALF alveolar macrophages on cytopins using immunofluorescence [240]. This suggests involvement of macrophage-secreted OPN in emphysema. Furthermore, at the protein level a 30kDa cleaved OPN fragment was present on western blots of murine BALF, although the protease responsible for cleavage was not deciphered. In support of the above findings, the double KO (*Ada*^{-/-} *OPN*^{-/-}) is significantly protected from emphysema compared with the *Ada*^{-/-} strain, once again suggesting involvement of OPN in emphysema. Knowledge of the involvement of MMP-12 in emphysema is also derived from KO mouse models. Macrophages derived from *MME*^{-/-} mice have <5% of the elastolytic activity of their wildtype [159] counterparts, making *MME*^{-/-} mice completely resistant to cigarette smoke-induced emphysema [203].

In humans MMP-12 and OPN RNA levels are upregulated in airway macrophages from smokers compared to non-smokers [280]. Furthermore, BALF OPN protein levels, measured by ELISA, are increased in smokers compared to non-smokers and inversely related to the degree of airflow obstruction [280]. Sputum OPN levels are also elevated in asthmatics compared to non-asthmatic subjects and smoking asthmatics compared to non-smoking asthmatics [281]. However, whether the OPN measured in these studies

was cleaved or full length is unknown. A 25kDa OPN fragment has been described in BALF in asthmatics, and a 17kDa fragment in asthmatic sputum, the latter noted to be more abundant in asthma compared to healthy subjects [246]. The authors suggested the 25kDa fragment resulted from thrombin proteolysis due to similar sized fragments obtained with *in vitro* cleavage of OPN by thrombin, yet the protease that produced the 17kDa fragment was not determined [246]. Similar studies have not yet been carried out in COPD patients. Therefore, while macrophages, OPN and MMP-12 are all associated with smoking, airway disease and emphysema, it is unknown whether all are linked in human COPD by one common mechanism involving MMP-12 cleavage of OPN.

Given the above evidence it was hypothesized that in COPD OPN may be present in the airways where it may be cleaved by MMP-12, with more cleavage occurring at exacerbation compared to stable disease. MMP-12-cleaved OPN, in turn, may increase the pro-inflammatory function of macrophages and their monocyte precursors. To detect the mechanism of cleavage of OPN in COPD, a novel *ex vivo* model was used whereby sputum was collected from COPD patients at exacerbation and recovery and spiked with recombinant OPN before detecting its cleavage using western blotting. To determine the pro-inflammatory effects of MMP-12-cleaved OPN, monocytes and macrophages were stimulated with full length or MMP-12-cleaved OPN and compared for markers of inflammation, including ROS production by monocytes and the presence of phenotypic markers of classical activation of macrophages.

3.1 Methods

3.1.1 *In vitro* cleavage assays

OPN (*R+D, Abingdon, UK*) was reconstituted at 100µg/ml in deionized water; 200ng OPN were incubated with 44ng active MMP-12 (*Enzo Life Sciences, Exeter, UK*) in

deionised water in a total volume of 12 μ L. The reaction was carried out at 37°C for 30, 60 and 120min. To inhibit MMP-12, 200ng of OPN were incubated with 44ng active MMP-12 at 37°C in a final concentration of 25 μ M Ilomastat (*Sigma Aldrich, Dorset, UK*) or 1mM EDTA and a total volume of 12 μ L. Thrombin (0.05U) and OPN (200ng) were used as positive control, the latter also as standard. Similarly, to test whether OPN was cleaved by NE and uPA, 500ng OPN was incubated with 0.05U NE or 55ng uPA (*all R+D*) at 37°C for 18h, with 500ng OPN as standard.

3.1.2 Patient cohort and study design

Patients with clinically proven COPD were recruited at presentation to hospital with an exacerbation (Visit 1) and were followed up 5-7 days later (Visit 2) and again after 4 weeks (Visit 3/ recovery visit). Sputum was obtained at all visits where possible. The study was approved by NRES, REC reference 10/H0403/85.

For monocyte and macrophage experiments blood was taken from healthy non-smoking volunteers under a different study approved by NRES, REC reference BT17012011. Written informed consent was obtained before all procedures which were carried out in accordance with the Declaration of Helsinki [273].

3.1.3 Spirometry and CT scans

Forced expiratory manoeuvres FEV₁ and FVC were measured in accordance with the ATS/ERS task force recommendations for lung function [274], as previously described (Section 2.2). The CT scan protocol is described in Section 2.4.

3.1.4 Sputum induction

Sputum was induced from COPD patients at 4 weeks if unable to expectorate spontaneously. The procedure is described in Section 2.5.

3.1.5 Sputum processing

Sputum was processed within 2 hours of expectoration as described in Section 2.6. Only samples with a cell viability of >50% and squamous cell contamination <30% were processed further. For cell counts 400 leukocytes were counted; results were expressed as absolute counts/g of sputum as well as a percentage of the total leukocyte count.

3.1.6 Sputum spiking *ex vivo* experiments

Each sputum supernatant sample was diluted 1:5 in PBS and spiked with 200ng recombinant HIS-tagged human OPN (*R+D, Abingdon, UK*). Samples were incubated in a total volume of 11 μ l at 37°C at the following time points: 15 min, 1h, 2h, 4h, 8h, 24h, 48h, 60h and 72h. To compare cleavage of OPN in the airways at exacerbation to cleavage at recovery, sputum obtained from visit 1 (exacerbation sample) was spiked with OPN as above for 120 minutes and compared with similarly OPN-spiked sputum obtained from visit 3 (recovery sample). Visit 2 sputum was used as the exacerbation sample for patients unable to produce sputum at visit 1. For assays involving protease inhibitors, 1:5 diluted sputum samples were pre-incubated with protease inhibitors for 1 hour at 37°C. Next, 200ng recombinant HIS-tagged human OPN was added to the sputum/ inhibitor mix for a further 120 minutes at 37°C. The following inhibitors at the following final concentrations were used: 25 μ M ilomastat (*Sigma Aldrich, Dorset, UK*), 50X-3.125X Serine Protease Inhibitor Cocktail (*Fisher Scientific, Loughborough, UK*), 10 μ M amiloride (*Sigma Aldrich*), 1 μ M sivelestat (*Sigma Aldrich*) and 0.5U-0.0625U hirudin (*Sigma Aldrich*). All procedures were carried out at least twice.

3.1.7 Western blotting

In vitro cleavage reaction products were diluted 1:2 in 2 X loading buffer, run on 10% gels (*Bio-Rad Laboratories, Hertfordshire, UK*) and transferred to PVDF membranes (*Hybond-P, GE Healthcare, Amersham, Buckinghamshire, UK*) which were probed with anti-human OPN rabbit polyclonal antibody (*AbCam, Cambridge, UK*) diluted 1:1000, followed by HRP-conjugated polyclonal goat anti-rabbit secondary antibody (*Sigma Aldrich, Dorset, UK*) diluted 1:10,000. Proteins were visualised by the addition of a chemiluminescent mixture (*GE Healthcare, Amersham, UK*) to the membranes followed by their exposure to autoradiography film (*GE Healthcare, Amersham, UK*). Experiments were carried out at least twice.

Similarly, sputum samples were diluted 1:2 in 2x loading buffer, run on 10% gels and then transferred to PVDF membranes which were probed with anti-human OPN rabbit polyclonal antibody (*R+D, Abingdon, UK*) diluted 1:1000, followed by HRP-conjugated polyclonal goat anti-rabbit secondary antibody. Blots were exposed to autoradiography film as above. Experiments were carried out at least twice.

Ex vivo sputum spiking experiments: following incubation of recombinant human HIS-tagged OPN in sputum, samples were diluted 1:2 in 2x loading buffer, run on 10% gels and then transferred to PVDF membranes which were probed with HRP-conjugated rabbit polyclonal anti-6XHIS antibody (*Abcam, Cambridge, UK*) diluted 1:5000, or anti-human OPN rabbit polyclonal antibody as above. Experiments were carried out at least twice.

3.1.8 Silver stain

Gels were fixed overnight at 4°C in a mixture of 50% methanol, 10% acetic acid, 10% fixative enhancer concentrate (*Bio-Rad, Munich, UK*) and 30% deionised water, by

volume. Next, gels were washed for 10 minutes in deionised water four times, followed by staining using the silver stain plus kit (*Bio-Rad*) as per the manufacturer's instructions. Once the desired level of staining was achieved gels were placed in 5% acetic acid solution. Gels were imaged using the GeneGenius bioimaging system (*Syngene, Cambridge, UK*)

3.1.9 Proteome profiler human protease array

Following sputum spiking experiments, sputum supernatant samples were arbitrarily divided into two groups: 1) samples that cleaved spiked OPN completely to a 20kDa fragment within 4 hours (termed fast OPN cleavers), and 2) samples that took longer than 4 hours (termed slow OPN cleavers). Protease levels in the two groups were compared using the Proteome Profiler Human Protease Array Kit (*R+D, Abingdon, UK*). Undiluted sputum was pooled into the above two groups to a total of 60µL per group and incubated with detection antibody cocktail at room temperature for 1 hour. Next, each sample/antibody mixture was added to a nitrocellulose membrane, coated with protease-specific capture antibodies, and incubated on a rocker overnight at 2-8°C. Next day, membranes were incubated in Streptavidin-HRP (*R+D*), followed by the addition of a chemiluminescent mixture (*R+D*). Protease levels in sputum were then visualised as specific duplicate spots of varying intensity following exposure to autoradiography film. The intensity signal for each protease was measured in pixel density using GIMP version 2.6 1.0 and normalised to the pixel density of a reference spot on the membrane.

3.1.10 Sputum Protein Level Determination

The protein concentration in COPD sputum supernatant was measured using the Bradford assay (*Bio-Rad, Munich, Germany*), as previously described (Section 2.7). The

optical density measured at 595nm wavelength using a microplate reader (*Flexstation 3, Sunnyvale, CA, USA*). The sample protein concentration was back calculated with reference to the standard curve which had an upper limit of detection of $2000\mu\text{gml}^{-1}$ and a lower limit of $62.5\mu\text{gml}^{-1}$. Samples were tested twice.

3.1.11 Human Monocyte Preparation

PBMC were obtained by venepuncture into EDTA tubes from healthy volunteers after giving written informed consent, REC reference BT17012011. Blood was processed for monocyte isolation as described in Section 2.18.

3.1.12 ROS Measurement

This is described in section 2.19.

3.1.13 Macrophage Differentiation Protocol

This is described in Section 2.20

3.1.14 qPCR

This is fully described in Section 2.21. Extracted RNA from monocyte derived macrophages was reverse transcribed using SuperScript Reverse Transcriptase (*Life technologies, Paisley, UK*) and cDNA was amplified using a Brilliant III Ultra-Fast SYBR Green qPCR Master Mix kit (*Agilent Technologies, CA, USA*) according to manufacturer's instructions. Target genes, Mannose Receptor (MR), a marker of macrophage M2 differentiation, and IL-12, a marker of macrophage M1 differentiation, as well as housekeeping gene β -actin transcripts were real-time quantified from cDNA using a QuantiFast SYBR Green PCR kit and gene specific primer assays (*Sigma Aldrich, Dorset, UK*). β -actin PCR was included in each reaction plate. PCRs were all set up in triplicate reactions. Primer sequences were as follows: IL-12 forward:

AGAAAGATAGAGTCTTCACGG; IL-12 reverse: AAGATGAGCTATAGTAGCGG; Mannose Receptor forward: AAATTTGAGGGCAGTGAAAG; Mannose Receptor reverse: GGATTTGGAGAAAATCTG; β -actin forward: GACGACATGGAGAAAATCTG; β -actin reverse: ATGATCTGGGTCATCTTCTC.

3.1.15 Analysis and Statistics

Normality of data was determined using the D'Agostino and Pearson omnibus normality test. Sputum neutrophil and macrophage counts were log 2 transformed to assume a normal distribution before analysis. Normally distributed data were compared using the paired or unpaired t-test as appropriate. All other data apart from optical densitometry assumed a normal distribution. The level of cleaved recombinant OPN after incubation in sputum was expressed as the optical densitometry of the spiked OPN 65kDa monomer normalized to the optical densitometry of the standard recombinant OPN 65kDa monomer on the same Western blot. Optical densitometry was measured in pixel density using GIMP version 2.6 1.0 (www.gimp.org). Differences in OPN cleavage between exacerbation and recovery visits were determined by comparing the optical densitometry of the normalized spiked 65kDa 6X HIS tagged-OPN monomer at each visit using the paired Wilcoxon matched pairs signed rank test. Data were analysed using GraphPad Prism version 6.05 (*GraphPad Software, San Diego, California, USA*). A p value < 0.05 was taken as statistically significant.

3.2 Results

3.2.1 MMP-12 cleaves osteopontin *in vitro*

The recombinant human OPN monomer has a size of 65kDa. After incubation with MMP-12 at 37°C for 30 minutes and 2 hours the 65kDa OPN monomer was completely cleaved to a \approx 20kDa fragment (fig. 3.1). Cleavage was partially inhibited in

the presence of 1mM EDTA (fig. 3.2) and completely inhibited by 25 μ M ilomastat (fig. 3.1). Following incubation of OPN with 0.05U human thrombin a sole OPN fragment in the 20-40kDa range was detected (fig. 3.2).

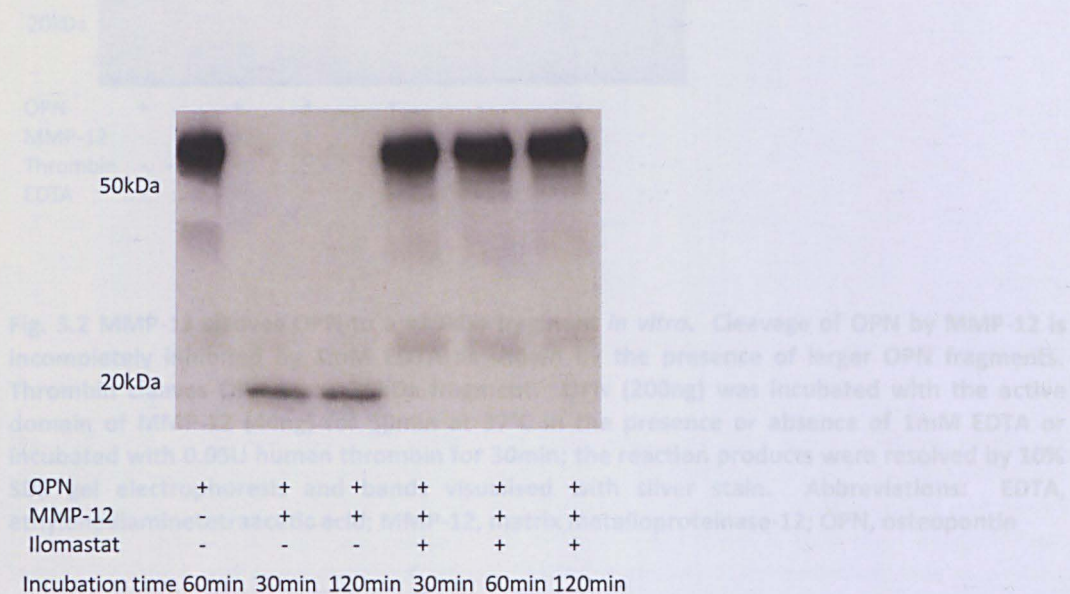


Fig. 3.1 MMP-12 cleaves OPN to a \approx 20kDa fragment *in vitro*. This fragment is not detected in the absence of MMP-12 or in the presence of the metalloprotease inhibitor ilomastat. OPN (200ng) was incubated with the active domain of MMP-12 (44ng) at the above time points at 37°C in the presence or absence of 25 μ M ilomastat. The reactions products were resolved by 10% SDS gel electrophoresis and transferred to a PVDF membrane probed with anti-OPN antibody. Abbreviations: MMP-12, matrix metalloproteinase-12; OPN, osteopontin; PVDF: polyvinylidene fluoride.

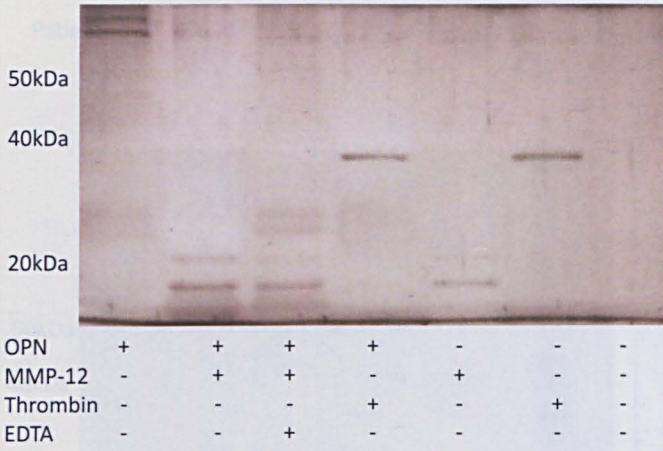


Fig. 3.2 MMP-12 cleaves OPN to a ≈ 20 kDa fragment *in vitro*. Cleavage of OPN by MMP-12 is incompletely inhibited by 1mM EDTA as shown by the presence of larger OPN fragments. Thrombin cleaves OPN to a ≈ 30 kDa fragment. OPN (200ng) was incubated with the active domain of MMP-12 (44ng) for 30min at 37°C in the presence or absence of 1mM EDTA or incubated with 0.05U human thrombin for 30min; the reaction products were resolved by 10% SDS gel electrophoresis and bands visualised with silver stain. Abbreviations: EDTA, ethylenediaminetetraacetic acid; MMP-12, matrix metalloproteinase-12; OPN, osteopontin

3.2.2 OPN is present in human COPD sputum in cleaved and uncleaved forms

Anti-OPN Western blot analysis of COPD sputum at exacerbation (n=8) and recovery (n=8) revealed the presence of OPN in polymeric and 65kDa monomeric forms. In addition, 4 main OPN fragments were noted at ≈ 40 kDa, ≈ 30 kDa, ≈ 25 and ≈ 20 kDa. Not all forms of OPN were present in all patients (fig 3.3). No differences in cleaved OPN fragments were noted between samples taken at exacerbation and recovery.

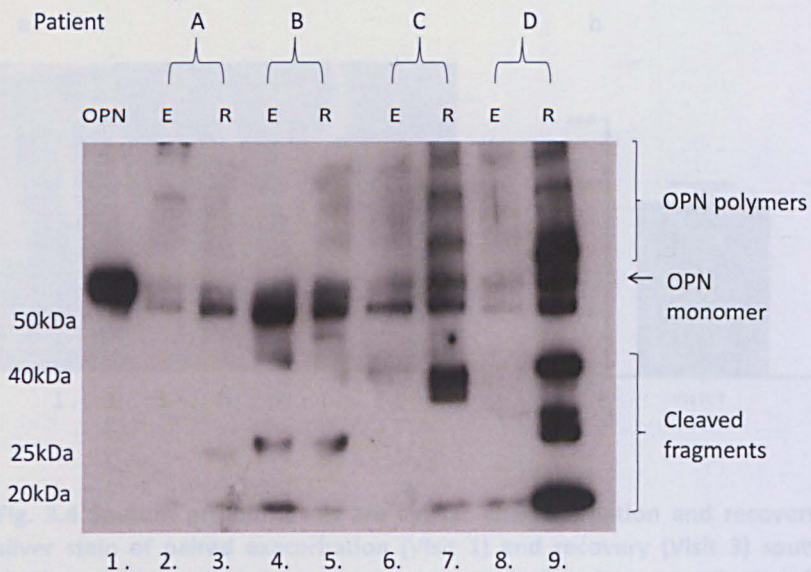


Fig. 3.3 OPN is present in COPD sputum in polymeric, monomeric and cleaved forms, at exacerbation and when patients have recovered. Representative anti-OPN Western blot from sputum from 4 COPD patients A, B, C and D, each sampled at exacerbation and when recovered. Lane 1: recombinant human OPN only; lane 2: Patient A sputum at exacerbation; lane 3: Patient A sputum at recovery; lane 4: Patient B sputum at exacerbation; lane 5: Patient B sputum at recovery; lane 6: Patient C sputum at exacerbation; lane 7: Patient C sputum at recovery; lane 8: Patient D sputum at exacerbation; lane 9: Patient D sputum at recovery. The OPN monomer is present at ≈ 65 kDa. Fragments are noted at ≈ 40 kDa, 30 kDa, 25 kDa and < 20 kDa; not all fragments are present in all patients. Bands > 65 kDa represent OPN polymers. Equal volumes of COPD sputum supernatant per patient and visit were resolved on 10% SDS gels by electrophoresis; proteins were then transferred to a PVDF membrane probed with anti-OPN antibody. Similar levels of protein were present between paired exacerbation and recovery samples as shown by silver stain (fig. 3.4a and b). 200ng recombinant human OPN was used as standard. Only PBS sputum supernatants were analysed. Abbreviations: E, exacerbation sputum; OPN, osteopontin; PVDF, polyvinylidene fluoride, R, recovery sputum.

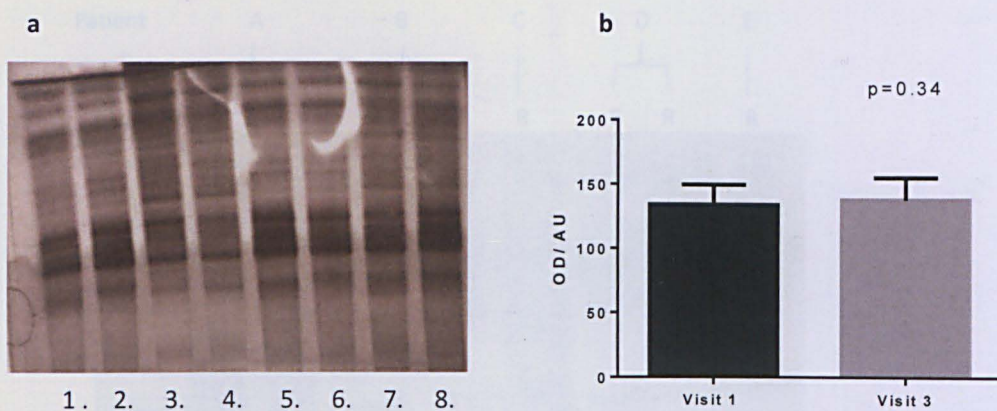


Fig. 3.4 Sputum protein levels are similar at exacerbation and recovery. **A)** Representative silver stain of paired exacerbation (Visit 1) and recovery (Visit 3) sputum samples showing similar stain intensity between visits. Lane 1: Patient A sputum at exacerbation; lane 2: Patient A sputum at recovery; lane 3: Patient B sputum at exacerbation; lane 4: Patient B sputum at recovery; lane 5: Patient C sputum at exacerbation; lane 6: Patient C sputum at recovery; lane 7: Patient D sputum at exacerbation; lane 8: Patient D sputum at exacerbation. **B)** Sputum protein stain was similar between exacerbation and recovery visits, as measured by optical densitometry following silver stain (n=10 paired samples, p=0.34, paired t-test). Abbreviations: OD, optical density; AU, arbitrary units.

3.2.3 MMP-12 is present in human COPD sputum

Anti-MMP-12 western blot analysis of COPD sputum at exacerbation and recovery (n=18, n=23, respectively, n=17 matched pairs) revealed the presence of MMP-12 in all its three forms: the 54kDa inactive, the 45kDa intermediately active and the 22kDa fully active form. All three forms of MMP-12 were present in all patients. No differences in intensity or expression of the three forms were noted between matched exacerbation and recovery samples. A representative blot is shown in fig 3.5.

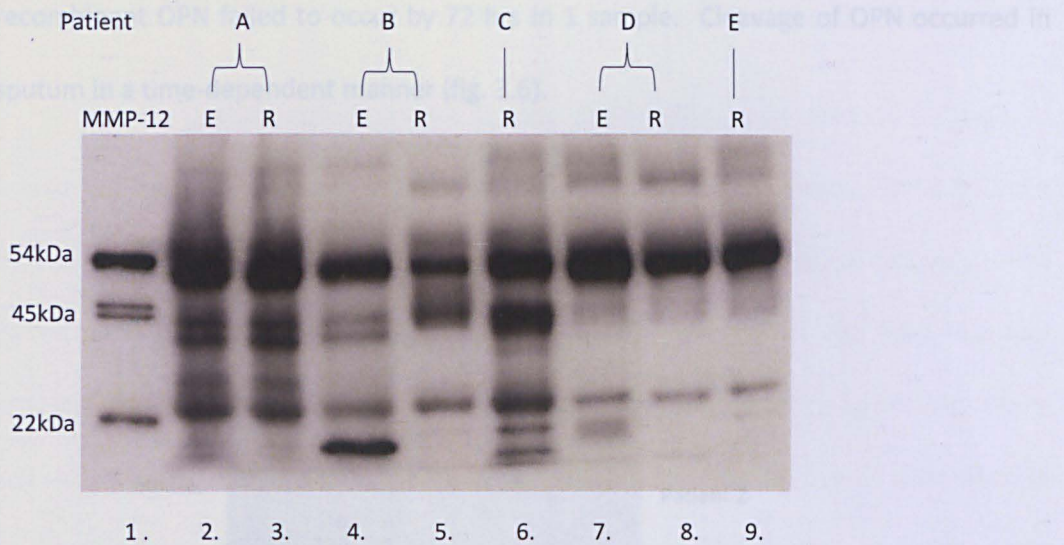


Fig. 3.5 All three forms of MMP-12 are present in COPD sputum at exacerbation and when patients have recovered: 54kDa inactive form, 45kDa intermediately active form and 22kDa fully active form. Representative anti-MMP-12 Western blot from sputum from 5 COPD patients A, B, C, D and E sampled at exacerbation and/or when recovered. Lane 1: recombinant human MMP-12 only; lane 2: Patient A sputum at exacerbation; lane 3: Patient A sputum at recovery; lane 4: Patient B sputum at exacerbation; lane 5: Patient B sputum at recovery; lane 6: Patient C sputum at recovery; lane 7: Patient D sputum at exacerbation; lane 8: Patient D sputum at recovery; lane 9: Patient E sputum at recovery. Equal volumes of COPD sputum supernatant per patient and visit were resolved on 10% SDS gels by electrophoresis; proteins were then transferred to a PVDF membrane probed with anti-MMP-12 antibody. 75ng recombinant human MMP-12 was used as standard. Only PBS sputum supernatants were analysed. Abbreviations: E, exacerbation; MMP-12, matrix metalloproteinase-12; PVDF, polyvinylidene fluoride, R, recovery.

3.2.4 OPN is cleaved *in situ* in human COPD sputum

To determine if OPN fragments present in sputum were due to sputum protease activity, 10 diluted 1:5 human COPD exacerbation and recovery sputum samples were spiked with recombinant 6X HIS tagged-human OPN and allowed to incubate at 37°C for 15min, 1h, 2h, 4h, 8h, 24h, 48h and 72h. Only PBS sputum supernatant samples were used in this experiment. Cleavage of recombinant OPN was seen within 15 min in 9 out of 10 samples, i.e. the ≈20kDa fragment appeared within 15 min. By 4h of incubation, the 65kDa recombinant OPN monomer was fully digested in 8 out of 10 samples; this time point was therefore arbitrarily used as the cut-off for distinguishing fast OPN-cleaving from slow OPN-cleaving sputum samples, in later experiments. Cleavage of

recombinant OPN failed to occur by 72 hrs in 1 sample. Cleavage of OPN occurred in sputum in a time-dependent manner (fig. 3.6).

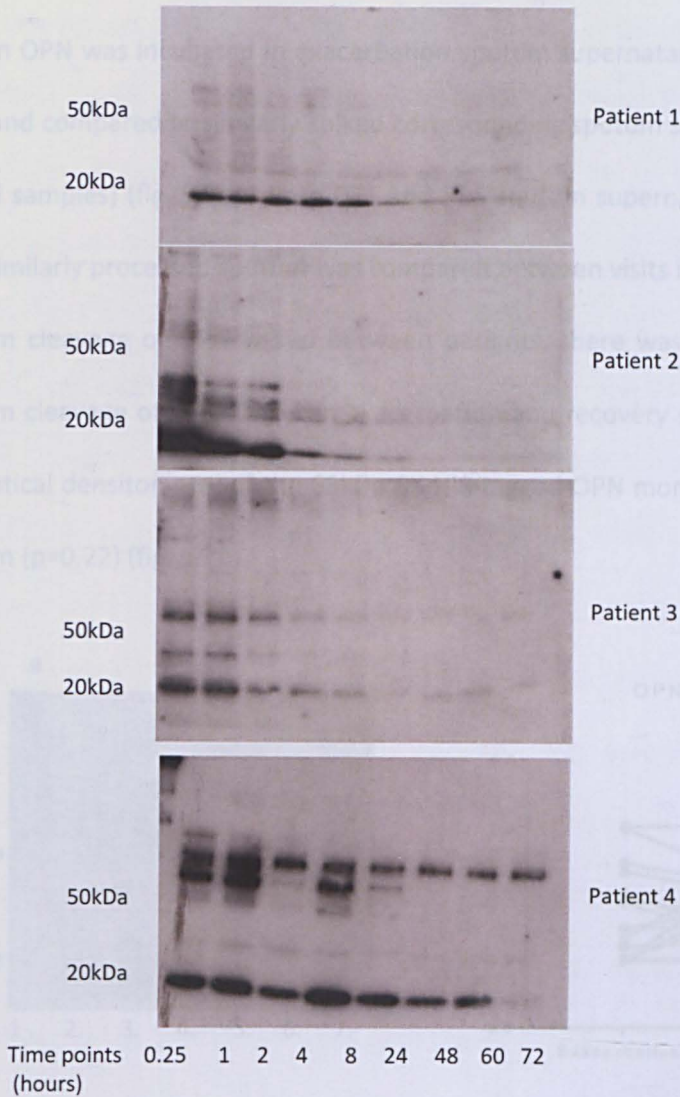


Fig. 3.6 Representative anti-OPN western blots from 4 patients showing time dependent cleavage of recombinant OPN to a final fragment of $\approx 20\text{kDa}$. Each sputum sample was first diluted 1:5 in PBS so that inherent OPN was undetectable and then spiked with 200ng of recombinant 6X HIS-tagged OPN. Samples were then incubated at 37°C at various time points from 15 minutes to 72 hours. Next, samples were resolved on 10% SDS gels by electrophoresis and then transferred to PVDF membranes probed with anti-OPN antibody. OPN monomer is visible at $\approx 65\text{kDa}$ and fragments visible $<50\text{kDa}$. Bands $>65\text{kDa}$ represent polymerization of recombinant OPN in COPD sputum. Loss of band signal with increasing incubation times represents OPN degradation. Only PBS sputum supernatant samples were used. Abbreviations: OPN, osteopontin; PVDF, polyvinylidene fluoride.

3.2.5 Comparison of OPN cleavage in COPD sputum at exacerbation and recovery

Further to the above sputum spiking experiments, recombinant HIS tagged-human OPN was incubated in exacerbation sputum supernatant samples for 4 hours at 37°C and compared to similarly spiked corresponding sputum samples at recovery (n=24 paired samples) (fig. 3.7a). Both DTT and PBS sputum supernatant was used, however only similarly processed sputum was compared between visits in any one patient. While sputum cleavage of OPN varied between patients, there was no overall difference in sputum cleavage of OPN between exacerbation and recovery samples, as measured by the optical densitometry of the 65kDa 6X HIS tagged-OPN monomer after incubation in sputum (p=0.22) (fig. 3.7b).

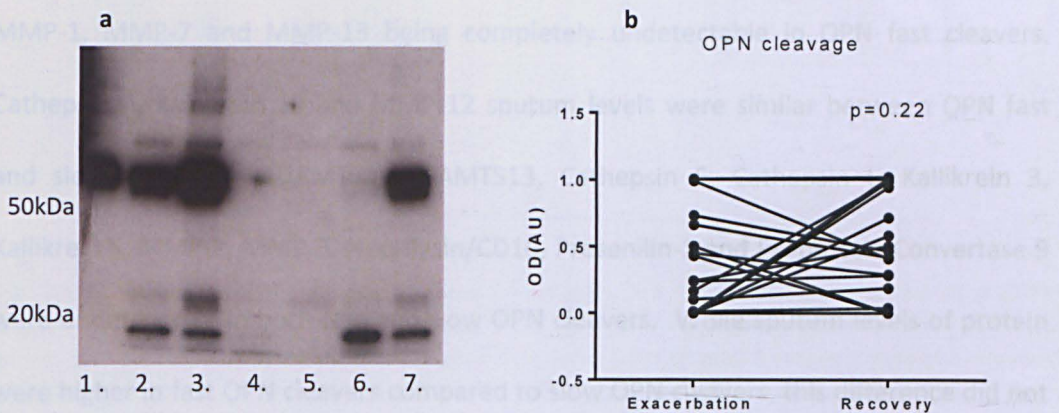


Fig. 3.7 Cleavage of 6X HIS tagged-OPN occurs at different rates in sputum from different COPD patients, but no overall difference was noted between OPN cleavage at exacerbation compared to recovery (n=24). a) Representative anti-6X HIS antibody probed western blot for 3 patient sputum samples A-C, sampled at exacerbation and when recovered: lane 1: recombinant OPN only; lane 2: Patient A sputum at exacerbation; lane 3: Patient A sputum at recovery; lane 4: Patient B sputum at exacerbation; lane 5: Patient B sputum at recovery; lane 6: Patient C sputum at exacerbation. Each sputum sample was diluted 1:5 in PBS, spiked with 200ng 6X HIS tagged-OPN and incubated at 37°C for 120 min. 200ng OPN was used as standard. The resultant western blot shows different rates of 6X HIS tagged-OPN cleavage which occurs fastest in Patient B and slowest in Patient A. OPN was not cleaved when incubated in PBS at 37°C for 120 min (lane 1). b) No significant difference in OPN cleavage was noted between exacerbation and recovery, as measured by the optical densitometry of the 65kDa 6X HIS tagged-OPN monomer after incubation in sputum (n=24, p=0.22 Wilcoxon matched-pairs signed rank test). Similar levels of protein were present between paired exacerbation and recovery sputum samples (fig. 4.6). Both DTT and PBS sputum supernatant was used, however only similarly processed sputum was compared between visits in any one patient. Abbreviations: OPN, osteopontin; OD, optical densitometry; AU, arbitrary units.

3.2.6 Proteome profiler assay

To explore further the differences in sputum proteases between fast and slow OPN-cleaving samples a proteome profiler assay was employed. Fig. 3.8 a-d show the differences in PBS sputum supernatant levels between fast OPN cleavers and slow OPN cleavers (n=3 patient in each group). Since data could not be analysed statistically, they were described qualitatively. Sputum levels of ADAM8, ADAM9, Cathepsin D, Kallikrein 6, Kallikrein 7 and uPA were increased in OPN fast cleavers in comparison to OPN slow cleavers, with Kallikrein 6 and 7 being undetectable in slow OPN cleavers. Conversely, sputum levels of Cathepsin B, Cathepsin C, Cathepsin S, Cathepsin V, Cathepsin X, DDPIV/CD26 (Dipeptidyl-peptidase 4), Kallikrein 13, MMP-1, MMP-7, MMP-13 and proteinase 3 were higher in OPN slow cleavers compared to OPN fast cleavers, with MMP-1, MMP-7 and MMP-13 being completely undetectable in OPN fast cleavers. Cathepsin A, Kallikrein 10 and MMP-12 sputum levels were similar between OPN fast and slow cleavers. ADAMTS1, ADAMTS13, Cathepsin E, Cathepsin L, Kallikrein 3, Kallikrein S, MMP-2, MMP-3, Neprilysin/CD10, Presenilin-1 and Proprotein Convertase 9 were undetectable in both fast and slow OPN cleavers. While sputum levels of protein were higher in fast OPN cleavers compared to slow OPN cleavers, this difference did not reach statistical significance (mean $1084 \pm 303.5 \mu\text{g/ml}$ v $872.9 \pm 339.8 \mu\text{g/ml}$, respectively, n=5, 6 respectively, p=0.31) (fig. 3.9).

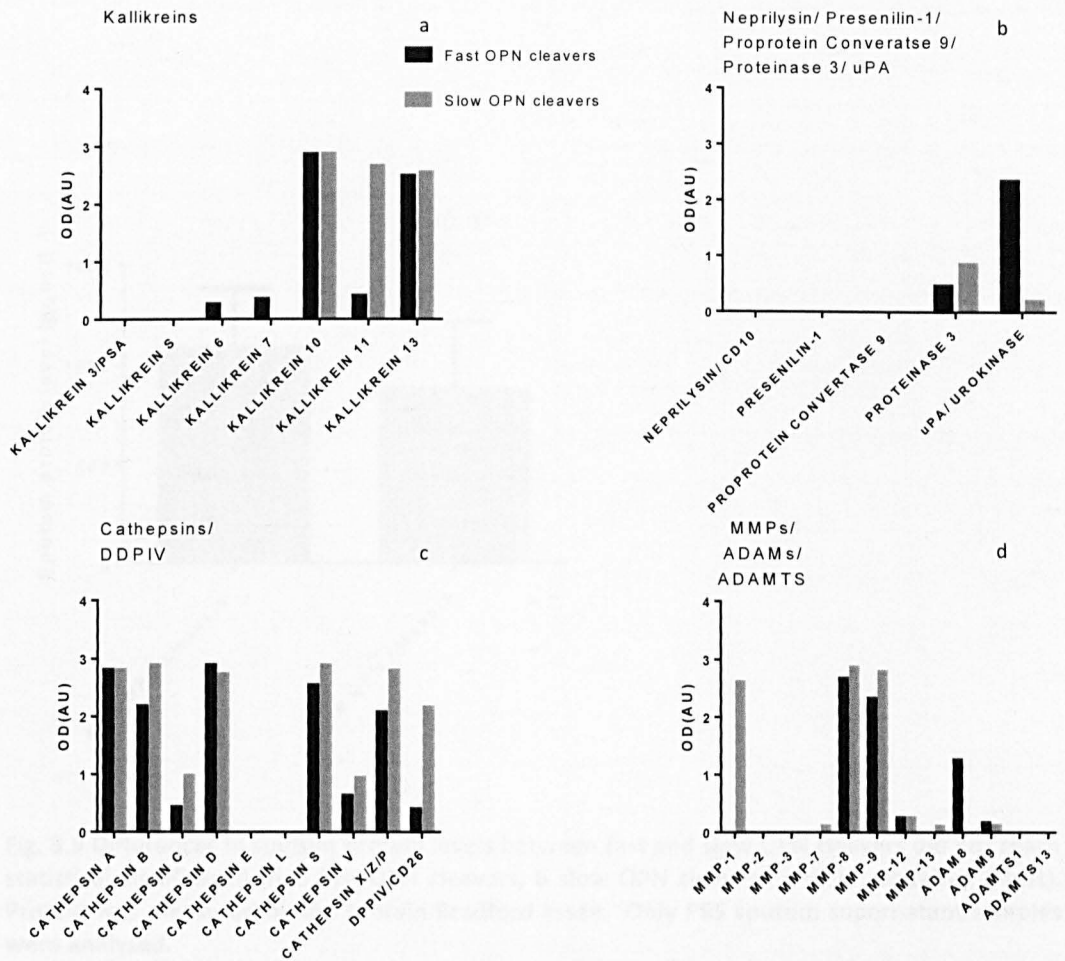


Fig. 3.8a-d Differences in sputum protease levels between fast OPN cleavers and slow OPN cleavers. PBS sputum supernatant samples were pooled from 3 patients at recovery in each group, fast and slow OPN cleavers, to a total of 50 μ L in each group. Sputum supernatant levels of ADAM8, ADAM9, Cathepsin D, Kallikrein 6, Kallikrein 7 and uPA were increased in OPN fast cleavers in comparison to OPN slow cleavers. Protein levels were similar between fast (black) and slow (grey) OPN cleavers (shown in fig. 3.9). The experiment was conducted once. Abbreviations: AU, arbitrary units; DDPIV, dipeptidyl-peptidase 4; MMP, matrix metalloproteinase; OD, optical densitometry; OPN, osteopontin; uPA, Urokinase-type plasminogen activator.

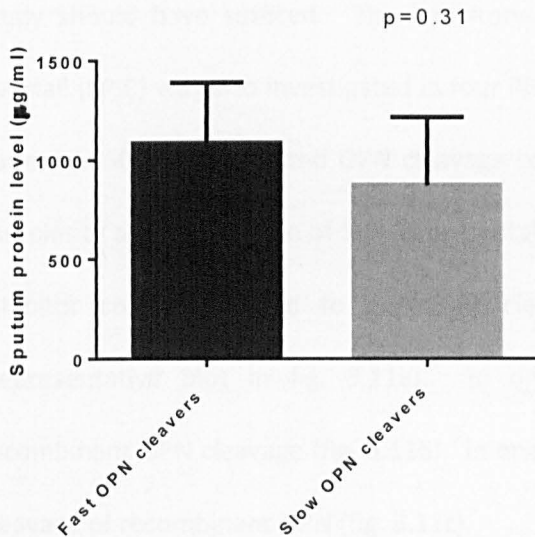


Fig. 3.9 Differences in sputum protein levels between fast and slow OPN cleavers did not reach statistical significance (n=5 fast OPN cleavers, 6 slow OPN cleavers, p=0.31, unpaired t-test). Protein was measured by the protein Bradford assay. Only PBS sputum supernatant samples were analysed.

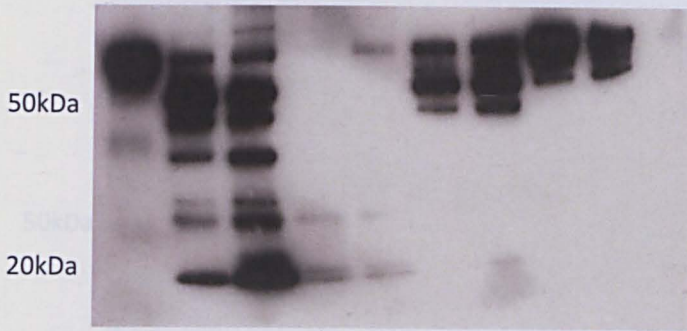
3.2.7: Inhibition Assays: *ex vivo* sputum cleavage of OPN in the presence of protease inhibitors

As the main differences in sputum protease levels between the two groups were higher levels in the fast cleavers of 1) the metalloproteases ADAM8 and ADAM 9, 2) the serine proteases Kallikrein 6, Kallikrein 7 and 3) the serine protease uPA, a series of inhibition assays were carried out to determine the main protease class/es involved in sputum OPN cleavage. Therefore, four Visit 3 PBS sputum supernatant samples from four COPD patients were spiked with recombinant 6X HIS-tagged OPN in the presence of 25µM of the metalloprotease inhibitor ilomastat or serine protease inhibitor cocktail.

Ilomastat failed to inhibit sputum cleavage of OPN in all patients (representative blots in fig. 3.10a and b). Since the product literature for ilomastat reports a K_i range of 0.1nM-27nM for MMPs-1, 2, 3, 7, 8, 9, 12, 14 and 26, the concentration used in this study should have sufficed. The inhibitory potential of a serine protease inhibitor cocktail (SPIC) was also investigated in four PBS sputum supernatant samples from four patients. 50X SPIC inhibited OPN cleavage completely in two out of the four sputum samples at a concentration of 50X (representative blot in fig. 3.11a). Serially diluting the inhibitor cocktail 1:2 led to increasing cleavage of OPN in both these samples (representative blot in fig. 3.11a). In one sample 50X SPIC partially inhibited recombinant OPN cleavage (fig. 3.11b). In one sputum sample 50X SPIC failed to inhibit cleavage of recombinant OPN (fig. 3.11c).

a)

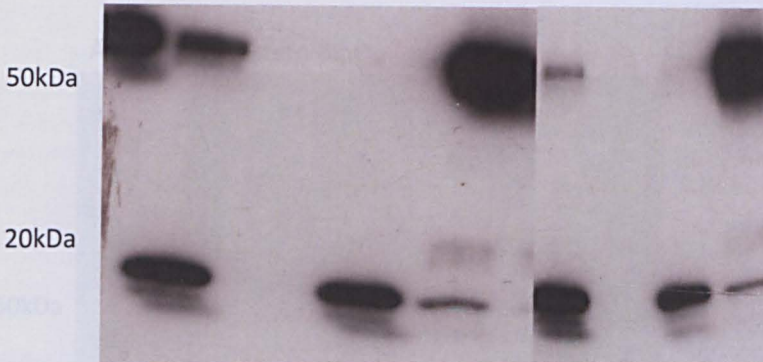
Anti-OPN Western Blot



OPN	+	+	+	+	+	+	+	+	+
Sputum	-	+	+	+	+	+	+	+	+
Ilomastat	-	+	-	+	-	+	-	+	-
Patient		A	A	B	B	C	C	D	D

b)

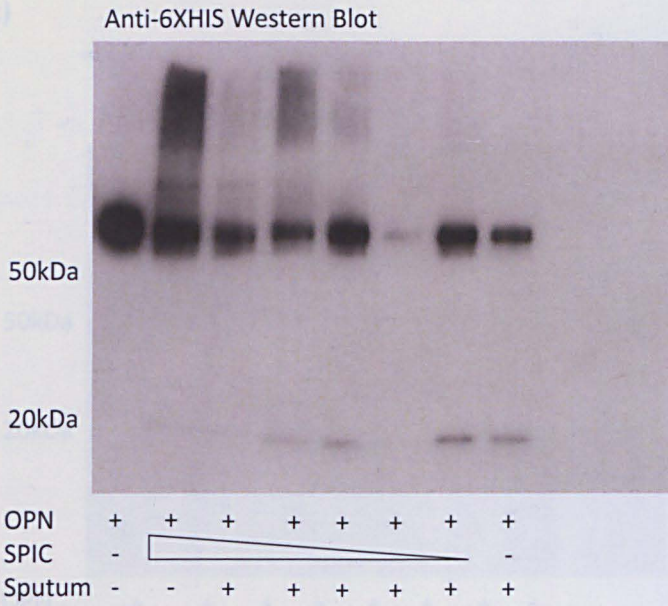
Anti-6XHIS Western Blot



OPN	+	+	+	+	+	+	+	+	+
Sputum	-	+	+	+	+	+	+	+	+
Ilomastat	-	-	-	-	-	+	+	+	+
Patient		A	B	C	D	A	B	C	D

Fig. 3.10 Ilomastat does not inhibit recombinant OPN cleavage in COPD sputum; a) immunoblot probed with anti-OPN antibody and b) immunoblot probed with anti-6XHIS tag antibody. Recombinant human 6XHIS tagged OPN was incubated in COPD sputum, patients A-C in the presence (+) or absence (-) of 25µM Ilomastat at 37°C for 2 hours and its cleavage in the same patient samples compared. Lower or lack of signal intensity reflects increased recombinant OPN degradation: patient B cleaves OPN more readily than patients A, C and D. Only PBS sputum supernatant was used. Abbreviations: OPN, osteopontin.

a)



b)

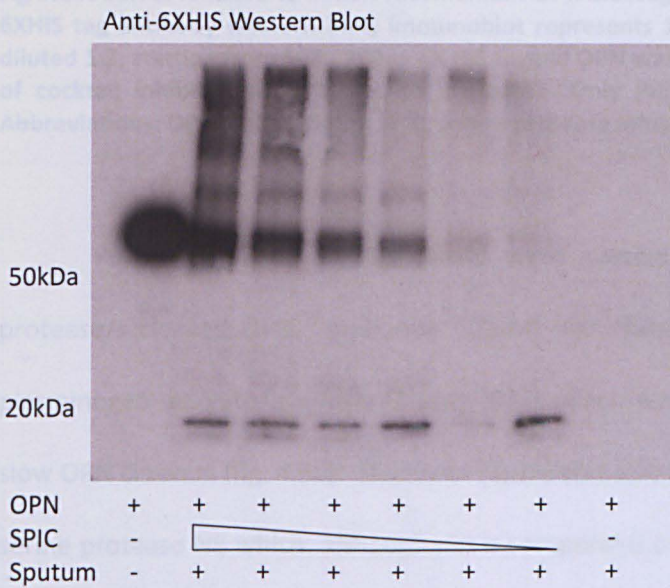


Fig. 3.11a and b 50X SPIC inhibits recombinant OPN cleavage in sputum; Anti-6XHIS tag antibody western blots; each immunoblot represents 1 COPD patient. SPIC was serially diluted 1:2, starting from 50X. 200ng 6X HIS tagged OPN was then added to each serial dilution of cocktail inhibitor and allowed to incubate. 50X SPIC inhibits recombinant OPN cleavage in sputum completely (a). This was noted in n=2 patients of 4 patients. 50X SPIC partially blocks recombinant OPN cleavage in sputum in n=1 of 4 patients (b). Only PBS sputum supernatant was used. Abbreviations: OPN, osteopontin; SPIC, serine protease inhibitor cocktail.

c)

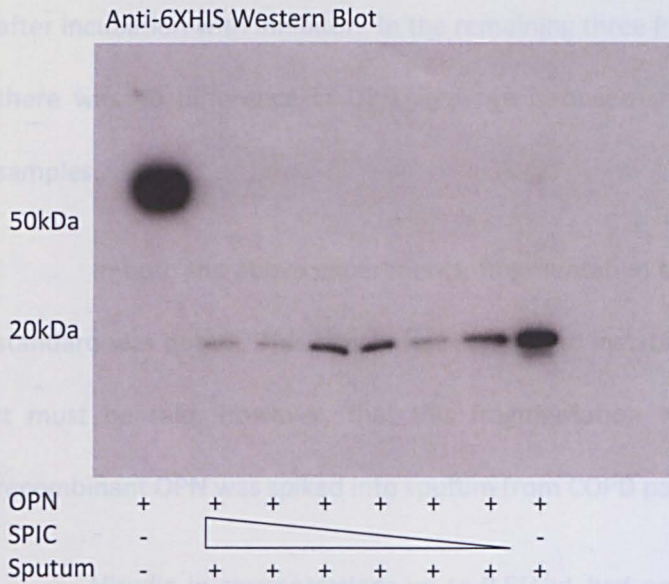


Fig 3.11c 50X SPIC failed to inhibit recombinant OPN cleavage in sputum from 1 patient. Anti-6XHIS tag antibody western blot; immunoblot represents 1 COPD patient. SPIC was serially diluted 1:2, starting from 50X. 200ng 6X HIS tagged OPN was then added to each serial dilution of cocktail inhibitor and allowed to incubate. Only PBS sputum supernatant was used. Abbreviations: OPN, osteopontin; SPIC, serine protease inhibitor cocktail.

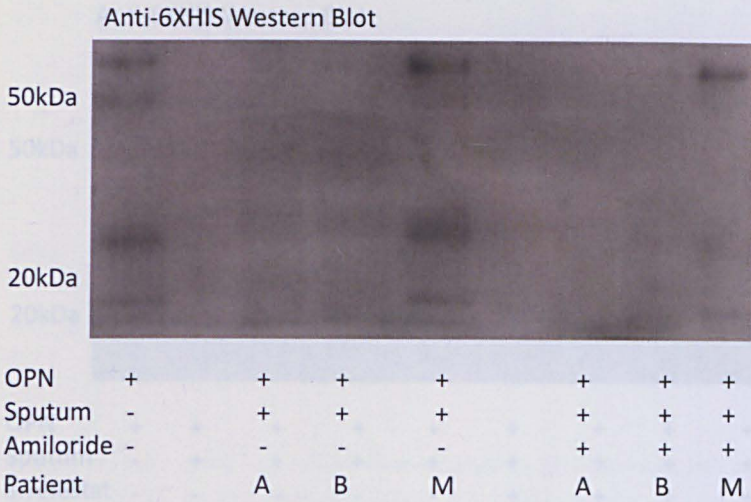
Further inhibition experiments were carried out to detect which serine protease/s cleaved OPN. Amiloride (10 μ M) was chosen as it inhibits Urokinase-type plasminogen activator (uPA)($K_i=7 \mu$ M) [282] which was elevated in fast compared to slow OPN cleavers (fig. 4.8b). Sivelestat (1 μ M) was also chosen as it is an inhibitor of the serine protease NE which, although not a component of the proteome profiler assay, is an important serine protease in COPD pathogenesis [17-20]. Similarly, the serine protease thrombin was not a component of the proteome profiler assay, but since OPN cleavage data in the literature centres around thrombin activity inhibition, assays with up to 0.5U/ μ L of the thrombin inhibitor hirudin were performed. No difference in OPN cleavage between amiloride treated and untreated PBS sputum supernatant samples

was noted (n=6) (fig. 3.12a and b). In contrast, in three sivelestat-treated PBS sputum supernatant samples (fig. 3.13a and b) OPN cleavage was reduced compared with matched untreated samples, as shown by the presence of the 65kDa OPN monomer after incubation with inhibitor. In the remaining three PBS sputum supernatant samples there was no difference in OPN cleavage between sivelestat treated and untreated samples.

In both the above experiments, fragmentation of recombinant OPN used as the standard was noted. This may have been due to instability of the recombinant protein. It must be said, however, that this fragmentation was less than that seen when recombinant OPN was spiked into sputum from COPD patients.

Hirudin in concentrations up to 0.5U/ μ L had no effect on OPN cleavage in PBS sputum supernatant samples (n=3). Since the range of sputum thrombin concentration is 1.15-10.2U/ml [283], this level of hirudin should inhibit the activity of thrombin activity if it were responsible for OPN cleavage. A representative immunoblot testing the dose response of Hirudin on OPN cleavage in one sputum sample is shown in fig. 3.14.

a)



b)

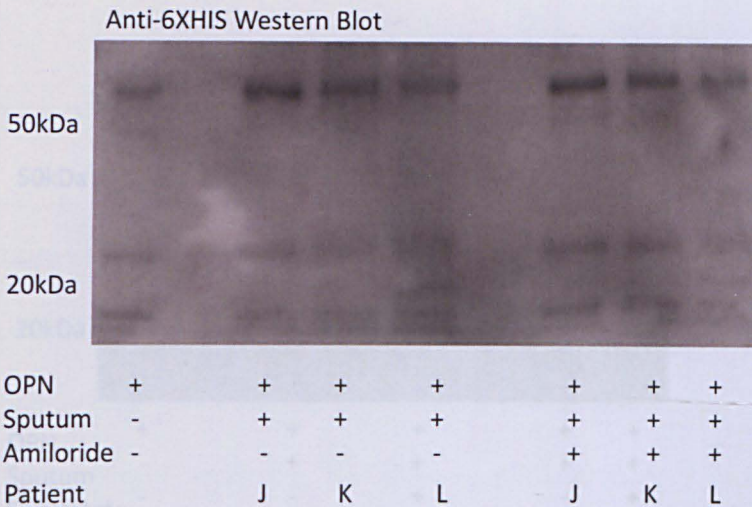
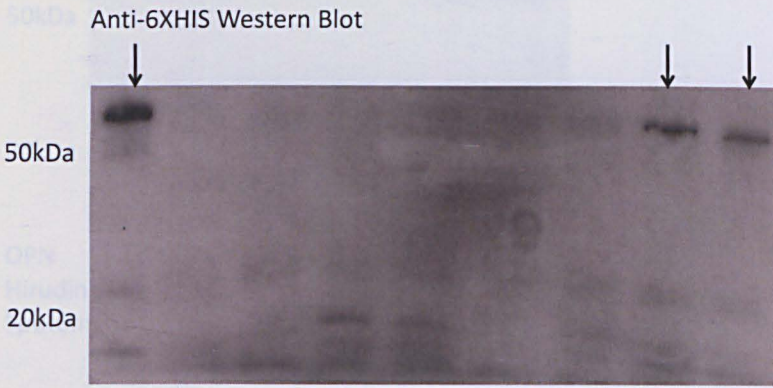


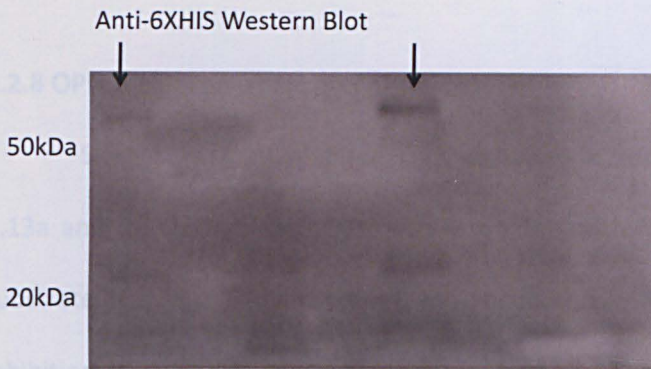
Fig. 3.12a and b Amiloride does not inhibit OPN cleavage in COPD sputum; immunoblots probed with anti-6X HIS tag antibody. Recombinant human 6X HIS tagged OPN (200ng) was incubated in COPD sputum, patients A, B, M (a) and J, K,L (b) (n=6) in the presence (+) or absence (-) of 10 μ M of the uPA inhibitor amiloride at 37°C for 2 hours. Only PBS sputum supernatant was used. Abbreviations: OPN, osteopontin; uPA, Urokinase-type plasminogen activator.

a)



OPN	+	+	+	+	+	+	+	+
Sputum	-	+	+	+	+	+	+	+
Sivelestat	-	-	-	-	-	+	+	+
Patient		A	B	C	D	A	B	C

b)



OPN	+	+	+	+	+
Sputum	-	+	+	+	+
Sivelestat	-	-	+	-	+
Patient		E	E	F	F

Fig. 3.13a and b Recombinant OPN cleavage decreased the presence of sivelestat in sputum from 3 patients; immunoblots probed with anti-6X HIS tag antibody. Recombinant human 6X HIS-tagged OPN (200ng) was incubated in COPD sputum, patients A-F (n=6) in the presence (+) or absence (-) of 1 μ M NE inhibitor sivelestat at 37°C for 2 hours minutes and its cleavage in the same patient samples compared. Arrows point to 65kDa OPN monomer. OPN degradation decreased in the presence of sivelestat in sputum from patients C and D (a) and patient E(b) but was unaffected by sivelestat-treated sputum from patients A, B (a) and F(b). Only PBS sputum supernatant was used. Abbreviations: NE, neutrophil elastase; OPN, osteopontin.

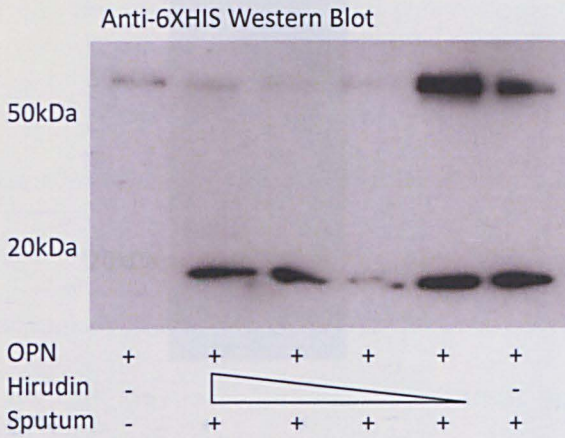


Fig 3.14 Hirudin does not inhibit recombinant OPN cleavage in sputum; immunoblot probed with anti-6X HIS tag antibody representing 1 COPD patient. Recombinant human 6X HIS tagged OPN (200ng) was incubated in COPD sputum in the absence (-) or presence (+) of 1:2 serial dilutions of the thrombin inhibitor hirudin, starting from 0.5U/ μ l. The experiment was repeated in 2 other patients. Only PBS sputum supernatant was used. Abbreviations: OPN, osteopontin.

3.2.8 OPN is cleaved by NE and uPA

Since sivelestat inhibited OPN cleavage in some of the sputum samples (fig. 3.13a and b), recombinant OPN was incubated with NE *in vitro*, to confirm OPN as a substrate for NE. Similarly, OPN was incubated with uPA *in vitro*, as although no inhibition of OPN cleavage was noted with the uPA inhibitor amiloride, levels of uPA were strikingly elevated in fast cleavers compared to slow cleavers (fig. 3.8b). OPN was cleaved by both NE and uPA *in vitro*. NE cleaved OPN to a <20kDa fragment (fig. 3.15) while uPA cleaved OPN to a \approx 20kDa fragment (fig. 3.16).

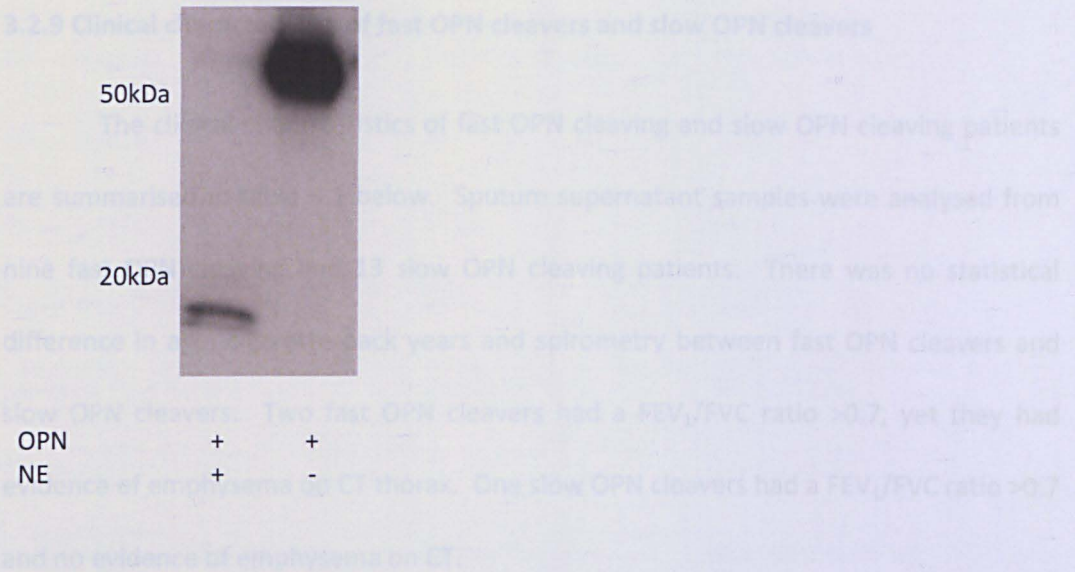


Fig. 3.15 NE cleaves OPN *in vitro* to a <20kDa fragment. OPN (500ng) was incubated with 0.05U NE *in vitro* at 37°C for 18h. The reactions products were resolved by 10% SDS gel electrophoresis and transferred to a PVDF membrane probed with anti-OPN antibody. Abbreviations: NE, neutrophil elastase; OPN, osteopontin; PVDF, polyvinylidene fluoride.

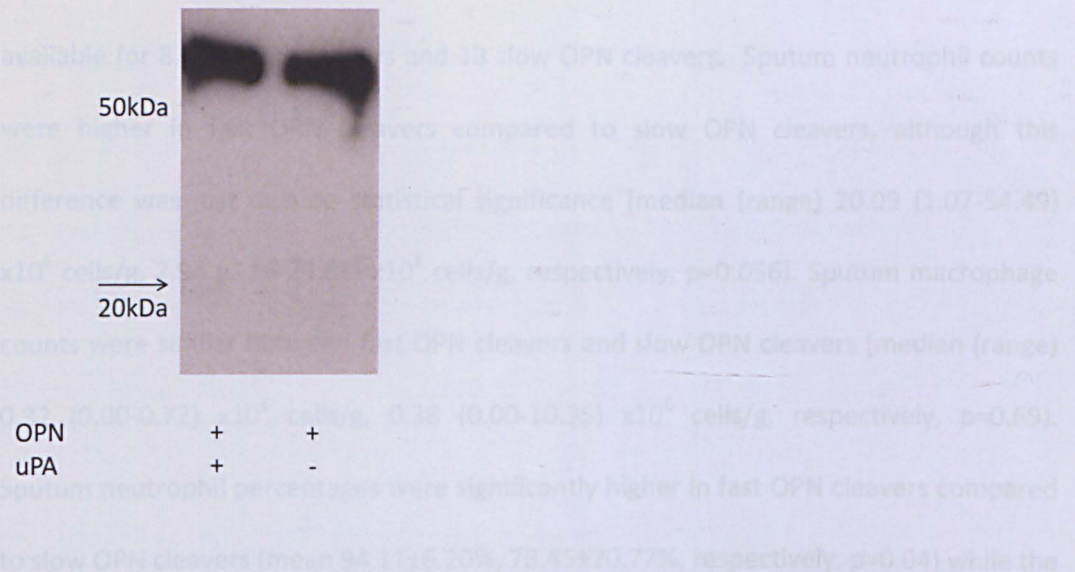


Fig. 3.16 uPA cleaves OPN *in vitro* to a ≈20kDa fragment (arrow). OPN (500ng) was incubated with 55ng uPA *in vitro* at 37°C for 18h. The reactions products were resolved by 10% SDS gel electrophoresis and transferred to a PVDF membrane probed with anti-OPN antibody. Abbreviations: OPN, osteopontin; PVDF, polyvinylidene fluoride; uPA, urokinase-type plasminogen activator.

3.2.9 Clinical characteristics of fast OPN cleavers and slow OPN cleavers

The clinical characteristics of fast OPN cleaving and slow OPN cleaving patients are summarised in table 3.1 below. Sputum supernatant samples were analysed from nine fast OPN cleaving and 13 slow OPN cleaving patients. There was no statistical difference in age, cigarette pack years and spirometry between fast OPN cleavers and slow OPN cleavers. Two fast OPN cleavers had a FEV₁/FVC ratio >0.7, yet they had evidence of emphysema on CT thorax. One slow OPN cleavers had a FEV₁/FVC ratio >0.7 and no evidence of emphysema on CT.

Fast OPN cleavers had higher sputum TCC than slow OPN cleavers (20.49±18.61 x10⁶ cells/g sputum, 7.95±9.50 x10⁶ cells/g sputum, respectively), yet this difference was not statistically significant (p=0.058). Sputum neutrophil and macrophage indices were available for 8 fast OPN cleavers and 13 slow OPN cleavers. Sputum neutrophil counts were higher in fast OPN cleavers compared to slow OPN cleavers, although this difference was just outside statistical significance [median (range) 20.09 (1.07-54.49) x10⁶ cells/g, 2.94 (0.16-25.63) x10⁶ cells/g, respectively, p=0.056]. Sputum macrophage counts were similar between fast OPN cleavers and slow OPN cleavers [median (range) 0.32 (0.00-0.72) x10⁶ cells/g, 0.38 (0.00-10.35) x10⁶ cells/g, respectively, p=0.69]. Sputum neutrophil percentages were significantly higher in fast OPN cleavers compared to slow OPN cleavers (mean 94.11±6.20%, 78.45±20.77%, respectively, p=0.04) while the reverse was true for sputum macrophage percentages (mean 4.69±5.08%, 15.75±15.42%, respectively, p=0.005) (fig. 3.17 a and b).

Table 3.1 Clinical characteristics of fast OPN cleavers and slow OPN cleavers

Demographics	Fast OPN cleavers	Slow OPN cleavers
Male/ Female (n)	8/1	10/3
Age/ Years*	67±8	68±11
Current/ex-smokers/never (n)	2/7/0	9/4/1
Cigarette Pack years*	60.22±35.39	47.29 ±21.40
ICS yes/ no/ N/A (n)	7/1/1	14/0/0
Lung function/ CT/ MRC grade	Fast OPN cleavers	Slow OPN cleavers
FEV ₁ / Ls ⁻¹ *	1.25±0.73	1.4 ±0.7
FEV ₁ / percent predicted*	46.00±22.83	49.14±17.98
FEV ₁ /FVC*	0.47±0.19	0.48 ±0.14
Emphysema on CT yes/ no /N/A (n)	5/3/1	8/4/2
MRC grades 3-5 (n)	Grade 3(1), 4 (3), 5(5)	Grade 3(5), 4(6), 5(3)
Sputum cell counts	Fast OPN cleavers	Slow OPN cleavers
Sputum TCC/ x10 ⁶ cells/g*	20.49±18.61	7.95±9.50
Sputum neutrophil count/ x10 ⁶ cells/g median (range)	20.09 (1.07-54.49)	2.94 (0.16-25.63)
Sputum macrophage count/ x10 ⁶ cells/g median (range)	0.32 (0.00-0.72)	0.38 (0.00-10.35)
Sputum neutrophil percentage*	94.11±6.20	78.45±20.77
Sputum macrophage percentage*	4.69±5.08%	15.75±15.42

*Data presented as mean ±standard deviation. Abbreviations: ICS, Inhaled corticosteroids (n), number; N/A, not available; TCC, total cell count

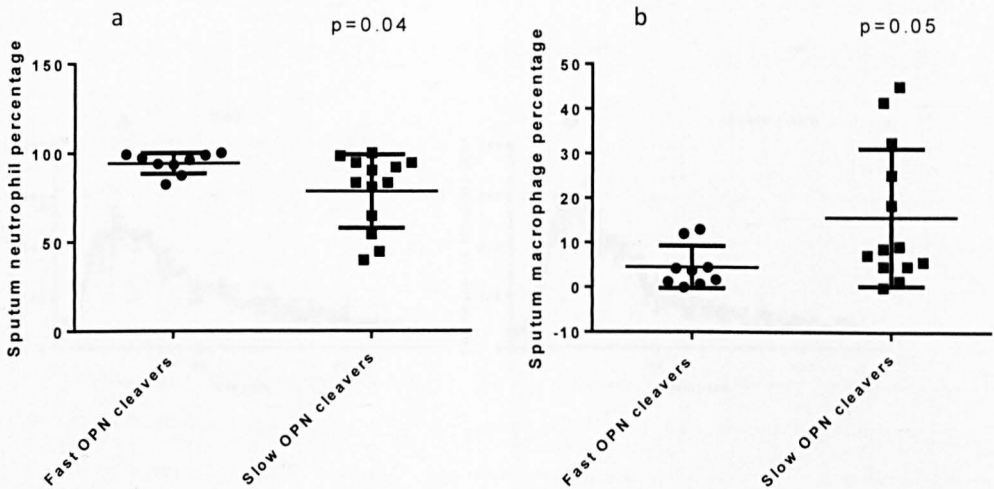


Fig. 3.17 Fast OPN cleavers have higher sputum neutrophil percentages a) and lower sputum macrophage percentages b) compared to slow OPN cleavers (n=8, 13; fast OPN cleavers, slow OPN cleavers, respectively, p=0.04, p=0.05, respectively, unpaired t-test)

3.2.10 Functional assays of MMP-12-cleaved OPN: ROS assay

To test whether OPN has a pro-inflammatory effect on PBMCs, as measured by increased ROS production, the effect of increasing OPN concentration on ROS production was tested. No difference in PBMC ROS production was noted with increasing concentrations of OPN (0.01-10 μ g/ml) (n=3 patients), nor any difference noted between OPN and PBS (n=3 patients) (figure 3.18). Next, to test whether MMP-12-cleaved OPN had an increased pro-inflammatory effect compared to uncleaved OPN, the effect of both on PBMC ROS production was tested. No difference in PBMC ROS production was noted between cells treated with uncleaved OPN and those treated with MMP-12-cleaved OPN (figure 3.19). Due to a lack of effect, this experiment was discontinued after n=2 patients.

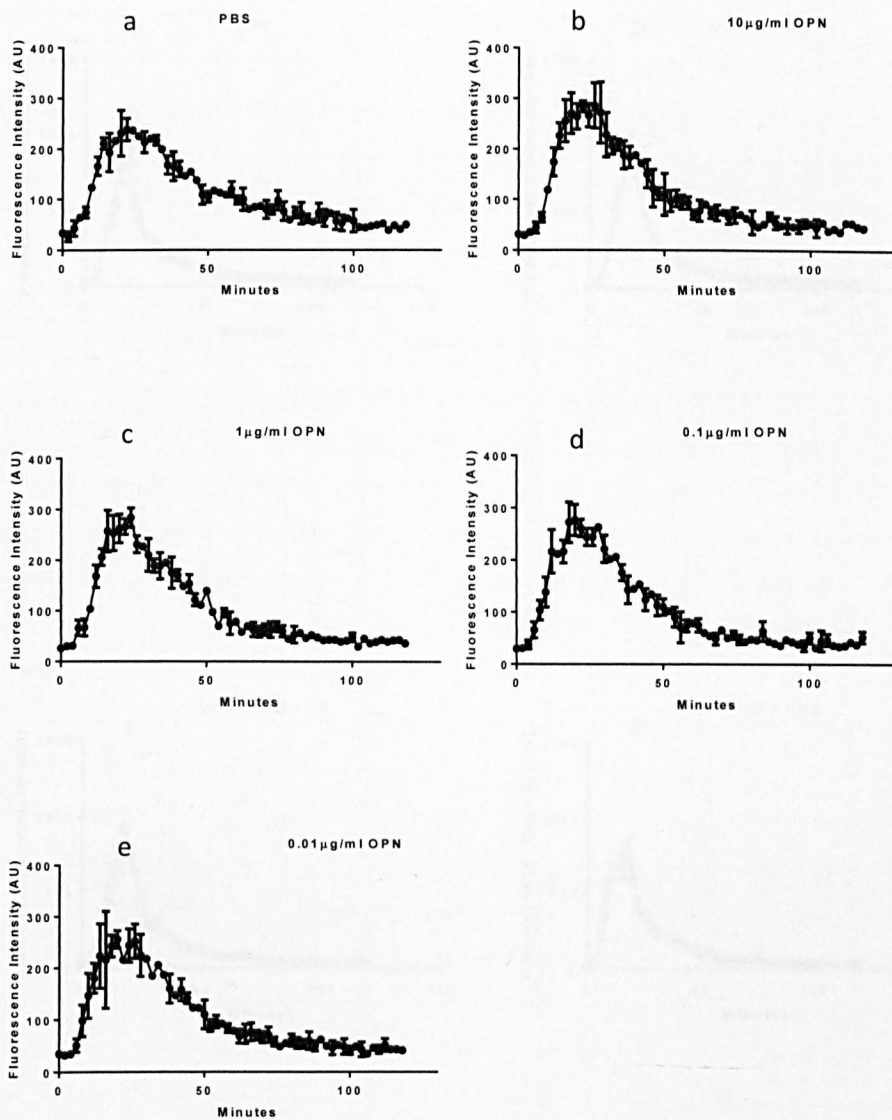


Fig. 3.18 ROS production by PBMC undergoing zymosan phagocytosis is not altered by OPN up to a concentration of 10µg/ml. PBMC derived from healthy volunteers were incubated with Buffer A containing PBS or increasing concentrations of OPN. Next, zymosan was added and their ROS production measured immediately and after every 2min for 2h. The experiment was carried out 3 times using PBMC from 3 individuals. Graphical data shown are from one individual. Abbreviations: OPN, osteopontin; PBMC, peripheral blood mononuclear cells; ROS, reactive oxidative species.

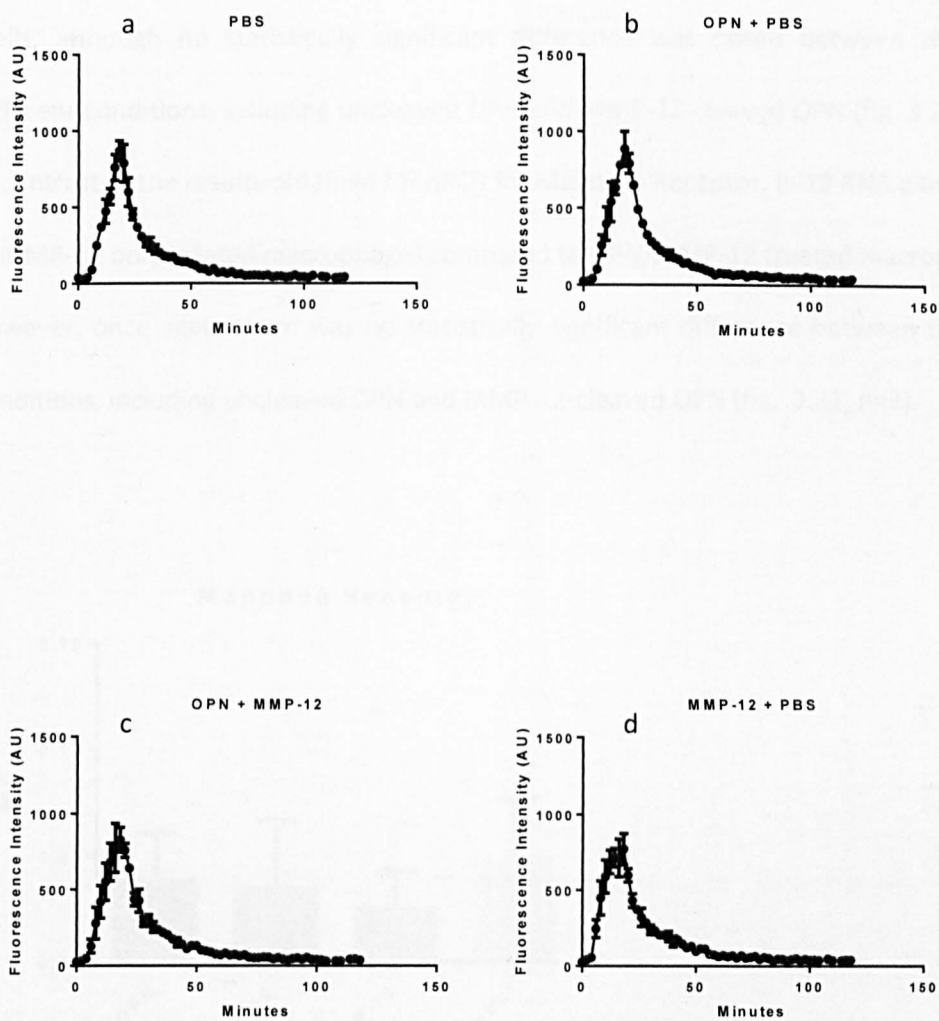


Fig. 3.19 No difference in PBMC ROS production was noted between uncleaved and MMP-12-cleaved OPN. PBMC derived from healthy volunteers were incubated with PBS a), uncleaved OPN (10 μ g/ml) b), MMP-12-cleaved OPN (10 μ g/ml) c) or MMP-12 d). ROS production was measured every 2 min for 2h. The experiment was carried out twice using PBMC from two individuals. Graphical data shown are from one individual. Abbreviations: MMP-12, matrix metalloproteinase-12; OPN, osteopontin; PBMC, peripheral blood mononuclear cells; ROS, reactive oxidative species.

3.2.11 Functional assays of MMP-12-cleaved OPN: qPCR

Mannose Receptor RNA levels were lowest in macrophages in the MMP-12 only wells, although no statistically significant difference was noted between the four different conditions, including uncleaved OPN and MMP-12-cleaved OPN (fig. 3.20 n=3). In contrast to the results obtained for qPCR for Mannose Receptor, IL-12 RNA was higher in MMP-12 only treated macrophages compared to OPN/MMP-12 treated macrophages; however, once again there was no statistically significant difference between the four conditions, including uncleaved OPN and MMP-12-cleaved OPN (fig. 3.21, n=3).

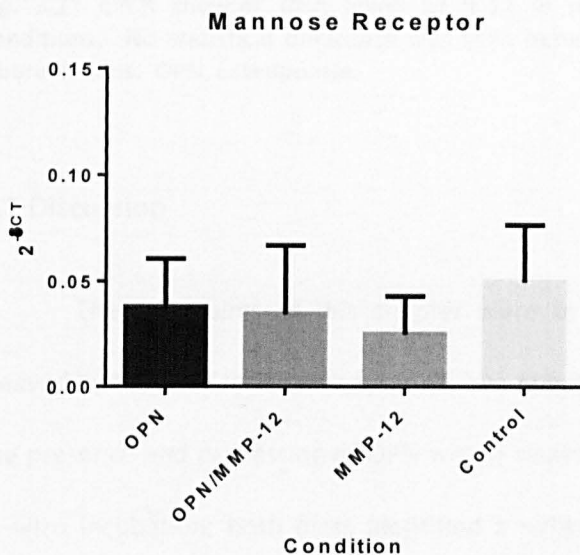


Fig. 3.20 qPCR showing RNA levels of Mannose Receptor in macrophages incubated under different conditions. Although levels of Mannose Receptor RNA were lowest in the MMP-12 only treated cells, no statistical difference was seen between the conditions using ANOVA (n=3). Abbreviations: OPN, osteopontin.

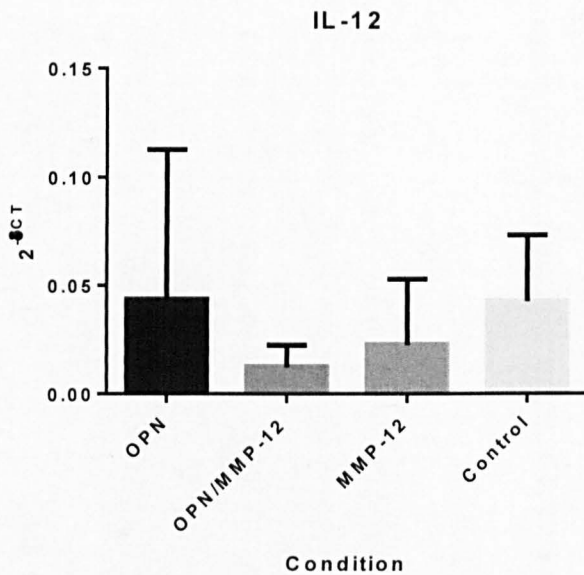


Fig. 3.21 qPCR showing RNA levels of IL-12 in macrophages incubated under different conditions. No statistical difference was seen between the conditions using ANOVA (n=3). Abbreviations: OPN, osteopontin.

3.3 Discussion

The main aims of this chapter were to determine if OPN was present and cleaved by MMP-12 in the airways in COPD. Western blotting of COPD sputum revealed the presence and processing of OPN with a cleavage signature similar to MMP-12/OPN *in vitro* incubation; both blots identified a ≈ 20 kDa OPN fragment. Similarly, spiking COPD sputum with HIS tagged-OPN, led to the *de novo* release of a ≈ 20 kDa HIS tagged-OPN fragment. However, while this may be suggestive of MMP-12 cleaving OPN *in vivo*, it does not rule out other proteases producing similar sized OPN fragments. Indeed, the *in vitro* studies in this chapter demonstrated the complexity of OPN cleavage. In addition to its cleavage by MMP-12, OPN was also susceptible to cleavage by two serine proteases *in vitro*, NE and uPA, leading to the release of a similar sized ≈ 20 kDa fragment. These *in vitro* findings, therefore suggest that OPN may be cleaved in the airways by any of these three proteases, or indeed all three.

On further exploration, ilomastat, a broad spectrum metalloprotease inhibitor, failed to inhibit the cleavage of OPN in sputum. Furthermore, there was no difference in sputum MMP-12 levels between fast and slow OPN cleavers, nor sputum macrophages, the main source of MMP-12 [198]. In contrast, cleavage of OPN in COPD sputum was noted to be serine protease cocktail dependent and in some samples NE dependent. Cleavage of OPN in COPD sputum was also related to neutrophilic inflammation, as shown by higher neutrophil levels in fast compared to slow OPN cleavers. While sputum uPA levels were higher in fast OPN cleavers, amiloride, an inhibitor of uPA [284] failed to inhibit OPN cleavage, suggesting that uPA was not responsible for OPN processing. Similarly, thrombin inhibition with hirudin failed to inhibit OPN cleavage in sputum, despite its use in sufficient concentrations [283]. The inhibition studies therefore show that in COPD OPN cleavage is serine protease, in particular NE, dependent, rather than metalloproteinase dependent.

NE is important in COPD pathogenesis [17-20]; it degrades ECM components to cause emphysema in animal models [17, 19] and in individuals deficient in its inhibitor α 1AT [18]. While most COPD studies have focused on ECM substrates of NE, there is recognition of non-ECM proteins as NE substrates, such as complement factor C3 [285] and immunoglobulin [286]. OPN has not been previously described as a NE substrate, and while it is a component of bone ECM[232], it also exists in soluble forms, as in the airways [231, 281, 287]. This study thus extends the non-ECM substrate profile of NE. The role of NE cleaved OPN is not known. Since cleavage of OPN by the serine protease thrombin potentiates its inflammatory role [288-290] by exposing its RGD motif to enhance integrin binding [248, 250, 252], it is tempting to speculate a similar role for NE-cleaved OPN. However, this is a role that remains unexplored and further studies are needed.

Of note, NE inhibition did not affect OPN cleavage in all sputum samples. This may reflect the heterogeneity of the proteases involved in cleavage of OPN in sputum, and/or the variety in activity and level of NE in different samples. Unfortunately, due to the technical difficulty in obtaining sputum samples it was not possible to match sputum samples for NE levels prior to the inhibition assays. Although airway neutrophils increase at exacerbation [80, 82, 84] there was no difference in OPN cleavage between sputum exacerbation and recovery samples. This may be due to the use of a semi-quantitative method of analysis by Western blotting which may not have been sensitive enough to detect differences in cleavage.

One limitation in the clinical part of the study was the inclusion of three patients with a FEV₁/FVC greater than 70%. While one of them had radiological evidence of emphysema on CT, the other two declined scanning. Despite this, the patients' data were included in the study to reflect a closer picture to that encountered in clinical practice.

The other aim of this chapter was to explore the functional role of MMP-12 cleaved OPN. Given the importance of macrophages and their monocyte precursors in COPD [70, 107, 108, 156, 157] and the up-regulation of OPN RNA in airway macrophages in smokers, the effect of MMP-12-cleaved OPN on monocyte ROS production and macrophage phenotype was studied. MR was chosen as a marker of the M2 phenotype due to its involvement in phagocytosis [151]; IL-12 is an accepted marker of the M1 phenotype [152]. No differences in monocyte ROS production were noted between controls, uncleaved and MMP-12- cleaved OPN, and as a result the experiment was stopped after n=2. Similarly, no effect on macrophage phenotype was noted. The results obtained in the ROS analysis are somewhat similar to a previous study where no effect was noted by OPN cleavage products on neutrophil ROS production [291].

The functional experiments had a number of limitations which may explain the lack of effect of MMP-12-cleaved OPN on monocytes/ macrophages. One possible explanation may be the use of monocytes/ macrophages from healthy volunteers rather than COPD patients, the latter likely to have been more pro-inflammatory. Unfortunately, only ethics approval for bloodletting from healthy individuals was available. To somewhat counteract this effect in macrophage experiments, the isolated monocytes were matured into a M1 phenotype to more closely resemble COPD cells. However, one still cannot exclude the possibility that MMP-12-cleaved OPN would have had more of a pro-inflammatory effect had COPD macrophages been used. One could also speculate that if MMP12-cleaved-OPN causes macrophages to acquire a M1 phenotype, then the decision to mature monocytes to M1 macrophages may have hindered detection of M1 macrophage polarization by MMP12-cleaved-OPN, as the M1 phenotype had already been attained. To test this speculation a similar experiment with M2 macrophages needs to be conducted. Another possible explanation for the lack of a pro-inflammatory effect with MMP-12-cleaved OPN may be due to the concentrations of OPN chosen being too low or the MMP-12 levels being too low to cause sufficient OPN cleavage. However, OPN levels were decided in accordance with available literature [292], and the MMP-12: OPN ratio and incubation times chosen were based on earlier *in vitro* cleavage findings.

In conclusion, this study reveals OPN as a new substrate of serine proteases, in particular NE within COPD airways. OPN processing within COPD airways is closely linked to neutrophilic inflammation. In contrast, while MMP-12 readily cleaved OPN *in vitro*, it did not appear to have a major role in its processing *in vivo*. Similarly, no link between airway macrophages and OPN cleavage was noted. In view of these findings, further studies should be directed at understanding the role of airway neutrophil involvement in OPN cleavage in COPD.

Chapter 4 The Presence and Cleavage of TFPI in COPD Airways

4.0 Background

In vitro studies employing NH₂-terminal sequencing demonstrate that MMP-12 cleaves TFPI at three sites, Lys²⁰-Leu²¹, Arg⁸³-Ile⁸⁴ and Ser¹⁷⁴-Thre¹⁷⁵ [221]. This results in COOH terminal processing of TFPI [221] which prevents its binding to Xa and its inhibition of coagulation [262]. Other MMPs, notably MMP-1, 7 and 9 also cleave TFPI *in vitro* and reduce its anticoagulant effect; however, this occurs less efficiently than with MMP-12 [221]. In addition to the MMPs, NE cleaves TFPI *in vitro* into three fragments, one of the cleavage sites being Thre⁸⁷-Thre⁸⁸ [293]. Similar to cleavage by MMPs, NE proteolysis of TFPI impairs its anticoagulant activity, although the mechanism differs. NE disrupts the peptide sequence of TFPI within its NH₂-terminal region; this impairs tightening of the TFPI-Xa complex needed to prevent coagulation [293]. In addition, NE proteolysis impairs TFPI inhibition of VIIa [293]. Therefore, *in vitro* TFPI is readily susceptible to proteolytic cleavage by various enzymes which results in loss of its anti-coagulant activity. However, the relative contribution of MMP-12 to loss of TFPI function *in vivo* is unclear.

Ex vivo and *in vivo* studies on TFPI proteolysis focus on cleavage by serine proteases, rather than MMP-12. Higuchi *et al.* [293] showed that stimulated human neutrophils restore TF activity from the Xa-TFPI-VIIa/TF quaternary structure *ex vivo*, a finding reversed by the specific NE inhibitor MeO-Suc-Ala-Ala-Pro-Val-CH₂Cl. The authors suggest that this effect may be mediated by NE proteolysis of TFPI. In a study by Massberg *et al* [145], double KO mice, lacking NE and Cathepsin G (NE^{-/-}Ctsg^{-/-}) had reduced thrombus formation and prolonged bleeding times compared to WT mice. *Ex vivo*, their neutrophils were inefficient at cleaving TFPI and only able to promote coagulation to the same level as WT mice in the presence of TFPI antibody.

Furthermore, anti-TFPI Western blots of intracardiac thrombus from the double KO mice showed a clear reduction in the NE-digested TFPI fragment compared to thrombus from WT mice. These studies present a role for NE proteolysis of TFPI in promoting intravascular coagulation *in vivo*. Whether similar findings occur with cleavage of TFPI by MMP-12 *in vivo* is unknown as such studies have not been carried out on the MMP-12 KO mouse.

Belaouaj *et al.* [221] investigated the role of MMP-12-cleaved TFPI in intravascular coagulation in human samples. Sections from two endarterectomy specimens were analysed for MMP-12 and TFPI mRNA by qPCR, and the presence of both proteins was determined by immunohistochemistry. MMP-12 and TFPI mRNA were detected within the atherosclerotic plaques, as was the presence of both proteins on stained tissue slides. Of note was that sections stained more intensely for TFPI in areas that did not reveal any MMP-12. While the study suggests that TFPI is degraded by MMP-12 at sites of intravascular coagulation in humans, more work is still needed to prove this. Nonetheless, it provides an interesting working hypothesis that TFPI proteolysis by MMP-12 promotes intravascular thrombosis and hence cardiovascular disease (CVD). If this were true, one might expect patients with CVD to have lower levels of circulating TFPI due to its enzymatic degradation. Unfortunately, results from such cohort studies are conflicting and difficult to compare as they are dependent on multiple factors. These include the type of CVD studied, the enrolment of patients during an acute coronary event or patients with chronic ischaemic heart disease recruited when stable, and whether TFPI antigen levels or TFPI activity levels were measured (reviewed in [294]).

To date no similar studies exist on the role of TFPI proteolysis in CVD in COPD. COPD increases the risk of CVD two to three fold greater than that attributed to smoking

[4]. Furthermore, CVD accounts for more than a quarter deaths in COPD [43]. Therefore, given the above data, and the aforementioned importance of the proteolytic enzyme MMP-12 in COPD, it was hypothesised that TFPI is a substrate for MMP-12 in the airways whereby its cleavage leads to lower circulating levels of TFPI and an increased risk of cardiovascular disease in COPD. To detect the mechanism and level of cleavage of TFPI in COPD, a novel *ex vivo* model was used whereby sputum was collected from COPD patients at exacerbation and recovery and spiked with recombinant TFPI before detecting its cleavage using Western blotting. This was correlated to plasma levels of TFPI which in turn were correlated to a non-invasive measure of future risk of CVD in a COPD cohort, measured by the aortic pulse wave velocity, a measure of aortic stiffness [276, 295-298].

4.1 Methods

4.1.1 *In vitro* cleavage

TFPI (*R+D, Abingdon, UK*) was reconstituted at 100µg/ml in 25mM Tris and 150mM NaCl, pH 7.5; 300ng TFPI were incubated with 44ng active MMP-12 (*Enzo Life Sciences, Exeter, UK*) in deionised water in a total volume of 12µL. The reaction was carried out at 37°C for 60, 120, 150 and 180min. To inhibit MMP-12, 300ng of TFPI were incubated with 44ng active MMP-12 at 37°C in a final concentration of 25µM Ilomastat (*Sigma Aldrich, Dorset, UK*). 300ng TFPI provided the standard. Similarly, to test whether TFPI was cleaved by NE and uPA, 500ng TFPI was incubated with 0.05U NE or 55ng uPA (*all R+D*) at 37°C for 18h, with 500ng TFPI as standard.

4.1.2 Patient cohort and study design

Patients with clinically proven COPD were recruited at presentation to hospital with an exacerbation (Visit 1) and were followed up 5-7 days later (Visit 2) and again after 4 weeks (visit 3 or recovery visit). Blood for lithium heparin plasma samples and sputum was obtained at all visits where possible. Ethical approvals were granted, REC reference 10/H0403/85.

EDTA plasma samples were obtained in a further study "The Effect of Statins in Patients with COPD" (clinical trials identifier NCT01151306). Samples were taken from clinically stable patients at the baseline visit, pre-statin treatment. Clinical stability was defined as no change in regular treatment and no symptom change beyond day-to-day variation in the previous four weeks. None of the patients had a history of diabetes mellitus or ischaemic heart disease. None had been prescribed statins prior to the start of the trial. Spirometry was between 30-80% predicted. Ethical (REC 10/H0408/10) and governance (including Medicines and Healthcare Products Regulatory agency) approvals were granted.

Written informed consent was obtained before the start of each study. All procedures which were carried out in accordance with the Declaration of Helsinki [273].

4.1.3 Spirometry and CT scans

Spirometry was carried out as described in Section 2.2. The thoracic CT scan protocol is described in Section 2.4.

4.1.4 Cardiovascular measurements

These were taken in the "The Effect of Statins in Patients with COPD" trial only. This is described in section 2.3.

4.1.5 Lithium heparin plasma preparation

Blood was collected into lithium heparin containing tubes. Whole blood was spun at 2000xg for 15 min at 4°C and the resultant supernatant divided into aliquots on ice. Samples were stored at -80°C till analysis.

4.1.6 EDTA plasma preparation

Blood was collected into EDTA containing tubes. Whole blood was spun at 1000xg for 15 min at 4°C and the resultant supernatant divided into aliquots on ice. Samples were stored at -80°C till analysis.

4.1.7 Sputum induction

This was carried out as described in section 2.5.

4.1.8 Sputum processing

This was carried out as described in section 2.6. Only supernatants derived from PBS processing were used in this chapter.

4.1.9 Sputum spiking *ex vivo* experiments

Each sputum supernatant sample was diluted 1:5 in PBS and spiked with 100ng recombinant 10X HIS-tagged human TFPI (*R+D, Abingdon, UK*). Samples were incubated in a final total volume of 11µl at 37°C at various time points: 15 min, 1h, 2h, 4h, 8h, 24h, 48h, 60h and 72h. To compare cleavage of TFPI in the airways at exacerbation to cleavage at recovery, sputum obtained from Visit 1 (exacerbation sample) was spiked with TFPI as above for 15 min and compared with similarly spiked sputum obtained from Visit 3 (recovery sample). Visit 2 sputum was used as the exacerbation sample for patients unable to produce sputum at visit 1. For assays involving protease inhibitors, 1:5 diluted sputum samples were pre-incubated with protease inhibitors for 1h at 37°C.

Next, 100ng recombinant HIS-tagged human TFPI was added to the sputum/ inhibitor mix for a further 15 minutes at 37°C. The following inhibitors at the following final concentrations were used: 25µM ilomastat (*Sigma Aldrich, Dorset, UK*), 10X Serine Protease Inhibitor Cocktail (*Fisher Scientific, Loughborough, UK*), P8340 Serine, Cysteine, Aspartate, Amidopeptidase Protease inhibitor cocktail diluted 1:100 (*Sigma Aldrich*), P2801 Protease Inhibitor Cocktail VIII for Broad Range Cysteine Proteases diluted 1:100 (*Melford Biolaboratories, Ipswich, UK*), 10µM amiloride (*Sigma Aldrich*), and 1µM sivelestat (*Sigma Aldrich*). Inhibitor concentrations were used as recommended by the manufacturer. All procedures were carried out at least twice.

4.1.10 Western blotting

In vitro cleavage reaction products were diluted 1:2 in 2x loading buffer, run on 10% gels (Bio-Rad Laboratories, Hertfordshire, UK) and transferred to PVDF membranes (*Hybond-P, GE Healthcare, Amersham, Buckinghamshire, UK*) which were probed with anti-human TFPI mouse monoclonal antibody (*R+D, Abingdon, UK*) diluted 1:250, followed by HRP-conjugated polyclonal goat anti-mouse secondary antibody (*Sigma Aldrich, Dorset, UK*) diluted 1:10,000. Proteins were visualised by the addition of a chemiluminescent mixture (*GE Healthcare, Amersham, UK*) to the membranes followed by their exposure to autoradiography film (*GE Healthcare*). Experiments were carried out at least twice.

Similarly, sputum samples were diluted 1:2 in 2x loading buffer, run on 10% gels and then transferred to PVDF membranes which were probed with anti-human TFPI mouse monoclonal antibody (*R+D*) diluted 1:500, followed by HRP-conjugated polyclonal goat anti-mouse secondary antibody. Blots were exposed to autoradiography film as above. Experiments were carried out at least twice.

Ex vivo sputum spiking experiments: following incubation of recombinant human HIS-tagged TFPI in sputum, samples were diluted 1:2 in 2x loading buffer, run on 10% gels and then transferred to PVDF membranes which were probed with HRP-conjugated rabbit polyclonal anti-6XHIS antibody (*Abcam, Cambridge, UK*) diluted 1:5000. Blots were exposed to autoradiography film as above. Experiments were carried out at least twice.

4.1.11 Proteome profiler human protease array

Following sputum spiking experiments, sputum supernatant samples were arbitrarily divided into two groups: 1) samples where fragmentation of the spiked recombinant TFPI monomer was evident on Western blot within 15 min of spiking (termed “fast TFPI cleavers”) and 2) samples in which the spiked recombinant TFPI monomer took longer than 15 min to fragment (termed “slow TFPI cleavers”). Undiluted sputum supernatant was pooled into the above two separate groups to a total of 60µL per group and their protease levels compared using the Proteome Profiler Human Protease Array Kit (*R+D*). The procedure was carried out twice with a total of five slow TFPI-cleaving and nine fast TFPI-cleaving PBS sputum supernatant samples were analysed. The procedure was carried out as detailed in section 2.16.

4.1.12 ELISA

TFPI-1 levels in heparin and EDTA plasma samples were measured in duplicate using a DuoSet ELISA kit (*R+D, Abingdon, UK*). Samples were diluted 1:50-150 and their optical density measured at 450nm and 570nm in a microplate reader (*Flex Station 3, Molecular Devices, Sunnyvale, CA, USA*). The final optical density for the samples was the value read at 570nm subtracted from the 450nm value. This value was read with

reference to a 7-point 4-parameter standard curve created by using 2-fold serial dilutions starting at 1000pg/ml.

4.1.13 Analysis and statistics

Normality of data was determined using the Kolmogorov-Smirnov test or the D'Agostino normality test. Data were compared using the unpaired t-test, Mann Whitney test or the Wilcoxon matched-pairs signed rank, as appropriate. Associations between variables and TFPI plasma levels were examined using Spearman's Correlation. The level of cleaved recombinant TFPI after incubation in sputum was expressed as the optical densitometry of the spiked TFPI 40kDa monomer normalized to the optical densitometry of the standard recombinant TFPI 40kDa monomer on the same Western blot. Optical densitometry was measured in pixel density using GIMP version 2.6 1.0 (www.gimp.org). Data from the "The Effect of Statins in Patients with COPD" trial were analysed using Statistical Package for the Social Sciences version 21.0 software (*SPSS, Chicago, IL, USA*). All other data were analysed using GraphPad Prism version 6.05 (*GraphPad Software, San Diego, California, USA*). Statistical significance was set at $p < 0.05$.

4.2 Results

4.2.1 MMP-12 cleaves TFPI *in vitro*

Recombinant human TFPI monomer has a size of 40kDa. After incubation with MMP-12 at 37°C for 180 min the 40kDa monomer was completely cleaved to a ≈20kDa fragment (fig. 4.1). Cleavage was completely inhibited by 25μM ilomastat (fig. 4.1).

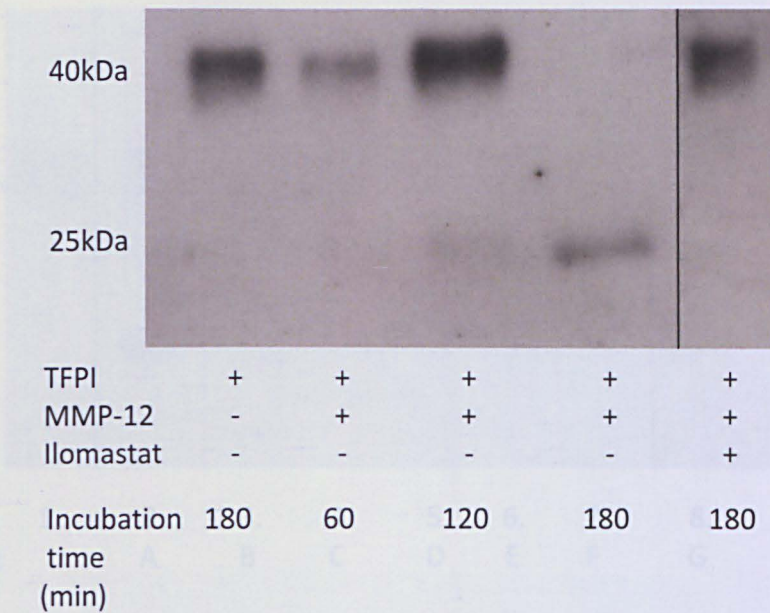


Fig. 4.1 MMP-12 cleaves TFPI *in vitro* to a \approx 20kDa fragment. Cleavage was inhibited by 25 μ M ilomastat. TFPI (300ng) was incubated with 44ng fully active MMP-12 *in vitro* at 37°C at the above time points in the presence or absence of 25 μ M ilomastat. The reactions products were resolved by 10% SDS gel electrophoresis and transferred to a PVDF membrane probed with anti-TFPI antibody. Abbreviations: MMP-12, matrix metalloproteinase-12; PVDF, polyvinylidene fluoride; TFPI, tissue factor pathway inhibitor.

4.2.2 TFPI is present in human COPD sputum in cleaved and uncleaved forms

Anti-TFPI Western blots of sputum taken from COPD patients (n=7) at the recovery visit revealed the presence of TFPI. TFPI was present in three molecular weight forms: the 40kDa monomer and 2 main fragments at \approx 30kDa and $<$ 20kDa (fig. 4.2).

with 10 μ g recombinant 10X-HIS tagged human TFPI and allowed to incubate at 37°C for 15min, 1h, 2h, 4h, 8h, 24h, 48h and 72h. Cleavage of TFPI occurred in sputum in a time-dependent manner (fig. 4.3). Recombinant TFPI was cleaved within 15 min incubation in seven samples, while cleavage took longer than 15 min in the remaining three samples. TFPI was degraded into three main fragments: \approx 30kDa, $<$ 20kDa and $<$ 15kD (fig. 4.4). Not all three fragments were visible in all samples. Since most recombinant TFPI/sputum incubations led to TFPI fragmentation within 15 min, this time point was arbitrarily taken as the cut-off for distinguishing fast TFPI-cleaving sputum samples from slow TFPI-

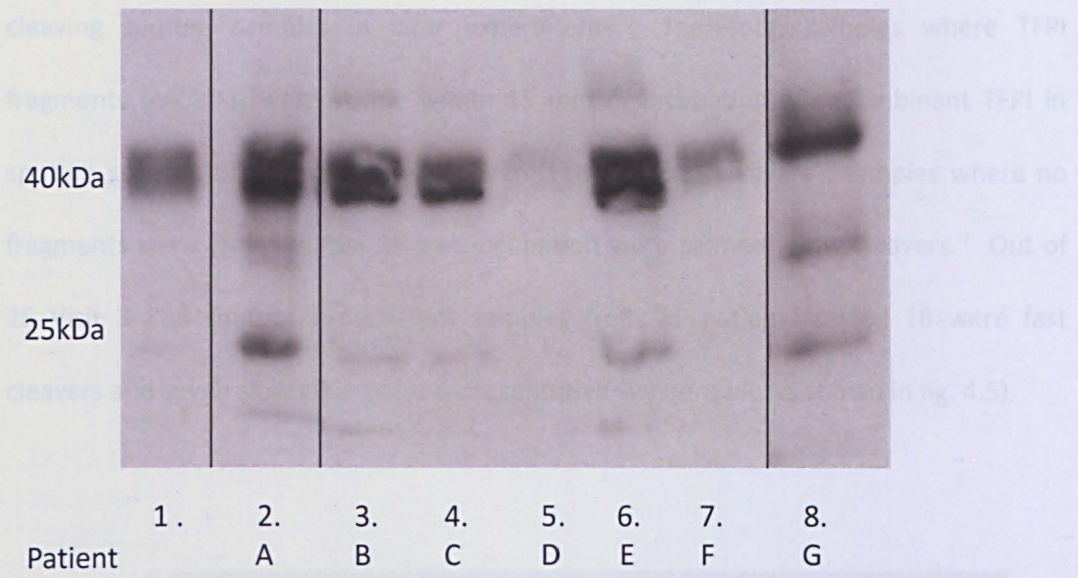


Fig. 4.2 TFPI monomer and fragments are present in human COPD sputum. Anti-TFPI Western blot: lane 1, 300ng recombinant human TFPI monomer (standard); lanes 2-8 TFPI monomer at 40kDa and TFPI fragments at \approx 30kDa and <20kDa in COPD Visit 3 sputum samples (n=7). Equal volumes of COPD sputum supernatant per patient were resolved on 10% SDS gels by electrophoresis. Proteins were then transferred to a PVDF membrane probed with anti-TFPI antibody. 300ng TFPI was used as standard. Abbreviations: PVDF, polyvinylidene fluoride; TFPI, tissue factor pathway inhibitor.

4.2.3 TFPI is cleaved *in situ* in human COPD sputum

To determine if TFPI fragments present in sputum were due to sputum protease activity, 15 diluted 1:5 human COPD sputum samples (n=3 paired exacerbation and recovery, n=3 unpaired exacerbation samples and n=6 recovery samples) were spiked with 100ng recombinant 10X HIS tagged-human TFPI and allowed to incubate at 37°C for 15min, 1h, 2h, 4h, 8h, 24h, 48h and 72h. Cleavage of TFPI occurred in sputum in a time-dependent manner (fig 4.3). Recombinant TFPI was cleaved within 15 min incubation in seven samples while cleavage took longer than 15 min in the remaining three samples. TFPI was degraded into three main fragments: \approx 30kDa, <20kDa and <15kD (fig. 4.4). Not all three fragments were visible in all samples. Since most recombinant TFPI/ sputum incubations led to TFPI fragmentation within 15 min, this time point was arbitrarily taken as the cut-off for distinguishing fast TFPI-cleaving sputum samples from slow TFPI-

cleaving sputum samples in later experiments. Therefore, samples where TFPI fragments (<40kDa) were visible within 15 min of incubation of recombinant TFPI in sputum supernatant on Western blot were termed “fast cleavers”, samples where no fragments were visible within 15 min incubation were termed “slow cleavers.” Out of 25 Visit 3 PBS sputum supernatant samples from 25 patients tested 18 were fast cleavers and seven slow cleavers (a representative Western blot is shown in fig. 4.5).

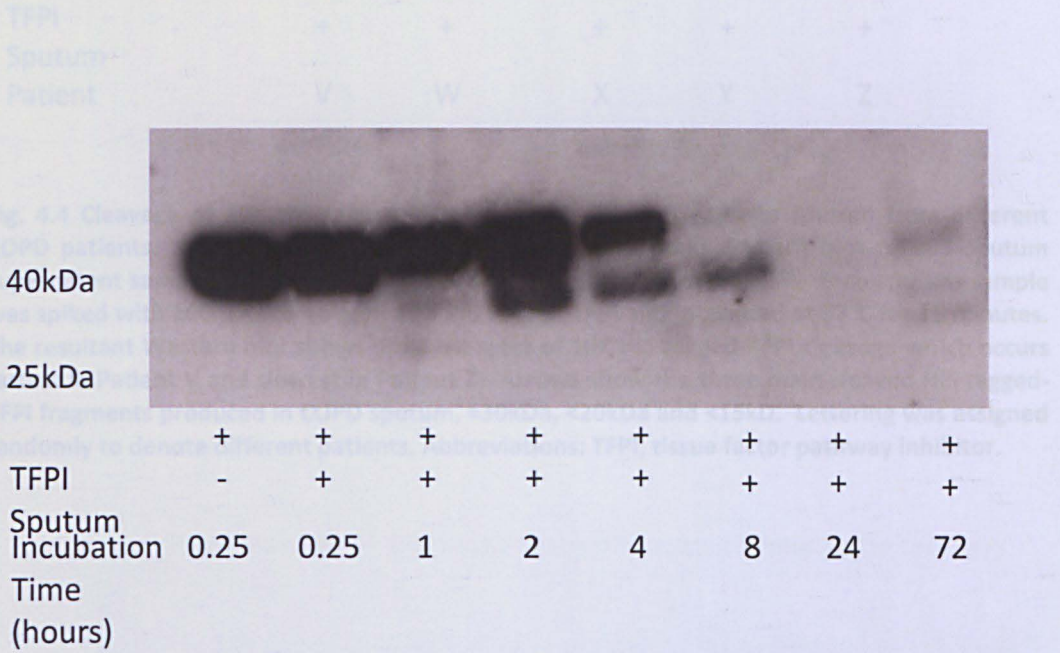


Fig. 4.3 TFPI cleavage in COPD sputum is time-dependent. Representative anti-6X HIS probed western blot of one PBS sputum supernatant sample shows increasing degradation of recombinant 10X HIS tagged-TFPI in COPD sputum with increasing duration of incubation in sputum at 37°C. Abbreviations: TFPI, tissue factor pathway inhibitor.

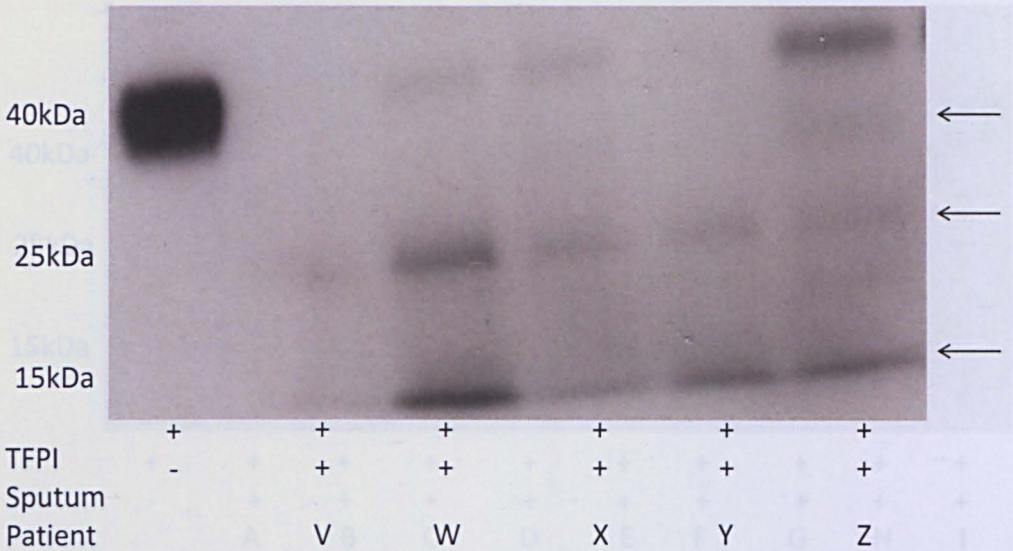


Fig. 4.4 Cleavage of 10X HIS tagged-TFPI occurs at different rates in sputum from different COPD patients. Representative anti-6X HIS antibody probed western blot of PBS sputum supernatant samples from 5 patients, V-Z, taken from the recovery visit. Each sputum sample was spiked with 100ng recombinant 10X HIS tagged-TFPI and incubated at 37°C for 15 minutes. The resultant Western blot shows different rates of 10X HIS tagged-TFPI cleavage which occurs fastest in Patient V and slowest in Patient Z. Arrows show the three main cleaved HIS tagged-TFPI fragments produced in COPD sputum, ~30kDa, <20kDa and <15kD. Lettering was assigned randomly to denote different patients. Abbreviations: TFPI, tissue factor pathway inhibitor.

4.2.4 Comparison of cleavage of TFPI in COPD sputum at exacerbation and recovery

Further to the above sputum spiking experiments recombinant 10X HIS tagged-human TFPI was incubated in exacerbation sputum samples for 15 min at 37°C and compared to similarly spiked matched sputum samples at recovery (n=16 paired samples). No difference in TFPI cleavage was noted between exacerbation and recovery sputum samples, as measured by the optical densitometry of the 40kDa 10X HIS tagged-TFPI monomer after incubation in sputum (p=0.28, Wilcoxon matched-pairs signed rank test) (fig. 4.5). A representative Western blot it shows in fig. 4.7.

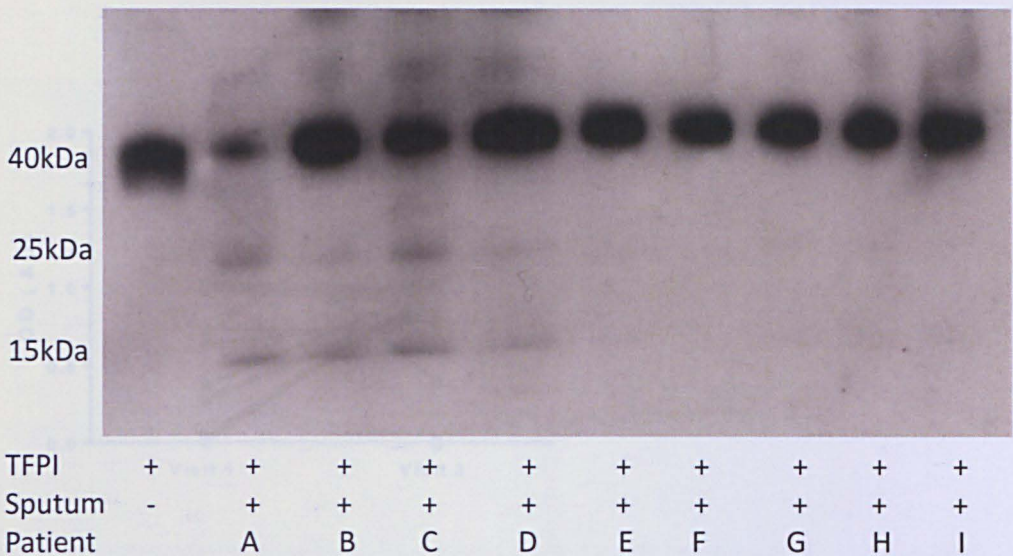


Fig. 4.5 Cleavage of 10X HIS tagged-TFPI occurs at different rates in sputum from different COPD patients. Representative anti-6X HIS antibody probed Western blot of PBS sputum supernatant samples from nine patients, A-I, taken from the recovery visit: each sputum sample was diluted 1:5 in PBS, spiked with 100ng 10X HIS tagged-TFPI and incubated at 37°C for 15 min. Lettering was assigned randomly to denote different patients. Abbreviations: TFPI, tissue factor pathway inhibitor.

4.2.4 Comparison of cleavage of TFPI in COPD sputum at exacerbation and recovery

Further to the above sputum spiking experiments recombinant 10X HIS tagged-human TFPI was incubated in exacerbation sputum samples for 15 min at 37°C and compared to similarly spiked matched sputum samples at recovery (n=16 paired samples). No difference in TFPI cleavage was noted between exacerbation and recovery sputum samples, as measured by the optical densitometry of the 40kDa 10X HIS tagged-TFPI monomer after incubation in sputum (p=0.28, Wilcoxon matched-pairs signed rank test) (fig. 4.6). A representative Western blot is shown in fig. 4.7.

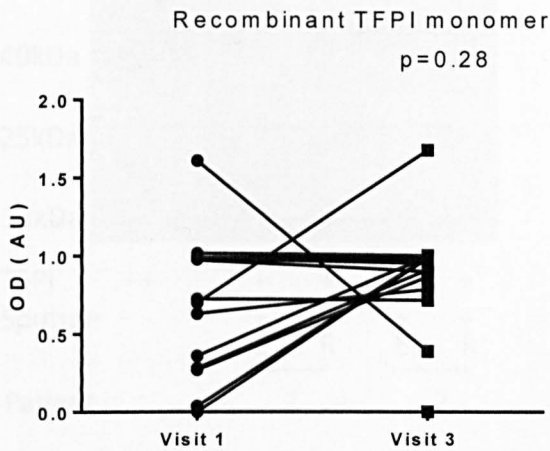


Fig. 4.6 Level of cleavage of human recombinant 10X HIS tagged-TFPI in sputum supernatant was similar at Visit 1 (exacerbation) and Visit 3 (recovery). 10X HIS tagged-TFPI (100ng/ per sputum sample) was incubated in paired Visit 1 and 3 PBS sputum supernatant samples for 15 min at 37°C. Sample proteins were then resolved by gel electrophoresis and transferred to a PVDF membrane which was then probed with anti-6X HIS tag antibody to measure the remaining recombinant TFPI after its incubation in sputum. The graph therefore represents the optical densitometry of the remaining signal of recombinant TFPI on Western blot. All values were normalised to the TFPI standard on each blot (n=16 paired samples p=0.28, Wilcoxon matched-pairs signed rank test). There was no statistical difference in protein signal between exacerbation and recovery samples as shown by silver stain of a representative group of paired sputum supernatant samples analysed from the cohort (fig. 3.4 a and b). Abbreviations: AU, arbitrary units; OD, optical densitometry; TFPI, tissue factor pathway inhibitor.



Fig. 4.7 Representative anti-6X HIS antibody probed western blot comparing degradation of 10X HIS tagged-TFPI in COPD PBS supernatant sputum in paired samples taken at exacerbation and recovery in two patients. Abbreviations: E, exacerbation; R, recovery; TFPI, tissue factor pathway inhibitor.

4.2.5 Proteome profiler assay

To explore further the differences in sputum proteases between fast and slow TFPI-cleaving samples a proteome profiler assay was employed. Fig. 4.8a-d show the differences in PBS sputum supernatant levels between fast TFPI cleavers and slow TFPI cleavers (n=9 fast cleavers, n=5 slow cleavers). Since data could not be analysed statistically, they were described qualitatively. Compared to slow TFPI cleavers, fast TFPI cleavers had ≥ 1.5 X higher mean levels of Neprilysin, Presenilin-1, uPA, Kallikrein 7, and the metalloproteases MMP-1, MMP-2, MMP-3, MMP-7, MMP-8, MMP-12, MMP-13, ADAM 8, ADAM 9, ADAMTS1 and ADAMTS13. Compared to fast TFPI cleavers, slow TFPI cleavers had ≥ 1.5 X higher mean levels of PR3 (proteinase 3) and Cathepsins E and L.

Inhibitors

A series of inhibition assays were carried out to determine the main protease classes involved in sputum TFPI cleavage. First 3 PBS sputum supernatant samples from five COPD patients were spiked with TFPI in the presence or absence of the following inhibitors: 1) the metalloprotease inhibitor EDTA, 2) a serine protease

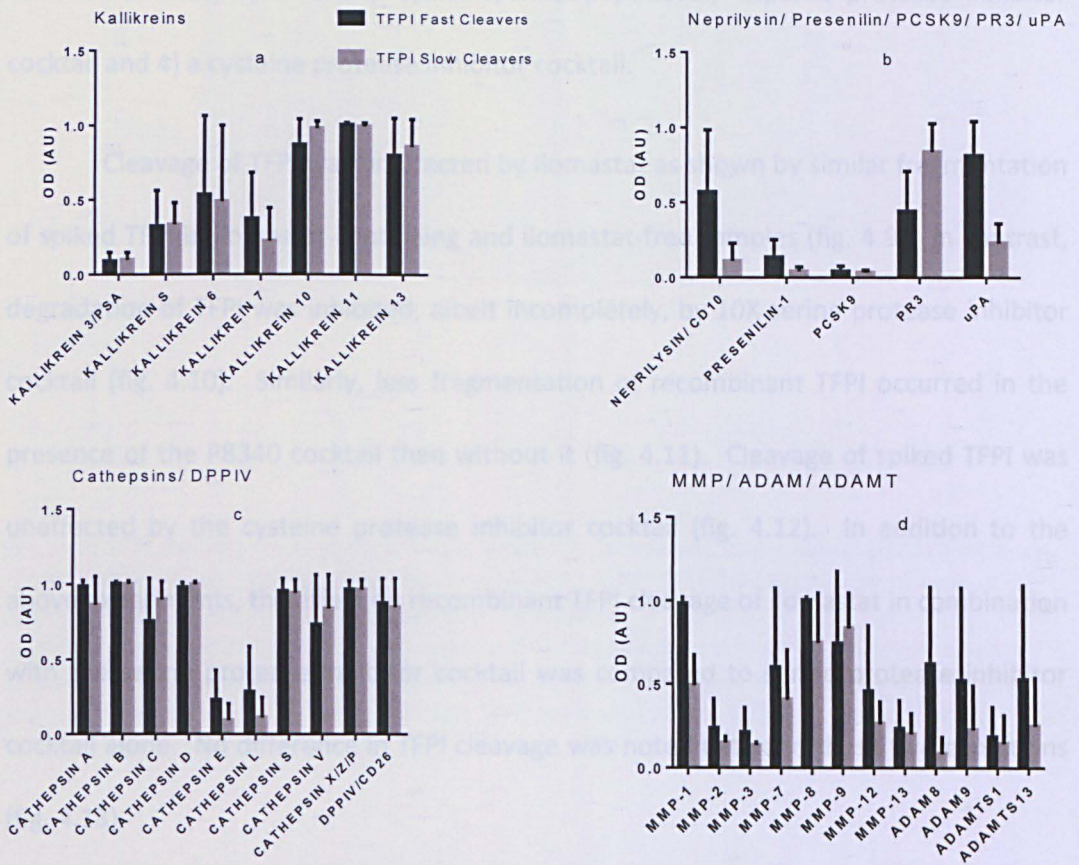


Fig. 4.8a-d Differences in sputum protease levels between fast (black) TFPI cleavers and slow (grey) TFPI cleavers. Over two experiments, PBS sputum supernatant recovery samples were pooled from nine fast TFPI cleavers and five slow TFPI cleavers. A total of 60 μ L sputum were pooled into each group each time the experiment was conducted. Compared to slow TFPI cleavers, fast TFPI cleavers had ≥ 1.5 X higher mean levels of Nepriylisin, Presenilin-1, uPA, Kallikrein 7, and the metalloproteases MMP-1, MMP-2, MMP-3, MMP-7, MMP-8, MMP-12, MMP-13, ADAM 8, ADAM 9, ADAMTS1 and ADAMTS13. Abbreviations: AU, arbitrary units; DDPIV, dipeptidyl-peptidase 4; MMP, matrix metalloproteinase; OD, optical densitometry; PCSK9, proprotein convertase 9; PR3, proteinase 3; TFPI, tissue factor pathway inhibitor; uPA, urokinase-type plasminogen activator.

4.2.6 Inhibition Assays: *ex vivo* sputum cleavage of TFPI in the presence of protease inhibitors

A series of inhibition assays were carried out to determine the main protease class/es involved in sputum TFPI cleavage. Visit 3 PBS sputum supernatant samples from five COPD patients were spiked with TFPI in the presence or absence of the following inhibitors: 1) the metalloprotease inhibitor Ilomastat, 2) a serine protease

inhibitor cocktail, 3) a serine/ cysteine/amidopeptidases/ aspartic protease inhibitor cocktail and 4) a cysteine protease inhibitor cocktail.

Cleavage of TFPI was unaffected by Ilomastat as shown by similar fragmentation of spiked TFPI in ilomastat-containing and ilomastat-free samples (fig. 4.9). In contrast, degradation of TFPI was inhibited, albeit incompletely, by 10X serine protease inhibitor cocktail (fig. 4.10). Similarly, less fragmentation of recombinant TFPI occurred in the presence of the P8340 cocktail than without it (fig. 4.11). Cleavage of spiked TFPI was unaffected by the cysteine protease inhibitor cocktail (fig. 4.12). In addition to the above experiments, the effect on recombinant TFPI cleavage of ilomastat in combination with the serine protease inhibitor cocktail was compared to serine protease inhibitor cocktail alone. No difference in TFPI cleavage was noted between these two conditions (fig. 4.13).

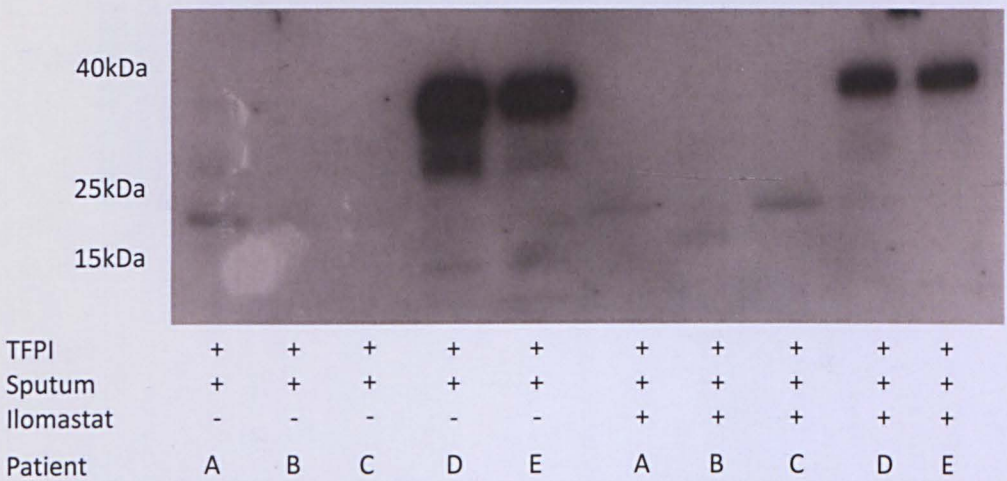


Fig. 4.9 Ilomastat does not inhibit TFPI cleavage in COPD sputum; immunoblot probed with anti-6X HIS tag antibody. Recombinant human 10X HIS tagged-TFPI (100ng) was incubated in COPD sputum, patients A-E (n=5) in the presence or absence of 25 μ M Ilomastat at 37°C for 15 minutes and its cleavage in the same patient samples compared. Lower or lack of signal intensity reflects increased recombinant TFPI degradation: patients A, B and C cleave TFPI more than patients D and E. Abbreviations: TFPI, tissue factor pathway inhibitor.



Fig. 4.10 TFPI cleavage in sputum is serine protease dependent; immunoblot probed with anti-6X HIS tag antibody. Recombinant human 10X HIS tagged-TFPI (100ng) was incubated in COPD sputum, patients A-E (n=5) in the presence or absence of 10X SPIC at 37°C for 15 min. Lower signal intensity and the presence of lower weight fragments reflect increased recombinant TFPI degradation in the absence of serine protease inhibitor; patients A, B and C cleave TFPI more than patients D and E. Abbreviations: SPIC, serine protease inhibitor cocktail; TFPI, tissue factor pathway inhibitor.

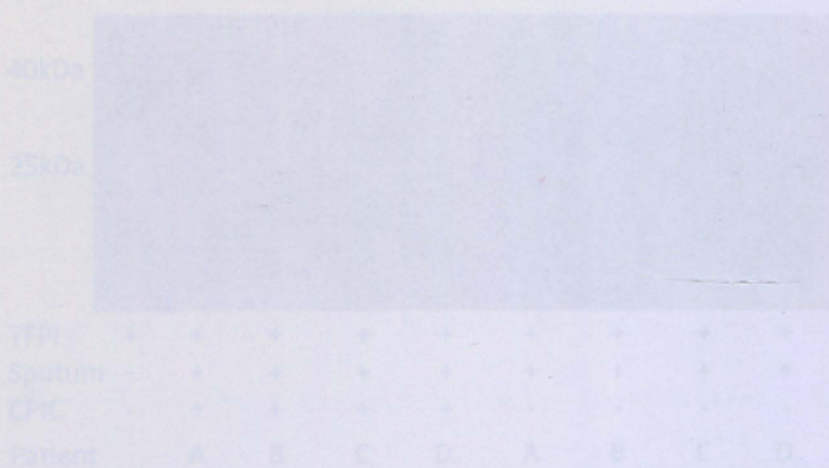


Fig. 4.11 Cysteine protease inhibition does not inhibit TFPI cleavage in COPD sputum; immunoblot probed with anti-6X HIS tag antibody. Recombinant human 10X HIS tagged-TFPI (100ng) was incubated in COPD sputum, patients A-D (n=4) in the presence or absence of cysteine protease inhibitor cocktail at 37°C for 15 min. Abbreviations: CPC, cysteine protease inhibitor cocktail; TFPI, tissue factor pathway inhibitor.

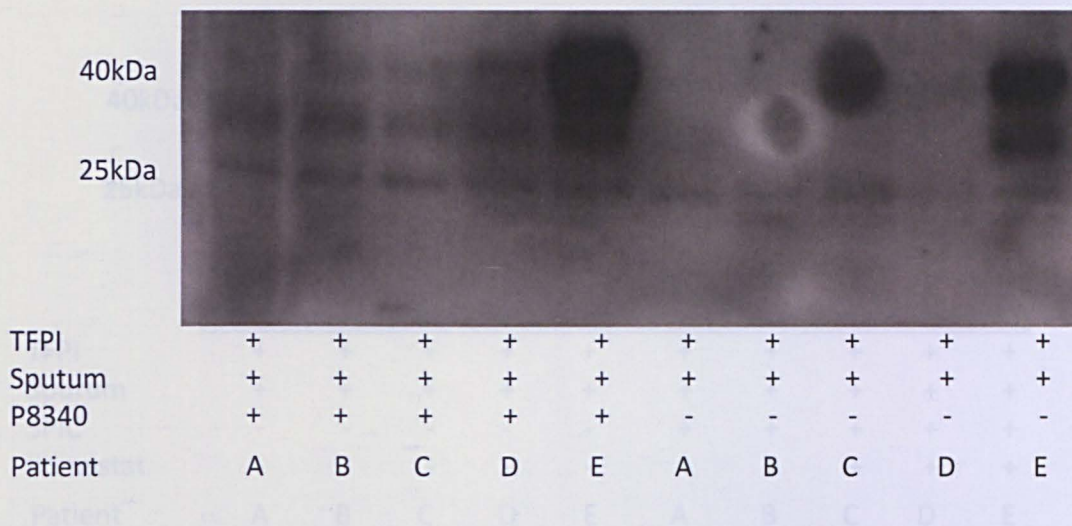


Fig. 4.11 TFPI cleavage in sputum is partially inhibited by a serine/cysteine/amidopeptidases/aspartic protease inhibitor cocktail P8340; immunoblot probed with anti-6X HIS tag antibody. Recombinant human 10X HIS tagged-TFPI (100ng) was incubated in COPD sputum, patients A-E (n=5) in the presence or absence of P8340 at 37°C for 15 min. Lower signal intensity and the presence of lower weight fragments reflect increased recombinant TFPI degradation in the absence of inhibitor cocktail; patients A, B, C and D cleave TFPI more than patient E. Abbreviations: TFPI, tissue factor pathway inhibitor.



Fig. 4.12 Cysteine protease inhibition does not inhibit TFPI cleavage in COPD sputum; immunoblot probed with anti-6X HIS tag antibody. Recombinant human 10X HIS tagged-TFPI (100ng) was incubated in COPD sputum, patients A-D (n=4) in the presence or absence of cysteine protease inhibitor cocktail at 37°C for 15 min. Abbreviations: CPIC, cysteine protease inhibitor cocktail; TFPI, tissue factor pathway inhibitor.

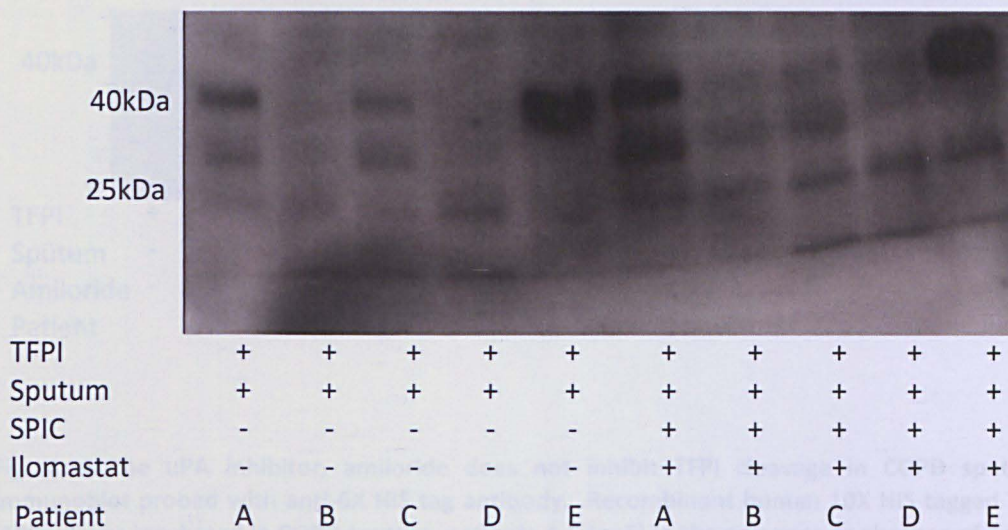


Fig. 4.13 No clear differences were noted between samples treated with 10X SPIC/ Iloprost and 10X SPIC only; immunoblot probed with anti- 6X HIS tag antibody. Recombinant human 10X HIS tagged-TFPI (100ng) was incubated in COPD sputum, patients A-E (n=5) in the presence of 10X SPIC alone or a combination of 10X SPIC/ Iloprost at 37°C for 15 min. Patients A, B, C and D cleave TFPI more than patient E. Abbreviations: SPIC, serine protease inhibitor cocktail; TFPI, tissue factor pathway inhibitor.

Further inhibition experiments were carried out to detect which serine protease/s cleaved TFPI. Amiloride (10 μ M) was chosen as it inhibits plasminogen (uPA) (K_i=7 μ M) [282] which was elevated in fast compared to slow TFPI cleavers (fig. 4.14). Sivelestat (1 μ M) was also chosen as it is an inhibitor of the serine protease NE which, although not a component of the proteome profiler assay, is an important serine protease in COPD pathogenesis. Amiloride at a concentration of 10 μ M failed to inhibit TFPI cleavage in five sputum supernatant samples from five different COPD patients while 1 μ M Sivelestat partially or completely inhibited TFPI cleavage in four of these five samples (fig. 4.15).



Fig. 4.14 The uPA inhibitor, amiloride does not inhibit TFPI cleavage in COPD sputum; immunoblot probed with anti-6X HIS tag antibody. Recombinant human 10X HIS tagged TFPI (100ng) was incubated in COPD sputum, patients A-E (n=5) in the presence or absence of a final concentration of 10 μ M Amiloride at 37°C for 15 min; its cleavage in the same patient samples was compared. Lower or lack of signal intensity reflects increased recombinant TFPI degradation. Abbreviations: TFPI, tissue factor pathway inhibitor; uPA, urokinase-type plasminogen activator.

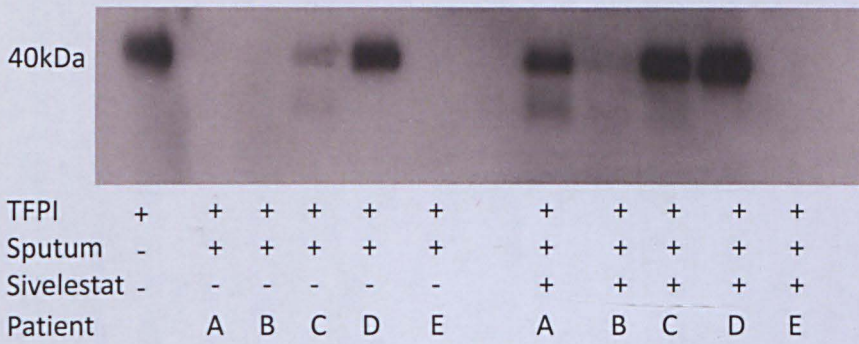


Fig. 4.15 The NE inhibitor, sivelestat inhibits TFPI cleavage in COPD sputum; immunoblot probed with anti-6X HIS tag antibody. Less TFPI degradation occurred in the presence of sivelestat (patients A-D), with the exception of patient E where complete degradation occurred irrespective of presence of the inhibitor. Recombinant human 10X HIS tagged-TFPI (100ng) was incubated in COPD sputum, patients A-E (n=5) in the presence or absence of a final concentration of 1 μ M sivelestat at 37°C for 15 min and its cleavage in the same patient samples compared. Lower or lack of signal intensity reflects increased recombinant TFPI degradation. Abbreviations: NE, neutrophil elastase, TFPI, tissue factor pathway inhibitor.

4.2.7 TFPI is cleaved by NE and uPA

Since sivelestat inhibited TFPI cleavage in some of the sputum samples (fig. 4.15), recombinant TFPI was incubated with NE *in vitro*, to confirm TFPI as a substrate for NE. Similarly, TFPI was incubated with uPA *in vitro*, as although no inhibition of TFPI cleavage was noted with the uPA inhibitor amiloride, levels of uPA were strikingly elevated in fast cleavers compared to slow cleavers (fig. 4.8b). TFPI was cleaved by both NE and uPA *in vitro*. NE cleaved TFPI to a <20kDa fragment (fig. 4.16) while uPA cleaved TFPI to a ≈35kDa fragment (fig. 4.17).

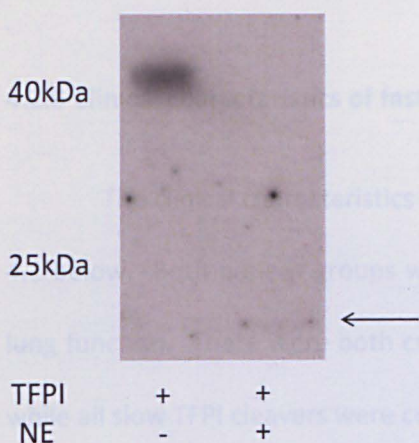


Fig. 4.16 NE cleaves TFPI *in vitro* to a <20kDa fragment (arrow). TFPI (500ng) was incubated with 0.05U NE *in vitro* at 37°C for 18h. The reactions products were resolved by 10% SDS gel electrophoresis and transferred to a PVDF membrane probed with anti-TFPI antibody. Abbreviations: NE, neutrophil elastase; PVDF, polyvinylidene fluoride; TFPI, tissue factor pathway inhibitor.

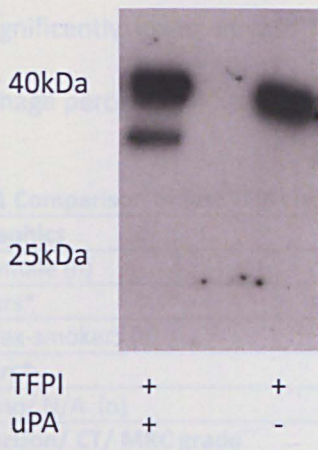


Fig. 4.17 uPA cleaves TFPI *in vitro* to a ≈ 35 kDa fragment. TFPI (500ng) was incubated with 55ng uPA *in vitro* at 37°C for 18h. The reactions products were resolved by 10% SDS gel electrophoresis and transferred to a PVDF membrane probed with anti-TFPI antibody. Abbreviations: PVDF, polyvinylidene fluoride; TFPI, tissue factor pathway inhibitor; uPA, urokinase-type plasminogen activator.

4.2.8 Clinical characteristics of fast TFPI cleavers and slow TFPI cleavers

The clinical characteristics of fast and slow TFPI cleavers are summarised in table 4.1 below. Both patient groups were similar in terms of age, cigarette pack years and lung function. There were both current and ex-smokers in the fast TFPI cleavers group while all slow TFPI cleavers were current smokers.

Sputum cell indices in the two groups are represented in fig. 4.18a-e. Sputum total cell counts (TCC) were higher in fast TFPI cleavers than slow TFPI cleavers [median (range) fast $7.18(0.50-54.90) \times 10^6$ cells/g, slow $1.29(0.37-2.78) \times 10^6$ cells/g, $p=0.001$]. Similarly, sputum neutrophil counts and sputum neutrophil percentages were higher in fast than in slow TFPI cleavers [median (range) sputum neutrophil count: fast $8.16(1.71-54.49) \times 10^6$ cells/g, slow $0.57(0.16-1.79) \times 10^6$ cells/g, $p=0.002$; mean sputum neutrophil percentage: fast $94.33\% \pm 5.25$, slow 51.04 ± 22.91 , $p=0.01$]. Sputum macrophage counts were similar between fast and slow TFPI cleavers [median (range) fast $0.36(0.00-2.49) \times 10^6$ cells/g, slow $0.35(0.15-0.90) \times 10^6$ cells/g, $p=0.71$. Sputum macrophage percentages

were significantly lower in fast TFPI cleavers than slow TFPI cleavers (mean sputum macrophage percentage: fast 5.14%±5.10 v. slow 30.78%±16.53, p<0.0001).

Table 4.1 Comparison of fast TFPI cleavers and slow TFPI cleavers

Demographics	Fast TFPI cleavers	Slow TFPI cleavers
Male/ Female (n)	17/3	6/1
Age/ Years*	68±9	64±10
Current/ex-smokers (n)	8/12	7/0
Pack years*	56±33	59±17
ICS yes/ no/ N/A (n)	16/3/1	6/1/0
Lung function/ CT/ MRC grade	Fast TFPI cleavers	Slow TFPI cleavers
FEV ₁ / L*	1.33±0.73	1.53±0.62
FEV ₁ / percent predicted*	47.5±20.79	51.86±6.40
FEV ₁ /FVC*	0.47±0.16	53.43±13.44
Emphysema on CT yes/ no /N/A (n)	10/7/3	5/0/2
MRC grades 3-5 (n)	Grade 3(5), 4 (6), 5(9)	Grade 3(2), 4 (2), 5(3)
Sputum cell counts	Fast TFPI cleavers	Slow TFPI cleavers
Sputum TCC/ x10 ⁶ cells/g median (range) ⁺	7.18(0.50-54.90)	1.29(0.37-2.78)
Sputum neutrophil count/ x10 ⁶ cells/g median (range) ⁺	8.16(1.71-54.49)	0.57(0.16-1.79)
Sputum macrophage count/ x10 ⁶ cells/g median (range)	0.36(0.00-2.49)	0.35(0.15-0.90)
Sputum neutrophil percentage* ⁺	94.33±5.25	51.04±22.91
Sputum macrophage percentage* ⁺	5.14±5.10	30.78±16.53
Plasma Measurements	Fast TFPI cleavers	Slow TFPI cleavers
Heparin Plasma TFPI levels/ngml ⁻¹ * ⁺	6.36±1.37	12.99±12.46

*Data presented as mean ±standard deviation; ⁺p<0.05. Abbreviations: ICS, Inhaled corticosteroids (n), number; N/A, not available; TCC, total cell count; TFPI, tissue factor pathway inhibitor

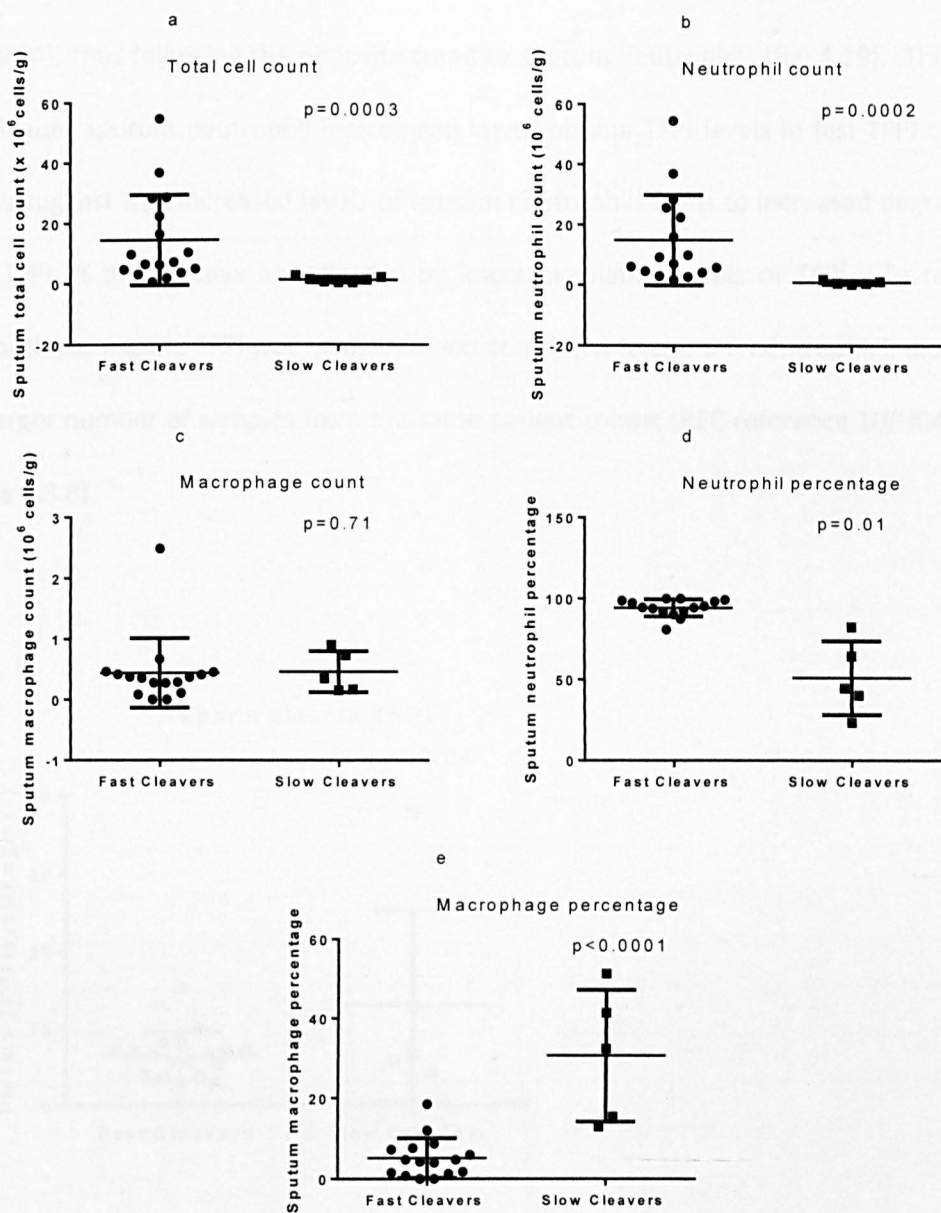


Fig. 4.18 Sputum indices were compared between fast and slow TFPI cleavers. Fast TFPI cleavers had higher TCC ($p=0.0003$) (a), higher neutrophil counts ($p=0.0002$) (b), higher neutrophil percentages (d) and lower macrophage percentages ($p<0.0001$) (e) compared to slow TFPI cleavers. There were similar macrophage counts between fast and slow cleavers ($p=0.71$) (c). TCC data were available for $n=17$ fast TFPI cleavers, $n=7$ slow TFPI cleavers; for all other sputum indices $n=16$ fast TFPI cleavers, $n=5$ slow cleavers, $p<0.05$ taken as significant. TCC, neutrophil counts and macrophage counts were compared using the Mann Whitney test. Neutrophil percentages and macrophage percentages were compared using the unpaired t-test. Abbreviations: TCC, total cell count; TFPI, tissue factor pathway inhibitor.

Heparin plasma TFPI levels were first measured in the above fast TFPI ($n=18$) and slow TFPI cleavers ($n=7$). Levels were significantly lower in fast TFPI cleavers

compared to slow TFPI cleavers (mean TFPI levels 6.36 ± 1.37 , 12.99 ± 12.46 respectively, $p=0.04$), thus following the opposite trend to sputum neutrophils (fig. 4.19). This trend of higher sputum neutrophil indices and lower plasma TFPI levels in fast TFPI cleavers may suggest that increased levels of sputum neutrophils leads to increased degradation of TFPI in the airways as reflected by lower circulating levels of TFPI. To test this hypothesis plasma TFPI was measured and correlated to sputum neutrophil indices in a larger number of samples from the same patient cohort (REC reference 10/H0403/85) (see 4.3.8).

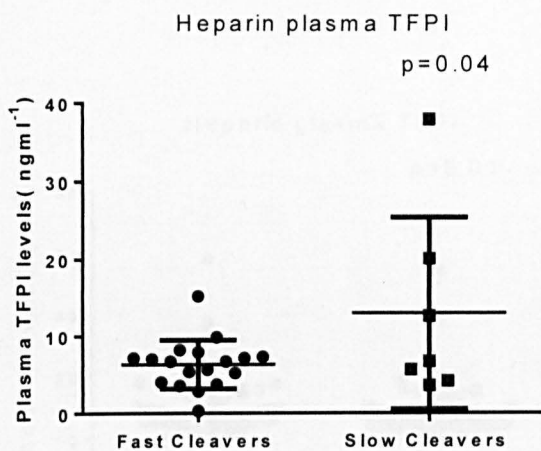


Fig. 4.19 Fast TFPI cleavers had lower heparin plasma TFPI levels compared to slow TFPI cleavers ($n=18$ fast TFPI cleavers, 7 slow TFPI cleavers, $p=0.04$, unpaired t-test). Abbreviations: TFPI, tissue factor pathway inhibitor.

4.2.9 Heparin plasma TFPI levels at exacerbation and recovery

TFPI levels were measured in 72 paired exacerbation (Visit 1) and recovery (Visit3) samples. Plasma TFPI levels were significantly raised at exacerbation compared to recovery [median (range) 6.45 ($0.00-58.20$) ng ml^{-1} , 5.55 ($0.30-54.13$) ng ml^{-1} respectively, $p=0.01$] (fig. 4.20). At visit 3 plasma TFPI levels negatively correlated to

sputum neutrophil counts ($r=-0.4$, $p=0.03$, $n=32$ patients fig. 4.21) No correlation was noted between plasma TFPI levels and sputum neutrophil counts at visit 1, although the direction of the relationship was similar to that seen at Visit 3 ($r=-0.1$, $p=0.63$, $n=26$ patients). Plasma TFPI levels did not correlate with sputum neutrophil percentages at Visits 1 or 3. Similarly, no correlation was noted between plasma TFPI levels and sputum macrophage counts, sputum macrophage percentages or sputum TCC at either visit. The correlation data between heparin plasma TFPI levels and sputum indices is summarised in table 4.2 below.

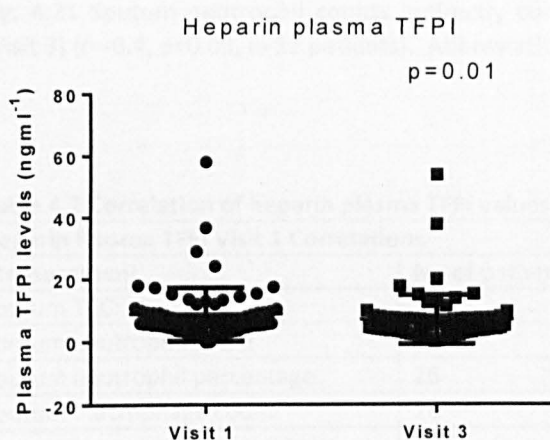


Fig. 4.20 Plasma TFPI levels are elevated at exacerbation (Visit 1) compared to recovery (Visit 3) ($n=72$ [median (range) 6.45 ($0.00-58.20$) ng ml^{-1} , 5.55 ($0.30-54.13$) ng ml^{-1} , respectively, $p=0.01$ Wilcoxon matched-pairs signed rank test]. Abbreviations: TFPI, tissue factor pathway inhibitor.

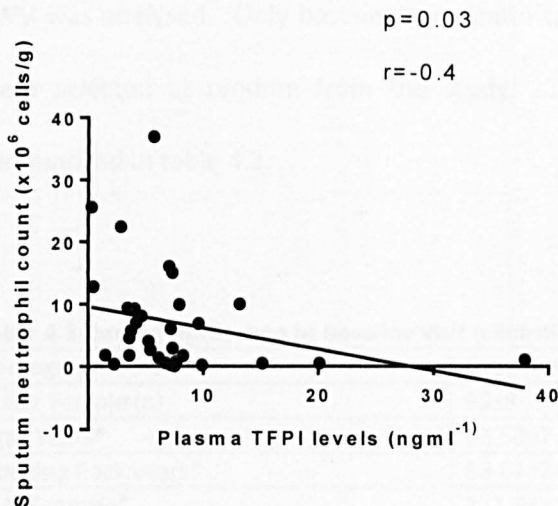


Fig. 4.21 Sputum neutrophil counts indirectly correlate with plasma TFPI levels at recovery (Visit 3) ($r=-0.4$, $p=0.03$, $n=32$ patients). Abbreviations: TFPI, tissue factor pathway inhibitor

Table 4.2 Correlation of heparin plasma TFPI values at Visit 1 and Visit 3 to sputum cell indices

Heparin Plasma TFPI Visit 1 Correlations			
Measurement	No of patients	r value	p value
Sputum TCC	30	0.06	0.74
Sputum neutrophil count	26	-0.11	0.60
Sputum neutrophil percentage	26	0.05	0.80
Sputum macrophage count	26	-0.10	0.63
Sputum macrophage percentage	26	0.11	0.57
Heparin Plasma TFPI Visit 3 Correlations			
Measurement	n	r value	p value
Sputum TCC	37	-0.30	0.09
Sputum neutrophil count*	32	-0.40	0.03
Sputum neutrophil percentage	32	-0.16	0.39
Sputum macrophage count	32	-0.24	0.19
Sputum macrophage percentage	32	0.14	0.44

Abbreviations: TCC, Total Cell Count; TFPI, tissue factor pathway inhibitor. * $p<0.05$

4.2.10 Correlation of plasma TFPI levels to aortic stiffness

To test the hypothesis that cleaved, *i.e.* lower TFPI levels were associated with increased aortic stiffness the relationship between EDTA plasma TFPI levels and aortic PWV was analysed. Only baseline (pre-statin treatment) data were used. 40 patients were selected at random from the study. The demographic data at baseline are summarized in table 4.3.

Table 4.3 Demographic data at baseline visit (clinical trial NCT01151306)

Demographic Data	Baseline Visit
Male/ Female (n)	32/8
Age/ Years*	63.50±7.25
Smoking Pack years*	53.61±24.99
MAP/ mmHg*	111.43±17.19
FEV ₁ / L*	1.55±0.56
FEV ₁ / percent predicted*	54.45±14.26
FEV ₁ /FVC*	47.05±12.03
Aortic PWV/ ms ⁻¹	9.65±3.26
EDTA Plasma TFPI levels/ngml ⁻¹ **	89.26±25.99

*Data presented as mean ±standard deviation Abbreviations: MAP, Mean Arterial Pressure; PWV, Pulse Wave Velocity; TFPI, tissue factor pathway inhibitor

Univariate analysis revealed a positive correlation between plasma TFPI levels and aortic PWV ($r=0.41$, $p=0.009$). There was no significant correlation between TFPI levels and FEV₁, FVC, gender, age or pack years. Similarly, there was no significant correlation between aortic PWV and gender, age or smoking pack years. PWV and MAP correlated positively ($r=0.48$, $p=0.02$). In the multivariate linear regression analysis aortic PWV was chosen as the dependent variable; age, smoking pack years, gender, MAP and plasma TFPI level as independent variables. This significant positive correlation between aortic PWV and plasma TFPI level persisted even after adjusting for age, smoking pack years, gender and MAP using multivariate linear regression (partial correlation= 0.39 , $p=0.014$).

4.3 Discussion

This chapter presents several novel findings. For the first time TFPI is shown to be present in the airways where it is also cleaved. Its cleavage is mainly neutrophil driven, occurring faster in the presence of higher sputum neutrophils, and most limited when NE is inhibited. In addition, circulating TFPI levels are indirectly correlated to sputum neutrophil counts, leading to speculation that its degradation by neutrophil enzymes results in lower detectable levels in blood. These findings are important as they not only reveal a new substrate for NE in COPD, but also uncover a potential new role for the airways – involvement in coagulation. The latter may be useful in understanding the link between airway inflammation and the risk of thrombotic events in COPD [4, 9, 40-42, 299].

The *in vitro* findings in this chapter which demonstrate TFPI cleavage by MMP-12 and NE are in agreement with previously published data [221, 293]. This study adds to the complexity of TFPI proteolysis by introducing uPA as another protease that cleaves TFPI *in vitro*. Indeed, this complexity may explain why none of the protease inhibitors used alone inhibited TFPI cleavage completely. *In vitro* cleavage of TFPI by MMP-12 and NE produced a <25kDa and a <20kDa fragment, respectively while uPA cleaved TFPI to a 35kDa fragment. Western blots of COPD sputum probed with anti-TFPI antibody as well as the sputum spiking experiments showed similar sized fragments to those obtained *in vitro*. This suggests TFPI is cleaved by these proteases in sputum, although it does not clarify whether the <20/25kDa fragments are produced by MMP-12 or NE alone, or indeed both.

With the exception of one sputum sample, the NE inhibitor sivelestat, prevented complete degradation of TFPI in sputum, but allowed partial cleavage to the 35kDa fragment, suggesting that while NE cleaves TFPI it is not involved in the release of this

particular 35kDa fragment. This appears to be produced by uPA. The broad spectrum ilomastat failed to inhibit TFPI cleavage in sputum. Since ilomastat inhibited *in vitro* TFPI cleavage by MMP-12 and since the literature reveals that lower levels of MMP-12 are present in COPD sputum [122] than those used in the *in vitro* assays, one would expect to see some inhibition of TFPI cleavage with ilomastat if MMP-12 were significantly involved in TFPI degradation. Furthermore, macrophage number, the source of MMP-12 [198], is not positively related to TFPI cleavage. However, one cannot rule out the possibility that MMP-12 cleavage of TFPI is overshadowed by a higher degree of NE activity given that both proteases produce a similar sized fragment.

The study in this chapter first centred on the cleavage of TFPI in the airways, as this is the main site of protease activity in COPD. While TFPI was found to be present in the airways the reason for this or the mechanism by which this occurs is unknown. TFPI is secreted by the endothelium [255] which, within the lungs, is in close proximity to alveoli. One possibility may be that TFPI diffuses across the endothelial-epithelial barrier. The next step was to look at how TFPI degradation in the airways was related to levels in the vasculature where thrombotic events occur. Due to a limited supply of samples it was not possible to directly correlate sputum and plasma TFPI levels. However, in the study it was noted that patients termed “fast cleavers” had a tendency to lower plasma TFPI levels. While accepting that sample numbers were rather low in the slow cleavers group, the findings suggested that increased degradation of TFPI in the airways was associated with lower TFPI levels in the circulation.

Unexpectedly, plasma TFPI was higher at exacerbation than recovery which is the reverse of what was expected given that airway neutrophil counts rise at exacerbation. These findings may partly be explained by increased production of TFPI in inflammatory states as a result of endothelial dysfunction [257]. Furthermore, perhaps

increased “leakiness” of the endothelium during heightened inflammatory states [300] allows more TFPI to travel across the endothelial-alveolar epithelial barrier. A less recognized function of TFPI is anti-bacterial activity. In a mouse model of severe sepsis the C-terminal fragment of recombinant TFPI activated complement leading to a microbicidal effect against *E.coli* [301]. This raises the possibility that increased circulating levels of TFPI at exacerbation may be a pathophysiological response to contain infection. Another discrepancy was that no difference in TFPI cleavage was noted between sputum exacerbation and recovery samples. This may be due to the use of a semi-quantitative method of analysis which may not have been sensitive enough to detect differences in cleavage.

Given that previous studies show loss of anticoagulant function following TFPI degradation [221, 293], it was hypothesized that low plasma TFPI would be associated with an increased risk of CVD, measured by a higher aortic PWV [276, 295, 296]. The results, however, showed the opposite findings. Higher plasma TFPI levels were positively correlated with higher aortic PWV; this relationship remained statistically significant even after multivariate analysis. Of note, however, is that this is in keeping with most CVD studies whereby higher TFPI levels predict CVD risk (reviewed in [294]). Similarly, in the previous study TFPI levels increased at exacerbation, a time of increased risk of thrombotic events [41, 42], although it must be pointed out that plasma was collected differently in the two studies which led to a difference in magnitude in TFPI measurements. TFPI has previously been identified as a marker of endothelial dysfunction [302]. Since endothelial dysfunction reportedly precedes angiographic or invasive ultrasonographic evidence of atherosclerotic plaques [303], TFPI may have potential use as an early biomarker of CVD in COPD. Another explanation for the strong positive relationship between TFPI and aortic PWV may be that wider pressure differences across arteries increase blood flow turbulence leading to direct stimulation

of the endothelium and subsequent release of TFPI. However this is only a speculative suggestion and currently there are no data to support this.

5.1 Background

In conclusion, TFPI is present in the airways in COPD where it is degraded by NE. Within the circulation TFPI levels increase at exacerbation and are positively related to aortic stiffness. TFPI may therefore be useful as an early biomarker of increased CVD risk in COPD. Further studies are needed to better understand the link between the presence and cleavage of TFPI in the airways and its role in the circulation.

Chapter 5 Identifying MMP-12 substrates in COPD

5.0 Background

In the previous two chapters a candidate based approach was used to determine whether substrates cleaved by MMP-12 *in vitro* were also targets of this enzyme in COPD. Similar to other biological systems [26, 304], a “protease web” exists in COPD airways [60, 99, 305] whereby substrate degradation is the result of a series of “cross talks” between various proteases. This makes it challenging to match cleavage of a substrate to the activity of a specific protease. Exploring a particular protease degradome *in vivo* therefore requires a more sophisticated high throughput technique that addresses such complexities.

MMP-12 was first identified in macrophages as an elastinolytic protease [197]. Discovery of resistance to cigarette smoke-induced emphysema in *Mmp-12*^{-/-} mice ensued [100]. This promoted the idea that MMP-12 was destructive. Yet more recent data has challenged this belief by extending the role of MMP-12 beyond elastin degradation to inactivation of pro-inflammatory mediators. *In vitro*, MMP-12 inactivates murine ELR⁺ chemokines CCL-2, 7, 8 and 13 by cleavage at position 4-5 which may explain the increased neutrophil and macrophage recruitment to LPS in airways of *Mmp-12*^{-/-} mice [115]. Similarly, MMP-12 is protective in viral infection in mice partly by its cleavage of interferon-alpha [306]. In a collagen-induced arthritis model *Mmp-12*^{-/-} mice suffered more severe neutrophilic joint inflammation due to lack of MMP-12 cleavage and subsequent inactivation of complement factors C3a and C5a [307]. This paradoxical role of MMP-12 in inflammation and its ever-expanding known substrate profile further adds to the difficulty in using a candidate approach to explore new MMP-12 substrates in COPD.

TAILS (terminal amine isotopic labelling of substrates) is a novel proteomic technique used to determine the substrate profile of a specific protease within a complex biological system. This involves labelling the N-terminal end of peptides (the N-terminome) within a sample, followed by their identification by LC-MS/MS analysis [228, 229]. Thus, a particular protease degradome may be determined by comparing the differentially labelled N-terminomes of protease-treated and control samples. Alternatively, the N-terminome of a specific protease KO mouse may be compared to its WT counterpart. In addition to the identification and relative quantification of peptides between samples, TAILS enables the determination of the precise cleavage sites of these peptides as well as the natural N-terminus of proteins. The previous use of gel electrophoresis for peptide resolution prior to identification is unnecessary with TAILS which enables more accurate identification of a larger number of peptides [308, 309]. Furthermore, while previous methods of degradome determination may have relied on genetic overexpression of a protease or its introduction into a cell line that constitutively lacks it, the sensitivity of TAILS [308-310] does away with this, allowing exploration under more physiological conditions. Indeed, TAILS has been successfully employed to identify new MMP-12 substrates in viral infections [306] and in a collagen-induced arthritis murine model [307]. This makes it a useful tool to determine the MMP-12 degradome in COPD airways by applying it to the *Mmp-12*^{-/-} smoking mouse model.

Human COPD sputum is a rich source of proteases [20, 60, 122, 213-215] resulting from the influx of inflammatory cells into the airways [66, 68, 69]. While the activity of proteases is thought to be linked to airway damage [18, 20, 98-100, 305] and airflow limitation in COPD [305] little is known about their proteolytic processed signatures. This would be useful to understand the underlying mechanism. Most studies focus on one protease only, thus failing to address the complexity of protease activity, or this “protease web”. Verrills et al [311] identified, using a proteomic

approach, peptide differences between asthmatic, COPD and healthy subjects. However, the study was carried out on blood samples which limits its use given that *airway* inflammation is central to COPD pathogenesis. In another study [312] the sputum degradome was analysed, using a shotgun proteomics approach following gel electrophoresis, leading to a low number of confident peptides. Therefore, there is an urgent need to use newer proteomics approaches to study the COPD sputum degradome: the sputome.

Based on previous observations [306, 307], MMP-12 plays a pivotal role in chemokine processing and affects the resolution of inflammation, thus extending its proteolytic substrates repertoire outside the ECM matrix substrates. The hypothesis was that in COPD MMP-12 targets immune and inflammatory components outside the extracellular matrix. The aims of this chapter were firstly to identify MMP-12 substrates using a smoking *Mmp-12*^{-/-} mouse model, and secondly to search for the newly identified murine MMP-12 substrates in human COPD sputum. TAILS was therefore used for the relative quantification of substrates in the BALF of *Mmp-12*^{-/-} mice and their WT counterparts. Next the MMP-12 targets identified in mice were searched for in nine paired exacerbation and recovery COPD sputum samples using TAILS. In doing so not only was the degradome and N-terminome of COPD sputum described, but peptide differences at exacerbation and recovery were also determined.

5.1 Methods

5.1.1 BALF samples from *Mmp-12^{-/-}* and *Mmp-12^{+/+}* mice

Mouse BALF samples were a very generous gift from Professor Steven D. Shapiro (Division of Pulmonary, Allergy and Critical Care Medicine, University of Pittsburgh). *Mmp-12^{-/-}* and *Mmp-12^{+/+}* mice (n = 4) were exposed to cigarette smoke from 2 unfiltered cigarettes (University of Kentucky) 6 days a week for 6 weeks, the time needed for *Mmp-12^{+/+}* mice to develop emphysema; *Mmp-12^{-/-}* mice remain emphysema-free [100]. Mice were then sacrificed followed by the insertion of a 22-gauge i.v. catheter into their trachea through which lungs were lavaged with 1 ml 0.9% saline. Lavage was repeated 3 times to obtain around 1ml BALF per mouse. The BALF was then centrifuged at maximum speed for 3 minutes and the resultant supernatant stored at -80°C until analysis.

Mmp-12^{-/-} mice were generated in Professor Shapiro's laboratory [146]. The construct was created by the insertion of the phosphoglycerolkinase promoter and neomycin resistance genes (PGK-neo) between intron 1 and 2 and electroincorporated into RW4 ES cells. Next, C57BL/6J blastocysts were microinjected with the correctly targeted clones. Mice which were homozygous for the *MMP-12* mutation were backcrossed 10 generations into the C57BL/6J background. *Mmp-12^{+/+}* were age and sex-matched to provide the controls. Only male mice were used in reported experiments.

5.1.2 Sputum samples

Sputum induction and processing was carried out as described in sections 2.5 and 2.6, respectively. Only sputum supernatant samples were used in the proteomics experiments. Both DTT and PBS processed sputum samples were utilized.

5.1.3 Whole Protein TMT Labelling

250µg for each sample was used per TMT label in each six-channel (6-plex) experiment and precipitated by centrifugation at 4,000 rpm for 8 min in a 4:2:3 methanol: chloroform: HPLC water volume ratio. The resulting pellet was then mixed with 4 volumes of methanol followed by centrifugation at 4000 rpm for 10 minutes. The supernatant was discarded and the air-dried protein precipitate dissolved in 30µL 6M guanidine HCL, 50µL HPLC water and 20µL 1M HEPES pH 8. Tris (2-carboxyethyl) phosphine (TCEP) was added in a final concentration of 10mM as a reducing agent. The pH of the mixture was adjusted to >6 and incubated at 55°C for 30 min. Alkylation was achieved by the addition of iodoacetamide in a final concentration of 25mM for 30 min at room temperature in the dark. Each TMT label (0.8mg) was dissolved in a volume of DMSO equal to the reaction mixture. To label peptide α- and ε-amines TMT labels were added to the sample and incubated at room temperature in the dark for 1 h. To quench the labels and prevent their carry-over to the trypsin digests, 25µL 1M ethanolamine was incubated with each label/sample mixture for 30 minutes at room temperature. All sample mixtures were then combined and cleaned in a 8:1 ice-cold acetone: methanol volume ratio for 2-18h at -80°C. The next day, the pellet was sedimented by centrifugation at 8,500 rpm for 15 min at 4°C. After discarding the supernatant the pellet was resuspended in ice-cold methanol and centrifuged at 8,500 rpm for 15min, the procedure repeated twice to remove any precipitated guanidine chloride. Once air-dried the protein pellet was resuspended in 200µL 100mM NaOH, 200µL 200mM HEPES (pH 7.5-8) and the volume adjusted to 1mL with HPLC water. After adjusting the pH to 6.5-8, the proteome was trypsinized by incubation with sequencing grade TrypsinGold (*Promega, Madison, Wisconsin, USA*) for 18h at 37°C at a 1:100, enzyme: proteome mass ratio. Trypsinization was assessed by 10% SDS-PAGE and Imperial stain (*Thermo Fisher Scientific, Rockford Illinois, USA*). Prior to the next step of N-terminal enrichment 100µL

of trypsinized sample was removed, acidified to pH <2.5 with 100% acetic acid and stored on C18 Stage tips for analysis of the pre-TAILS sample.

5.1.4 Whole Protein Dimethylation

Samples were precipitated. Human sputum or mouse BALF supernatant was incubated in quarter of its volume of 100% trichloroacetic acid (TCA) on ice for 10 min. The mixture was then centrifuged at 4°C at 14,000 rpm for 10 min. The supernatant was discarded and the pellet centrifuged in 1ml ice-cold acetone at 4°C at 14,000 rpm for 5min, repeated twice, centrifuging increased to 10 minutes on the last spin. Once air-dried the pellet was resuspended in a final concentration of 4M guanidine HCL (pH 7.0), 100mM HEPES (pH 8.0) and 10mM DTT and incubated at 65°C for 30 min. Once cooled to room temperature, alkylation of the sample was achieved by incubation with a final concentration of 15mM iodoacetamide for 30 min in the dark at room temperature. The pH was next adjusted to 6.5 with NaOH or HCL. Next, to label peptide α - and ϵ -amines, samples were incubated for 18h at 37°C with isotopically super-heavy [40mM heavy formaldehyde ($^{13}\text{CD}_2\text{O}$) + 20mM NaBD_3CN (sodium cyanoborodeuteride)], heavy [40mM $^{13}\text{CD}_2\text{O}$ + 20mM NaBH_3CN (sodium cyanoborohydride)], medium [40mM medium formaldehyde (CD_2O) + 20mM NaBH_3CN] or light labels [40mM light formaldehyde (CH_2O) + 20mM NaBH_3CN], all final concentrations. The labels used varied depending on the experiment. The following day, the labelling step was repeated at half the final concentration of labels used the day before, and the sample mixture incubated for a further 2h at 37°C. Next, sample mixtures were cleaned in acetone: methanol, followed by protein precipitation, trypsinization and storage as described in Section 5.2.3.

5.1.5 N-terminal Enrichment

To negatively select against unlabelled α -amines of trypsinized peptides, samples were incubated with a 3-5 fold excess (w/w) of dendritic polyglycerol aldehyde polymer and 1M ALD for 18h at 37°C, following pH adjustment to 6-6.5 with 1M HCL. Ten microliters 1M ALD was added for each 1mg protein in the sample to ensure catalysis of the binding reaction of the polymer to free α -amines of peptides. Unbound peptides were separated from polymer-bound peptides by filtration using centrifugal filter units with 10kDa cut-off membranes (*Amicon, Millipore, Billerica, Massachusetts, USA*). Once concentrated to ~100 μ L, the polymer was washed with 100 μ L of 100mM ammonium bicarbonate. The polymer-bound peptides on the filter were then discarded while the filtrate was collected, acidified with 100% acetic acid to pH <2.5 and stored on C18 Stage tips till analysis.

5.1.6 High Performance Liquid Chromatography (HPLC) and Mass Spectrometry (MS)

All HPLC and MS experiments were carried out by the UBC Centre for High Throughput Biology. Analysis was performed on a nanoHPLC system (Thermo Scientific) consisting of a nanospray ionization source coupled to a LTQ-Orbitrap hybrid mass spectrometer (LTQ-Orbitrap XL, Thermo Scientific). The ionization source included a fused-silica trap column (length, 2 cm; inner diameter, 100 μ m; packed with 5- μ m-diameter Aqua C-18 beads; Phenomenex), fused-silica fritted analytical column (length, 20 cm; inner diameter, 50 μ m; packed with 3- μ m-diameter Reprosil-Pur C-18-AQ beads; Dr. Maisch GmbH) and a silica gold-coated spray tip (20- μ m inner diameter, 6- μ m diameter opening, pulled on a P-2000 laser puller; Sutter Instruments; coated on EM SCD005 Super Cool Sputtering Device, *Leica Microsystems*). Peptides were eluted from Stage tips in 80% ACN (acetonitrile), 0.1% formic acid mobile phase, then SpeedVac concentrated to near-dryness and dissolved in 20 μ l mobile phase 2% ACN, 0.1% formic

acid. Ten microliters were loaded onto the column. Buffer A was 0.5% formic acid, buffer B 0.5% acetic acid/ 80% ACN. Gradients were run from 0% B to 15% B over 15 min, then from 15% B to 40% B in the next 65 min, then increased to 100% B over 10 min period, held at 100% B for 30 min. The LTQ-Orbitrap was set to acquire a full-range scan at 60,000 resolution (m/z 350–1,800) in the Orbitrap and to simultaneously fragment the top five peptide ions in each cycle in the LTQ (minimum intensity 200 counts). Parent ions were then excluded from MS/MS for the next 180s. The Orbitrap was continuously recalibrated against protonated $(\text{Si}(\text{CH}_3)_2\text{O})_6$ at $m/z = 445.120025$ using the lock-mass function.

5.1.7 Spectrum-to-sequence Matching and Statistics

Data acquired with the Orbitrap XL spectra were matched to peptide sequences in the mouse or human UniProt protein database (October 2013) with added standard laboratory and common contamination protein entries and reverse decoy sequences using the Andromeda algorithm²⁹ as implemented in the MaxQuant software package v1.4.12 [313], with a peptide false discovery rate (FDR) set at 0.01. Searches were performed using the following parameters: a mass tolerance of 5 p.p.m. for the parent ion, 0.5 Da for the fragment ions, carbamidomethylation of cysteine residues (+57.021464 Da), variable N-terminal modification by acetylation (+42.010565 Da), methionine oxidation (+15.994915 Da), and amino acid cyclization, semi-Arg-C cleavage specificity with up to two missed cleavages and (KR|X) as simple cleavage site rule for trypsin with up to three missed cleavages. In addition the following were set as variable modification at the peptide N termini and fixed modification at the peptide lysine residues: isobaric mass tag for TMT labelling and superheavy (+36.0757 Da), heavy (+34.0631) medium (+32.0564 Da) and light (+28.0313 Da) for dimethyl labelling. For murine experiments *Mmp-12^{-/-}* / *Mmp12^{+/+}* ratios of ≤ 0.67 and ≥ 1.5 were analysed

further; similarly for human experiments exacerbation/ recovery ratios of ≤ 0.67 and ≥ 1.5 were reported as significant. Demographic data were analysed GraphPad Prism version 6.05 (GraphPad Software, San Diego, California, USA).

5.2 Results

5.2.1 Mice samples

TAILS was used to identify potential MMP-12 targets in COPD by the relative quantification of substrates in four cigarette smoke-exposed *Mmp-12^{-/-}* and *Mmp-12^{+/+}* mice. Pre-TAILS identified a total of 1778 N-terminal peptides in the BALF proteome of *Mmp-12^{-/-}* and *Mmp-12^{+/+}* mice. Following N-terminal enrichment by TAILS a total of 62 unique mature and cleaved neo-N-terminal peptides were identified. Using the cut off *Mmp-12^{-/-}* / *Mmp-12^{+/+}* ratios of ≤ 0.67 and ≥ 1.5 , 22 neo-N-terminal peptides (corresponding to 19 proteins) were identified which were differentially cleaved in *Mmp-12^{-/-}* and *Mmp-12^{+/+}*. Of these, 15 peptides (corresponding to 13 proteins) were found to have a level ≥ 1.5 in *Mmp-12^{-/-}* compared to *Mmp-12^{+/+}*. In contrast, seven peptides, corresponding to seven proteins were ≤ 0.67 times lower in *Mmp-12^{-/-}* compared to *Mmp-12^{+/+}*. The sites of cleavage and ratios for the differentially cleaved peptides are summarized below in table 5.1

In this protease KO smoking mouse model, the potential MMP-12 substrates identified were similar to validated MMP-12 targets in published data derived from *Mmp-12^{-/-}* embryonic fibroblasts, *Mmp-12^{-/-}* macrophages and *Mmp-12^{-/-}* peritonitis murine models [10]. These included: alpha-2-HS glycoprotein, anti-thrombin III, clusterin, complement C3, complement C4b, complement factor H-related protein-1, hemopexin, serotransferrin and serum albumin. In addition to the aforementioned potential MMP-12 substrates, alpha-2-macroglobulin, beta-1, 4-galactosyltransferase 2,

transmembrane protease 7, DEP domain-containing mTOR-interacting protein, kininogen-1, pleckstrin homology domain-containing family H member 1, tumour necrosis factor ligand superfamily member 11 and zinc finger protein 518B were identified as potential new substrates of MMP-12. Furthermore, the current smoking mouse KO model identified new cleavage sites for the already known MMP-12 substrates: alpha-2-HS-glycoprotein, complement C3 and clusterin.

Table 5.1 Cleavage sites and *Mmp-12*^{-/-}/*Mmp-12*^{+/+} ratios for the differentially cleaved peptides. Numbers in *italics* represent known cleavage sites

Gene Ontology	Protein	Average ratios of neo-N-terminal peptides (<i>Mmp-12</i> ^{-/-} / <i>Mmp-12</i> ^{+/+})	Start position of neo N-terminal peptides (P1')	Cleavage site (P1-P1')
Acute phase	Alpha-2-HS-glycoprotein	18.92, 1.52	19, 24	S-A, T-G
Acute phase	Serum albumin	3.58, 1.53	25, 473	R-E, C-V
Acute phase	Hemopexin	2.67	24	A-S
Acute phase	Serotransferrin	0.53	642	S-T
Blood coagulation	Alpha-2-macroglobulin	0.13	730	Y-S
Blood coagulation	Antithrombin-III	2.07	35	G-N
Blood coagulation	Kininogen-1	2.88	389	R-S
Transmembrane serine protease	Transmembrane protease serine 7	0.43	294	Y-D
Negative regulator of the mTORC1 and mTORC2 signaling pathways	DEP domain-containing mTOR-interacting protein	0.61	147	G-V
Transcription	Zinc finger protein 518B	1.60	293	K-V
Cell death regulation	Clusterin	3.22	22	G-E
Complement system	Complement factor H-related protein-1	4.14	24	G-E
Complement system	Complement factor B	1.84	23	A-T
Complement system	Complement C4-B	0.41	953	R-T
Complement system	Complement C3	10.79; 0.37; 2.87	671, 749, 960	R-S, R-S, K-V
Bone metabolism	Tumor necrosis factor ligand superfamily member 11	1.96	195	K-V
Cytoskeletal remodelling	Pleckstrin homology domain-containing family H member 1	0.03	164	D-A
Carbohydrate metabolism	Beta-1,4-galactosyltransferase 2	2.32	237	I-A

5.2.2 Human COPD exacerbation and recovery samples

Of the potential MMP-12 substrates detected in mice, alpha-2-HS-glycoprotein, anti-thrombin III, complement factors C3 and C4b, hemopexin and serum albumin were identified in both exacerbation and recovery human sputum by TAILS. Of note, a similar cleavage site was identified between murine and human anti-thrombin III, at G³⁵N and G³⁵S respectively, strongly suggestive of MMP-12 cleavage in sputum. The proteins cleaved in both COPD sputum and mouse BALF are summarised in table 5.2.

TAILS enabled comparison of substrate proteolysis in human COPD sputum at exacerbation and recovery. Proteolysis of 16 substrates occurred with increased intensity both at exacerbation as well as recovery, depending on the site of cleavage. For instance, cathepsin G was cleaved with increased intensity at A³⁷Y and R¹²³N at exacerbation, and also cleaved with increased intensity at T¹⁰⁶Q at recovery. The cleavage sites of these 16 peptides are shown in table 5.3.

Table 5.2 Murine MMP-12 targets are present in human COPD sputum. This table reveals the MMP-12-cleaved peptides and their cleavage sites in the murine cigarette smoke exposed-model as well as the corresponding human peptides detected by TAILS in COPD exacerbation and recovery sputum.

Protein	Protein cleavage site/s for MMP-12 substrates in mouse BALF	Protein cleavage site/s identified in human exacerbation or recovery sputum
Alpha-2-HS glycoprotein	T ²⁴ G	R ³⁴¹ T
Anti-thrombin III	G ³⁵ N	C ³³ H, G ³⁵ S
Complement 3	R ⁶⁷¹ S, R ⁷⁴⁹ S, K ⁹⁶⁰ V	K ²⁷³ V, A ⁷⁴⁸ R, I ¹⁵⁶⁶ E
Complement C4b	R ⁹⁵³ T	E ⁷⁶⁰ I, T ⁹⁸² I, R ¹⁴⁵⁴ E
Hemopexin	A ²⁴ S	H ³³ G
Serum albumin	R ²⁵ E, C ⁴⁷³ V	C ⁷⁹ H, T ²⁶⁸ E

Table 5.3 Proteins with peptides increased both at exacerbation and recovery; the numbers in the columns by the cleavage sites represent the recovery/exacerbation peptide ratios.

Protein	Cleavage sites for peptides increased at exacerbation	Average ratios of neo-N-terminal peptides (recovery/exacerbation)	Cleavage sites for peptides increased at recovery	Average ratios of neo-N-terminal peptides (recovery/exacerbation)
Cathepsin G	A ³⁷ Y R ¹²³ N	0.41 0.30	T ¹⁰⁶ Q	1.52
Coronin	C ⁵² E	0.50	I ⁵¹ C, T ¹⁷⁰ L	1.79 1.85
Cystatin-S	A ³⁸ D	0.58	C ¹¹⁹ S	1.55
Histone H2A type 1-C	I ⁸⁹ R	0.50	L ⁵⁷ E	1.67
Ig alpha-1 chain C region	V ²⁹ Q L ³²³ A	0.53 0.55	L ³⁸ S	1.89
Integrin-alpha M	T ⁵²⁶ V V ⁶⁷⁵ T I ⁹⁶⁸ S	0.51 0.6 0.5	I ²⁵⁷ T S ¹⁰⁰⁷ H	1.82 1.75
MMP-9	S ²⁷ T L ²⁹ V L ⁷⁹ S T ¹²⁶ Q R ³²³ D I ⁵⁵⁷ A L ⁶⁶⁰ D V ⁶⁹⁸ T	0.1 0.05 0.56 0.39 0.24 0.49 0.44 0.37	R ⁴²⁵ F T ⁴²⁷ E	2.31 1.98
MPO	A ²⁴⁵ S R ³³¹ L T ³³⁴ E R ⁴⁴² V R ⁴⁶⁵ Q A ⁵⁶⁸ C C ⁵⁶⁹ I V ⁶¹⁸ S	0.60 0.24 0.34 0.37 0.42 0.31 0.55 0.53	I ²³⁶ N T ²⁴⁰ S	3.17 1.66
Myosin-9	I ¹²³⁹ A	0.56	V ²³⁹ S	1.68

Table 5.3 continued Proteins with peptides increased both at exacerbation and recovery

Mucin-5AC	A ⁵⁸ T	0.48	Y ⁶²⁷ A	1.69
	N ⁵⁷⁶ S	0.40		
	F ⁷⁴⁹ L	0.53		
	V ⁸⁰² C	0.60		
	V ¹⁰⁵⁵ V	0.56		
	V ¹²⁹⁰ I	0.14		
	R ¹⁴³¹ A	0.14		
	V ¹⁷⁵⁶ D	0.58		
	H ¹⁷⁶⁴ G	0.15		
	C ⁴⁵⁷² A	0.49		
Mucin-5B	C ⁵⁴¹⁵ V	0.47	S ⁶⁰⁴ F	1.81
Neutrophil defensin 3	V ⁴⁶ S	0.12	I ³⁷ A	3.75
	A ⁷³ C	0.50		
	T ⁸³ C	0.36		
Polymeric Immunoglobulin Receptor	T ⁴⁰ C	0.55	R ²⁷³ Q	1.70
	C ⁴¹ Y	0.39		
	V ⁹⁵ V	0.35		
	V ⁹⁶ N	0.42		
	F ²⁰⁴ S	0.38		
	Q ²³⁷ V	0.11		
	F ³⁰⁹ S	0.51		
	V ⁴²⁷ I	0.16		
	L ⁵²⁹ T	0.28		
	A ⁵⁵⁷ A	0.20		
	A ⁵⁵⁸ V	0.07		
	V ⁵⁷⁴ S	0.08		
	K ⁵⁷⁸ A	0.25		
Protein SET	V ¹⁰¹ T	0.58	S ⁸² A	1.71
Serum albumin	C ⁷⁹ H	0.61	T ²⁶⁸ E	1.82
UPF0762 protein C6orf58	T ²³ S	0.56	S ²¹⁴ T	1.78

51 proteins were cleaved with increased intensity at exacerbation; their cleavage sites and the relative quantification of their cleaved peptides at exacerbation and recovery are summarized in table 5.4. The function of the corresponding proteins is shown in table 5.7.

Table 5.4 Proteins with peptides increased at exacerbation only; peptide cleavage sites and peptide recovery/exacerbation ratios are shown.

Protein	Peptides increased at exacerbation	Average ratios of neo-N-terminal peptides (recovery/exacerbation)
Actin-related protein 2/3 complex subunit 2	I ²²⁴ T	0.51
Adenosylhomocysteinase	V ¹⁹¹ A	0.54
Alpha-actinin-4	A ⁴⁴⁵ T I ⁷⁹⁶ S	0.51 1.59
Alpha-enolase	V ²² S	0.57
Annexin	G ¹⁴³ T	0.50
Antileukoproteinase	K ⁷² C	0.21
Anti-thrombin III	C ³³ H G ³⁵ S	0.10 0.09
ARP2 actin-related protein 2	T ¹⁸³ T	1.53
AZU1 protein	V ⁹⁴ V	0.61
Beta-2-microglobulin	Y ³⁹ Y	0.34
Calreticulin	L ⁵² S S ⁵³ S	0.08 0.18
Calpain-1 catalytic subunit	I ³⁶ K	0.59
Carcinoembryonic antigen-related cell adhesion molecule 8	V ⁸⁴ I I ⁸⁵ S	0.59 0.05
Cathelicidin antimicrobial peptide	A ¹³⁴ L	0.51
Choline transporter-like protein 4	S ¹⁶⁶ F	0.58
Complement C3	K ²⁷³ V I ¹⁵⁶⁶ E	0.02 0.03
Complement C4B	E ⁷⁶⁰ I T ⁹⁸² A R ¹⁴⁵⁴ E	0.25 0.13 0.23
Cystatin-SA	C ¹¹⁹ S	0.57
Cystatin-SN	C ¹¹⁹ S	0.56
Cytochrome c oxidase subunit 2	T ¹⁶⁸ L	0.54
Deleted in malignant brain tumors 1 protein	I ²⁹⁷ V E ⁷⁶⁰ I T ⁹⁸² A R ¹⁴⁵⁴ E	0.26 0.25 0.13 0.23
Enolase	V ¹⁹⁸ G	0.51
Elongation factor 1-alpha 1	V ¹¹⁷ A	0.52

Table 5.4 continued: Proteins with peptides increased at exacerbation only

Filamin-A	K ⁸⁶⁶ V	0.52
Gelsolin	T ³⁶³ S	0.56
Glycogen phosphorylase, liver form	V ³⁵⁷ D	0.52
Haptoglobin	I ¹⁶⁷ C	0.55
Heat shock cognate 71 kDa protein	V ⁶⁰ A V ²²⁰ K T ²²³ A I ²⁹² D	0.49 0.001 0.16 0.07
Heat shock protein HSP 90-alpha	I ⁴⁹⁵ T	0.51
Hematopoietic lineage cell-specific protein	I ²⁹⁴ R	0.54
Hemopexin	H ³³ G	0.57
Histone H4	I ⁴⁸ S	0.52
Ig alpha-2 chain C region	C ¹³⁵ T	0.47
Integrin beta-2	A ²⁸⁴ A V ⁴²¹ T	0.46 0.44
Lactotransferrin	V ⁸³ A A ¹⁶² S C ³⁵⁴ A L ⁵¹³ C	0.59 0.57 0.50 0.55
Leukocyte elastase inhibitor	S ²⁴⁴ Y A ²⁵² R V ²⁵⁶ Q	0.52 0.54 0.48
Macrophage capping protein	V ⁸³ H	0.15
Major vault protein	L ⁷¹³ S	0.52
Neutrophil elastase	I ¹³⁰ N N ¹³¹ A N133V L ¹⁵³ A M ¹⁵⁵ G V ²⁴⁰ N	0.02 0.31 0.34 0.55 0.53 0.63
Phosphoglycerate mutase 1	M ¹²¹ Q	0.51
Protein disulfide-isomerase A3	V ⁷⁴ S	0.50
Pulmonary surfactant -related protein	V ¹²⁹ G	0.51
P35-related protein	V ⁴⁰ G,	0.50
Rab GDP dissociation inhibitor beta	A ⁴⁵ S	0.57

Table 5.4 continued: Proteins with peptides increased at exacerbation only

Ras-related protein Ral-A	I ⁶⁵ D	0.55
Resistin	I ⁴⁵ S	0.53
Septin-2	V ²⁵¹ T	0.57
Septin-9	V ¹⁹² I	0.52
SH3 domain-binding glutamic acid-rich-like protein	I ³³ G	0.52
Transitional endoplasmic reticulum ATPase	A ³⁰⁰ I	0.55
	V ⁵⁷⁴ L	0.55
Twinfilin-2	I ²¹³ E	0.52

27 proteins were cleaved with increased intensity at recovery; their cleavage sites and the relative quantification of their cleaved peptides at exacerbation and recovery are summarized in table 5.5 below. The function of the corresponding proteins is shown in table 5.7.

Table 5.5 Proteins with peptides increased at recovery only; peptide cleavage sites and peptide recovery/exacerbation ratios are shown.

Protein	Peptides increased at recovery	Average ratios of neo-N-terminal peptides (recovery/exacerbation)
Acyl-protein thioesterase 1	A ⁶⁰ S	1.78
Aldehyde dehydrogenase family 3 member B1	I ³⁰⁶ V	1.57
Alpha-1-antichymotrypsin	P ²⁹ L	8.36
Annexin	T ¹¹⁷ S	1.68
Annexin A4	T ⁸⁸ V	1.71
Catalase	A ⁴⁴⁶ F	1.59
cDNA FLJ53963	V ⁶⁹ S	1.52
Complement decay-accelerating factor	G ³⁵ D	1.67
Cornulin	V ²²⁸ T	1.71
Clathrin heavy chain 1	V ³⁵⁴ R	1.52
Cysteine-rich secretory protein 3	T ³⁰ A	1.71
Glucose-6-phosphate isomerase	A ⁴²⁸ N	1.64
Glutathione S-transferase P	A ⁸⁸ A	1.76
Growth factor receptor-bound protein 2	V ¹²¹ Q	1.59
Heat shock cognate 71 kDa protein	S ²²² T	2.39
Ig delta chain C region	V ¹⁷¹ Y V ²⁰⁷ A	1.86 1.74
Ig mu heavy chain disease protein	V ⁴⁴ I	1.51
Neutrophil collagenase	V ³⁵² Q	1.89
Peptidoglycan recognition protein 1	I ¹⁴⁶ R	1.51
Plastin-2	S ¹⁶⁵ V A ³⁶⁶ F	1.83 1.79

Table 5.5 continued: Proteins with peptides increased at recovery only

Proteasome subunit beta type-1	I ⁴⁹ A	1.64
Protein-arginine deiminase type-4	I ⁴⁰² S	1.67
Ras GTPase-activating-like protein IQGAP1	V ⁴⁸⁴ T	1.90
	V ⁵⁷² L	1.70
Tubulin alpha-4A chain	G ³⁶⁵ G	1.52
Tubulin beta chain	I ³⁰ S	1.53
Vinculin	V ²⁹ S	1.78
6-phosphogluconate dehydrogenase, decarboxylating	I ⁶⁸ L	1.79

5.2.3 The human sputum degradome in COPD

Clinical data and sputum cell counts for the nine patients whose sputum samples were used in the TAILS analysis are summarized in table 5.6 below. All patients had a FEV₁ % predicted <80%, and all, apart from 1 with a FEV₁/FVC =0.75, had a ratio <0.7. Sputum cell counts were available for eight patients at exacerbation and all nine patients at recovery. Data derived from TAILS analysis of COPD exacerbation and recovery sputum led to the identification of 1,116 peptides. These peptide sequences were matched in the UniProt database, www.uniprot.org, to determine the corresponding proteins and their functions. Sputum proteins were grouped into the following categories according to their function: cell adhesion/migration, complement system, acute phase response, extracellular matrix structure/function, anti-microbicidal activity, cytoskeletal function/ remodelling, carbohydrate metabolism, oxidoreductase activity, cell death regulation/ DNA synthesis/repair, immune response, protease activity, protease inhibition and ATP synthesis/ function. Proteins with an unclear, or not yet known, function were grouped into an “other/unknown” category. These protein groups are summarized in table 5.7. Proteins marked *are described as MMP-12 targets in published data.

Table 5.6 Clinical and sputum characteristics of COPD patients

Demographics	
Male/ Female (n)	5/4
Age/ Years*	71 (8)
Current/ex-smokers (n)	5/4
Pack years*	47 (18)
ICS yes/ no/ (n)	8/1
Lung function/ CT/ MRC grade	
FEV1/ Ls-1*	1.18 (0.65)
FEV1/ percent predicted*	48.11 (16.99)
FEV1/FVC*	0.48 (0.15)
Emphysema on CT yes/ no /N/A (n)	3/2/4
MRC grades 3-5 (n)	Grade 3(4)/ Grade 4 (2)/ Grade 5 (3)
Sputum cell counts at exacerbation	
Sputum TCC/ x10 ⁶ cells/g median (range)	20.30 (2.04-148.00)
Sputum neutrophil count/ x10 ⁶ cells/g median (range)	20.28 (0.46-148.00)
Sputum macrophage count/ x10 ⁶ cells/g median (range)	0.00 (0.00-0.21)
Sputum neutrophil percentage median (range)	99.88 (21.25-100.00)
Sputum macrophage percentage median (range)	0.00 (0.00-51.00)
Sputum cell counts at recovery	
Sputum TCC/ x10 ⁶ cells/g median (range)	9.77 (0.39-54.90)
Sputum neutrophil count/ x10 ⁶ cells/g median (range)	9.40 (0.17-54.49)
Sputum macrophage count/ x10 ⁶ cells/g median (range)	0.36 (0.00-0.73)
Sputum neutrophil percentage median (range)	95.75 (40.00-100.00)
Sputum macrophage percentage median (range)	3.75 (0.00-51.75)

*Data presented as mean ±standard deviation; †p<0.05. Abbreviations: ICS, Inhaled corticosteroids (n), number; N/A, not available; TCC, total cell count.

Table 5.7 Proteins identified in human COPD sputum by TAILS grouped according to their function/s. *=described as MMP-12 targets in published data.

<p>Cell adhesion/migration</p> <p>Annexin A1*</p> <p>Annexin A3</p> <p>Annexin A5</p> <p>Annexin A6</p> <p>Carcinoembryonic antigen-related cell adhesion molecule 1</p> <p>Carcinoembryonic antigen-related cell adhesion molecule 6</p> <p>Carcinoembryonic antigen-related cell adhesion molecule 8</p> <p>Fermitin family homolog 3*</p> <p>Galectin-3-binding protein</p> <p>Histidine-rich glycoprotein*</p> <p>Integrin alpha-M</p> <p>Integrin beta-2</p> <p>Moesin</p> <p>Olfactomedin-4</p> <p>Ras-related C3 botulinum toxin substrate 3</p> <p>Ras-related protein Ral-B</p> <p>Rho GDP-dissociation inhibitor 1</p> <p>Rho GDP-dissociation inhibitor 2</p> <p>Rho-related GTP-binding protein RhoG</p> <p>Septin-2*</p> <p>Septin-9</p> <p>Sialic acid-binding Ig-like lectin 5</p> <p>Trefoil factor 3</p> <p>Vinculin</p>	<p>Complement system</p> <p>Complement C3*</p> <p>Complement C4 beta chain*</p> <p>Complement decay-accelerating factor</p> <p>Complement factor B</p>
<p>Acute phase response</p> <p>Alpha-1-acid glycoprotein 1</p> <p>Alpha-2-HS-glycoprotein*</p> <p>Annexin A1*</p> <p>Arachidonate 5-lipoxygenase</p> <p>CCL16</p> <p>Coronin-1A*</p> <p>Glucose-6-phosphate isomerase</p> <p>Granulins*</p> <p>Heat shock 70 kDa protein 1A/1B*</p> <p>Heat shock 70 kDa protein 6</p> <p>Heat shock cognate 71 kDa protein</p> <p>Heat shock protein HSP 90-alpha*</p> <p>Hemopexin*</p> <p>Leukotriene A-4 hydrolase</p> <p>Lymphocyte-specific protein 1</p> <p>Pantetheinase</p> <p>Peptidyl-prolyl cis-trans isomerase FKBP1A*</p> <p>Protein S100-A8</p> <p>Serum albumin*</p>	<p>Extracellular matrix structure and function</p> <p>Fibrinogen beta chain</p> <p>Fibrinogen gamma chain</p> <p>Galectin-3*</p> <p>IgGfc-binding protein</p> <p>Mucin-4</p> <p>Mucin-5AC</p> <p>Mucin-5B</p> <p>Pulmonary surfactant-associated protein A1</p>

Table 5.7 continued: Proteins identified in human COPD sputum by TAILS

Antimicrobial activity	Cytoskeletal function/ remodelling
Bactericidal permeability-increasing protein	Adipocyte plasma membrane-associated protein
Cathelicidin antimicrobial peptide	Alpha-actinin-1*
Lactotransferrin	Alpha-actinin-4*
Neutrophil defensin 3	Actin*, cytoplasmic 1
	Actin-related protein 2/3 complex subunit 1B*
	Actin-related protein 3
	Calpain-1 catalytic subunit
	Copine-3
	Coronin-1A*
	Dysferlin
	Endoplasmic
	Eukaryotic initiation factor 4A-II
	F-actin-capping protein subunit beta*
	Filamin-A*
	Gelsolin*
	Glia maturation factor gamma
	Hematopoietic lineage cell-specific protein
	Macrophage-capping protein*
	Myosin-9*
	Myosin regulatory light chain 12A
	Na(+)/H(+) exchange regulatory cofactor
	Nesprin-1
	NHE-RF1
	Plastin-3
	Profilin-1*
	Ras-related C3 botulinum toxin substrate 2
	Ras GTPase-activating-like protein IQGAP1
	Ras-related protein Rap-1b
	Transitional endoplasmic reticulum ATPase*
	Thioredoxin reductase 1, cytoplasmic
	Thymosin beta-4
	Tropomyosin alpha-3 chain
	Tubulin alpha-4A chain
	Tubulin beta chain
	Twinfilin-2
	Unconventional myosin-1f
	Vesicular integral-membrane protein VIP36
	Vimentin*

Table 5.7 continued: Proteins identified in human COPD sputum by TAILS

Carbohydrate metabolism	Oxidoreductase activity
Alpha-amylase 2B	Aldehyde dehydrogenase family 16 member A1
Alpha-enolase	Catalase
Beta-glucuronidase	Ceruloplasmin
Citrate synthase	Clusterin*
Di-N-acetylchitobiase	Cytochrome c oxidase subunit 5B
Enolase	ERO1-like protein alpha
Fructose-bisphosphate aldolase A	Glutaredoxin-1
Fructose-bisphosphate aldolase C	Glutathione S-transferase P
Glycogenin-1	Glyceraldehyde-3-phosphate dehydrogenase
Glycogen phosphorylase, liver form	Nicotinamide phosphoribosyltransferase
Glucose-6-phosphate isomerase	Nicotinate phosphoribosyltransferase
Hexokinase-3	Pyridoxal kinase
Malate dehydrogenase	Sulfhydryl oxidase 1
N-acetylglucosamine-6-sulfatase	Thioredoxin
Phosphoglucomutase-1	Thioredoxin domain-containing protein 17
Phosphoglycerate kinase 1	Transcobalamin-1
Protein kinase C beta type	
Pyruvate kinase PKM	
Resistin	
Transketolase	
Triosephosphate isomerase	
6-phosphogluconolactonase	

Table 5.7 continued: Proteins identified in human COPD sputum by TAILS

Cell death regulation/ DNA synthesis and repair	Immune response
Adenosylhomocysteinase	Basic salivary proline-rich protein 3
Adenylosuccinate synthetase isozyme 2	Beta-2-microglobulin*
Calcineurin-like phosphoesterase domain-containing protein 1	Calreticulin*
Clusterin*	Clathrin heavy chain 1
Cullin-4A	Cysteine-rich secretory protein 3
Cytidine deaminase	Deleted in malignant brain tumors 1 protein
Elongation factor 1-gamma	EH domain-containing protein 1
Elongation factor 2	Galectin-3-binding protein
Eukaryotic translation initiation factor 5A-1	Ficolin-1
Heterogeneous nuclear ribonucleoprotein A1	Histidine-rich glycoprotein*
Heterogeneous nuclear ribonucleoproteins A2/B1	HLA class I histocompatibility antigen, Cw-14 alpha chain
Heterogeneous nuclear ribonucleoprotein D0	Ig alpha-1 chain C region
Heterogeneous nuclear ribonucleoprotein K	Ig delta chain C region
Heterogeneous nuclear ribonucleoprotein U-like protein 1	Ig J chain
Heterogeneous nuclear ribonucleoprotein U-like protein 2	Ig kappa chain C region
Histone H1t	Ig kappa chain V-I region EU
Histone H1.5	Ig kappa chain V-IV region Len
Histone H2A type 1-C	Ig lambda-2 chain C regions
Histone H2B type1-L	Ig mu heavy chain disease protein
Histone H3.2	Lysozyme C
Histone H4	Monocyte differentiation antigen CD14*
Hypoxanthine-guanine phosphoribosyltransferase	Myeloid cell nuclear differentiation antigen
Inosine-5-monophosphate dehydrogenase 1	Peptidoglycan recognition protein 1
Programmed cell death 6-interacting protein*	Polymeric immunoglobulin receptor
Prolactin-inducible protein	Protein-arginine deiminase type-4
Protein SET	Protein S100-A8
Purine nucleoside phosphorylase	Tapasin
Serine/threonine-protein phosphatase 2A 65 kDa regulatory subunit A beta isoform	Tyrosine-protein kinase HCK
Thymidine phosphorylase	
Ubiquitin-conjugating enzyme E2 D3	
Ubiquitin-like modifier-activating enzyme 1	
14-3-3 protein zeta/delta	

Table 5.7 continued: Proteins identified in human COPD sputum by TAILS

<p>Protease inhibition Alpha-1-antichymotrypsin Alpha-2-HS-glycoprotein* Alpha-2-macroglobulin Antileukoproteinase Cystatin-B Cystatin-C Cystatin-S Cystatin-SA Cystatin-SN Haptoglobin* Leukocyte elastase inhibitor</p>	<p>Protease activity ADP-sugar pyrophosphatase Cathepsin G Cathepsin S Dipeptidyl peptidase 3 Matrix metalloproteinase-9 Mitochondrial peptide methionine sulfoxide reductase Myeloblastin Myeloperoxidase Neutrophil collagenase Neutrophil elastase Proteasome subunit alpha type-5 Proteasome subunit alpha type-7 Proteasome subunit beta type-1 Proteasome subunit beta type-4* Proteasome subunit beta type-6 Proteasome subunit beta type-9 Tripeptidyl-peptidase 1</p>
<p>Neutrophilic inflammation Azurocidin Bactericidal permeability-increasing protein Cathepsin G Matrix metalloproteinase-9 Myeloblastin Myeloperoxidase Neutrophil collagenase Neutrophil elastase Protein-arginine deiminase type-4 Protein S100-A8</p>	<p>Lipid metabolism Chloride intracellular channel protein 1 Phospholipase B-like 1 Putative lipocalin 1-like protein 1 Zinc-alpha-2-glycoprotein</p>
<p>Regulation of cellular proliferation Major vault protein Retinoic acid receptor responder protein 1 Serotransferrin*</p>	<p>Coagulation Antithrombin-III* WD repeat-containing protein 1 6-phosphogluconate dehydrogenase, decarboxylating</p>
<p>Natural killer cell toxicity Syntaxin-binding protein 2</p>	<p>T-cell regulation CCL16 Eosinophil lysophospholipase/Galectin-10 Signal-regulatory protein gamma Receptor-type tyrosine-protein phosphatase C</p>

Table 5.7 continued: Proteins identified in human COPD sputum by TAILS

ATP synthesis and function	Other/ unknown
ATP-citrate synthase	Acyl-protein thioesterase 1
ATP-dependent RNA helicase DDX39A	Alpha-1B-glycoprotein
ATP synthase subunit alpha	Alpha-2-macroglobulin-like protein 1
ATP synthase subunit beta	Apolipoprotein A-I*
Nucleoside diphosphate kinase	Arginase-1
Synaptic vesicle membrane protein VAT-1 homolog	Beta-microseminoprotein
T-complex protein 1 subunit beta	BPI fold-containing family B member 1
Tryptophan-tRNA ligase	BPI fold-containing family B member 2
78 kDa glucose-regulated protein	cAMP-dependent protein kinase type I-alpha regulatory subunit
	Coactosin-like protein
	Cornulin
	Docking protein 3D-dopachrome decarboxylase
	Dolichyl-diphosphooligosaccharide--protein glycosyltransferase subunit 1
	EF-hand domain-containing protein D2
	Fatty acid binding protein, epidermal
	G-protein coupled receptor family C group 6 member A
	Growth factor receptor-bound protein 2
	Guanine nucleotide-binding protein G(i) subunit alpha-2
	Guanine nucleotide-binding protein G(I)/G(S)/G(T) subunit beta-1
	Haemoglobin subunit beta
	Importin subunit beta-1
	Inositol 1,4,5-trisphosphate receptor-interacting protein
	Osteoclast-stimulating factor 1
	Peptidyl-prolyl cis-trans isomerase
	POTE ankyrin domain family member E
	Proline and serine rich-protein 2
	Rab GDP dissociation inhibitor beta
	Ribonuclease pancreatic
	Salivary acidic proline-rich phosphoprotein 1
	SH3 domain-binding glutamic acid-rich-like protein
	Signal-regulatory protein beta-1 isoform 3
	Sorcin
	Syntenin-1
	Translin
	UPF0762 protein C6orf58
	14-3-3 protein eta
	60S ribosomal protein L4
	78 kDa glucose-regulated protein

5.3 Discussion

This chapter presents for the first time the degradome and N-terminome of MMP-12 in COPD and describes the most comprehensive analysis to date of the COPD sputome. The murine MMP-12 degradome reveals the striking versatility of the protease which includes substrates with opposing functions, such as proteases and their inhibitors, pro-coagulants and anti-coagulants as well as complement factors, pro-inflammatory mediators, signalling peptides, and modulators of cytoskeletal function. While most of these MMP-12 substrates are novel in terms of their discovery in the setting of COPD, others, such as transmembrane serine protease-7 and RANK, are novel in their actual discovery as MMP-12 substrates. The human COPD sputome study reveals MMP-12 substrates described in the current murine model as well as several others discovered identified in other studies [307]. The findings in this chapter therefore demonstrate MMP-12 activity outside degradation of the extracellular matrix. This suggests a pivotal role for MMP-12 in COPD.

The human sputum study provides a clear insight into proteolytic events in COPD. Proteolysis is a constant process occurring both at exacerbation and recovery. Interestingly, while there is a tendency for different substrates to be targeted at exacerbation and recovery, similar substrates were also cleaved, albeit at different sites. Also of note, a larger number of substrates were targeted at exacerbation compared to recovery, reflecting increased proteolysis at exacerbation. Similar to the murine MMP-12 study, the substrates degraded were heterogeneous, often with opposing functions, *e.g.* alpha-2-macroglobulin (protease inhibitor) and transmembrane serine protease-7 (protease), anti-thrombin III (anti-coagulant) and kininogen-1 (pro-coagulant). This highlights the complexity of COPD pathogenesis and demonstrates that the widely held view of the disease resulting from an imbalance of protease over anti-protease activity,

with proteolysis viewed solely as harmful, is incorrect and incomplete. Indeed, this complexity may explain the inefficacy of a MMP-12 inhibitor in a clinic trial [22], highlighting the need for more tailored therapeutic targeting downstream of proteases.

Complement C3 and anti-thrombin III were both identified as potential MMP-12 substrates in the murine study as well as cleaved peptides in COPD sputum. C3, which is cleaved into C3a and C3b, plays a central role in the complement system and innate and adaptive immunity. C3a, an anaphylatoxin, is involved in the recruitment of leukocytes to sites of infection and inflammation while C3b ensures continuation of the complement cascade and promotes opsonisation and subsequent phagocytosis of pathogens [314]. Data suggest the involvement of both fragments in T-cell activation during infection and inflammation [314-316]. Bellac et al [307] demonstrated that MMP-12 cleavage of C3a leads to its inactivation while MMP-12 cleavage of C3b leads to an increase in phagocytosis. This suggests that cleavage of C3 promotes resolution of inflammation. The increased cleavage of C3 in exacerbation compared to recovery sputum in the present study may reveal a negative feedback loop that sets in as a defence mechanism to aid resolution of heightened inflammation at exacerbation. MMP-12 cleavage of anti-thrombin III causes a decrease in its anticoagulation function both *in vitro* and *in vivo*, the latter demonstrated by *Mmp-12^{-/-}* mice having a higher activated partial thromboplastin time [307]. In this study there was an increase in anti-thrombin III cleavage at exacerbation compared to recovery which may provide further understanding of the mechanisms responsible for the increased risk of thrombotic events seen during COPD exacerbations [41, 42].

One of strengths of the study is that in both instances as close to physiological conditions were used. The murine model did away with the addition of recombinant proteases to the tested sample. In the case of human COPD sputum, samples were

analysed both at exacerbation and during stable disease to reflect the nature of the illness. Several of the MMP-12 substrates discovered using the *Mmp-12^{-/-}* model are in agreement with published data [307], increasing confidence in the findings. Similarly, several of the sputum peptides discovered are in agreement with earlier proteomic studies on COPD blood [311] and BAL [317], with the added benefit of discovering a larger number of peptides. In addition, several of the peptides discovered are in keeping with the known pathology of COPD, adding to the strength of the study. These include peptides derived from oxidoreductive enzymes, such as catalase and glutaredoxin-1, and others, such as neutrophil defensin and NE linked to neutrophilic inflammation. Intriguingly, other peptides are derived from more recently discovered proteins in COPD which have a less clear function, such as Clara Cell 6 [318, 319].

Using BALF, several challenges arose. Firstly, a low diversity of proteins was found. This may represent the low protein content in BALF. Analysing lung homogenates as well as BALF may have provided a sample with a higher protein yield. Secondly, BALF collection is technically difficult and involves the addition of saline to the airways to increase sample yield. This results in a dilute sample. Thirdly, there is a high cost in the use of animal models to study the substrate profile of a protease. The potential MMP-12 substrates described in this murine model have not been validated in the present study by *in vitro* cleavage and gel electrophoresis. This is, however, an ongoing study where further work is being carried out. In addition, several of these peptides have already been confirmed as MMP-12 substrates in published data [307], albeit in non-COPD murine models, which might indicate that MMP12 plays a larger inflammatory role in various diseases and is not localized to the lungs specifically. Similarly, while several COPD peptides discovered in this study have previously been validated as MMP-12 substrates in murine or cell culture studies, this has not yet been confirmed in human studies. MMP-12 was not detected by TAILS in human COPD

sputum. Perhaps this reflects its presence in low quantities, making it undetectable with current mass spectrometers. However, given the paradoxical function of MMP-12 seen in this study, as well as others [115, 220, 306, 307], one could argue that studying or confirming the protease involved is of much less value than focusing downstream on the peptides identified. Indeed, this study highlights the need for a change in the current thinking model whereby the protease is viewed as “bad” and the anti-protease as “good”. It is time to focus attention on the degraded peptides in studying the pathogenesis of COPD, not just the proteases that produce them. One limitation to the study is that one of the patients had a $FEV_1/FVC = 0.75$, *i.e.* outside the range for COPD. Patients were recruited at hospital with a physician diagnosis of COPD exacerbation when often too ill to perform spirometry. Despite this being a limitation it reflects a more realistic picture of the illness, reflecting patients who are seen and treated in clinical practice.

In summary, the COPD mouse model reveals the involvement of MMP-12 activity outside the extracellular matrix. Several MMP-12 targets are also present in human airways, often with opposing functions. This strongly highlights the need to study COPD using a different model whereby the protease targets, rather than the proteases are centre-stage. This study provides a library of peptides for such studies and confirms TAILS as an ideal tool to use in studying the protease degradome in COPD.

Chapter 6 Discussion and Further Work

6.0 Introduction

MMP-12 has been implicated in COPD in animal studies and human genetic studies. However, few studies have focused on its activity at the protein level in COPD airways. As a result the mechanisms by which it is associated with COPD pathology remain unclear. This as well as the disappointing results of MMP inhibitors means that further understanding of MMP-12 biology is needed. This thesis sought to discover its substrate repertoire as this will lead to the design of more specific safer drugs designed to target mediators downstream of the protease. The following chapter summarizes the main findings and further work that should be followed on from this thesis.

6.1 MMP-12 is present and active in COPD sputum

One of the first steps in this thesis was to demonstrate the presence of active MMP-12 in human COPD sputum. Chaudhuri *et al.* [122] measured the presence of MMP-12 by ELISA and measured activity of the enzyme by a FRET assay. The disadvantages of such assays are their cross-reactivity with other MMPs and the need to activate the MMP in the biological sample under investigation by the operator prior to the activity assay. In this thesis human COPD sputum was analysed by Western blotting to detect the MMP-12. For this first time the presence of active MMP-12 in COPD airways was noted without prior manipulation of biological samples. In addition, this thesis also revealed the presence of the inactive and intermediately active forms alongside the fully active form, suggesting that activation of MMP-12 occurs *in situ* in the airways. This adds further weight to the findings by Chaudhuri *et al.* [122] that MMP-12 is present and active in human airways in COPD.

A limitation of note is that a semi-quantitative method was used to identify MMP-12 in sputum. When ELISA was used to quantify MMP-12 in sputum supernatant, levels were below the lower limit of detection of the kit (*Dendritics, Lyon, France*). Unfortunately, due to the limited sputum supernatant samples available, it was not possible to optimize detection with this kit or ELISA kits from other manufacturers.

6.2 OPN and TFPI were identified as new substrates for NE, rather than MMP-12, in human COPD

Following the identification of active MMP-12 in COPD sputum, the next step was to use a candidate-based approach to determine which *in vitro* substrates of MMP-12 were present in COPD airways. The *in vitro* data in the first two results chapters confirmed the literature findings that OPN and TFPI are both cleaved by MMP-12. To determine whether the *in vitro* findings could be translated to the airways, COPD sputum was analysed by Western blotting for OPN and TFPI fragments. Both were present in cleaved forms, with some fragments of a similar size to the MMP-12-cleaved OPN and TFPI fragments obtained following *in vitro* cleavage. Furthermore, the addition of recombinant OPN and TFPI to COPD sputum led to their cleavage into fragments, some of which were similar in size to those produced by MMP-12 cleavage *in vitro*. While this suggested that MMP-12 was responsible for cleaving OPN and TFPI *in vivo*, further studies were needed to confirm this. This task proved challenging. At first, an experiment was designed to immunoprecipitate MMP-12 out of sputum, followed by the addition of OPN or TFPI to sputum. If different sized fragments were obtained on spiking sputum with OPN and TFPI, with and without MMP-12 immunoprecipitation, then this would further suggest that MMP-12 was responsible for OPN and TFPI fragments. Unfortunately, immunoprecipitation of MMP-12 in sputum supernatant was unsuccessful, perhaps due to its presence in low amounts.

Since immunoprecipitation was unsuccessful a series of inhibition assays were conducted. Broad spectrum inhibitors were initially employed, followed by specific protease ones. Surprisingly, both TFPI and OPN cleavage occurred in sputum despite the presence of the metalloprotease inhibitors, suggesting that MMP-12 was not the main protease responsible for the degradation. In contrast, inhibition, albeit incomplete, of OPN and TFPI cleavage in sputum was seen with a broad spectrum serine protease inhibitor complex. By using a more specific serine protease inhibitor targeting NE only, notable inhibition of both OPN and TFPI cleavage was noted. Furthermore, higher sputum neutrophils were linked with increased OPN and TFPI cleavage in sputum. Further weight was added to these findings by *in vitro* experiments demonstrating that NE cleaves both OPN and TFPI. This is all suggestive of OPN and TFPI proteolysis in COPD airways being driven by NE. While MMP inhibition had no effect on OPN and TFPI cleavage in sputum, one cannot rule out MMP-12 activity still being present as there is the possibility that serine proteases are present in larger amounts than MMP-12 and therefore overshadow its activity. Had more sputum samples been available sputum neutrophil elastase levels could have been measured and compared in fast and slow OPN and TFPI-cleaving samples.

6.3 Protease activity in COPD airways is complex with different proteases targeting similar substrates

Complete inhibition of OPN and TFPI cleavage was never achieved with any inhibitor despite using high enough doses, often in combination too. This is due to the complexity of protease activity in the airways whereby different proteases target the same substrates. This highlights the difficulty in using a candidate based approach to determine the substrate profile of a particular protease. Indeed, the newer and more sophisticated technique of TAILS was next used to identify MMP-12 substrates.

6.4 MMP-12 targets a large variety of substrates outside the ECM

TAILS on mouse BAL samples provided a library of potential MMP-12 substrates for the first time in COPD. This included substrates with opposing functions, such as proteases and their inhibitors, pro-coagulants and anti-coagulants as well as complement factors, pro-inflammatory mediators, signalling peptides, and modulators of cytoskeletal function. Of note was the identification of C3 as a MMP-12 target. Earlier studies demonstrate that C3 is activated by MMP-12 leading to its pro-inflammatory role through its recruitment of inflammatory cells [307]. Also of interest, anti-thrombin III was identified as another potential substrate; its cleavage by MMP-12 has been shown cause loss of its anti-coagulant function [307]. This makes for interesting findings if further studies lead to their therapeutic manipulation. In the case of C3, preventing its cleavage may decrease inflammatory cell recruitment to the airways; targeting anti-thrombin III could reduce the intravascular thrombotic events and perhaps the incidence of CVD in COPD. Naturally, further studies are required to confirm that these are true MMP-12 substrates. This would be done by incubating the recombinant potential substrates identified by TAILS with recombinant MMP-12 and analysing the fragments obtained by gel electrophoresis followed by Edman sequencing. If this sequencing matches that detected by TAILS the substrates will be confirmed as MMP-12 targets.

6.5 TAILS on human COPD sputum identified the presence of MMP-12 substrates

Human COPD sputum was analysed for the first time by TAILS to determine whether the potential MMP-12 substrates identified in the mouse BAL study were present in the human COPD sputum degradome. There were peptides derived from 5

common proteins in the mouse and human study. Of note, these included complement C3 and anti-thrombin III whose importance in inflammatory cell recruitment and coagulation, respectively have been highlighted. In addition several peptides that were identified as MMP-12 substrates in previous MMP-12 murine studies were detected by TAILS in COPD sputum. Further studies are still needed to confirm that these peptides are cleaved by MMP-12 in human COPD. However this provides an important direction and basis for planning future studies aimed at improving the understanding of MMP-12 biology in COPD.

TAILS identified the presence of peptides with opposing functions. These included substrates such as proteases and anti-proteases, pro-inflammatory and anti-inflammatory mediators, as well as pro-coagulants and anti-coagulants. This suggests that airway proteolysis involves the targeting of substrates with opposing functions and may therefore be more complex than previously thought. Indeed, this study highlights the need for a change in the current thinking model in COPD whereby the protease is viewed as “bad” and the anti-protease as “good”. It is time to focus attention on the degraded peptides in studying the pathogenesis of COPD, not just the proteases that produce them.

6.6 TAILS was used successfully to identify the human COPD sputum degradome

For the first time, human COPD sputum was analysed by TAILS. Matched samples were analysed at exacerbation and recovery. This led to the identification of 1,116 peptides, providing the most comprehensive analysis to date of human COPD sputum. The variety of peptides identified highlighted the importance of proteolysis, anti-microbicidal, inflammatory cell recruitment, coagulation, complement system and redox activity, among other processes, providing further insight into the complexity of

the airway environment in COPD. Further studies are needed to compare COPD human sputum with samples from smokers without airflow obstruction and never smokers. Furthermore, TAILS on plasma samples will provide a clearer understanding of the link between airway and systemic inflammation in COPD.

6.7 Neutrophils are chiefly involved in proteolytic events in COPD airways

All three results chapters highlight the importance of neutrophils as a source of proteolysis in COPD. Inhibition of both OPN and TFPI cleavage in the airways was most notably achieved by serine protease or neutrophil elastase inhibitors. Sputum neutrophil counts were associated with increased and faster cleavage of OPN and TFPI in sputum *ex vivo*. Both OPN and TFPI were cleaved by NE *in vitro*. Furthermore, TAILS identified several peptides of neutrophil origin, such as NE, myeloperoxidase, myeloblastin, MMP-9, Cathepsin G, MMP-8 and MMP-9.

6.8 The lungs are involved in coagulation in COPD

When determining whether MMP-12 targeted TFPI in COPD it was noted that TFPI was present in COPD airways where it was actively cleaved. This identified a role for the airways in coagulation in COPD. This was of particular importance given the association between airway inflammation and CVD risk in COPD, CVD being often associated with intravascular thrombotic events. While cleavage of TFPI in the airways was driven by neutrophils, the precise functional role for this occurrence remained unclear. It was suspected that increased degradation of TFPI in the airways may lead to lower circulating TFPI levels thereby reducing the anti-coagulant properties of blood. However, contrary to the expected, higher peripheral TFPI levels were associated with increased risk of cardiovascular events. It must be noted that this study was restricted by a limited supply of human sputum samples; hence the use of Western blotting which

only allows semi-quantitative measurement. In order to better understand the functional role of TFPI cleavage in COPD airways and the utility of TFPI as a biomarker, more accurate measurement of sputum TFPI by methods such as ELISA is needed. Furthermore, this needs to be supplemented by measurements of other components of the coagulation pathways in the airways. This will allow more accurate comparison of airway and peripheral TFPI and provide a better understanding of the role of the lungs in coagulation.

6.9 Conclusion

The role of proteolysis in the airways in COPD is a lot more complex than previously thought. While proteolysis and peptide identification are central to improving understanding of COPD, the disease must no longer be simply viewed as an imbalance of proteases over anti-proteases. This thesis has highlighted novel roles for COPD airways, the complexity and paradoxical role of airway proteases, including MMP-12 and NE, and provided a library of potential MMP-12 substrates as well as the most comprehensive description of degradome in COPD airways. These findings will hopefully be used in the development of better drugs in the continued battle against COPD.

7.0 References

1. Calderón-Larrañaga, A., et al., *Association of population and primary healthcare factors with hospital admission rates for chronic obstructive pulmonary disease in England: national cross-sectional study*. Thorax, 2010.
2. Lozano, R., et al., *Global and regional mortality from 235 causes of death for 20 age groups in 1990 and 2010: a systematic analysis for the Global Burden of Disease Study 2010*. The Lancet. **380**(9859): p. 2095-2128.
3. Hurd, S., *The Impact of COPD on Lung Health Worldwide**. Chest, 2000. **117**(2 suppl): p. 1S-4S.
4. Sin, D.D. and S.F.P. Man, *Chronic Obstructive Pulmonary Disease as a Risk Factor for Cardiovascular Morbidity and Mortality*. Proceedings of the American Thoracic Society, 2005. **2**(1): p. 8-11.
5. www.goldcopd.org, *Global strategy for the diagnosis, management, and prevention of chronic obstructive pulmonary disease 2011*.
6. Halpin, D.M.G. and M. Miravittles, *Chronic Obstructive Pulmonary Disease*. Proceedings of the American Thoracic Society, 2006. **3**(7): p. 619-623.
7. Halbert, R.J., et al., *Interpreting COPD prevalence estimates: what is the true burden of disease?* Chest, 2003. **123**(5): p. 1684-92.
8. Buist, A.S., et al., *International variation in the prevalence of COPD (The BOLD Study): a population-based prevalence study*. The Lancet. **370**(9589): p. 741-750.
9. Divo, M., et al., *Comorbidities and Risk of Mortality in Patients with Chronic Obstructive Pulmonary Disease*. American Journal of Respiratory and Critical Care Medicine, 2012. **186**(2): p. 155-161.
10. Rennard, S., et al., *Impact of COPD in North America and Europe in 2000: subjects' perspective of Confronting COPD International Survey*. European Respiratory Journal, 2002. **20**(4): p. 799-805.
11. Sullivan, S.D., S.D. Ramsey, and T.A. Lee, *The economic burden of COPD*. Chest, 2000. **117**(2 Suppl): p. 5S-9S.
12. Thun, M.J., et al., *50-Year Trends in Smoking-Related Mortality in the United States*. New England Journal of Medicine, 2013. **368**(4): p. 351-364.
13. *Cigarette smoking among adults and trends in smoking cessation - United States, 2008*. MMWR Morb Mortal Wkly Rep, 2009. **58**(44): p. 1227-32.
14. Chung, K., G. Caramori, and I. Adcock, *Inhaled corticosteroids as combination therapy with β -adrenergic agonists in airways disease: present and future*. European Journal of Clinical Pharmacology, 2009. **65**(9): p. 853-871.
15. Calverley, P.M.A., et al., *Salmeterol and Fluticasone Propionate and Survival in Chronic Obstructive Pulmonary Disease*. New England Journal of Medicine, 2007. **356**(8): p. 775-789.
16. Hanania, N.A., K.R. Chapman, and S. Kesten, *Adverse effects of inhaled corticosteroids*. The American Journal of Medicine, 1995. **98**(2): p. 196-208.
17. Lesser, M., M.L. Padilla, and C. Cardozo, *Induction of emphysema in hamsters by intratracheal instillation of cathepsin B*. Am Rev Respir Dis, 1992. **145**(3): p. 661-8.
18. Janciauskiene, S.M., et al., *The discovery of α 1-antitrypsin and its role in health and disease*. Respiratory Medicine, 2011. **105**(8): p. 1129-1139.

19. Kao, R.C., et al., *Proteinase 3. A distinct human polymorphonuclear leukocyte proteinase that produces emphysema in hamsters.* J Clin Invest, 1988. **82**(6): p. 1963-73.
20. Burnett, D., et al., *Neutrophils from subjects with chronic obstructive pulmonary disease show enhanced chemotaxis and extracellular proteolysis.* The Lancet, 1987. **330**(8567): p. 1043-1046.
21. Magnussen, H., et al., *Safety and tolerability of an oral MMP-9 and -12 inhibitor, AZD1236, in patients with moderate-to-severe COPD: A randomised controlled 6-week trial.* Pulmonary Pharmacology & Therapeutics, 2011. **24**(5): p. 563-570.
22. Dahl, R., et al., *Effects of an oral MMP-9 and -12 inhibitor, AZD1236, on biomarkers in moderate/severe COPD: A randomised controlled trial.* Pulmonary Pharmacology & Therapeutics, 2012. **25**(2): p. 169-177.
23. Kuna, P., et al., *AZD9668, a neutrophil elastase inhibitor, plus ongoing budesonide/formoterol in patients with COPD.* Respir Med, 2012. **106**(4): p. 531-9.
24. Bramhall, S.R., et al., *Marimastat as maintenance therapy for patients with advanced gastric cancer: a randomised trial.* Br J Cancer, 2002. **86**(12): p. 1864-70.
25. King, J., et al., *Randomised double blind placebo control study of adjuvant treatment with the metalloproteinase inhibitor, Marimastat in patients with inoperable colorectal hepatic metastases: significant survival advantage in patients with musculoskeletal side-effects.* Anticancer Res, 2003. **23**(1B): p. 639-45.
26. Fortelny, N., et al., *Network analyses reveal pervasive functional regulation between proteases in the human protease web.* PLoS Biol, 2014. **12**(5): p. e1001869.
27. Yoshida, T. and R.M. Tuder, *Pathobiology of Cigarette Smoke-Induced Chronic Obstructive Pulmonary Disease.* Physiological Reviews, 2007. **87**(3): p. 1047-1082.
28. Mannino, D.M. and A.S. Buist, *Global burden of COPD: risk factors, prevalence, and future trends.* The Lancet. **370**(9589): p. 765-773.
29. Sexton, P., et al., *Fixed airflow obstruction among nonsmokers with asthma: a case-comparison study.* J Asthma, 2013. **50**(6): p. 606-12.
30. Pillai, S.G., et al., *A genome-wide association study in chronic obstructive pulmonary disease (COPD): identification of two major susceptibility loci.* PLoS Genet, 2009. **5**(3): p. e1000421.
31. Schirmer, H., et al., *Matrix metalloproteinase gene polymorphisms: lack of association with chronic obstructive pulmonary disease in a Brazilian population.* Genet Mol Res, 2009. **8**(3): p. 1028-34.
32. Castaldi, P.J., et al., *Genome-Wide Association Identifies Regulatory Loci Associated with Distinct Local Histogram Emphysema Patterns.* American Journal of Respiratory and Critical Care Medicine, 2014. **190**(4): p. 399-409.
33. Gordon, S.B., et al., *Respiratory risks from household air pollution in low and middle income countries.* The Lancet Respiratory Medicine, 2014. **2**(10): p. 823-860.
34. Alahmari, A.D., et al., *Influence of weather and atmospheric pollution on physical activity in patients with COPD.* Respir Res, 2015. **16**: p. 71.
35. Song, Q., et al., *The global contribution of outdoor air pollution to the incidence, prevalence, mortality and hospital admission for chronic obstructive pulmonary disease: a systematic review and meta-analysis.* Int J Environ Res Public Health, 2014. **11**(11): p. 11822-32.
36. Atkinson, R.W., et al., *Long-term exposure to outdoor air pollution and the incidence of chronic obstructive pulmonary disease in a national English cohort.* Occup Environ Med, 2015. **72**(1): p. 42-8.

37. Peto, R., Z.-M. Chen, and J. Boreham, *Tobacco-the growing epidemic*. Nat Med, 1999. **5**(1): p. 15-17.
38. Cosio Piqueras, M.G. and M.G. Cosio, *Disease of the airways in chronic obstructive pulmonary disease*. European Respiratory Journal, 2001. **18**(34 suppl): p. 41s-49s.
39. Saetta, M., et al., *Cellular and Structural Bases of Chronic Obstructive Pulmonary Disease*. American Journal of Respiratory and Critical Care Medicine, 2001. **163**(6): p. 1304-1309.
40. Gan, W.Q., S.F.P. Man, and D.D. Sin, *The Interactions Between Cigarette Smoking and Reduced Lung Function on Systemic Inflammation**. CHEST Journal, 2005. **127**(2): p. 558-564.
41. Donaldson, G.C., et al., *Increased risk of myocardial infarction and stroke following exacerbation of copd*. CHEST Journal, 2010. **137**(5): p. 1091-1097.
42. Patel, A.R.C., et al., *Cardiovascular Risk, Myocardial Injury, and Exacerbations of Chronic Obstructive Pulmonary Disease*. American Journal of Respiratory and Critical Care Medicine, 2013. **188**(9): p. 1091-1099.
43. McGarvey, L.P., et al., *Ascertainment of cause-specific mortality in COPD: operations of the TORCH Clinical Endpoint Committee*. Thorax, 2007. **62**(5): p. 411-415.
44. Donaldson, G.C., et al., *Airway and systemic inflammation and decline in lung function in patients with copd**. CHEST Journal, 2005. **128**(4): p. 1995-2004.
45. Hogg, J.C., P.T. Macklem, and W.M. Thurlbeck, *Site and Nature of Airway Obstruction in Chronic Obstructive Lung Disease*. New England Journal of Medicine, 1968. **278**(25): p. 1355-1360.
46. Van Brabandt, H., et al., *Partitioning of pulmonary impedance in excised human and canine lungs*. Journal of Applied Physiology, 1983. **55**(6): p. 1733-1742.
47. Yanai, M., et al., *Site of airway obstruction in pulmonary disease: direct measurement of intrabronchial pressure*. Journal of Applied Physiology, 1992. **72**(3): p. 1016-1023.
48. Hogg, J., et al., *The nature of small-airway obstruction in chronic obstructive pulmonary disease*. N Engl J Med, 2004. **350**: p. 2645 - 2653.
49. Mead, J., et al., *Significance of the relationship between lung recoil and maximum expiratory flow*. J Appl Physiol, 1967. **22**(1): p. 95-108.
50. Otis, A.B., et al., *Mechanical Factors in Distribution of Pulmonary Ventilation*. Journal of Applied Physiology, 1956. **8**(4): p. 427-443.
51. Hogg, J.C., *Pathophysiology of airflow limitation in chronic obstructive pulmonary disease*. The Lancet, 2004. **364**(9435): p. 709-721.
52. Rutgers, S.R., et al., *Ongoing airway inflammation in patients with COPD who do not currently smoke*. Thorax, 2000. **55**(1): p. 12-8.
53. Willemse, B., et al., *Effect of 1-year smoking cessation on airway inflammation in COPD and asymptomatic smokers*. Eur Respir J, 2005. **26**: p. 835 - 845.
54. Doz, E., et al., *Cigarette Smoke-Induced Pulmonary Inflammation Is TLR4/MyD88 and IL-1R1/MyD88 Signaling Dependent*. The Journal of Immunology, 2008. **180**(2): p. 1169-1178.
55. Mercer, B.A., et al., *The Epithelial Cell in Lung Health and Emphysema Pathogenesis*. Curr Respir Med Rev, 2006. **2**(2): p. 101-142.
56. Fuke, S., et al., *Chemokines in bronchiolar epithelium in the development of chronic obstructive pulmonary disease*. Am J Respir Cell Mol Biol, 2004. **31**(4): p. 405-12.

57. de Boer, W.I., et al., *Monocyte chemoattractant protein 1, interleukin 8, and chronic airways inflammation in COPD*. J Pathol, 2000. **190**(5): p. 619-26.
58. Traves, S.L., et al., *Specific CXC but not CC chemokines cause elevated monocyte migration in COPD: a role for CXCR2*. Journal of Leukocyte Biology, 2004. **76**(2): p. 441-450.
59. Burnett, D., et al., *Neutrophils from subjects with chronic obstructive lung disease show enhanced chemotaxis and extracellular proteolysis*. Lancet, 1987. **2**(8567): p. 1043-6.
60. Finlay, G., et al., *Matrix Metalloproteinase Expression and Production by Alveolar Macrophages in Emphysema*. American Journal of Respiratory and Critical Care Medicine, 1997. **156**(1): p. 240-247.
61. Lee, S.H., et al., *Antielastin autoimmunity in tobacco smoking-induced emphysema*. Nat Med, 2007. **13**(5): p. 567-9.
62. Feghali-Bostwick, C.A., et al., *Autoantibodies in Patients with Chronic Obstructive Pulmonary Disease*. American Journal of Respiratory and Critical Care Medicine, 2008. **177**(2): p. 156-163.
63. Polverino, F., et al., *A Novel Insight into Adaptive Immunity in Chronic Obstructive Pulmonary Disease*. American Journal of Respiratory and Critical Care Medicine, 2010. **182**(8): p. 1011-1019.
64. Saetta, M., et al., *CD8 + ve Cells in the Lungs of Smokers with Chronic Obstructive Pulmonary Disease*. American Journal of Respiratory and Critical Care Medicine, 1999. **160**(2): p. 711-717.
65. Saetta, M., et al., *Activated T-lymphocytes and macrophages in bronchial mucosa of subjects with chronic bronchitis*. Am Rev Respir Dis, 1993. **147**(2): p. 301-6.
66. Martin, T.R., et al., *The effects of chronic bronchitis and chronic air-flow obstruction on lung cell populations recovered by bronchoalveolar lavage*. Am Rev Respir Dis, 1985. **132**(2): p. 254-60.
67. Thompson, A.B., et al., *Intraluminal airway inflammation in chronic bronchitis. Characterization and correlation with clinical parameters*. Am Rev Respir Dis, 1989. **140**(6): p. 1527-37.
68. O'Donnell, R.A., et al., *Relationship between peripheral airway dysfunction, airway obstruction, and neutrophilic inflammation in COPD*. Thorax, 2004. **59**(10): p. 837-842.
69. Stanescu, D., et al., *Airways obstruction, chronic expectoration, and rapid decline of FEV1 in smokers are associated with increased levels of sputum neutrophils*. Thorax, 1996. **51**(3): p. 267-71.
70. Di Stefano, A., et al., *Severity of Airflow Limitation Is Associated with Severity of Airway Inflammation in Smokers*. American Journal of Respiratory and Critical Care Medicine, 1998. **158**(4): p. 1277-1285.
71. de Jong, J.W., et al., *Peripheral blood lymphocyte cell subsets in subjects with chronic obstructive pulmonary disease: association with smoking, IgE and lung function*. Respir Med, 1997. **91**(2): p. 67-76.
72. Pauwels, R., et al., *COPD exacerbations: the importance of a standard definition*. Respiratory Medicine, 2004. **98**(2): p. 99-107.
73. Burge, S. and J.A. Wedzicha, *COPD exacerbations: definitions and classifications*. Eur Respir J Suppl, 2003. **41**: p. 46s-53s.
74. Donaldson, G.C., et al., *Relationship between exacerbation frequency and lung function decline in chronic obstructive pulmonary disease*. Thorax, 2002. **57**(10): p. 847-852.
75. Kanner, R.E., N.R. Anthonisen, and J.E. Connett, *Lower Respiratory Illnesses Promote FEV1 Decline in Current Smokers But Not Ex-Smokers with Mild Chronic Obstructive Pulmonary Disease*. American Journal of Respiratory and Critical Care Medicine, 2001. **164**(3): p. 358-364.

76. Seemungal, T.A.R., et al., *Effect of Exacerbation on Quality of Life in Patients with Chronic Obstructive Pulmonary Disease*. American Journal of Respiratory and Critical Care Medicine, 1998. **157**(5): p. 1418-1422.
77. Price, L.C., et al., *UK National COPD Audit 2003: impact of hospital resources and organisation of care on patient outcome following admission for acute COPD exacerbation*. Thorax, 2006. **61**(10): p. 837-842.
78. Halpin, D.M., et al., *Exacerbation frequency and course of COPD*. Int J Chron Obstruct Pulmon Dis, 2012. **7**: p. 653-61.
79. Hurst, J.R., et al., *Susceptibility to Exacerbation in Chronic Obstructive Pulmonary Disease*. New England Journal of Medicine, 2010. **363**(12): p. 1128-1138.
80. Fujimoto, K., et al., *Airway inflammation during stable and acutely exacerbated chronic obstructive pulmonary disease*. European Respiratory Journal, 2005. **25**(4): p. 640-646.
81. Maestrelli, P., et al., *Comparison of leukocyte counts in sputum, bronchial biopsies, and bronchoalveolar lavage*. American Journal of Respiratory and Critical Care Medicine, 1995. **152**(6): p. 1926-1931.
82. Papi, A., et al., *Infections and Airway Inflammation in Chronic Obstructive Pulmonary Disease Severe Exacerbations*. American Journal of Respiratory and Critical Care Medicine, 2006. **173**(10): p. 1114-1121.
83. Saetta, M., et al., *Airway eosinophilia in chronic bronchitis during exacerbations*. American Journal of Respiratory and Critical Care Medicine, 1994. **150**(6): p. 1646-1652.
84. Gompertz, S., et al., *Changes in bronchial inflammation during acute exacerbations of chronic bronchitis*. Eur Respir J, 2001. **17**(6): p. 1112-9.
85. Mercer, P., et al., *MMP-9, TIMP-1 and inflammatory cells in sputum from COPD patients during exacerbation*. Respiratory Research, 2005. **6**(1): p. 151.
86. Kwiatkowska, S., et al., *Enhanced Exhalation of Matrix Metalloproteinase-9 and Tissue Inhibitor of Metalloproteinase-1 in Patients with COPD Exacerbation: A Prospective Study*. Respiration, 2012. **84**(3): p. 231-241.
87. Connors, A.F., et al., *Outcomes following acute exacerbation of severe chronic obstructive lung disease. The SUPPORT investigators (Study to Understand Prognoses and Preferences for Outcomes and Risks of Treatments)*. American Journal of Respiratory and Critical Care Medicine, 1996. **154**(4): p. 959-967.
88. Sethi, S., et al., *New Strains of Bacteria and Exacerbations of Chronic Obstructive Pulmonary Disease*. New England Journal of Medicine, 2002. **347**(7): p. 465-471.
89. Sethi, S., et al., *Airway Bacterial Concentrations and Exacerbations of Chronic Obstructive Pulmonary Disease*. American Journal of Respiratory and Critical Care Medicine, 2007. **176**(4): p. 356-361.
90. George, S.N., et al., *Human rhinovirus infection during naturally occurring COPD exacerbations*. European Respiratory Journal, 2014.
91. Stockley, R.A., et al., *RElationship of sputum color to nature and outpatient management of acute exacerbations of copd**. CHEST Journal, 2000. **117**(6): p. 1638-1645.
92. Rohde, G., et al., *Respiratory viruses in exacerbations of chronic obstructive pulmonary disease requiring hospitalisation: a case-control study*. Thorax, 2003. **58**(1): p. 37-42.
93. Donaldson, G.C., et al., *Effect of temperature on lung function and symptoms in chronic obstructive pulmonary disease*. Eur Respir J, 1999. **13**(4): p. 844-9.

94. MacNee, W. and K. Donaldson, *Exacerbations of COPD: environmental mechanisms*. Chest, 2000. **117**(5 Suppl 2): p. 390S-7S.
95. Viegi, G., et al., *Epidemiology of chronic obstructive pulmonary disease: Health effects of air pollution*. Respirology, 2006. **11**(5): p. 523-532.
96. Dominici, F., et al., *Fine particulate air pollution and hospital admission for cardiovascular and respiratory diseases*. JAMA, 2006. **295**(10): p. 1127-1134.
97. Ling, S.H. and S.F. van Eeden, *Particulate matter air pollution exposure: role in the development and exacerbation of chronic obstructive pulmonary disease*. Int J Chron Obstruct Pulmon Dis, 2009. **4**: p. 233-43.
98. Janoff, A., et al., *Experimental emphysema induced with purified human neutrophil elastase: tissue localization of the instilled protease*. Am Rev Respir Dis, 1977. **115**(3): p. 461-78.
99. Shapiro, S.D., et al., *Neutrophil Elastase Contributes to Cigarette Smoke-Induced Emphysema in Mice*. The American Journal of Pathology, 2003. **163**(6): p. 2329-2335.
100. Hautamaki, R.D., et al., *Requirement for Macrophage Elastase for Cigarette Smoke-Induced Emphysema in Mice*. Science, 1997. **277**(5334): p. 2002-2004.
101. Gadek, J.E., et al., *Antielastases of the human alveolar structures. Implications for the protease-antiprotease theory of emphysema*. The Journal of Clinical Investigation, 1981. **68**(4): p. 889-898.
102. Russell, R.E.K., et al., *Release and Activity of Matrix Metalloproteinase-9 and Tissue Inhibitor of Metalloproteinase-1 by Alveolar Macrophages from Patients with Chronic Obstructive Pulmonary Disease*. American Journal of Respiratory Cell and Molecular Biology, 2002. **26**(5): p. 602-609.
103. Borregaard, N. and J.B. Cowland, *Granules of the human neutrophilic polymorphonuclear leukocyte*. Blood, 1997. **89**(10): p. 3503-21.
104. Amulic, B., et al., *Neutrophil Function: From Mechanisms to Disease*. Annual Review of Immunology, 2012. **30**(1): p. 459-489.
105. Korkmaz, B., et al., *Neutrophil Elastase, Proteinase 3, and Cathepsin G as Therapeutic Targets in Human Diseases*. Pharmacological Reviews, 2010. **62**(4): p. 726-759.
106. Scapini, P., et al., *Neutrophils produce biologically active macrophage inflammatory protein-3 α (MIP-3 α) / CCL20 and MIP-3 β / CCL19*. European Journal of Immunology, 2001. **31**(7): p. 1981-1988.
107. Shapiro, S.D., *The Macrophage in Chronic Obstructive Pulmonary Disease*. American Journal of Respiratory and Critical Care Medicine, 1999. **160**(supplement_1): p. S29-S32.
108. Barnes, P.J., S.D. Shapiro, and R.A. Pauwels, *Chronic obstructive pulmonary disease: molecular and cellular mechanisms*. European Respiratory Journal, 2003. **22**(4): p. 672-688.
109. Barnes, P.J., *Mediators of Chronic Obstructive Pulmonary Disease*. Pharmacological Reviews, 2004. **56**(4): p. 515-548.
110. Soehnlein, O., C. Weber, and L. Lindbom, *Neutrophil granule proteins tune monocytic cell function*. Trends in Immunology, 2009. **30**(11): p. 538-546.
111. Tetley, T.D., *Macrophages and the pathogenesis of copd**. CHEST Journal, 2002. **121**(5_suppl): p. 156S-159S.
112. Smith, M.E., K. van der Maesen, and F.P. Somera, *Macrophage and microglial responses to cytokines in vitro: Phagocytic activity, proteolytic enzyme release, and free radical production*. Journal of Neuroscience Research, 1998. **54**(1): p. 68-78.
113. Churg, A., et al., *Macrophage Metalloelastase Mediates Acute Cigarette Smoke-induced Inflammation via Tumor Necrosis Factor- α Release*.

- American Journal of Respiratory and Critical Care Medicine, 2003. **167**(8): p. 1083-1089.
114. Gearing, A.J.H., et al., *Processing of tumour necrosis factor-[alpha] precursor by metalloproteinases*. Nature, 1994. **370**(6490): p. 555-557.
 115. Dean, R.A., et al., *Macrophage-specific metalloelastase (MMP-12) truncates and inactivates ELR+ CXC chemokines and generates CCL2, -7, -8, and -13 antagonists: potential role of the macrophage in terminating polymorphonuclear leukocyte influx*. Blood, 2008. **112**(8): p. 3455-3464.
 116. Starr, A.E., et al., *Biochemical Analysis of Matrix Metalloproteinase Activation of Chemokines CCL15 and CCL23 and Increased Glycosaminoglycan Binding of CCL16*. Journal of Biological Chemistry, 2012. **287**(8): p. 5848-5860.
 117. Cox, J.H., et al., *Matrix Metalloproteinase Processing of CXCL11/I-TAC Results in Loss of Chemoattractant Activity and Altered Glycosaminoglycan Binding*. Journal of Biological Chemistry, 2008. **283**(28): p. 19389-19399.
 118. Gibson, T.L.B. and P. Cohen, *Inflammation-related neutrophil proteases, cathepsin G and elastase, function as insulin-like growth factor binding protein proteases*. Growth Hormone & IGF Research, 1999. **9**(4): p. 241-253.
 119. Koolwijk, P., et al., *Proteolysis of the urokinase-type plasminogen activator receptor by metalloproteinase-12: implication for angiogenesis in fibrin matrices*. Blood, 2001. **97**(10): p. 3123-3131.
 120. Boschetto, P., et al., *Association between markers of emphysema and more severe chronic obstructive pulmonary disease*. Thorax, 2006. **61**(12): p. 1037-42.
 121. Culpitt, S.V., et al., *Sputum matrix metalloproteases: comparison between chronic obstructive pulmonary disease and asthma*. Respiratory Medicine, 2005. **99**(6): p. 703-710.
 122. Chaudhuri, R., et al., *Sputum matrix metalloproteinase-12 in patients with chronic obstructive pulmonary disease and asthma: Relationship to disease severity*. Journal of Allergy and Clinical Immunology, 2012. **129**(3): p. 655-663.e8.
 123. D'Armiento, J.M., et al., *Increased matrix metalloproteinase (MMPs) levels do not predict disease severity or progression in emphysema*. PLoS One, 2013. **8**(2): p. e56352.
 124. Babior, B.M., *The respiratory burst of phagocytes*. The Journal of Clinical Investigation, 1984. **73**(3): p. 599-601.
 125. Repine, J.E., A. Bast, and I. Lankhorst, *Oxidative stress in chronic obstructive pulmonary disease*. Oxidative Stress Study Group. Am J Respir Crit Care Med, 1997. **156**(2 Pt 1): p. 341-57.
 126. Halliwell, B. and J.M. Gutteridge, *Oxygen toxicity, oxygen radicals, transition metals and disease*. Biochem J, 1984. **219**(1): p. 1-14.
 127. Nelson, M.E., A.R. O'Brien-Ladner, and L.J. Wesselius, *Regional variation in iron and iron-binding proteins within the lungs of smokers*. American Journal of Respiratory and Critical Care Medicine, 1996. **153**(4): p. 1353-1358.
 128. Wesselius, L.J., M.E. Nelson, and B.S. Skikne, *Increased release of ferritin and iron by iron-loaded alveolar macrophages in cigarette smokers*. American Journal of Respiratory and Critical Care Medicine, 1994. **150**(3): p. 690-695.
 129. Morrow, J.D., et al., *Increase in Circulating Products of Lipid Peroxidation (F2-Isoprostanes) in Smokers — Smoking as a Cause of Oxidative Damage*. New England Journal of Medicine, 1995. **332**(18): p. 1198-1203.

130. Schaberg, T., et al., *Subpopulations of alveolar macrophages in smokers and nonsmokers: relation to the expression of CD11/CD18 molecules and superoxide anion production*. American Journal of Respiratory and Critical Care Medicine, 1995. **151**(5): p. 1551-1558.
131. Dekhuijzen, P.N., et al., *Increased exhalation of hydrogen peroxide in patients with stable and unstable chronic obstructive pulmonary disease*. American Journal of Respiratory and Critical Care Medicine, 1996. **154**(3): p. 813-816.
132. Pinamonti, S., et al., *Xanthine oxidase activity in bronchoalveolar lavage fluid from patients with chronic obstructive pulmonary disease*. Free Radical Biology and Medicine, 1996. **21**(2): p. 147-155.
133. Cavarra, E., et al., *Human SLPI inactivation after cigarette smoke exposure in a new in vivo model of pulmonary oxidative stress*. American Journal of Physiology - Lung Cellular and Molecular Physiology, 2001. **281**(2): p. L412-L417.
134. Fischer, B.M., et al., *Neutrophil elastase increases airway epithelial nonheme iron levels*. Clin Transl Sci, 2009. **2**(5): p. 333-9.
135. Okamoto, T., et al., *Activation of human neutrophil procollagenase by nitrogen dioxide and peroxynitrite: a novel mechanism for procollagenase activation involving nitric oxide*. Arch Biochem Biophys, 1997. **342**(2): p. 261-74.
136. Gu, Z., et al., *S-Nitrosylation of Matrix Metalloproteinases: Signaling Pathway to Neuronal Cell Death*. Science, 2002. **297**(5584): p. 1186-1190.
137. Peppin, G., Weiss, S., *Activation of the endogenous metalloproteinase, gelatinase, by triggered human neutrophils*. Proceedings of the American Thoracic Society, 1986. **83**: p. 4322-6.
138. Owen, C.A., *Proteinases and oxidants as targets in the treatment of chronic obstructive pulmonary disease*. Proc Am Thorac Soc, 2005. **2**(4): p. 373-85; discussion 394-5.
139. Keatings, V.M., et al., *Effects of inhaled and oral glucocorticoids on inflammatory indices in asthma and COPD*. Am J Respir Crit Care Med, 1997. **155**(2): p. 542-8.
140. Peleman, R.A., et al., *The cellular composition of induced sputum in chronic obstructive pulmonary disease*. Eur Respir J, 1999. **13**(4): p. 839-43.
141. Saetta, M., et al., *Inflammatory Cells in the Bronchial Glands of Smokers with Chronic Bronchitis*. American Journal of Respiratory and Critical Care Medicine, 1997. **156**(5): p. 1633-1639.
142. Panzner, P., et al., *MARked up-regulation of T lymphocytes and expression of interleukin-9 in bronchial biopsies from patients with chronic bronchitis with obstruction**. CHEST Journal, 2003. **124**(5): p. 1909-1915.
143. Parr, D., et al., *Inflammation in sputum relates to progression of disease in subjects with COPD: a prospective descriptive study*. Respiratory Research, 2006. **7**(1): p. 136.
144. Sapey, E., et al., *Behavioral and Structural Differences in Migrating Peripheral Neutrophils from Patients with Chronic Obstructive Pulmonary Disease*. American Journal of Respiratory and Critical Care Medicine, 2011. **183**(9): p. 1176-1186.
145. Massberg, S., et al., *Reciprocal coupling of coagulation and innate immunity via neutrophil serine proteases*. Nat Med, 2010. **16**(8): p. 887-96.
146. Houghton, A.M., et al., *Elastin fragments drive disease progression in a murine model of emphysema*. The Journal of Clinical Investigation, 2006. **116**(3): p. 753-759.

147. Gordon, S. and P. Taylor, *Monocyte and macrophage heterogeneity*. Nat Rev Immunol, 2005. **5**: p. 953 - 964.
148. Landsman, L. and S. Jung, *Lung Macrophages Serve as Obligatory Intermediate between Blood Monocytes and Alveolar Macrophages*. The Journal of Immunology, 2007. **179**(6): p. 3488-3494.
149. Yona, S. and S. Jung, *Monocytes: subsets, origins, fates and functions*. Curr Opin Hematol, 2010. **17**(1): p. 53-9.
150. Murray, P.J. and T.A. Wynn, *Protective and pathogenic functions of macrophage subsets*. Nat Rev Immunol, 2011. **11**(11): p. 723-37.
151. Gordon, S., *Alternative activation of macrophages*. Nat Rev Immunol, 2003. **3**(1): p. 23-35.
152. Liu, G. and H. Yang, *Modulation of macrophage activation and programming in immunity*. J Cell Physiol, 2013. **228**(3): p. 502-12.
153. Mantovani, A., A. Sica, and M. Locati, *Macrophage Polarization Comes of Age*. Immunity, 2005. **23**(4): p. 344-346.
154. Novak, M.L. and T.J. Koh, *Macrophage phenotypes during tissue repair*. Journal of Leukocyte Biology, 2013. **93**(6): p. 875-881.
155. Benoit, M., B. Desnues, and J.-L. Mege, *Macrophage Polarization in Bacterial Infections*. The Journal of Immunology, 2008. **181**(6): p. 3733-3739.
156. Kaku, Y., et al., *Overexpression of CD163, CD204 and CD206 on alveolar macrophages in the lungs of patients with severe chronic obstructive pulmonary disease*. PLoS One, 2014. **9**(1): p. e87400.
157. Finkelstein, R., et al., *Alveolar inflammation and its relation to emphysema in smokers*. American Journal of Respiratory and Critical Care Medicine, 1995. **152**(5): p. 1666-72.
158. Traves, S.L., et al., *Increased levels of the chemokines GRO α and MCP-1 in sputum samples from patients with COPD*. Thorax, 2002. **57**(7): p. 590-595.
159. Caramori, G., et al., *Nuclear localisation of p65 in sputum macrophages but not in sputum neutrophils during COPD exacerbations*. Thorax, 2003. **58**(4): p. 348-351.
160. Wang, M.H., Y.Q. Zhou, and Y.Q. Chen, *Macrophage-Stimulating Protein and RON Receptor Tyrosine Kinase: Potential Regulators of Macrophage Inflammatory Activities*. Scandinavian Journal of Immunology, 2002. **56**(6): p. 545-553.
161. Shaykhiev, R., et al., *Smoking-dependent reprogramming of alveolar macrophage polarization: Implication for pathogenesis of chronic obstructive pulmonary disease*. J Immunol, 2009. **183**: p. 2867 - 2883.
162. Chen, H., et al., *Tobacco Smoking Inhibits Expression of Proinflammatory Cytokines and Activation of IL-1R-Associated Kinase, p38, and NF- κ B in Alveolar Macrophages Stimulated with TLR2 and TLR4 Agonists*. The Journal of Immunology, 2007. **179**(9): p. 6097-6106.
163. Yang, S.-R., et al., *Cigarette smoke induces proinflammatory cytokine release by activation of NF- κ B and posttranslational modifications of histone deacetylase in macrophages*. American Journal of Physiology - Lung Cellular and Molecular Physiology, 2006. **291**(1): p. L46-L57.
164. Kunz, L.I., et al., *Smoking status and anti-inflammatory macrophages in bronchoalveolar lavage and induced sputum in COPD*. Respir Res, 2011. **12**: p. 34.
165. Chana, K.K., et al., *Identification of a distinct glucocorticosteroid-insensitive pulmonary macrophage phenotype in patients with chronic obstructive pulmonary disease*. Journal of Allergy and Clinical Immunology, (0).
166. Gross, J. and C.M. Lapiere, *Collagenolytic activity in amphibian tissues: a tissue culture assay*. Proc Natl Acad Sci U S A, 1962. **48**: p. 1014-22.

167. Verma, R.P. and C. Hansch, *Matrix metalloproteinases (MMPs): Chemical-biological functions and (Q)SARs*. Bioorganic & Medicinal Chemistry, 2007. **15**(6): p. 2223-2268.
168. Nagase, H., R. Visse, and G. Murphy, *Structure and function of matrix metalloproteinases and TIMPs*. Cardiovascular Research, 2006. **69**(3): p. 562-573.
169. Matsumura, S.-i., et al., *Targeted deletion or pharmacological inhibition of MMP-2 prevents cardiac rupture after myocardial infarction in mice*. The Journal of Clinical Investigation, 2005. **115**(3): p. 599-609.
170. Johnson, J.L., et al., *Divergent effects of matrix metalloproteinases 3, 7, 9, and 12 on atherosclerotic plaque stability in mouse brachiocephalic arteries*. Proceedings of the National Academy of Sciences of the United States of America, 2005. **102**(43): p. 15575-15580.
171. Matsumoto, S.-i., et al., *Expression and Localization of Matrix Metalloproteinase-12 in the Aorta of Cholesterol-Fed Rabbits: Relationship to Lesion Development*. The American Journal of Pathology, 1998. **153**(1): p. 109-119.
172. D'Armiento, J., et al., *Collagenase expression in the lungs of transgenic mice causes pulmonary emphysema*. Cell, 1992. **71**(6): p. 955-961.
173. Shapiro, S.D., *Elastolytic Metalloproteinases Produced by Human Mononuclear Phagocytes: Potential Roles in Destructive Lung Disease*. Am. J. Respir. Crit. Care Med., 1994. **150**(6_Pt_2): p. S160-164.
174. Bruner-Tran, K.L., et al., *Steroid and Cytokine Regulation of Matrix Metalloproteinase Expression in Endometriosis and the Establishment of Experimental Endometriosis in Nude Mice*. Journal of Clinical Endocrinology & Metabolism, 2002. **87**(10): p. 4782-4791.
175. Carnevale, D., et al., *Placental Growth Factor Regulates Cardiac Inflammation Through the Tissue Inhibitor of Metalloproteinases-3/Tumor Necrosis Factor- α -Converting Enzyme Axis / Clinical Perspective*. Circulation, 2011. **124**(12): p. 1337-1350.
176. Tandara, A.A. and T.A. Mustoe, *MMP- and TIMP-secretion by human cutaneous keratinocytes and fibroblasts - impact of coculture and hydration*. Journal of Plastic, Reconstructive & Aesthetic Surgery, 2011. **64**(1): p. 108-116.
177. Hou, P., et al., *Matrix metalloproteinase-12 (MMP-12) in osteoclasts: new lesson on the involvement of MMPs in bone resorption*. Bone, 2004. **34**(1): p. 37-47.
178. Chun, T.-H., et al., *MT1-MMP-dependent neovessel formation within the confines of the three-dimensional extracellular matrix*. The Journal of Cell Biology, 2004. **167**(4): p. 757-767.
179. Ardi, V.C., et al., *Human neutrophils uniquely release TIMP-free MMP-9 to provide a potent catalytic stimulator of angiogenesis*. Proceedings of the National Academy of Sciences, 2007. **104**(51): p. 20262-20267.
180. Oviedo-Orta, E., et al., *Comparison of MMP-2 and MMP-9 secretion from T helper 0, 1 and 2 lymphocytes alone and in coculture with macrophages*. Immunology, 2008. **124**(1): p. 42-50.
181. Baker, A.H., D.R. Edwards, and G. Murphy, *Metalloproteinase inhibitors: biological actions and therapeutic opportunities*. Journal of Cell Science, 2002. **115**(19): p. 3719-3727.
182. Mott, J.D., et al., *Post-translational Proteolytic Processing of Procollagen C-terminal Proteinase Enhancer Releases a Metalloproteinase Inhibitor*. Journal of Biological Chemistry, 2000. **275**(2): p. 1384-1390.

183. Petitclerc, E., et al., *New Functions for Non-collagenous Domains of Human Collagen Type IV*. Journal of Biological Chemistry, 2000. **275**(11): p. 8051-8061.
184. Herman, M.P., et al., *Tissue factor pathway inhibitor-2 is a novel inhibitor of matrix metalloproteinases with implications for atherosclerosis*. The Journal of Clinical Investigation, 2001. **107**(9): p. 1117-1126.
185. Murphy, G. and A.J.P. Docherty, *The Matrix Metalloproteinases and Their Inhibitors*. Am. J. Respir. Cell Mol. Biol., 1992. **7**(2): p. 120-125.
186. Nagase, H., et al., *Stepwise activation mechanisms of the precursor of matrix metalloproteinase 3 (stromelysin) by proteinases and (4-aminophenyl)mercuric acetate*. Biochemistry, 1990. **29**(24): p. 5783-5789.
187. Cao, J., et al., *The Propeptide Domain of Membrane Type 1-Matrix Metalloproteinase Acts as an Intramolecular Chaperone when Expressed in trans with the Mature Sequence in COS-1 Cells*. Journal of Biological Chemistry, 2000. **275**(38): p. 29648-29653.
188. Klaus, M., *Crystal structures of MMPs in complex with physiological and pharmacological inhibitors*. Biochimie, 2005. **87**(3-4): p. 249-263.
189. Lovejoy, B., et al., *Crystal structures of MMP-1 and -13 reveal the structural basis for selectivity of collagenase inhibitors*. Nat Struct Mol Biol, 1999. **6**(3): p. 217-221.
190. Visse, R. and H. Nagase, *Matrix Metalloproteinases and Tissue Inhibitors of Metalloproteinases: Structure, Function, and Biochemistry*. Circulation Research, 2003. **92**(8): p. 827-839.
191. Bode, W., F.-X. Gomis-Rüth, and W. Stöckler, *Astacins, serralysins, snake venom and matrix metalloproteinases exhibit identical zinc-binding environments (HEXXHXXGXXH and Met-turn) and topologies and should be grouped into a common family, the 'metzincins'*. FEBS Letters, 1993. **331**(1-2): p. 134-140.
192. Park, H.I., et al., *The Intermediate S1' Pocket of the Endometase/Matrilysin-2 Active Site Revealed by Enzyme Inhibition Kinetic Studies, Protein Sequence Analyses, and Homology Modeling*. Journal of Biological Chemistry, 2003. **278**(51): p. 51646-51653.
193. Piccard, H., P.E. Van den Steen, and G. Opdenakker, *Hemopexin domains as multifunctional liganding modules in matrix metalloproteinases and other proteins*. Journal of Leukocyte Biology, 2007. **81**(4): p. 870-892.
194. Curci, J.A., et al., *Expression and localization of macrophage elastase (matrix metalloproteinase-12) in abdominal aortic aneurysms*. J Clin Invest, 1998. **102**(11): p. 1900-10.
195. Werb, Z. and S. Gordon, *Elastase secretion by stimulated macrophages. Characterization and regulation*. The Journal of Experimental Medicine, 1975. **142**(2): p. 361-377.
196. Banda, M.J. and Z. Werb, *Mouse macrophage elastase. Purification and characterization as a metalloproteinase*. Biochem. J., 1981. **193**(2): p. 589-605.
197. Shapiro, S.D., et al., *Molecular cloning, chromosomal localization, and bacterial expression of a murine macrophage metalloelastase*. Journal of Biological Chemistry, 1992. **267**(7): p. 4664-71.
198. Shapiro, S.D., D.K. Kobayashi, and T.J. Ley, *Cloning and characterization of a unique elastolytic metalloproteinase produced by human alveolar macrophages*. Journal of Biological Chemistry, 1993. **268**(32): p. 23824-23829.
199. Nar, H., et al., *Crystal structure of human macrophage elastase (MMP-12) in complex with a hydroxamic acid inhibitor*. Journal of Molecular Biology, 2001. **312**(4): p. 743-751.

200. Xie, S., et al., *Induction and regulation of matrix metalloproteinase-12 in human airway smooth muscle cells*. *Respir Res*, 2005. **6**: p. 148.
201. Salmela, M.T., et al., *Upregulation and differential expression of matrix metalloproteinase (MMP-7) and metalloelastase (MMP-12) and their inhibitors TIMP-1 and TIMP-3 in Barrett's oesophageal adenocarcinoma*. *Br J Cancer*, 2001. **85**(3): p. 383-392.
202. Overall, C.M. and O. Kleinfeld, *Tumour microenvironment - opinion: validating matrix metalloproteinases as drug targets and anti-targets for cancer therapy*. *Nat Rev Cancer*, 2006. **6**(3): p. 227-39.
203. Shipley, J.M., et al., *Metalloelastase is required for macrophage-mediated proteolysis and matrix invasion in mice*. *Proceedings of the National Academy of Sciences*, 1996. **93**(9): p. 3942-3946.
204. Hunninghake, G.W., et al., *Elastin fragments attract macrophage precursors to diseased sites in pulmonary emphysema*. *Science*, 1981. **212**(4497): p. 925-7.
205. Senior, R.M., G.L. Griffin, and R.P. Mecham, *Chemotactic activity of elastin-derived peptides*. *J Clin Invest*, 1980. **66**(4): p. 859-62.
206. Senior, R.M., et al., *Val-Gly-Val-Ala-Pro-Gly, a repeating peptide in elastin, is chemotactic for fibroblasts and monocytes*. *The Journal of Cell Biology*, 1984. **99**(3): p. 870-874.
207. Shapiro, S.D., *Mighty mice: Transgenic technology "knocks out" questions of matrix metalloproteinase function*. *Matrix Biology*, 1997. **15**(8-9): p. 527-533.
208. Churg, A., D.D. Sin, and J.L. Wright, *Everything Prevents Emphysema*. *American Journal of Respiratory Cell and Molecular Biology*, 2011. **45**(6): p. 1111-1115.
209. Haq, I., et al., *Association of MMP - 12 polymorphisms with severe and very severe COPD: A case control study of MMPs - 1, 9 and 12 in a European population*. *BMC Medical Genetics*, 2010. **11**(1): p. 7.
210. Joos, L., et al., *The role of matrix metalloproteinase polymorphisms in the rate of decline in lung function*. *Human Molecular Genetics*, 2002. **11**(5): p. 569-576.
211. Haq, I., et al., *Matrix metalloproteinase-12 (MMP-12) SNP affects MMP activity, lung macrophage infiltration and protects against emphysema in COPD*. *Thorax*, 2011. **66**(11): p. 970-976.
212. Jormsjö, S., et al., *Allele-Specific Regulation of Matrix Metalloproteinase-7 Promoter Activity Is Associated With Coronary Artery Luminal Dimensions Among Hypercholesterolemic Patients*. *Arteriosclerosis, Thrombosis, and Vascular Biology*, 2001. **21**(11): p. 1834-1839.
213. Babusyte, A., et al., *Patterns of airway inflammation and MMP-12 expression in smokers and ex-smokers with COPD*. *Respir Res*, 2007. **8**: p. 81.
214. Molet, S., et al., *Increase in macrophage elastase (MMP-12) in lungs from patients with chronic obstructive pulmonary disease*. *Inflammation Research*, 2005. **54**(1): p. 31-36.
215. Demedts, I.K., et al., *Elevated MMP-12 protein levels in induced sputum from patients with COPD*. *Thorax*, 2006. **61**(3): p. 196-201.
216. LaPan, P., et al., *Optimization of total protein and activity assays for the detection of MMP-12 in induced human sputum*. *BMC Pulmonary Medicine*, 2010. **10**(1): p. 40.
217. Ishii, T., et al., *Alveolar macrophage proteinase/antiproteinase expression in lung function and emphysema*. *Eur Respir J*, 2014. **43**(1): p. 82-91.
218. Chandler, S., et al., *Macrophage Metalloelastase Degrades Matrix and Myelin Proteins and Processes a Tumour Necrosis Factor- α Fusion*

- Protein*. Biochemical and Biophysical Research Communications, 1996. **228**(2): p. 421-429.
219. Gronski, T.J., et al., *Hydrolysis of a Broad Spectrum of Extracellular Matrix Proteins by Human Macrophage Elastase*. Journal of Biological Chemistry, 1997. **272**(18): p. 12189-12194.
 220. Goncalves DaSilva, A., L. Liaw, and V.W. Yong, *Cleavage of Osteopontin by Matrix Metalloproteinase-12 Modulates Experimental Autoimmune Encephalomyelitis Disease in C57BL/6 Mice*. The American Journal of Pathology, 2010. **177**(3): p. 1448-1458.
 221. Belaaouaj, A.a., et al., *Matrix Metalloproteinases Cleave Tissue Factor Pathway Inhibitor*. Journal of Biological Chemistry, 2000. **275**(35): p. 27123-27128.
 222. Dong, Z., et al., *Macrophage-Derived Metalloelastase Is Responsible for the Generation of Angiostatin in Lewis Lung Carcinoma*. Cell, 1997. **88**(6): p. 801-810.
 223. Banda, M.J., et al., *Alpha 1-proteinase inhibitor is a neutrophil chemoattractant after proteolytic inactivation by macrophage elastase*. Journal of Biological Chemistry, 1988. **263**(9): p. 4481-4484.
 224. Coussens, L.M., B. Fingleton, and L.M. Matrisian, *Matrix Metalloproteinase Inhibitors and Cancer—Trials and Tribulations*. Science, 2002. **295**(5564): p. 2387-2392.
 225. Rabilloud, T., *Paleoproteomics explained to youngsters: how did the wedding of two-dimensional electrophoresis and protein sequencing spark proteomics on: Let there be light*. J Proteomics, 2014.
 226. Morrison, C.J., et al., *Matrix metalloproteinase proteomics: substrates, targets, and therapy*. Curr Opin Cell Biol, 2009. **21**(5): p. 645-53.
 227. Dean, R.A. and C.M. Overall, *Proteomics Discovery of Metalloproteinase Substrates in the Cellular Context by iTRAQ™ Labeling Reveals a Diverse MMP-2 Substrate Degradome*. Molecular & Cellular Proteomics, 2007. **6**(4): p. 611-623.
 228. Kleifeld, O., et al., *Isotopic labeling of terminal amines in complex samples identifies protein N-termini and protease cleavage products*. Nat Biotech, 2010. **28**(3): p. 281-288.
 229. Kleifeld, O., et al., *Identifying and quantifying proteolytic events and the natural N terminome by terminal amine isotopic labeling of substrates*. Nat. Protocols, 2011. **6**(10): p. 1578-1611.
 230. Prudova, A., et al., *Multiplex N-terminome Analysis of MMP-2 and MMP-9 Substrate Degradomes by iTRAQ-TAILS Quantitative Proteomics*. Molecular & Cellular Proteomics, 2010. **9**(5): p. 894-911.
 231. Samitas, K., et al., *Osteopontin expression and relation to disease severity in human asthma*. European Respiratory Journal, 2011. **37**(2): p. 331-341.
 232. Goldsmith, H.L., et al., *Homotypic Interactions of Soluble and Immobilized Osteopontin*. Annals of Biomedical Engineering, 2002. **30**(6): p. 840-850.
 233. Hirose, M., et al., *Role of osteopontin in early phase of renal crystal formation: immunohistochemical and microstructural comparisons with osteopontin knock-out mice*. Urological Research, 2012. **40**(2): p. 121-129.
 234. Wang-Rodriguez, J., et al., *Elevated osteopontin and thrombospondin expression identifies malignant human breast carcinoma but is not indicative of metastatic status*. Breast Cancer Res, 2003. **5**(5): p. R136-43.
 235. Mi, Z., et al., *Thrombin-Cleaved COOH-Terminal Osteopontin Peptide Binds with Cyclophilin C to CD147 in Murine Breast Cancer Cells*. Cancer Research, 2007. **67**(9): p. 4088-4097.

236. Weber, G.F., et al., *Phosphorylation-dependent interaction of osteopontin with its receptors regulates macrophage migration and activation*. Journal of Leukocyte Biology, 2002. **72**(4): p. 752-761.
237. O'Regan, A.W., et al., *Osteopontin (Eta-1) in cell-mediated immunity: teaching an old dog new tricks*. Immunology Today, 2000. **21**(10): p. 475-478.
238. Kazanekki, C.C., D.J. Uzwiak, and D.T. Denhardt, *Control of osteopontin signaling and function by post-translational phosphorylation and protein folding*. Journal of Cellular Biochemistry, 2007. **102**(4): p. 912-924.
239. van der Windt, G.J., et al., *Osteopontin impairs host defense during pneumococcal pneumonia*. J Infect Dis, 2011. **203**(12): p. 1850-8.
240. Schneider, D.J., et al., *Adenosine and osteopontin contribute to the development of chronic obstructive pulmonary disease*. The FASEB Journal, 2010. **24**(1): p. 70-80.
241. Beninati, S., et al., *Osteopontin: Its Transglutaminase-Catalyzed Posttranslational Modifications and Cross-Linking to Fibronectin*. Journal of Biochemistry, 1994. **115**(4): p. 675-682.
242. Kaartinen, M.T., et al., *Cross-linking of Osteopontin by Tissue Transglutaminase Increases Its Collagen Binding Properties*. Journal of Biological Chemistry, 1999. **274**(3): p. 1729-1735.
243. Kaartinen, M.T., et al., *Osteopontin Upregulation and Polymerization by Transglutaminase 2 in Calcified Arteries of Matrix Gla Protein-deficient Mice*. Journal of Histochemistry & Cytochemistry, 2007. **55**(4): p. 375-386.
244. Rosenthal, A.K., et al., *Osteopontin promotes pathologic mineralization in articular cartilage*. Matrix Biol, 2007. **26**(2): p. 96-105.
245. Nishimichi, N., et al., *Polymeric Osteopontin Employs Integrin $\alpha 9 \beta 1$ as a Receptor and Attracts Neutrophils by Presenting a de Novo Binding Site*. Journal of Biological Chemistry, 2009. **284**(22): p. 14769-14776.
246. Arjomandi, M., et al., *Secreted Osteopontin Is Highly Polymerized in Human Airways and Fragmented in Asthmatic Airway Secretions*. PLoS ONE, 2011. **6**(10): p. e25678.
247. Senger, D.R., et al., *Osteopontin at the Tumor/Host Interface*. Annals of the New York Academy of Sciences, 1995. **760**(1): p. 83-100.
248. Smith, L.L., et al., *Osteopontin N-terminal Domain Contains a Cryptic Adhesive Sequence Recognized by $\alpha 9 \beta 1$ Integrin*. Journal of Biological Chemistry, 1996. **271**(45): p. 28485-28491.
249. Agnihotri, R., et al., *Osteopontin, a Novel Substrate for Matrix Metalloproteinase-3 (Stromelysin-1) and Matrix Metalloproteinase-7 (Matrilysin)*. Journal of Biological Chemistry, 2001. **276**(30): p. 28261-28267.
250. Senger, D.R., et al., *Adhesive properties of osteopontin: regulation by a naturally occurring thrombin-cleavage in close proximity to the GRGDS cell-binding domain*. Molecular Biology of the Cell, 1994. **5**(5): p. 565-74.
251. Barry, S.T., et al., *Analysis of the $\alpha 4 \beta 1$ Integrin-Osteopontin Interaction*. Experimental Cell Research, 2000. **258**(2): p. 342-351.
252. Grassinger, J., et al., *Thrombin-cleaved osteopontin regulates hemopoietic stem and progenitor cell functions through interactions with $\alpha 9 \beta 1$ and $\alpha 4 \beta 1$ integrins*. Blood, 2009. **114**(1): p. 49-59.
253. Yamaguchi, Y., et al., *Thrombin-cleaved Fragments of Osteopontin Are Overexpressed in Malignant Glial Tumors and Provide a Molecular Niche with Survival Advantage*. Journal of Biological Chemistry, 2013. **288**(5): p. 3097-3111.
254. Wun, T.C., et al., *Cloning and characterization of a cDNA coding for the lipoprotein-associated coagulation inhibitor shows that it consists of*

- three tandem Kunitz-type inhibitory domains. *Journal of Biological Chemistry*, 1988. **263**(13): p. 6001-6004.
255. Bajaj, M.S., et al., *Structure and biology of tissue factor pathway inhibitor*. *Thromb Haemost*, 2001. **86**(4): p. 959-72.
256. Bajaj, M.S., et al., *Cultured normal human hepatocytes do not synthesize lipoprotein-associated coagulation inhibitor: evidence that endothelium is the principal site of its synthesis*. *Proceedings of the National Academy of Sciences*, 1990. **87**(22): p. 8869-8873.
257. Ameri, A., et al., *Expression of tissue factor pathway inhibitor by cultured endothelial cells in response to inflammatory mediators*. *Blood*, 1992. **79**(12): p. 3219-3226.
258. Novotny, W., et al., *Platelets secrete a coagulation inhibitor functionally and antigenically similar to the lipoprotein associated coagulation inhibitor*. *Blood*, 1988. **72**(6): p. 2020-2025.
259. Rana, S., et al., *Expression of tissue factor and factor VIIa/tissue factor inhibitor activity in endotoxin or phorbol ester stimulated U937 monocyte-like cells*. *Blood*, 1988. **71**(1): p. 259-262.
260. Rao, C.N., et al., *Extracellular matrix-associated serine protease inhibitors (Mr 33,000, 31,000, and 27,000) are single-gene products with differential glycosylation: cDNA cloning of the 33-kDa inhibitor reveals its identity to tissue factor pathway inhibitor-2*. *Arch Biochem Biophys*, 1996. **335**(1): p. 82-92.
261. Petersen, L.C., et al., *Inhibitory properties of a novel human Kunitz-type protease inhibitor homologous to tissue factor pathway inhibitor*. *Biochemistry*, 1996. **35**(1): p. 266-72.
262. Wesselschmidt, R., et al., *Tissue factor pathway inhibitor: the carboxy-terminus is required for optimal inhibition of factor Xa*. *Blood*, 1992. **79**(8): p. 2004-2010.
263. Girard, T.J., et al., *Functional significance of the Kunitz-type inhibitory domains of lipoprotein-associated coagulation inhibitor*. *Nature*, 1989. **338**(6215): p. 518-20.
264. Li, A. and T.C. Wun, *Proteolysis of tissue factor pathway inhibitor (TFPI) by plasmin: effect on TFPI activity*. *Thromb Haemost*, 1998. **80**(3): p. 423-7.
265. Brown, S., et al., *Quest for selectivity in inhibition of matrix metalloproteinases*. *Curr Top Med Chem*, 2004. **4**(12): p. 1227-38.
266. Moy, F.J., et al., *Impact of Mobility on Structure-Based Drug Design for the MMPs*. *Journal of the American Chemical Society*, 2002. **124**(43): p. 12658-12659.
267. Houghton, A.M., et al., *Macrophage Elastase (Matrix Metalloproteinase-12) Suppresses Growth of Lung Metastases*. *Cancer Research*, 2006. **66**(12): p. 6149-6155.
268. Saghatelian, A., et al., *Activity-based probes for the proteomic profiling of metalloproteases*. *Proceedings of the National Academy of Sciences of the United States of America*, 2004. **101**(27): p. 10000-10005.
269. Devel, L., et al., *Development of Selective Inhibitors and Substrate of Matrix Metalloproteinase-12*. *Journal of Biological Chemistry*, 2006. **281**(16): p. 11152-11160.
270. Li, W., et al., *A Selective Matrix Metalloprotease 12 Inhibitor for Potential Treatment of Chronic Obstructive Pulmonary Disease (COPD): Discovery of (S)-2-(8-(Methoxycarbonylamino)dibenzo[b,d]furan-3-sulfonamido)-3-methylbutanoic acid (MMP408)*. *Journal of Medicinal Chemistry*, 2009. **52**(7): p. 1799-1802.
271. Wu, Y., et al., *Discovery of potent and selective matrix metalloprotease 12 inhibitors for the potential treatment of chronic*

- obstructive pulmonary disease (COPD)*. *Bioorganic & Medicinal Chemistry Letters*, 2012. **22**(1): p. 138-143.
272. Devel, L., et al., *Insights from Selective Non-phosphinic Inhibitors of MMP-12 Tailored to Fit with an S1' Loop Canonical Conformation*. *Journal of Biological Chemistry*, 2010. **285**(46): p. 35900-35909.
273. World Medical, A., *World medical association declaration of helsinki: Ethical principles for medical research involving human subjects*. *JAMA*, 2013. **310**(20): p. 2191-2194.
274. Miller, M.R., et al., *Standardisation of spirometry*. *European Respiratory Journal*, 2005. **26**(2): p. 319-338.
275. John, M.E., et al., *Cardiovascular and inflammatory effects of simvastatin therapy in patients with COPD: a randomized controlled trial*. *Int J Chron Obstruct Pulmon Dis*, 2015. **10**: p. 211-21.
276. Sabit, R., et al., *Arterial Stiffness and Osteoporosis in Chronic Obstructive Pulmonary Disease*. *American Journal of Respiratory and Critical Care Medicine*, 2007. **175**(12): p. 1259-1265.
277. Laurent, S., et al., *Expert consensus document on arterial stiffness: methodological issues and clinical applications*. *Eur Heart J*, 2006. **27**(21): p. 2588-605.
278. Oakley, B.R., D.R. Kirsch, and N.R. Morris, *A simplified ultrasensitive silver stain for detecting proteins in polyacrylamide gels*. *Analytical Biochemistry*, 1980. **105**(1): p. 361-363.
279. Zhao, W., et al., *Differential Expression of Intracellular and Secreted Osteopontin Isoforms by Murine Macrophages in Response to Toll-like Receptor Agonists*. *Journal of Biological Chemistry*, 2010. **285**(27): p. 20452-20461.
280. Woodruff, P.G., et al., *A Distinctive Alveolar Macrophage Activation State Induced by Cigarette Smoking*. *American Journal of Respiratory and Critical Care Medicine*, 2005. **172**(11): p. 1383-1392.
281. Hillas, G., et al., *Increased levels of osteopontin in sputum supernatant of smoking asthmatics*. *Cytokine*, 2013. **61**(1): p. 251-255.
282. Matthews, H., et al., *Synthesis and preliminary evaluation of amiloride analogs as inhibitors of the urokinase-type plasminogen activator (uPA)*. *Bioorganic & Medicinal Chemistry Letters*, 2011. **21**(22): p. 6760-6766.
283. Kanazawa, H. and T. Yoshikawa, *UP-regulation of thrombin activity induced by vascular endothelial growth factor in asthmatic airways**. *CHEST Journal*, 2007. **132**(4): p. 1169-1174.
284. Bauer, T.W., et al., *Targeting of Urokinase Plasminogen Activator Receptor in Human Pancreatic Carcinoma Cells Inhibits c-Met- and Insulin-like Growth Factor-I Receptor-Mediated Migration and Invasion and Orthotopic Tumor Growth in Mice*. *Cancer Research*, 2005. **65**(17): p. 7775-7781.
285. Nordahl, E.A., et al., *Activation of the complement system generates antibacterial peptides*. *Proceedings of the National Academy of Sciences of the United States of America*, 2004. **101**(48): p. 16879-16884.
286. Prince, H.E., J.D. Folds, and J.K. Spitznagel, *Proteolysis of human IgG by human polymorphonuclear leucocyte elastase produces an Fc fragment with in vitro biological activity*. *Clin Exp Immunol*, 1979. **37**(1): p. 162-8.
287. Delimpoura, V., et al., *Increased levels of osteopontin in sputum supernatant in severe refractory asthma*. *Thorax*, 2010. **65**(9): p. 782-786.
288. Koh, A., et al., *Role of osteopontin in neutrophil function*. *Immunology*, 2007. **122**(4): p. 466-475.

289. Marroquin, C.E., et al., *Osteopontin increases CD44 expression and cell adhesion in RAW 264.7 murine leukemia cells*. Immunology Letters, 2004. **95**(1): p. 109-112.
290. Scatena, M., L. Liaw, and C.M. Giachelli, *Osteopontin*. Arteriosclerosis, Thrombosis, and Vascular Biology, 2007. **27**(11): p. 2302-2309.
291. Kim, M.K., et al., *Collagen-binding motif peptide, a cleavage product of osteopontin, stimulates human neutrophil chemotaxis via pertussis toxin-sensitive G protein-mediated signaling*. FEBS Lett, 2008. **582**(23-24): p. 3379-84.
292. Zheng, W., et al., *Role of osteopontin in induction of monocyte chemoattractant protein 1 and macrophage inflammatory protein 1beta through the NF-kappaB and MAPK pathways in rheumatoid arthritis*. Arthritis Rheum, 2009. **60**(7): p. 1957-65.
293. Higuchi, D.A., et al., *The effect of leukocyte elastase on tissue factor pathway inhibitor*. Blood, 1992. **79**(7): p. 1712-9.
294. Winckers, K., H. ten Cate, and T.M. Hackeng, *The role of tissue factor pathway inhibitor in atherosclerosis and arterial thrombosis*. Blood Reviews, 2013. **27**(3): p. 119-132.
295. Mattace-Raso, F.U.S., et al., *Arterial Stiffness and Risk of Coronary Heart Disease and Stroke: The Rotterdam Study*. Circulation, 2006. **113**(5): p. 657-663.
296. Blacher, J., et al., *Aortic Pulse Wave Velocity as a Marker of Cardiovascular Risk in Hypertensive Patients*. Hypertension, 1999. **33**(5): p. 1111-1117.
297. Ben-Shlomo, Y., et al., *Aortic Pulse Wave Velocity Improves Cardiovascular Event Prediction An Individual Participant Meta-Analysis of Prospective Observational Data From 17,635 Subjects*. Journal of the American College of Cardiology, 2014. **63**(7): p. 636-646.
298. Laurent, S., et al., *Aortic stiffness is an independent predictor of all-cause and cardiovascular mortality in hypertensive patients*. Hypertension, 2001. **37**(5): p. 1236-41.
299. Thomsen, M., et al., *Inflammatory Biomarkers and Comorbidities in Chronic Obstructive Pulmonary Disease*. American Journal of Respiratory and Critical Care Medicine, 2012. **186**(10): p. 982-988.
300. McDonald, D.M., G. Thurston, and P. Baluk, *Endothelial Gaps as Sites for Plasma Leakage in Inflammation*. Microcirculation, 1999. **6**(1): p. 7-22.
301. Schirm, S., et al., *Fragmented tissue factor pathway inhibitor (TFPI) and TFPI C-terminal peptides eliminate serum-resistant Escherichia coli from blood cultures*. J Infect Dis, 2009. **199**(12): p. 1807-15.
302. Cheng, G., et al., *Relationship between endothelial dysfunction, oxidant stress and aspirin resistance in patients with stable coronary heart disease*. J Clin Pharm Ther, 2007. **32**(3): p. 287-92.
303. Mano, T., et al., *Endothelial dysfunction in the early stage of atherosclerosis precedes appearance of intimal lesions assessable with intravascular ultrasound*. Am Heart J, 1996. **131**(2): p. 231-8.
304. Overall, C.M. and R.A. Dean, *Degradomics: systems biology of the protease web. Pleiotropic roles of MMPs in cancer*. Cancer Metastasis Rev, 2006. **25**(1): p. 69-75.
305. Hill, A., D. Bayley, and R. Stockley, *The Interrelationship of Sputum Inflammatory Markers in Patients with Chronic Bronchitis*. American Journal of Respiratory and Critical Care Medicine, 1999. **160**(3): p. 893-898.
306. Marchant, D.J., et al., *A new transcriptional role for matrix metalloproteinase-12 in antiviral immunity*. Nat Med, 2014. **20**(5): p. 493-502.

307. Bellac, Caroline L., et al., *Macrophage Matrix Metalloproteinase-12 Dampens Inflammation and Neutrophil Influx in Arthritis*. Cell Reports. **9**(2): p. 618-632.
308. Doucet, A. and C.M. Overall, *Broad Coverage Identification of Multiple Proteolytic Cleavage Site Sequences in Complex High Molecular Weight Proteins Using Quantitative Proteomics as a Complement to Edman Sequencing*. Molecular & Cellular Proteomics, 2011. **10**(5).
309. Rogers, L.D. and C.M. Overall, *Proteolytic post-translational modification of proteins: proteomic tools and methodology*. Mol Cell Proteomics, 2013. **12**(12): p. 3532-42.
310. Boersema, P.J., et al., *Triplex protein quantification based on stable isotope labeling by peptide dimethylation applied to cell and tissue lysates*. Proteomics, 2008. **8**(22): p. 4624-32.
311. Verrills, N.M., et al., *Identification of Novel Diagnostic Biomarkers for Asthma and Chronic Obstructive Pulmonary Disease*. American Journal of Respiratory and Critical Care Medicine, 2011. **183**(12): p. 1633-1643.
312. Nicholas, B., et al., *Shotgun proteomic analysis of human-induced sputum*. Proteomics, 2006. **6**(15): p. 4390-401.
313. Cox, J. and M. Mann, *MaxQuant enables high peptide identification rates, individualized p.p.b.-range mass accuracies and proteome-wide protein quantification*. Nat Biotech, 2008. **26**(12): p. 1367-1372.
314. Clarke, E.V. and A.J. Tenner, *Complement modulation of T cell immune responses during homeostasis and disease*. Journal of Leukocyte Biology, 2014. **96**(5): p. 745-756.
315. Dunkelberger, J.R. and W.C. Song, *Role and mechanism of action of complement in regulating T cell immunity*. Mol Immunol, 2010. **47**(13): p. 2176-86.
316. Kemper, C. and J. Kohl, *Novel roles for complement receptors in T cell regulation and beyond*. Mol Immunol, 2013. **56**(3): p. 181-90.
317. Merkel, D., et al., *Proteomic study of human bronchoalveolar lavage fluids from smokers with chronic obstructive pulmonary disease by combining surface-enhanced laser desorption/ionization-mass spectrometry profiling with mass spectrometric protein identification*. PROTEOMICS, 2005. **5**(11): p. 2972-2980.
318. Braido, F., et al., *Clara cell 16 protein in COPD sputum: A marker of small airways damage?* Respiratory Medicine, 2007. **101**(10): p. 2119-2124.
319. Celli, B.R., et al., *Inflammatory Biomarkers Improve Clinical Prediction of Mortality in Chronic Obstructive Pulmonary Disease*. American Journal of Respiratory and Critical Care Medicine, 2012. **185**(10): p. 1065-1072.